UC Berkeley
UC Berkeley Electronic Theses and Dissertations

Title
Glucocorticoids and Metabolic Disorders

Permalink
https://escholarship.org/uc/item/4d75g55b

Author
Chen, Tzu-Chieh

Publication Date
2016

Peer reviewed|Thesis/dissertation

eScholarship.org Powered by the California Digital Library
University of California

Glucocorticoids and Metabolic Disorders

By

Tzu-Chieh Chen

A dissertation submitted in partial satisfaction of the Requirements

for the degree of

Doctor of Philosophy

in

Metabolic Biology

in the

Graduate Division

of the

University of California, Berkeley

Committee in charge:
Professor Jen-Chywan Wally Wang, Chair
Professor Gary Firestone
Professor Dale Leitman
Professor Hei Sook Sul

Fall 2016

Abstract

Glucocorticoids and Metabolic Disorders

by

Tzu-Chieh Chen

Doctor of Philosophy in Metabolic Biology

University of California, Berkeley

Professor Jen-Chywan (Wally) Wang, Chair

Glucocorticoids (GC) are steroid hormones that exert necessary metabolic adaptation under stress, such as fasting/starvation, for the survival of mammals. To maintain blood glucose level during stress GC suppress insulin actions to promote hepatic gluconeogenesis and inhibit glucose utilization in muscle and adipose tissues. Chronic and/or excess GC exposure, however, leads to various metabolic disorders such as insulin resistance, dyslipidemia. Notably, the molecular mechanisms of GC-induced metabolic disorders are largely unclear. In this dissertation, we focus on two GC primary target genes: *Angptl4* and *Pik3r1* to study their roles in GC induced physiological/metabolic changes and insulin resistance *in vivo*.

In Chapter I, we identified a Glucocorticoids-Angiopoietin-like 4- ceramide axis as a mechanism for GC induced hepatic insulin resistance. Under Dex treatment, wild type mice developed hepatic insulin resistance with high hepatic ceramide level, increased expression of several ceramide synthesis associated genes, and increased PP2A and PKCζ activity. However, all these observations can be reversed by *Angptl4* depletion in *Angptl4* null mice.

In Chapter II, we found that Pik3r1 plays roles in the process to recruit PKA toward lipid droplet for Plin1 phosphorylation. Therefore, *Pik3r1* knockout does not impair the activation of cytosolic HSL and PKA, but does impair the phosphorylation of Plin1 on lipid droplet. Therefore, less phosphor-HSL (the activated HSL) can be recruited to lipid droplet to mediate lipolysis. As a consequence, under Dex treatment, with less lipolysis, the adipose tissues specific *Pik3r1* knockout (AKO) mice shown reduced fatty liver and dyslipidemia compared to wild type mice.

In Chapter III, we found that the expression of *Pik3r1* is regulated by GC in skeletal muscle *in vivo*. In the molecular level, the GC induced Pik3r1 expression is mediated by p300 induced histone H3 and H4 acetylation. In the physiological level, the *Pik3r1* expression in muscle is important for GC induced insulin resistance. Therefore, muscle specific *Pik3r1* knockout (MKO) mice show improved glucose tolerance under Dex treatment. This result is consistent with the findings *in vitro* using C2C12 myotubes.

In total, this dissertation demonstrated that *Angptl4* and *Pik3r1* are two important genes mediating GC-induced metabolic disorders including insulin resistance, fatty liver and dyslipidemia.

Dedication

To my family and friends.

Acknowledgements

I would like to thank my advisor Dr. Jen-Chywan (Wally) Wang for his guidance and encouragement throughout my PhD study. Wally was a very supportive and inspiring mentor. He always encourages me to explore unknown territories of my research projects, and to present my research studies in scientific conferences. In addition, Wally's "survival guide" in the US is also helpful to me as an international student. I appreciate his kindness for sharing all his knowledge and experience with me.

I appreciate Dr. Hei Sook Sul, Dr. Dale Leitman, and Dr. Gary Firestone for being my dissertation committee members. I want to give special thanks to Dr. Sul for revising all of my paper manuscripts, and encouraging me to keep going. I also want to thank Dr. Danica Chen and Dr. Kathleen Collins for serving as my qualifying exam committees.

Many Wang Lab members helped a lot for my studies. I am grateful to have them in my PhD life. Dr. Taiyi (Diana) Kuo, Dr. Nora Gray and Dr. Deepthi Kanamaluru introduced me to many of my research studies. My wonderful colleagues Allison Mcqueen, Rebecca Lee, and Damian Costello created an amiable atmosphere in the lab. I enjoyed everyday life working in the lab. Simplicia Flor-Cruz, our animal technician, helped me and taught me different animal experiments. Besides, I couldn't have finished these studies with the help from my talent and hard working undergraduates: Nguyen Nguyen, Augusta Broughton, Stacey Tran, Thanh Nguyen, Julie Cheng, Jenny Chen, Danyun Zhang, Mei Lan Lee, Kenneth Wu, Darryl Mar, Jessica Chen, and Rachel Lee.

I would like to thank my collaborators for broadening my horizons during my graduate study. Dr. Daniel Nomura was kind enough to give me the chance to study my research topic with metabolomics analysis. Dr. Daniel Benjamin and Breanna Ford helped me a lot to process my samples and showed me how to interpret the data. Dr. Michael Stallcup and Dr. Chen-Yin Ou from USC helped me to further understand CCAR1. Dr. Miles Pufall from University of Iowa helped me to perform the ChIP-sequencing and gave me helpful guidance for ChIP-seq analysis. Dr. Chulho Kang from Berkeley Transgenic Center helped us to generate the CCAR1 knockout mice.

I've been lucky to have wonderful classmates and friends in NST. I enjoyed teaching, discussing experimental problems, and brainstorming what the future would like with them. I also received a lot of good suggestions and encouragement from them. These interactions made me feel optimistic and positive. Faith Enemark, the NST graduate advisor, helped me a lot to deal the the course enrollment, and filing fee application. I really appreciate her patience to listen to my questions.

Last but not least, I would like to express my sincere gratitude to my college friends and family members especially my wonderful parents Cheng-Chih Chen, I-Yuan Cheng and my dear husband Hsiao-Wu Hsieh. Without their endless support and heart-warming care, I wouldn't have to been able to obtain my PhD degree.

Table of Contents

Introduction

Over 80 years ago, the first clinical evidence demonstrated that the animal adrenocortical tissue extract could treat human adrenal failure [1]. Since then, glucocorticoids (GC) and their synthetic analogs have been widely used as potent anti-inflammatory drugs to treat both acute and chronic inflammatory diseases such as asthma, inflammatory bowel disease, rheumatoid arthritis, multiple sclerosis, and various autoimmune diseases. Additionally, they are also used in immunosuppressive regimes for organ transplantation. However, prolonged and excess GC exposure could have significant impacts on several metabolic tissues such as liver, white adipose tissues, and skeletal muscles leading to severe metabolic disorders including insulin resistance, dyslipidemia, hypertension, osteoporosis, and muscle atrophy [2]. These adverse effects make GC and its relative steroid drugs a double-edged sword. Therefore, to improve therapeutic usage of these drugs, it is essential to study the mechanisms that mediate GC induced metabolic disorders.

I. Glucocorticoids and its molecular mechanism

I-1. The regulation of Glucocorticoids availability

Glucocorticoids (GC, cortisol in humans and corticosterone in rodents) are cholesterol-derived hormones which are secreted by the adrenal glands under the control of hypothalamic-pituitary-adrenal (HPA) axis [3]. In the biological system, the secretion of GC is usually regulated by the circadian, ultradian rhythm and physiological stress. Upon stimulation, the hypothalamus secretes corticotropin-releasing hormone (CRH), which then stimulates the anterior pituitary gland to release adrenocorticotropic hormone (ACTH). ACTH works as an endocrine to stimulate the cortex of adrenal glands to synthesize and secrete GC into the blood system. Once secreted, the GC can be transported by corticosteroid-binding globulin in the serum. The availability of GC in tissues is regulated by not only the HPA axis and GC transportation but also the local expression of 11β-hydroxysteroid dehydrogenase 1 (11β-HSD1) which converts the inert cortisone to active cortisol and 11β-HSD2 which carries out the opposite reaction [4]. With these, the secretion and tissue specific activity of GC are under tight control for proper metabolic regulation in response to alterations in physiological conditions.

I-2. Molecular mechanism of glucocorticoids action

I-2-A. Glucocorticoid signaling

Glucocorticoids convey their signaling via genomic or non-genomic mechanisms. In the non-genomic signaling, GC bind to membrane or intracellular receptors to alter the amount of intracellular secondary messengers or to modulate the activity of certain kinases to impact cellular responses [5]. However, this dissertation will mainly focus on the genomic signaling as shown in Figure 1a. In the absence of GC, GR stays in an inactive form by forming complex with chaperone protein complex consists of several protein members including heat shock protein 90 (HSP90), HSP70, Immunophilins, FKBPs, CyP-40, P23 and others [6-8]. This chaperone protein complex traps GR in the cytosol and keeps the ligand-binding pocket of GR exposed. Once GC binds to LBD of GR, GR will undergo a transformational change, which allows it to dissociate from the chaperone protein complex. Then, the GC-GR complex translocates to the nucleus where it forms a homo-dimer, binds to the GRE, and recruits different transcription cofactors to modulate downstream gene expression [9]. These GR primary target genes then confer the physiological and pathophysiological responses of GC.

I-2-B. Major players in glucocorticoid signaling

Once GC have entered cells by simple or facilitated diffusion, at the cellular level, they conveys their physiological effects through the glucocorticoid receptor (GR). Glucocorticoid receptor, also known as NR3C1 (nuclear receptor subfamily 3, group C, member 1), is a type I nuclear hormone receptor. Its molecular structure, as shown in Figure 1b, is composed of several domains each with distinct functionalities: The N-terminal domain (NTD) contains the transactivation function domain, AF-1 (hormone independent transactivation function domain-1). An additional transactivation domain, AF-2 (hormone independent transactivation function domain-2) was found on the C-terminal ligand-binding domain (LBD). A relatively uncharacterized transactivation domain, tau2 activation domain, was found in the hinge region of GR [10]. The DNA-binding domain (DBD) contains two alpha-helices, which form zinc-finger motifs that are critical for GR dimerization, recognition of the glucocorticoid response element (GRE), protein-nucleotide interaction, and transactivation of GR. Alternatively, the ligand-binding domain (LBD) is in charge of ligand recognition, ligand binding and providing interacting surface with transcription co-regulators once it binds to ligands. The hinge region joins the DBD and LDB together.

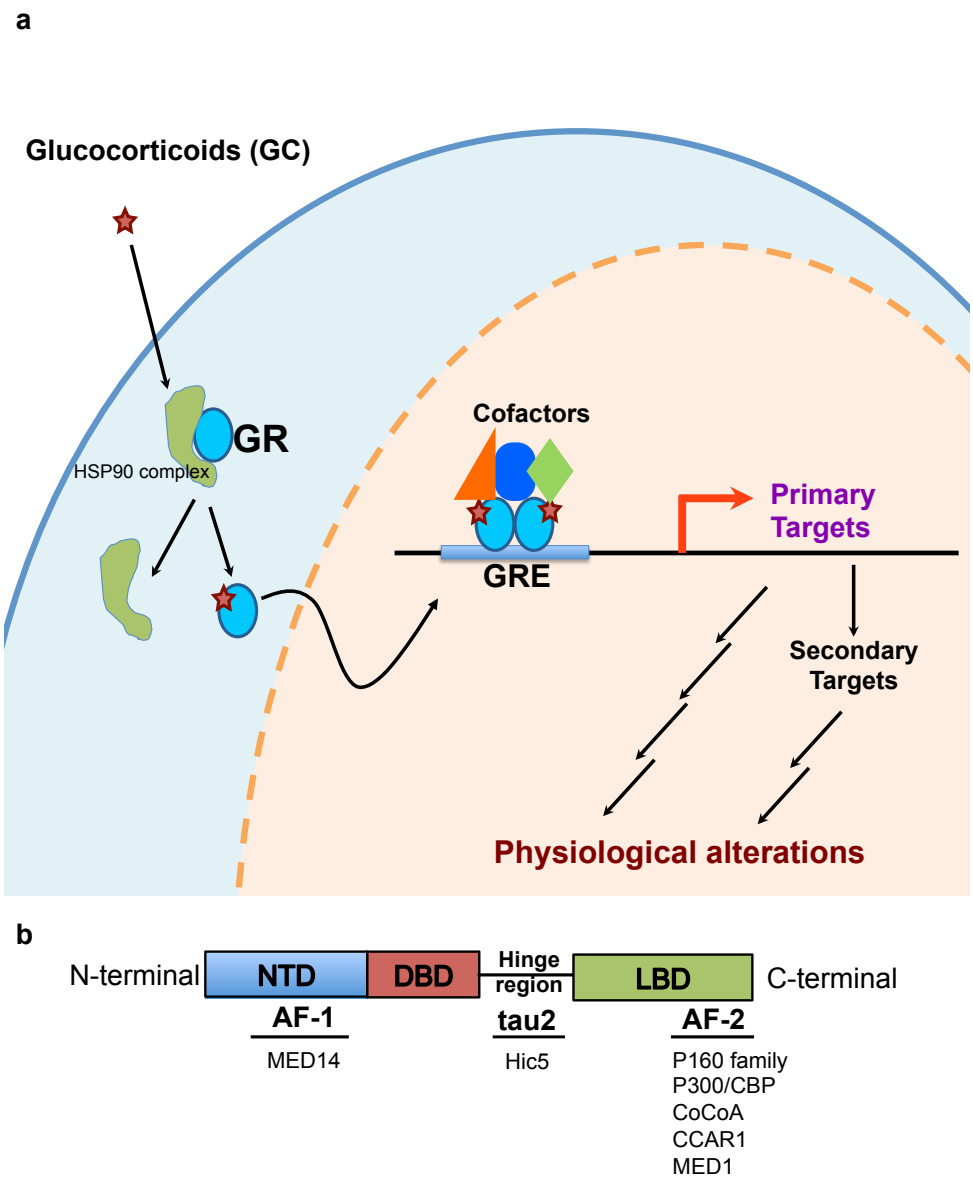

Figure 1. Glucocorticoid receptor and glucocorticoid signaling.

(a) Glucocorticoid signaling is shown. Upon entering the cell, glucocorticoids (GC) bind to the glucocorticoid receptor (GR). The GC-bound GR then dissociates from HSP90 chaperone protein complex, and translocate into the nucleus where it binds to the glucocorticoid response element (GRE). It then recruits transcription cofactors to induce the downstream gene expression of GC primary target genes. Its the expression of primary target genes as well as the potential secondary target genes that mediate the regular GC-associated physiological alterations and the development of GC-related adverse effects. (b) The Glucocorticoid receptor is structurally composed of a N-terminal domain (NTD), a DNA-binding domain (DBD), a hinge region, and the C-terminal ligand-binding domain (LBD). Three transactivation domains: AF-1, AF-2, and tau2 are embedded in the NTD, LBD, and hinge region respectively. Each of them can interact with several transcription cofactors as listed below each of the domains.

Glucocorticoid binding regions (GBRs) are genomic segments that were determined via chromatin immunoprecipitation (ChIP) coupled with quantitative PCR or ChIP sequencing to have GR occupancy. In the GBRs, the specific glucocorticoid receptor binding sites are called glucocorticoid response element (GRE). The GRE is a genomic segment that confers the transcriptional regulatory effect of GC *in vivo* by serving as centers for the assembly of multi-factor transcriptional regulatory complexes. The classical GRE has a palindromic sequence represented as 5'-AGAACAnnnTGTTCT-3', where the n is any nucleotide. Activated GR usually forms an inverted homo-dimer with each monomer binding to each half part of the palindrome [11, 12]. GBRs may be located far upstream or downstream of the target genes. With the help of transcription cofactors to provide necessary protein-protein interactions, the GR triggers chromatin looping or chromatin structural changes to bring together the GRE, the multi-factor transcriptional regulatory complex, and the promoter of GR target genes for GR mediated transcriptional activation or suppression [13, 14]. Interestingly, GC induces distinct patterns of genomic GBRs. This is in agreement with the fact that GC induces distinct gene expression patterns in different cell types. Regardless, not all GBRs have an identical GRE motif. Notably, a perfect GRE motif is rarely found in GBRs. Many GR target genes lack a canonical GRE. For some genes, one-half of the canonical palindrome is sufficient for monomeric GR to induce genetic transactivation [15-17]. Other GR target genes have been found to contain GBRs with degenerate but functional GREs [18, 19] or to have multiple copies of GREs [20].

Transcription cofactors are proteins that act with nuclear hormone receptors and numerous DNA-binding transcription factors to modulate the rate of transcription of specific genes. The mechanism by which the transcription cofactors modulate gene transcription varies from one cofactor to another. The expression pattern of cofactors could differ in tissues temporally and spatially. This contributes to the differential control of gene expression by the same transcription factor in different tissues during development, differentiation, and metabolism regulation [21].

Several transcription cofactors such as p160, p300/CBP, HDAC2, Hic-5, MED1, MED14, MED10, MED23, and the SWI/SNF complex have been found to work with GR to induce gene transactivation [22]. These co-activators are usually recruited via interaction with the AF-1, AF-2 or tau2 domain of glucocorticoid receptor [23] as listed in Figure 1b. Many of them serve to alter histone modification, chromatin structure, recruitment of RNA polymerase II basal transcription machinery or the stability of transcriptional machinery for transcriptional activation.

The p160 proteins including SRC1, SRC2/GRIP1/TIF2, and SRC3/pCIP/ACTR/AIB-1/RAC-3/TRAM-1 [24-32] interact with the LxxLL sequence motif on the AF-2 domain of GR [33-35]. The members of p160 proteins contain trans-activation domains (AD1 and AD2) that form docking sites for the recruitment of other co-activators. The AD1 transactivation domain of p160 family is found capable to recruit p300/CBP [36, 37]. P300/CBP has histone acyltransferase (HAT) activity, which acetylates specific lysine residues within the N-terminal tail of histone H3 and histone H4. These acetylations neutralize the positive charge of the histone N-terminal tails and decreases their interaction with the negatively charged phosphate groups of DNA. As a result, the

condensed higher-order chromatin is loosened to a more relaxed chromatin structure. The unwinding chromatin especially at gene promoter or transcription start site is critical because it increases the accessibility of these genomic regions to recruit transcription machinery for gene transactivation. Additionally, p300/CBP also serves as a protein bridge or protein scaffold to connect different transcription factors/co-factors to form multicomponent transcriptional regulatory complex [38]. Other HAT such as GCN5, Tip60, and PCAF are also shown to interact and coactivate with GR. Glucocorticoid receptors are also shown to react with histone deacetylase 2 (HDAC2) to induce gene expression for some genes. On the other hand, the AD2 transactivation domain of p160 family is associated with the recruitment of CARM1 (coactivator-associated arginine methyltransferase 1), which is a protein arginine methyltransferase (PRMT) that methylates arginine 17 on the N-terminal tail of histone H3. This methylation is associated with transcriptional activation. Besides, CARM1 also methylate p300/CBP to enhance the GR mediated gene expression [39]. CoCoA (coiled-coil coactivator) is another transcriptional cofactor that is recruited by p160 [40]. The C-terminal trans-activation domain of CoCoA is essential for its coactivation function [41]. One function of CoCoA in transactivation is to recruit CCAR1 (cell cycle and apoptosis regulator 1) which is important for the recruitment of mediator complex. In other words, CCAR1 provides a bridge to link activities of GR, p160, CoCoA to mediator complexes [42]. Other co-factors that can be recruited to p160 includes G9a, another histone methyltransferase [43], GAC63 [44], and Fli [45]. All of them are found to facilitate transcriptional activation.

Hic-5 (TGFB1I1, hydrogen peroxide-inducible clone-5) serves as an on/off switch for GC to regulate the transactivation of many genes. Its recruitment is mediated by tau2 activation domain of GR. For the GC induced genes, the major function of Hic-5 is to facilitate the recruitment of mediator complex. As for the suppressed genes, Hic-5 helps to prevent the GR occupancy and chromatin remodeling. Therefore, only when the Hic-5 is removed, these genes can be transactivate by GC [10].

MED1, MED14, MED10, and MED23 are components of the mediator complex. Mediator is a large, multi-components complex that provides a link to the basal transcription machinery for the regulation of RNA polymerase II assembly, pausing and elongation as well as the reorganization of chromatin architecture [46, 47]. Some mediator proteins physically interact with GR. For instance, MED1 and MED14 can directly interact with GR via the AF-2 and AF-1 domain respectively. However, others mediate transactivation by being recruited by other transcriptional cofactor. For example, CCAR1 is capable of recruiting MED10/NUT2, MED23 [48], and MED1/ TRAP220 [42].

The SWI/SNF complex is an ATP-dependent nucleosome-remodeling complex that remodels chromatin structure to increase the accessibility of transcription factors/ cofactors for their binding sites [49, 50]. The SWI/SNF complex contains about 10 BRG1-associated factor (BAF) protein components [51, 52]. The core subunit contains BRG1/Brm, BAF155, BAF170, BAF60, BAF47 (hSNF/Ini1) and BAF57. The BGR1 or Brm is the catalytic ATPase subunit. BAF155 and BAF170 exist as heterodimer or homodimers via a leucine zipper motif [52]. Both of them contain the SANT domain and

SWIRM domain as a module for histone tail binding and proline-protein interactions respectively [53-55]. Whereas, the BAF57 contains a proline rich region, a HMG domain, a NHRLI domain, and a putative coiled coil domain. The main function of BAF57 is to help recruit the SWI/SNF complex to the promoter for transactivation [56]. Several studies have shown that the expression of components of SWI/SNF complex is tightly controlled and coordinated [57]. SWI/SNF complex remodels nucleosome structure by sliding and facilitating the ejection and insertion of histone octamers [58]. With this, SWI/SNF complex helps to expose specific DNA regions and increase the accessibility for the recruitment of downstream transcription factors for gene transactivation.

II. Glucocorticoids and its biological functions

Serving as an endocrine hormone, GC is found to have impacts in a variety of biological processes in mammals. During fetal development, GC is required for the lung development and the production of many proteins important for lung function including surfactants, which are critical proteins to reduce the surface tension on alveoli, the epithelial sodium channel, the sodium/potassium ATPase, and many antioxidant enzymes [59]. Additionally, GC are also found to play roles in the development of mature adipose tissues. Disruption GC mediated transactivation by knocking down CCAR1 expression is found to impair the differentiation of both 3T3-L1 preadipocyte and mouse embryonic fibroblast to mature adipocytes [42]. In the immune system, GC serves as a negative regulator to suppress the host immune and inflammation responses. GC is capable of increasing the expression of anti-inflammatory proteins such as secretory leukocyte proteinase inhibitor (SLPI) [60] and mitogen-activated kinase phosphatase-1 (MKP-1) [61]; in the meantime, reducing the expression of pro-inflammatory proteins such as interleukin-6 (IL-6) [62]. In addition, GR can also interfere the actions of NF-κB (Nuclear Factor-κB) and AP-1 (Activator Protein-1), two key inflammatory transcriptional regulators, via direct interaction with these proteins [63, 64]. In terms of suppression of immune response, GC is able to induce the apoptosis of immune cells and regulate T-cell development [65, 66]. Despite the functions in development and immunosuppression, GC also plays key roles in regulating metabolism. The impacts of GC on metabolism are the major focus of this dissertation. In the next section, the main influence of GC on metabolism will be discussed in detail.

III. Glucocorticoids and metabolic physiology

III-1. Glucocorticoids and lipid homeostasis

Glucocorticoids are known as anabolic hormones in metabolism, which liberate stored energy for metabolic needs during stresses. The major impact of GC in the lipid metabolism in adipose tissue is to induce lipolysis [67]. Lipolysis is an enzymatic

process to break down the triacylglycerol (TAG), the major storage form of energy, to glycerol and free fatty acids. During lipolysis, TAGs are first converted to diacylglycerol (DAG) with the release of one free fatty acid. This conversion is mediated by adipose triglyceride lipase (ATGL) which may be the rate limiting enzyme for lipolysis [68]. In the second step, hormone sensitive lipase (HSL) will convert DAG to monoacylglycerol (MAG) and release another free fatty acid. HSL is found to be a regulatory pivot since its localization determines the onset/offset of lipolysis. In the basal status, HSL is located in the cytosol and has low activity. However, under stimulation, HSL will be phosphorylated/activated and translocate to the lipid droplet to facilitate lipolysis [69-72]. In the last step, MAG will then be broken down to glycerol and the third free fatty acid by monoacylglycerol lipase [73]. All of these released free fatty acids and glycerol can then be further processed and used by other tissues as energy sources [74].

Several mechanisms are stated for GC mediated lipolysis. First, GC can directly activate the expression of ATGL and HSL [71, 75-77]. Second, GC also regulates lipolysis by a nongenomic mechanism, the cAMP-PKA axis [71]: to increase intracellular cyclic adenosine monophosphate (cAMP) level. Increased cAMP activate cAMP-dependent protein kinase A (PKA), which phosphorylates Ser 660 and Ser 563 on HSL. Then, this phosphorylated HSL can translocate to lipid droplets to facilitate lipolysis [78]. Activated PKA can also phosphorylate perilipin1 (Plin1), a lipid droplet surface protein, whose phosphorylation is important for HSL translocation from cytosol to lipid droplet [79, 80]. Furthermore, Plink phosphorylation is also required to release comparative gene identification 58 (CGI-58) to cytosol to enhance the activity of ATGL [81, 82]. This cAMP-mediated regulation pathway can be suppressed by cAMP breakdown which is usually mediated by phosphodiesterase 3 B (PDE3B) [83]. Insulin, as a counterpart of GC in anabolic metabolism, is the major hormone that activates PDE3B through phosphoinositide 3-kinase (PI3 kinase)/Akt dependent or independent pathway to inhibit lipolysis [84, 85].

Recently, *Angptl4*, a glucocorticoid primary target gene, is also found to play a role in GC induced adipose tissue lipolysis (Fig. 2) [86]. *Angptl4* encodes a protein called Angiopoietin-like 4 (Angptl4). Angptl4 is a secreted protein whose induction can be up-regulated by GC. Angptl4 has two functionalities: to inhibit extracellular lipoprotein lipase (LPL) activity and to promote intracellular lipolysis in adipose tissues [87-89]. Mice lacking Angplt4 have an impaired GC-stimulated adipose tissue lipolysis with an improved tolerance to GC-induced hepatic steatosis and hyperlipidemia [88]. The receptor of Angplt4 has not been identified yet, but Angptl4 is thought to induce lipolysis by elevating intracellular cAMP levels to activate the cAMP-PKA axis. Angptl4 null mice show reduced cAMP accumulation under GC treatment. Catecholamine induced lipolysis (mainly via cAMP-PKA axis) is also impaired in adipocytes isolated from Angptl4 null mice [88].

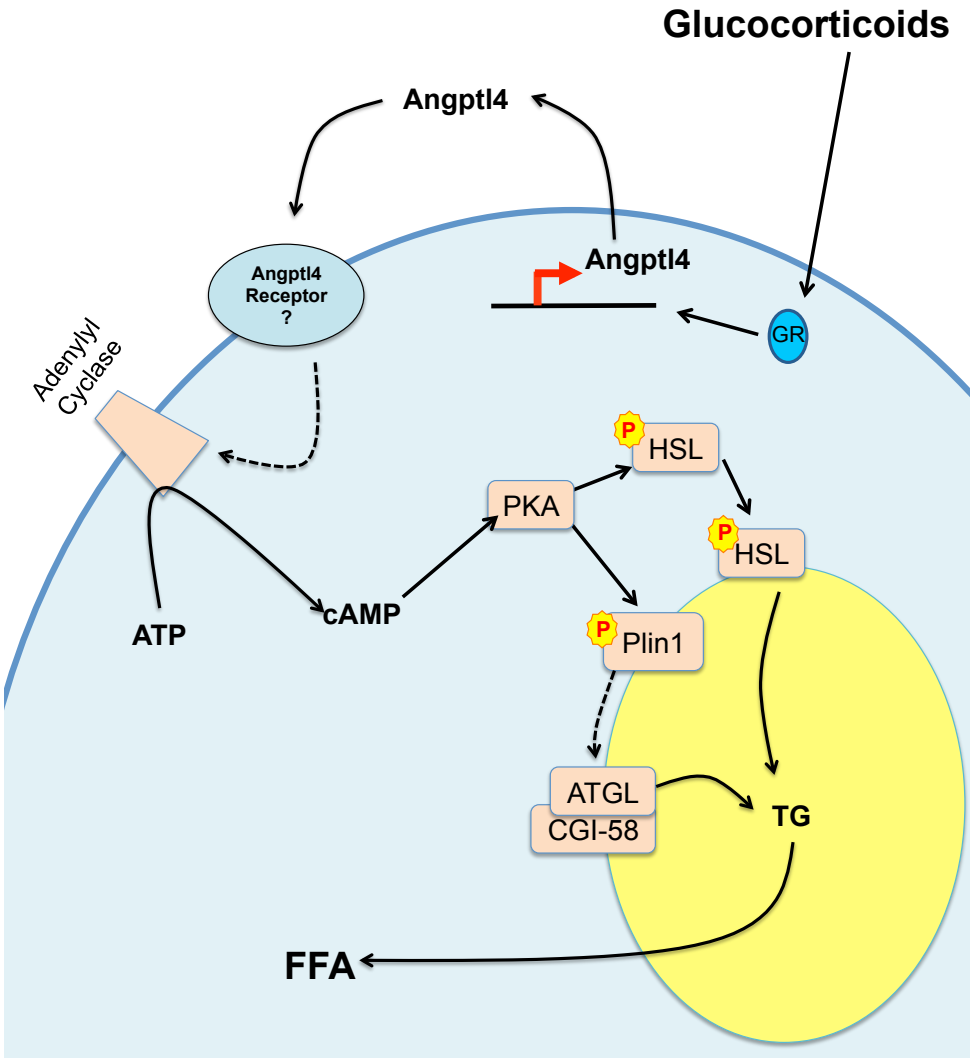

Figure 2. Glucocoritcoids-Angiopoietin-like 4 induced lipolysis.

Glucocorticoids induces Angiopoietin-like 4 (Angptl4) expression in adipose tissues. The Angptl4 can then be secreted and binds to an unknown receptor which mediates the activation of adenylyl cyclase that converts ATP to cAMP. The accumulated cAMP activates Protein kinase A (PKA). PKC then phosphorylates HSL in the cytosol and the perilipin 1 (Plin1) on the lipid droplet. The former, phosphor-HSL, then translocates to lipid droplet. Whereas the latter, phosphor-Plin1 help to dissociate GCI-58 from ATGL. Then, phosphor-HSL and ATGL work together to facilitate the lipolysis process to break down triglyceride (TG) into glycerol and free fatty acids (FAA).

III-2. Glucocorticoids and glucose homeostasis

GC play critical roles in regulating plasma glucose level. Newborn mice rely on GC to trigger gluconeogenesis for survival. Mice without GR will behave normally without stress, but will die with stress treatment. The major function of GC during stress conditions is to maintain the blood glucose level and preserve the glucose for important tissues including brain and red blood cells, which use only glucose as an energy source. GC achieve this goal by affecting a wide variety of biological processes in many tissues. In the liver, GC promote gluconeogenesis and increase glycogen storage. In skeletal muscle, GC reduce glucose utilization, and glycogen storage, but increase protein degradation. In white adipose tissues, GC reduce glucose utilization but increases lipolysis. In the pancreas, GC suppress insulin secretion, increase glucagon secretion, and induce beta cell hyperplasia. The effects of GC on glucose metabolism will be the major focus for this section.

Gluconeogenesis, which usually takes place in liver, is a process via which non-carbohydrate gluconeogenic substrates are converted to glucose. Major gluconeogenic substrates during stress conditions include glycerol from adipose tissue lipolysis and amino acids such as alanine and glutamine from skeletal muscle protein degradation. In the liver, alanine can be converted to pyruvate by alanine transaminase, then to oxaloacetate (OAA) by pyruvate carboxylase (PC) [90, 91] in mitochondria. Also in mitochondria, glutamine can be converted to alpha-ketoglutarate. With several enzymatic reactions, alpha-ketoglutarate can also be converted into OAA. OAA can then be transferred to cytosol via malate-aspartate shuttle system. In the cytosol, OAA will be converted by phosphoenolpyruvate carboxykinase (PCK1) to phosphoenolpyruvate (PEP) [92, 93] which then enter the gluconeogenic pathway. During gluconeogenesis, PEP will be converted to fructose-1,6-biphosphate (F1,6BP) then to fructose-6-phosphate (F6P) by fructose 1,6-bisphosphatase [94]. To generate glucose, F6P is catalyzed to glucose-6-phosphate (G6P). Then by glucose-6-phosphatase (G6PC), G6P is converted to glucose [95-97]. Besides alanine and glutamine, metabolites that can be converted to TCA cycle intermediates can all be converted to OAA to enter gluconeogenesis. Glycerol enters gluconeogenesis by being metabolized by glycerol kinase and glycerol 3-phosphate dehydrogenase to dihydroxyacetone phosphate (DHAP), which will then be converted to F1,6BP and finally glucose as described before [98, 99].

GC activates gluconeogenesis not only by increasing the supply of gluconeogenic precursors from adipose tissue lipolysis and skeletal muscle breakdown, but also by directly up-regulating genes involved in gluconeogenesis. The expression of PC, PCK1 [100-104], G6PC [105, 106] are all positively regulated by GC.

To elevate plasma glucose level, in peripheral tissues including adipose tissues and skeletal muscle, GC not only induces anabolic effects but also suppresses glucose utilization. Adipose tissues and skeletal muscle are two major tissues that execute insulin stimulated glucose utilization. Insulin conveys its function by binding to insulin receptor, which is a tyrosine kinase receptor, leading to the activation of kinase activity

and the phosphorylation of many downstream signaling molecules such as IRS1. Then, the signaling molecules further activate other important players in insulin signaling pathway including Akt, PI3 kinase and MAPK to stimulate many downstream events such as glucose uptake [107]. Under insulin stimulation, glucose transporter 4 (GLUT4), the insulin sensitive glucose transporter can be translocate to cell membrane to increase glucose uptake [108, 109]. GC is found to increase expression of GLUT4 in these tissues. However, the insulin induced GLUT4 translocation is suppressed in the presence of GC [110-114].

IV. Glucocorticoids and metabolic disorders

Chronic elevation of GC could result in pathological outcomes known as Cushing's syndrome [115]. Patients with Cushing's syndrome are characterized by central obesity with thin arms and legs, high blood pressure, moon face, muscle atrophy and diabetes mellitus. Endogenous Cushing's syndrome usually results from a tumor on the pituitary gland, which disrupts the HPA axis by increasing secretion of ACTH, which induces high cortisol production. This endogenous Cushing's syndrome is also called Cushing's disease. However, this disease is relatively rare among humans. Ever since the inception of synthetic glucocorticoids such as dexamethasone (Dex), predinisone and budesonide as drugs for clinical treatment, GC medication has become the most common cause of Cushing's syndrome. This phenomenon is also called exogenous Cushing's syndrome. Unfortunately, potent alternative medications are not available for many patients with diseases such as autoimmune disease and asthma. Therefore, it is imperative to develop improved GC medication for medical use.

Most pathological outcomes of excess or chronic GC exposure are results of over-stimulation of physiological pathways regulated by GC (Fig. 3). However, several studies have demonstrated that blocking key players downstream of GC could help to reduce GC induced pathological consequences. Therefore, understanding the mechanisms by which GC mediate the metabolic disorders and identifying critical players in the development of GC associated metabolic disorders could help developing better strategy to reduce the adverse effects of GC treatment. Important discoveries for GC induced metabolic disorders are discussed in the following sections.

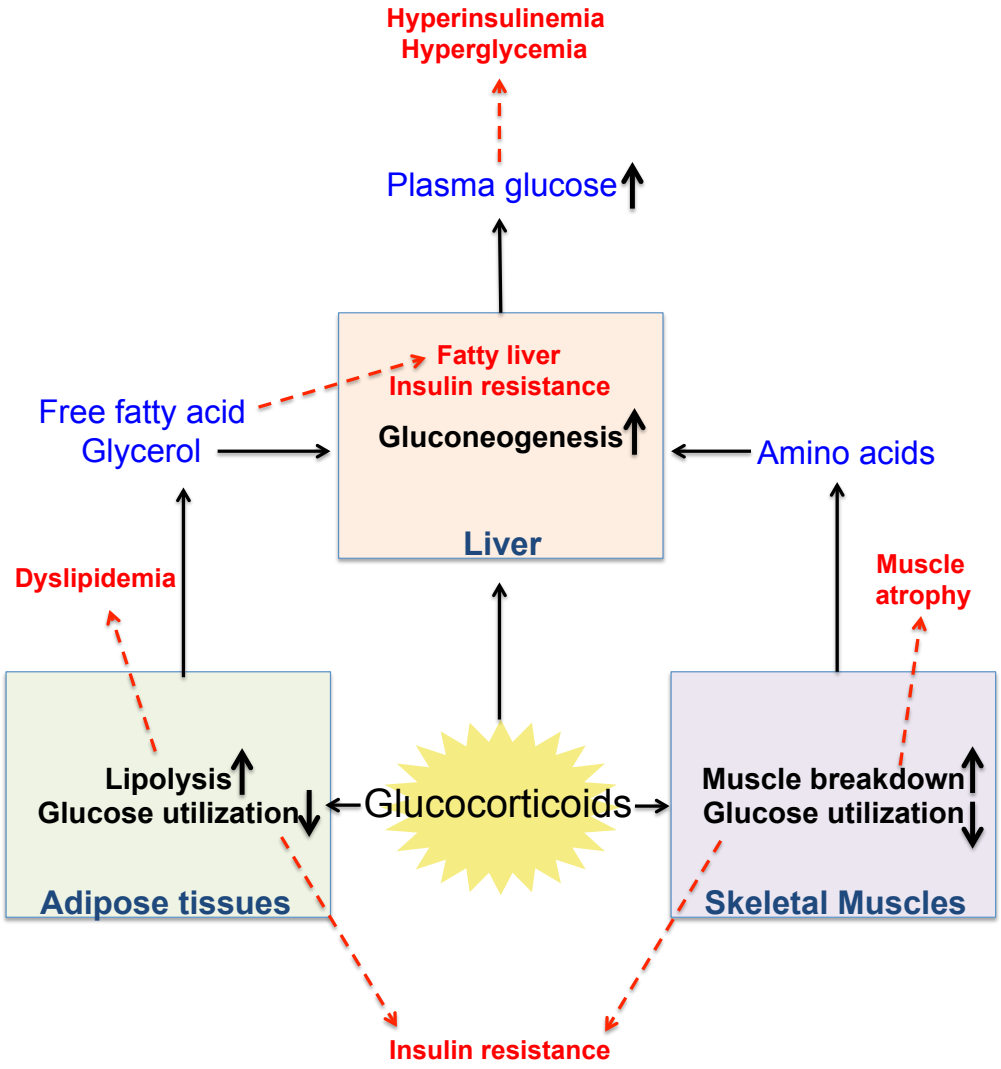

Figure 3. Impact of glucocorticoids on physiology and potential adverse effects.

Regular metabolic adaptation in lipid and glucose metabolisms mediated by GC are shown with blood arrows in three tissues including adipose tissues, skeletal muscles and liver. Read arrows shows the potential adverse effects of prolong or excess GC exposure.

IV-1. Glucocorticoids and lipid metabolism disorders

By inducing lipolysis, excess or chronic GC exposure mobilizes fat from adipose tissues into other peripheral tissues leading to pathological outcomes such as dyslipidemia (high amount of TAG in blood), fatty liver, and hepatic steatosis.

Besides dyslipidemia, fatty liver, and hepatic steatosis, GC induced lipolysis may also play a role in GC induced insulin resistance. A strong association of insulin resistance and high circulating free fatty acid levels has been demonstrated in both animals and humans. A recent review demonstrates that infusion of free fatty acids induces insulin resistance in human subjects [116]. Inhibiting lipolysis by Acipimox is found to improve GC induced insulin resistance in healthy humans [117]. In obese diabetic and non-diabetic subjects, giving Acipimox to suppress lipolysis also improves resistance by enhancing insulin stimulated glucose uptake in peripheral tissues [118]. One hypothesis to explain the function of lipolysis in GC induced insulin resistance is that the released lipid metabolites from lipolysis may work as signaling molecules to impact whole body metabolism. Two of the lipid mediators that are found to serve this function are DAG and ceramide [119].

In rodent systems, GC treatment is found to increase the ceramide level in liver and circulatory system. Suppressing ceramide synthesis by Myriocin significantly improves glucose intolerance and reverses insulin resistance in GC treated or obese rodents [120, 121]. An increasing number of studies have demonstrated that ceramide is involved in the development of insulin resistance [122-124]. At the molecular level, ceramide is found to reduce Akt phosphorylation by activating phosphatase, which de-phosphorylate phosphor-Akt or activating PKCζ, which phosphorylate Akt on another residue to suppress normal Akt phosphorylation for activation [125, 126]. GC treatment may elevate ceramide production by increasing the supply of ceramide synthesis precursors from adipocyte lipolysis and inducing the expression of genes involved in ceramide synthesis. Hepatic expression of serine palmitoyltransferase isoform2 (SPT2) and ceramide synthase 1 (Cers1) is found to be induced by GC treatment [120]. However, the comprehensive mechanism for how GC induce insulin resistance via inducing adipocyte lipolysis is still not fully understood.

GC are mostly studied for their lipolytic effect. Many downstream adverse effects are also partially resulted from this lipolytic effect. However, long-term excess exposure is also linked to increased adiposity. Patients with Cushing's syndrome or under corticosteroid treatment showed decreased muscle weight and bone mass, increased weight gain and visceral adiposity, with increased risk of developing type II diabetes [127-130]. In rodents, there is also evidence showing GC may have anabolic effects to increase the adipose mass as reported in humans [71, 131]. Over expression of 11β-HSD1 in adipose tissues to increase GC action also showed increased fat accumulation in visceral fat depots. This observation indicated that GC may have a direct impact to induce these anabolic effects [132, 133]. Though the mechanism by which the GC switches between the catabolic effect (to increase lipolysis) and anabolic effect (to increase adiposity) to regulate fat contents is not well understood, the anabolic effects

induced by GC is believed to be mediated by several factors. First of all, the GC tend to increase feeding [134] and causes humans and rodents favor high-caloric foods [135, 136]. Secondly, GC may increase fatty acid availability by increasing the lipoprotien lipase activity in omental fat [137]. Thirdly, GC are known to increase the amount of mature adipocytes by promoting the differentiation of adipose stream cells, preadipocytes, into mature adipocytes [138]. Forth, Dex, a synthetic GC, is shown to enhance insulin promoted lipogenesis [139]. Last but not least, the local expression level of 11β-HSD1 is reported to be higher in visceral fat depots compared to subcutaneous fat depots. This suggests that GC may have a greater impact in visceral fat depots. This observation also partially explains the differential physiological consequences of GC treatment in these two fat depots [140-142].

In total, acute and high dose GC treatment tends to induce GC mediated lipolysis. However, prolonged low dose GC treatment tends to eventually increase visceral adiposity. Though the mechanism in these observations is still unclear, in terms of the lipid metabolism, this dissertation will mainly focus on the former.

IV-2. Glucocorticoids and glucose metabolism disorders

Due to its critical role in regulating glucose homeostasis, excess or chronic GC exposure usually disrupts glucose metabolism. Patients with GC commonly develop hyperglycemia, a status of high blood glucose level, resulting from increased hepatic gluconeogenesis and decreased peripheral glucose utilization [143]. By counteracting insulin actions, GC also contribute to glucose intolerance and insulin resistance [144]. Many recent studies have examined the molecular mechanism of GC induced insulin resistance in a tissue specific manner *in vitro* and *in vivo*. In skeletal muscle, GC decrease expression of IRS-1 and increase expression of protein tyrosine phosphatase type 1 B (PTP1B) which counteracts insulin actions [145]. Using mouse C2C12 myotubes as a model system, Pik3r1 is found to mediate GC mediated insulin resistance. *Pik3r1*, also known as *p85α*, encodes a regulatory subunit of PI3 kinase which is a key player in insulin signaling. PI3 kinase is composed of p110, the catalytic subunit, and Pik3r1. To transduce the signal, PI3 kinase is first recruited to plasma membrane via the interaction between SRC homology 2 (SH2) domain of Pik3r1 and IRS-1 on the membrane. Then, the p110 catalyzes the reaction to phosphorylate phosatidylinositol 4,5-bisphosphate (PIP_2) to phosphatidylinositol 3,4,5-triphosphate (PIP_3) [146, 147] which anchors Akt protein kinase to plasma membrane for insulin signaling. [146] In C2C12 myotubes, Pik3r1 is found to be a potential GC primary target gene. Its expression can be up-regulated by GC treatment [148]. Although Pik3r1 is a key component of PI3 kinase, overexpression of monomeric Pik3r1 is found to suppress insulin signaling by competing with Pik3r1/p110 heterodimer (functional PI3 kinase) to the interaction with IRS-1. In this case, overexpression of Pik3r1 suppresses insulin signaling and induces insulin resistance [149, 150]. In agreement, reduction of Pik3r1 expression in C2C12 myotubes is sufficient to reduce GC induced insulin resistance [148]. Pik3r1 heterozygous mice have improved whole body insulin sensitivity [151,

152]. Additionally, patients with insulin resistance are found to have higher Pik3r1 expression [153].

Elevated blood glucose levels result in GC induced hyperglycemia and insulin resistance will also signal pancreatic beta cells to secrete more insulin leading to another pathological outcome known as hyperinsulinemia. Due to insulin resistance, the elevated insulin won't be able to induce skeletal muscle or adipose tissues to uptake glucose. Eventually, GC will lead to beta cell hyperplasia, beta cell exhaustion and beta cell dysfunction leading to the development of type II diabetes [154-156].

V. The goal of this dissertation

The goal of this dissertation is to study and expend our understanding of mechanisms for GC induced metabolic disorders. Here, we focus on two GC primary target genes: *Angptl4* and *Pik3r1. Angptl4* and *Pik3r1* are found to be strong GC primary target genes in both C2C12 myotubes and 3T3-L1 adipocytes, These two genes are further examined in this dissertation to study their roles in GC induced physiological/metabolic changes and insulin resistance *in vivo*.

Previously, our lab has found that the GC induced lipolysis is impaired in *Angptl4* null mice. In Chapter I, we hypothesize that Angptl4 by regulating lipolysis may also work to affect the release of insulin resistance associated lipid mediators and contribute to GC induced insulin resistance. We test this hypothesis by performing a lipidomics screening. In this study, we identify a Glucocorticoids-Angiopoietin-like 4- ceramide axis as a mechanism for GC induced hepatic insulin resistance.

In Chapter II, the adipose tissue specific *Pik3r1* knockout (AKO) mice were generated to study the function of Pik3r1 in GC regulated lipid metabolic homeostasis. AKO mice show impaired GC-induced-lipolysis under dexamethasone (Dex, a synthetic glucocorticoid) treatment. As a consequence, with less lipolysis, AKO mice show reduced fatty liver and dyslipidemia compared to wild type mice. In this chapter, we study and identify a potential mechanism that contributes to these phenotypes.

Pik3r1 is also found to mediate GC induced insulin resistance in C2C12 myotubes. In the Chpater III, we further examine this observation in the animal system. First of all, the molecular mechanism for GC induced transactivation of Pik3r1 is studied in mouse gastrocnemius muscle. Next, the muscle specific Pik3r1 knockout (MKO) mouse system is established to test if Pik3r1 is involved in GC induced insulin resistance *in vivo*.

In total, I hope this dissertation has extended our understanding of GC induced metabolic alterations that could further help us to identify specific ways to reduce GC associated adverse metabolic effects and improve the therapeutic use of GC.

References

[1] T. G. Benedek, "History of the development of corticosteroid therapy," *Clin Exp Rheumatol,* vol. 29, pp. S-5-12, Sep-Oct 2011.

[2] A. Vegiopoulos and S. Herzig, "Glucocorticoids, metabolism and metabolic diseases," *Mol Cell Endocrinol,* vol. 275, pp. 43-61, Sep 15 2007.

[3] S. C. Biddie, B. L. Conway-Campbell, and S. L. Lightman, "Dynamic regulation of glucocorticoid signalling in health and disease," *Rheumatology (Oxford),* vol. 51, pp. 403-12, Mar 2012.

[4] A. R. Clark and M. G. Belvisi, "Maps and legends: the quest for dissociated ligands of the glucocorticoid receptor," *Pharmacol Ther,* vol. 134, pp. 54-67, Apr 2012.

[5] C. Stahn and F. Buttgereit, "Genomic and nongenomic effects of glucocorticoids," *Nat Clin Pract Rheumatol,* vol. 4, pp. 525-33, Oct 2008.

[6] W. B. Pratt and D. O. Toft, "Steroid receptor interactions with heat shock protein and immunophilin chaperones," *Endocr Rev,* vol. 18, pp. 306-60, Jun 1997.

[7] Y. Morishima, K. C. Kanelakis, P. J. Murphy, E. R. Lowe, G. J. Jenkins, Y. Osawa*, et al.*, "The hsp90 cochaperone p23 is the limiting component of the multiprotein hsp90/hsp70-based chaperone system in vivo where it acts to stabilize the client protein: hsp90 complex," *J Biol Chem,* vol. 278, pp. 48754-63, Dec 5 2003.

[8] W. B. Pratt and D. O. Toft, "Regulation of signaling protein function and trafficking by the hsp90/hsp70-based chaperone machinery," *Exp Biol Med (Maywood),* vol. 228, pp. 111-33, Feb 2003.

[9] S. P. Umland, R. P. Schleimer, and S. L. Johnston, "Review of the molecular and cellular mechanisms of action of glucocorticoids for use in asthma," *Pulm Pharmacol Ther,* vol. 15, pp. 35-50, 2002.

[10] R. Chodankar, D. Y. Wu, B. J. Schiller, K. R. Yamamoto, and M. R. Stallcup, "Hic-5 is a transcription coregulator that acts before and/or after glucocorticoid receptor genome occupancy in a gene-selective manner," *Proc Natl Acad Sci U S A,* vol. 111, pp. 4007-12, Mar 18 2014.

[11] U. Strahle, G. Klock, and G. Schutz, "A DNA sequence of 15 base pairs is sufficient to mediate both glucocorticoid and progesterone induction of gene expression," *Proc Natl Acad Sci U S A,* vol. 84, pp. 7871-5, Nov 1987.

[12] M. J. Tsai and B. W. O'Malley, "Molecular mechanisms of action of steroid/thyroid receptor superfamily members," *Annu Rev Biochem,* vol. 63, pp. 451-86, 1994.

[13] S. Kadauke and G. A. Blobel, "Chromatin loops in gene regulation," *Biochim Biophys Acta,* vol. 1789, pp. 17-25, Jan 2009.

[14] T. Sexton, F. Bantignies, and G. Cavalli, "Genomic interactions: chromatin loops and gene meeting points in transcriptional regulation," *Semin Cell Dev Biol,* vol. 20, pp. 849-55, Sep 2009.

[15] D. M. Faust, A. M. Catherin, S. Barbaux, L. Belkadi, T. Imaizumi-Scherrer, and M. C. Weiss, "The activity of the highly inducible mouse phenylalanine hydroxylase gene promoter is dependent upon a tissue-specific, hormone-inducible enhancer," *Mol Cell Biol,* vol. 16, pp. 3125-37, Jun 1996.

[16] A. Bristeau, A. M. Catherin, M. C. Weiss, and D. M. Faust, "Hormone response of rodent phenylalanine hydroxylase requires HNF1 and the glucocorticoid receptor," *Biochem Biophys Res Commun,* vol. 287, pp. 852-8, Oct 5 2001.

[17] B. J. Schiller, R. Chodankar, L. C. Watson, M. R. Stallcup, and K. R. Yamamoto, "Glucocorticoid receptor binds half sites as a monomer and regulates specific target genes," *Genome Biol,* vol. 15, p. 418, 2014.

[18] D. J. Rozansky, H. Wu, K. Tang, R. J. Parmer, and D. T. O'Connor, "Glucocorticoid activation of chromogranin A gene expression. Identification and characterization of a novel glucocorticoid response element," *J Clin Invest,* vol. 94, pp. 2357-68, Dec 1994.

[19] T. Sugiyama, D. K. Scott, J. C. Wang, and D. K. Granner, "Structural requirements of the glucocorticoid and retinoic acid response units in the phosphoenolpyruvate carboxykinase gene promoter," *Mol Endocrinol,* vol. 12, pp. 1487-98, Oct 1998.

[20] A. A. Heinrichs, R. Bortell, S. Rahman, J. L. Stein, E. S. Alnemri, G. Litwack*, et al.*, "Identification of multiple glucocorticoid receptor binding sites in the rat osteocalcin gene promoter," *Biochemistry,* vol. 32, pp. 11436-44, Oct 26 1993.

[21] C. Goi, P. Little, and C. Xie, "Cell-type and transcription factor specific enrichment of transcriptional cofactor motifs in ENCODE ChIP-seq data," *BMC Genomics,* vol. 14 Suppl 5, p. S2, 2013.

[22] V. Perissi and M. G. Rosenfeld, "Controlling nuclear receptors: the circular logic of cofactor cycles," *Nat Rev Mol Cell Biol,* vol. 6, pp. 542-54, Jul 2005.

[23] E. M. McInerney, D. W. Rose, S. E. Flynn, S. Westin, T. M. Mullen, A. Krones*, et al.*, "Determinants of coactivator LXXLL motif specificity in nuclear receptor transcriptional activation," *Genes Dev,* vol. 12, pp. 3357-68, Nov 1 1998.

[24] S. A. Onate, S. Y. Tsai, M. J. Tsai, and B. W. O'Malley, "Sequence and characterization of a coactivator for the steroid hormone receptor superfamily," *Science,* vol. 270, pp. 1354-7, Nov 24 1995.

[25] H. Hong, K. Kohli, A. Trivedi, D. L. Johnson, and M. R. Stallcup, "GRIP1, a novel mouse protein that serves as a transcriptional coactivator in yeast for the hormone binding domains of steroid receptors," *Proc Natl Acad Sci U S A,* vol. 93, pp. 4948-52, May 14 1996.

[26] J. J. Voegel, M. J. Heine, C. Zechel, P. Chambon, and H. Gronemeyer, "TIF2, a 160 kDa transcriptional mediator for the ligand-dependent activation function AF-2 of nuclear receptors," *EMBO J,* vol. 15, pp. 3667-75, Jul 15 1996.

[27] T. P. Yao, G. Ku, N. Zhou, R. Scully, and D. M. Livingston, "The nuclear hormone receptor coactivator SRC-1 is a specific target of p300," *Proc Natl Acad Sci U S A,* vol. 93, pp. 10626-31, Oct 1 1996.

[28] S. L. Anzick, J. Kononen, R. L. Walker, D. O. Azorsa, M. M. Tanner, X. Y. Guan*, et al.*, "AIB1, a steroid receptor coactivator amplified in breast and ovarian cancer," *Science,* vol. 277, pp. 965-8, Aug 15 1997.

[29] H. Chen, R. J. Lin, R. L. Schiltz, D. Chakravarti, A. Nash, L. Nagy*, et al.*, "Nuclear receptor coactivator ACTR is a novel histone acetyltransferase and forms a multimeric activation complex with P/CAF and CBP/p300," *Cell,* vol. 90, pp. 569-80, Aug 8 1997.

[30] H. Li, P. J. Gomes, and J. D. Chen, "RAC3, a steroid/nuclear receptor-associated coactivator that is related to SRC-1 and TIF2," *Proc Natl Acad Sci U S A,* vol. 94, pp. 8479-84, Aug 5 1997.

[31] J. Torchia, D. W. Rose, J. Inostroza, Y. Kamei, S. Westin, C. K. Glass*, et al.*, "The transcriptional co-activator p/CIP binds CBP and mediates nuclear-receptor function," *Nature,* vol. 387, pp. 677-84, Jun 12 1997.

[32] D. M. Lonard and W. O'Malley B, "Nuclear receptor coregulators: judges, juries, and executioners of cellular regulation," *Mol Cell,* vol. 27, pp. 691-700, Sep 7 2007.

[33] B. D. Darimont, R. L. Wagner, J. W. Apriletti, M. R. Stallcup, P. J. Kushner, J. D. Baxter*, et al.*, "Structure and specificity of nuclear receptor-coactivator interactions," *Genes Dev,* vol. 12, pp. 3343-56, Nov 1 1998.

[34] X. F. Ding, C. M. Anderson, H. Ma, H. Hong, R. M. Uht, P. J. Kushner*, et al.*, "Nuclear receptor-binding sites of coactivators glucocorticoid receptor interacting protein 1 (GRIP1) and steroid receptor coactivator 1 (SRC-1): multiple motifs with different binding specificities," *Mol Endocrinol,* vol. 12, pp. 302-13, Feb 1998.

[35] E. Kalkhoven, J. E. Valentine, D. M. Heery, and M. G. Parker, "Isoforms of steroid receptor co-activator 1 differ in their ability to potentiate transcription by the oestrogen receptor," *EMBO J,* vol. 17, pp. 232-43, Jan 2 1998.

[36] I. Rogatsky, H. F. Luecke, D. C. Leitman, and K. R. Yamamoto, "Alternate surfaces of transcriptional coregulator GRIP1 function in different glucocorticoid receptor activation and repression contexts," *Proc Natl Acad Sci U S A,* vol. 99, pp. 16701-6, Dec 24 2002.

[37] Y. Chinenov, R. Gupte, J. Dobrovolna, J. R. Flammer, B. Liu, F. E. Michelassi*, et al.*, "Role of transcriptional coregulator GRIP1 in the anti-inflammatory actions of glucocorticoids," *Proc Natl Acad Sci U S A,* vol. 109, pp. 11776-81, Jul 17 2012.

[38] H. M. Chan and N. B. La Thangue, "p300/CBP proteins: HATs for transcriptional bridges and scaffolds," *J Cell Sci,* vol. 114, pp. 2363-73, Jul 2001.

[39] W. Xu, H. Chen, K. Du, H. Asahara, M. Tini, B. M. Emerson*, et al.*, "A transcriptional switch mediated by cofactor methylation," *Science,* vol. 294, pp. 2507-11, Dec 21 2001.

[40] J. H. Kim and M. R. Stallcup, "Role of the coiled-coil coactivator (CoCoA) in aryl hydrocarbon receptor-mediated transcription," *J Biol Chem,* vol. 279, pp. 49842-8, Nov 26 2004.

[41] J. H. Kim, C. K. Yang, and M. R. Stallcup, "Downstream signaling mechanism of the C-terminal activation domain of transcriptional coactivator CoCoA," *Nucleic Acids Res,* vol. 34, pp. 2736-50, 2006.

[42] J. H. Kim, C. K. Yang, K. Heo, R. G. Roeder, W. An, and M. R. Stallcup, "CCAR1, a key regulator of mediator complex recruitment to nuclear receptor transcription complexes," *Mol Cell,* vol. 31, pp. 510-9, Aug 22 2008.

[43] D. Y. Lee, J. P. Northrop, M. H. Kuo, and M. R. Stallcup, "Histone H3 lysine 9 methyltransferase G9a is a transcriptional coactivator for nuclear receptors," *J Biol Chem,* vol. 281, pp. 8476-85, Mar 31 2006.

[44] Y. H. Chen, J. H. Kim, and M. R. Stallcup, "GAC63, a GRIP1-dependent nuclear receptor coactivator," *Mol Cell Biol,* vol. 25, pp. 5965-72, Jul 2005.

[45] Y. H. Lee, H. D. Campbell, and M. R. Stallcup, "Developmentally essential protein flightless I is a nuclear receptor coactivator with actin binding activity," *Mol Cell Biol,* vol. 24, pp. 2103-17, Mar 2004.

[46] A. B. Hittelman, D. Burakov, J. A. Iniguez-Lluhi, L. P. Freedman, and M. J. Garabedian, "Differential regulation of glucocorticoid receptor transcriptional activation via AF-1-associated proteins," *EMBO J,* vol. 18, pp. 5380-8, Oct 1 1999.

[47] B. L. Allen and D. J. Taatjes, "The Mediator complex: a central integrator of transcription," *Nat Rev Mol Cell Biol,* vol. 16, pp. 155-66, Mar 2015.

[48] S. Sato, C. Tomomori-Sato, T. J. Parmely, L. Florens, B. Zybailov, S. K. Swanson*, et al.*, "A set of consensus mammalian mediator subunits identified by multidimensional protein identification technology," *Mol Cell,* vol. 14, pp. 685-91, Jun 4 2004.

[49] P. Sudarsanam and F. Winston, "The Swi/Snf family nucleosome-remodeling complexes and transcriptional control," *Trends Genet,* vol. 16, pp. 345-51, Aug 2000.

[50] L. Tang, E. Nogales, and C. Ciferri, "Structure and function of SWI/SNF chromatin remodeling complexes and mechanistic implications for transcription," *Prog Biophys Mol Biol,* vol. 102, pp. 122-8, Jun-Jul 2010.

[51] W. Wang, J. Cote, Y. Xue, S. Zhou, P. A. Khavari, S. R. Biggar*, et al.*, "Purification and biochemical heterogeneity of the mammalian SWI-SNF complex," *EMBO J,* vol. 15, pp. 5370-82, Oct 1 1996.

[52] W. Wang, Y. Xue, S. Zhou, A. Kuo, B. R. Cairns, and G. R. Crabtree, "Diversity and specialization of mammalian SWI/SNF complexes," *Genes Dev,* vol. 10, pp. 2117-30, Sep 1 1996.

[53] R. Aasland, A. F. Stewart, and T. Gibson, "The SANT domain: a putative DNA-binding domain in the SWI-SNF and ADA complexes, the transcriptional co-repressor N-CoR and TFIIIB," *Trends Biochem Sci,* vol. 21, pp. 87-8, Mar 1996.

[54] L. Aravind and L. M. Iyer, "The SWIRM domain: a conserved module found in chromosomal proteins points to novel chromatin-modifying activities," *Genome Biol,* vol. 3, p. RESEARCH0039, Jul 24 2002.

[55] L. A. Boyer, R. R. Latek, and C. L. Peterson, "The SANT domain: a unique histone-tail-binding module?," *Nat Rev Mol Cell Biol,* vol. 5, pp. 158-63, Feb 2004.

[56] K. A. Link, C. J. Burd, E. Williams, T. Marshall, G. Rosson, E. Henry*, et al.*, "BAF57 governs androgen receptor action and androgen-dependent proliferation through SWI/SNF," *Mol Cell Biol,* vol. 25, pp. 2200-15, Mar 2005.

[57] J. Chen and T. K. Archer, "Regulating SWI/SNF subunit levels via protein-protein interactions and proteasomal degradation: BAF155 and BAF170 limit expression of BAF57," *Mol Cell Biol,* vol. 25, pp. 9016-27, Oct 2005.

[58] A. Saha, J. Wittmeyer, and B. R. Cairns, "Chromatin remodelling: the industrial revolution of DNA around histones," *Nat Rev Mol Cell Biol,* vol. 7, pp. 437-47, Jun 2006.

[59] D. G. Grier and H. L. Halliday, "Effects of glucocorticoids on fetal and neonatal lung development," *Treat Respir Med,* vol. 3, pp. 295-306, 2004.

[60] J. M. Abbinante-Nissen, L. G. Simpson, and G. D. Leikauf, "Corticosteroids increase secretory leukocyte protease inhibitor transcript levels in airway epithelial cells," *Am J Physiol,* vol. 268, pp. L601-6, Apr 1995.

[61] M. Lasa, S. M. Abraham, C. Boucheron, J. Saklatvala, and A. R. Clark, "Dexamethasone causes sustained expression of mitogen-activated protein kinase (MAPK) phosphatase 1 and phosphatase-mediated inhibition of MAPK p38," *Mol Cell Biol,* vol. 22, pp. 7802-11, Nov 2002.

[62] A. Ray, K. E. Prefontaine, and P. Ray, "Down-modulation of interleukin-6 gene expression by 17 beta-estradiol in the absence of high affinity DNA binding by the estrogen receptor," *J Biol Chem,* vol. 269, pp. 12940-6, Apr 29 1994.

[63] S. Heck, M. Kullmann, A. Gast, H. Ponta, H. J. Rahmsdorf, P. Herrlich*, et al.*, "A distinct modulating domain in glucocorticoid receptor monomers in the repression of activity of the transcription factor AP-1," *EMBO J,* vol. 13, pp. 4087-95, Sep 1 1994.

[64] K. De Bosscher, W. Vanden Berghe, and G. Haegeman, "The interplay between the glucocorticoid receptor and nuclear factor-kappaB or activator protein-1: molecular mechanisms for gene repression," *Endocr Rev,* vol. 24, pp. 488-522, Aug 2003.

[65] J. A. Cidlowski, K. L. King, R. B. Evans-Storms, J. W. Montague, C. D. Bortner, and F. M. Hughes, Jr., "The biochemistry and molecular biology of glucocorticoid-induced apoptosis in the immune system," *Recent Prog Horm Res,* vol. 51, pp. 457-90; discussion 490-1, 1996.

[66] M. J. Herold, K. G. McPherson, and H. M. Reichardt, "Glucocorticoids in T cell apoptosis and function," *Cell Mol Life Sci,* vol. 63, pp. 60-72, Jan 2006.

[67] J. C. Wang, N. E. Gray, T. Kuo, and C. A. Harris, "Regulation of triglyceride metabolism by glucocorticoid receptor," *Cell Biosci,* vol. 2, p. 19, 2012.

[68] D. P. Macfarlane, S. Forbes, and B. R. Walker, "Glucocorticoids and fatty acid metabolism in humans: fuelling fat redistribution in the metabolic syndrome," *J Endocrinol,* vol. 197, pp. 189-204, May 2008.

[69] J. N. Fain, A. Dodd, and L. Novak, "Enzyme regulation in gluconeogenesis and lipogenesis. Relationship of protein synthesis and cyclic AMP to lipolytic action of growth hormone and glucocorticoids," *Metabolism,* vol. 20, pp. 109-18, Feb 1971.

[70] T. Rhen and J. A. Cidlowski, "Antiinflammatory action of glucocorticoids--new mechanisms for old drugs," *N Engl J Med,* vol. 353, pp. 1711-23, Oct 20 2005.

[71] J. E. Campbell, A. J. Peckett, M. D'Souza A, T. J. Hawke, and M. C. Riddell, "Adipogenic and lipolytic effects of chronic glucocorticoid exposure," *Am J Physiol Cell Physiol,* vol. 300, pp. C198-209, Jan 2011.

[72] A. J. Peckett, D. C. Wright, and M. C. Riddell, "The effects of glucocorticoids on adipose tissue lipid metabolism," *Metabolism,* vol. 60, pp. 1500-10, Nov 2011.

[73] C. Y. Yu, O. Mayba, J. V. Lee, J. Tran, C. Harris, T. P. Speed*, et al.*, "Genome-wide analysis of glucocorticoid receptor binding regions in adipocytes reveal gene network involved in triglyceride homeostasis," *PLoS One,* vol. 5, p. e15188, 2010.

[74] J. A. Villena, S. Roy, E. Sarkadi-Nagy, K. H. Kim, and H. S. Sul, "Desnutrin, an adipocyte gene encoding a novel patatin domain-containing protein, is induced by fasting and glucocorticoids: ectopic expression of desnutrin increases triglyceride hydrolysis," *J Biol Chem,* vol. 279, pp. 47066-75, Nov 5 2004.

[75] J. N. Fain and R. Saperstein, "The involvement of RNA synthesis and cyclic AMP in the activation of fat cell lipolysis by growth hormone and glucocorticoids," *Horm Metab Res,* vol. 2, pp. Suppl 2:20-7, 1970.

[76] B. G. Slavin, J. M. Ong, and P. A. Kern, "Hormonal regulation of hormone-sensitive lipase activity and mRNA levels in isolated rat adipocytes," *J Lipid Res,* vol. 35, pp. 1535-41, Sep 1994.

[77] J. Zhou and J. A. Cidlowski, "The human glucocorticoid receptor: one gene, multiple proteins and diverse responses," *Steroids,* vol. 70, pp. 407-17, May-Jun 2005.

[78] S. Martin, S. Okano, C. Kistler, M. A. Fernandez-Rojo, M. M. Hill, and R. G. Parton, "Spatiotemporal regulation of early lipolytic signaling in adipocytes," *J Biol Chem,* vol. 284, pp. 32097-107, Nov 13 2009.

[79] J. T. Tansey, C. Sztalryd, E. M. Hlavin, A. R. Kimmel, and C. Londos, "The central role of perilipin a in lipid metabolism and adipocyte lipolysis," *IUBMB Life,* vol. 56, pp. 379-85, Jul 2004.

[80] W. J. Shen, S. Patel, H. Miyoshi, A. S. Greenberg, and F. B. Kraemer, "Functional interaction of hormone-sensitive lipase and perilipin in lipolysis," *J Lipid Res,* vol. 50, pp. 2306-13, Nov 2009.

[81] T. Yamaguchi, N. Omatsu, E. Morimoto, H. Nakashima, K. Ueno, T. Tanaka*, et al.*, "CGI-58 facilitates lipolysis on lipid droplets but is not involved in the vesiculation of lipid droplets caused by hormonal stimulation," *J Lipid Res,* vol. 48, pp. 1078-89, May 2007.

[82] A. Gruber, I. Cornaciu, A. Lass, M. Schweiger, M. Poeschl, C. Eder*, et al.*, "The N-terminal region of comparative gene identification-58 (CGI-58) is important for lipid droplet binding and activation of adipose triglyceride lipase," *J Biol Chem,* vol. 285, pp. 12289-98, Apr 16 2010.

[83] V. C. Manganiello, E. Degerman, M. Taira, T. Kono, and P. Belfrage, "Type III cyclic nucleotide phosphodiesterases and insulin action," *Curr Top Cell Regul,* vol. 34, pp. 63-100, 1996.

[84] T. Kitamura, Y. Kitamura, S. Kuroda, Y. Hino, M. Ando, K. Kotani*, et al.*, "Insulin-induced phosphorylation and activation of cyclic nucleotide phosphodiesterase 3B by the serine-threonine kinase Akt," *Mol Cell Biol,* vol. 19, pp. 6286-96, Sep 1999.

[85] S. M. Choi, D. F. Tucker, D. N. Gross, R. M. Easton, L. M. DiPilato, A. S. Dean*, et al.*, "Insulin regulates adipocyte lipolysis via an Akt-independent signaling pathway," *Mol Cell Biol,* vol. 30, pp. 5009-20, Nov 2010.

[86] S. K. Koliwad, T. Kuo, L. E. Shipp, N. E. Gray, F. Backhed, A. Y. So*, et al.*, "Angiopoietin-like 4 (ANGPTL4, fasting-induced adipose factor) is a direct glucocorticoid receptor target and participates in glucocorticoid-regulated triglyceride metabolism," *J Biol Chem,* vol. 284, pp. 25593-601, Sep 18 2009.

[87] L. Shan, X. C. Yu, Z. Liu, Y. Hu, L. T. Sturgis, M. L. Miranda*, et al.*, "The angiopoietin-like proteins ANGPTL3 and ANGPTL4 inhibit lipoprotein lipase activity through distinct mechanisms," *J Biol Chem,* vol. 284, pp. 1419-24, Jan 16 2009.

[88] N. E. Gray, L. N. Lam, K. Yang, A. Y. Zhou, S. Koliwad, and J. C. Wang, "Angiopoietin-like 4 (Angptl4) protein is a physiological mediator of intracellular lipolysis in murine adipocytes," *J Biol Chem,* vol. 287, pp. 8444-56, Mar 9 2012.

[89] F. Mattijssen and S. Kersten, "Regulation of triglyceride metabolism by Angiopoietin-like proteins," *Biochim Biophys Acta,* vol. 1821, pp. 782-9, May 2012.

[90] S. Jitrapakdee and J. C. Wallace, "Structure, function and regulation of pyruvate carboxylase," *Biochem J,* vol. 340 (Pt 1), pp. 1-16, May 15 1999.

[91] A. L. Menefee and T. N. Zeczycki, "Nearly 50 years in the making: defining the catalytic mechanism of the multifunctional enzyme, pyruvate carboxylase," *FEBS J,* vol. 281, pp. 1333-54, Mar 2014.

[92] R. W. Hanson and A. J. Garber, "Phosphoenolpyruvate carboxykinase. I. Its role in gluconeogenesis," *Am J Clin Nutr,* vol. 25, pp. 1010-21, Oct 1972.

[93] R. W. Hanson and Y. M. Patel, "Phosphoenolpyruvate carboxykinase (GTP): the gene and the enzyme," *Adv Enzymol Relat Areas Mol Biol,* vol. 69, pp. 203-81, 1994.

[94] F. Marcus, J. Rittenhouse, B. Gontero, and P. B. Harrsch, "Function, structure and evolution of fructose-1,6-bisphosphatase," *Arch Biol Med Exp (Santiago),* vol. 20, pp. 371-8, 1987.

[95] A. Burchell and I. D. Waddell, "The molecular basis of the hepatic microsomal glucose-6-phosphatase system," *Biochim Biophys Acta,* vol. 1092, pp. 129-37, Apr 17 1991.

[96] E. van Schaftingen and I. Gerin, "The glucose-6-phosphatase system," *Biochem J,* vol. 362, pp. 513-32, Mar 15 2002.

[97] J. C. Hutton and R. M. O'Brien, "Glucose-6-phosphatase catalytic subunit gene family," *J Biol Chem,* vol. 284, pp. 29241-5, Oct 23 2009.

[98] J. H. Exton, L. E. Mallette, L. S. Jefferson, E. H. Wong, N. Friedmann, T. B. Miller, Jr*., et al.*, "The hormonal control of hepatic gluconeogenesis," *Recent Prog Horm Res,* vol. 26, pp. 411-61, 1970.

[99] R. K. Menon and M. A. Sperling, "Carbohydrate metabolism," *Semin Perinatol,* vol. 12, pp. 157-62, Apr 1988.

[100] E. Imai, P. E. Stromstedt, P. G. Quinn, J. Carlstedt-Duke, J. A. Gustafsson, and D. K. Granner, "Characterization of a complex glucocorticoid response unit in the phosphoenolpyruvate carboxykinase gene," *Mol Cell Biol,* vol. 10, pp. 4712-9, Sep 1990.

[101] D. K. Scott, P. E. Stromstedt, J. C. Wang, and D. K. Granner, "Further characterization of the glucocorticoid response unit in the phosphoenolpyruvate carboxykinase gene. The role of the glucocorticoid receptor-binding sites," *Mol Endocrinol,* vol. 12, pp. 482-91, Apr 1998.

[102] B. T. Schurter, S. S. Koh, D. Chen, G. J. Bunick, J. M. Harp, B. L. Hanson*, et al.*, "Methylation of histone H3 by coactivator-associated arginine methyltransferase 1," *Biochemistry,* vol. 40, pp. 5747-56, May 15 2001.

[103] D. Y. Lee, C. Teyssier, B. D. Strahl, and M. R. Stallcup, "Role of protein methylation in regulation of transcription," *Endocr Rev,* vol. 26, pp. 147-70, Apr 2005.

[104] R. K. Hall, X. L. Wang, L. George, S. R. Koch, and D. K. Granner, "Insulin represses phosphoenolpyruvate carboxykinase gene transcription by causing the rapid disruption

of an active transcription complex: a potential epigenetic effect," *Mol Endocrinol,* vol. 21, pp. 550-63, Feb 2007.

[105] B. T. Vander Kooi, H. Onuma, J. K. Oeser, C. A. Svitek, S. R. Allen, C. W. Vander Kooi*, et al.*, "The glucose-6-phosphatase catalytic subunit gene promoter contains both positive and negative glucocorticoid response elements," *Mol Endocrinol,* vol. 19, pp. 3001-22, Dec 2005.

[106] H. Onuma, B. T. Vander Kooi, J. N. Boustead, J. K. Oeser, and R. M. O'Brien, "Correlation between FOXO1a (FKHR) and FOXO3a (FKHRL1) binding and the inhibition of basal glucose-6-phosphatase catalytic subunit gene transcription by insulin," *Mol Endocrinol,* vol. 20, pp. 2831-47, Nov 2006.

[107] S. B. Biddinger and C. R. Kahn, "From mice to men: insights into the insulin resistance syndromes," *Annu Rev Physiol,* vol. 68, pp. 123-58, 2006.

[108] E. Ferrannini, D. C. Simonson, L. D. Katz, G. Reichard, Jr., S. Bevilacqua, E. J. Barrett*, et al.*, "The disposal of an oral glucose load in patients with non-insulin-dependent diabetes," *Metabolism,* vol. 37, pp. 79-85, Jan 1988.

[109] R. A. DeFronzo and D. Tripathy, "Skeletal muscle insulin resistance is the primary defect in type 2 diabetes," *Diabetes Care,* vol. 32 Suppl 2, pp. S157-63, Nov 2009.

[110] S. P. Weinstein, T. Paquin, A. Pritsker, and R. S. Haber, "Glucocorticoid-induced insulin resistance: dexamethasone inhibits the activation of glucose transport in rat skeletal muscle by both insulin- and non-insulin-related stimuli," *Diabetes,* vol. 44, pp. 441-5, Apr 1995.

[111] L. Coderre, G. A. Vallega, P. F. Pilch, and S. R. Chipkin, "In vivo effects of dexamethasone and sucrose on glucose transport (GLUT-4) protein tissue distribution," *Am J Physiol,* vol. 271, pp. E643-8, Oct 1996.

[112] G. Dimitriadis, B. Leighton, M. Parry-Billings, S. Sasson, M. Young, U. Krause*, et al.*, "Effects of glucocorticoid excess on the sensitivity of glucose transport and metabolism to insulin in rat skeletal muscle," *Biochem J,* vol. 321 (Pt 3), pp. 707-12, Feb 1 1997.

[113] S. P. Weinstein, C. M. Wilson, A. Pritsker, and S. W. Cushman, "Dexamethasone inhibits insulin-stimulated recruitment of GLUT4 to the cell surface in rat skeletal muscle," *Metabolism,* vol. 47, pp. 3-6, Jan 1998.

[114] S. A. Morgan, M. Sherlock, L. L. Gathercole, G. G. Lavery, C. Lenaghan, I. J. Bujalska*, et al.*, "11beta-hydroxysteroid dehydrogenase type 1 regulates glucocorticoid-induced insulin resistance in skeletal muscle," *Diabetes,* vol. 58, pp. 2506-15, Nov 2009.

[115] M. Kadmiel and J. A. Cidlowski, "Glucocorticoid receptor signaling in health and disease," *Trends Pharmacol Sci,* vol. 34, pp. 518-30, Sep 2013.

[116] D. E. Kelley, M. Mokan, J. A. Simoneau, and L. J. Mandarino, "Interaction between glucose and free fatty acid metabolism in human skeletal muscle," *J Clin Invest,* vol. 92, pp. 91-8, Jul 1993.

[117] L. Tappy, D. Randin, P. Vollenweider, L. Vollenweider, N. Paquot, U. Scherrer*, et al.*, "Mechanisms of dexamethasone-induced insulin resistance in healthy humans," *J Clin Endocrinol Metab,* vol. 79, pp. 1063-9, Oct 1994.

[118] A. T. Santomauro, G. Boden, M. E. Silva, D. M. Rocha, R. F. Santos, M. J. Ursich*, et al.*, "Overnight lowering of free fatty acids with Acipimox improves insulin resistance and glucose tolerance in obese diabetic and nondiabetic subjects," *Diabetes,* vol. 48, pp. 1836-41, Sep 1999.

[119] D. M. Erion and G. I. Shulman, "Diacylglycerol-mediated insulin resistance," *Nat Med,* vol. 16, pp. 400-2, Apr 2010.

[120] W. L. Holland, J. T. Brozinick, L. P. Wang, E. D. Hawkins, K. M. Sargent, Y. Liu*, et al.*, "Inhibition of ceramide synthesis ameliorates glucocorticoid-, saturated-fat-, and obesity-induced insulin resistance," *Cell Metab,* vol. 5, pp. 167-79, Mar 2007.

[121] C. Schmitz-Peiffer, "Targeting ceramide synthesis to reverse insulin resistance," *Diabetes,* vol. 59, pp. 2351-3, Oct 2010.

[122] M. Straczkowski and I. Kowalska, "The role of skeletal muscle sphingolipids in the development of insulin resistance," *Rev Diabet Stud,* vol. 5, pp. 13-24, Spring 2008.

[123] S. A. Summers, "Sphingolipids and insulin resistance: the five Ws," *Curr Opin Lipidol,* vol. 21, pp. 128-35, Apr 2010.

[124] C. Lipina and H. S. Hundal, "Sphingolipids: agents provocateurs in the pathogenesis of insulin resistance," *Diabetologia,* vol. 54, pp. 1596-607, Jul 2011.

[125] R. Cazzolli, L. Carpenter, T. J. Biden, and C. Schmitz-Peiffer, "A role for protein phosphatase 2A-like activity, but not atypical protein kinase Czeta, in the inhibition of protein kinase B/Akt and glycogen synthesis by palmitate," *Diabetes,* vol. 50, pp. 2210-8, Oct 2001.

[126] E. Hajduch, S. Turban, X. Le Liepvre, S. Le Lay, C. Lipina, N. Dimopoulos*, et al.*, "Targeting of PKCzeta and PKB to caveolin-enriched microdomains represents a crucial step underpinning the disruption in PKB-directed signalling by ceramide," *Biochem J,* vol. 410, pp. 369-79, Mar 1 2008.

[127] T. C. Friedman, G. Mastorakos, T. D. Newman, N. M. Mullen, E. G. Horton, R. Costello*, et al.*, "Carbohydrate and lipid metabolism in endogenous hypercortisolism: shared features with metabolic syndrome X and NIDDM," *Endocr J,* vol. 43, pp. 645-55, Dec 1996.

[128] V. Abad, G. P. Chrousos, J. C. Reynolds, L. K. Nieman, S. C. Hill, R. S. Weinstein*, et al.*, "Glucocorticoid excess during adolescence leads to a major persistent deficit in bone mass and an increase in central body fat," *J Bone Miner Res,* vol. 16, pp. 1879-85, Oct 2001.

[129] A. K. McDonough, J. R. Curtis, and K. G. Saag, "The epidemiology of glucocorticoid-associated adverse events," *Curr Opin Rheumatol,* vol. 20, pp. 131-7, Mar 2008.

[130] P. M. Stewart and S. Petersenn, "Rationale for treatment and therapeutic options in Cushing's disease," *Best Pract Res Clin Endocrinol Metab,* vol. 23 Suppl 1, pp. S15-22, Dec 2009.

[131] J. W. Jahng, N. Y. Kim, V. Ryu, S. B. Yoo, B. T. Kim, D. W. Kang*, et al.*, "Dexamethasone reduces food intake, weight gain and the hypothalamic 5-HT concentration and increases plasma leptin in rats," *Eur J Pharmacol,* vol. 581, pp. 64-70, Feb 26 2008.

[132] H. Masuzaki, J. Paterson, H. Shinyama, N. M. Morton, J. J. Mullins, J. R. Seckl*, et al.*, "A transgenic model of visceral obesity and the metabolic syndrome," *Science,* vol. 294, pp. 2166-70, Dec 7 2001.

[133] R. Desbriere, V. Vuaroqueaux, V. Achard, S. Boullu-Ciocca, M. Labuhn, A. Dutour*, et al.*, "11beta-hydroxysteroid dehydrogenase type 1 mRNA is increased in both visceral and subcutaneous adipose tissue of obese patients," *Obesity (Silver Spring),* vol. 14, pp. 794-8, May 2006.

[134] A. M. Strack, R. J. Sebastian, M. W. Schwartz, and M. F. Dallman, "Glucocorticoids and insulin: reciprocal signals for energy balance," *Am J Physiol,* vol. 268, pp. R142-9, Jan 1995.

[135] E. Epel, R. Lapidus, B. McEwen, and K. Brownell, "Stress may add bite to appetite in women: a laboratory study of stress-induced cortisol and eating behavior," *Psychoneuroendocrinology,* vol. 26, pp. 37-49, Jan 2001.

[136] M. F. Dallman, N. C. Pecoraro, and S. E. la Fleur, "Chronic stress and comfort foods: self-medication and abdominal obesity," *Brain Behav Immun,* vol. 19, pp. 275-80, Jul 2005.

[137] S. K. Fried, D. A. Bunkin, and A. S. Greenberg, "Omental and subcutaneous adipose tissues of obese subjects release interleukin-6: depot difference and regulation by glucocorticoid," *J Clin Endocrinol Metab,* vol. 83, pp. 847-50, Mar 1998.

[138] I. J. Bujalska, S. Kumar, M. Hewison, and P. M. Stewart, "Differentiation of adipose stromal cells: the roles of glucocorticoids and 11beta-hydroxysteroid dehydrogenase," *Endocrinology,* vol. 140, pp. 3188-96, Jul 1999.

[139] Y. Wang, B. Jones Voy, S. Urs, S. Kim, M. Soltani-Bejnood, N. Quigley*, et al.*, "The human fatty acid synthase gene and de novo lipogenesis are coordinately regulated in human adipose tissue," *J Nutr,* vol. 134, pp. 1032-8, May 2004.

[140] M. Rebuffe-Scrive, M. Bronnegard, A. Nilsson, J. Eldh, J. A. Gustafsson, and P. Bjorntorp, "Steroid hormone receptors in human adipose tissues," *J Clin Endocrinol Metab,* vol. 71, pp. 1215-9, Nov 1990.

[141] J. Sjogren, M. Weck, A. Nilsson, M. Ottosson, and P. Bjorntorp, "Glucocorticoid hormone binding to rat adipocytes," *Biochim Biophys Acta,* vol. 1224, pp. 17-21, Oct 20 1994.

[142] I. J. Bujalska, S. Kumar, and P. M. Stewart, "Does central obesity reflect "Cushing's disease of the omentum"?," *Lancet,* vol. 349, pp. 1210-3, Apr 26 1997.

[143] A. Perez, S. Jansen-Chaparro, I. Saigi, M. R. Bernal-Lopez, I. Minambres, and R. Gomez-Huelgas, "Glucocorticoid-induced hyperglycemia," *J Diabetes,* vol. 6, pp. 9-20, Jan 2014.

[144] R. C. Andrews and B. R. Walker, "Glucocorticoids and insulin resistance: old hormones, new targets," *Clin Sci (Lond),* vol. 96, pp. 513-23, May 1999.

[145] R. R. Almon, D. C. DuBois, and W. J. Jusko, "A microarray analysis of the temporal response of liver to methylprednisolone: a comparative analysis of two dosing regimens," *Endocrinology,* vol. 148, pp. 2209-25, May 2007.

[146] L. C. Cantley, "The phosphoinositide 3-kinase pathway," *Science,* vol. 296, pp. 1655-7, May 31 2002.

[147] J. M. Backer, "The regulation of class IA PI 3-kinases by inter-subunit interactions," *Curr Top Microbiol Immunol,* vol. 346, pp. 87-114, 2010.

[148] T. Kuo, M. J. Lew, O. Mayba, C. A. Harris, T. P. Speed, and J. C. Wang, "Genome-wide analysis of glucocorticoid receptor-binding sites in myotubes identifies gene networks modulating insulin signaling," *Proc Natl Acad Sci U S A,* vol. 109, pp. 11160-5, Jul 10 2012.

[149] L. A. Barbour, J. Shao, L. Qiao, W. Leitner, M. Anderson, J. E. Friedman*, et al.*, "Human placental growth hormone increases expression of the p85 regulatory unit of phosphatidylinositol 3-kinase and triggers severe insulin resistance in skeletal muscle," *Endocrinology,* vol. 145, pp. 1144-50, Mar 2004.

[150] B. Draznin, "Molecular mechanisms of insulin resistance: serine phosphorylation of insulin receptor substrate-1 and increased expression of p85alpha: the two sides of a coin," *Diabetes,* vol. 55, pp. 2392-7, Aug 2006.

[151] Y. Terauchi, Y. Tsuji, S. Satoh, H. Minoura, K. Murakami, A. Okuno*, et al.*, "Increased insulin sensitivity and hypoglycaemia in mice lacking the p85 alpha subunit of phosphoinositide 3-kinase," *Nat Genet,* vol. 21, pp. 230-5, Feb 1999.

[152] F. Mauvais-Jarvis, K. Ueki, D. A. Fruman, M. F. Hirshman, K. Sakamoto, L. J. Goodyear*, et al.*, "Reduced expression of the murine p85alpha subunit of phosphoinositide 3-kinase improves insulin signaling and ameliorates diabetes," *J Clin Invest,* vol. 109, pp. 141-9, Jan 2002.

[153] G. K. Bandyopadhyay, J. G. Yu, J. Ofrecio, and J. M. Olefsky, "Increased p85/55/50 expression and decreased phosphotidylinositol 3-kinase activity in insulin-resistant human skeletal muscle," *Diabetes,* vol. 54, pp. 2351-9, Aug 2005.

[154] C. Besse, N. Nicod, and L. Tappy, "Changes in insulin secretion and glucose metabolism induced by dexamethasone in lean and obese females," *Obes Res,* vol. 13, pp. 306-11, Feb 2005.

[155] A. Rafacho, L. Marroqui, S. R. Taboga, J. L. Abrantes, L. R. Silveira, A. C. Boschero*, et al.*, "Glucocorticoids in vivo induce both insulin hypersecretion and enhanced glucose

sensitivity of stimulus-secretion coupling in isolated rat islets," *Endocrinology,* vol. 151, pp. 85-95, Jan 2010.

[156] L. Fransson, S. Franzen, V. Rosengren, P. Wolbert, A. Sjoholm, and H. Ortsater, "beta-Cell adaptation in a mouse model of glucocorticoid-induced metabolic syndrome," *J Endocrinol,* vol. 219, pp. 231-41, Dec 2013.

Chapter I:

Glucocorticoid-Angiopoietin-like 4-Ceramide Axis induces insulin resistance

Abstract

Chronic glucocorticoid (GC) exposure is associated with the development of insulin resistance, but the underlying mechanism has remained elusive. Here, we show that GC-induced insulin resistance is attenuated upon ablation of angiopoietin-like 4 (*Angptl4*$^{-/-}$), a GC target gene encoding a secreted protein that mediates GC inducted lipolysis in white adipose tissue. Through metabolomic profiling, we reveal that GC treatment elevates hepatic ceramide levels by inducing enzymes in the ceramide synthetic pathway in an Angptl4-dependent manner. Angptl4 is also required for GCs to stimulate activities of ceramide downstream effectors, protein phosphatase 2A and protein kinase ζ. We further show that inhibition of ceramide synthesis prevents GC-induced glucose intolerance in wild type, but not in *Angptl4*$^{-/-}$ mice. Overall, our study demonstrates the key role of Angptl4 in GC-augmented hepatic ceramide production that induces whole body insulin resistance.

Introduction

Insulin resistance is a major risk factor for type 2 diabetes and cardiovascular diseases. Chronic and/or excess glucocorticoid (GC) exposure has long been associated with the development of insulin resistance [1-3]. GCs reduce insulin-stimulated glucose utilization in skeletal muscle and white adipose tissue (WAT). GC exposure also suppresses insulin responsiveness in liver and potentiates gluconeogenesis, which is inhibited by insulin. Several mechanisms have been proposed to explain GC-induced insulin resistance. First, GCs have been shown to directly inhibit insulin signaling and insulin-stimulated glucose uptake in myotubes and adipocytes [4-7]. In addition, osteocalcin secreted from bone has been reported to play a positive role in insulin secretion and insulin sensitivity [8]. Third, the ability of GCs to promote lipolysis in WAT has also been associated with insulin resistance. Administration of acipimox, an inhibitor of WAT lipolysis, reduces GC-induced insulin resistance in humans [9]. Similarly, injecting nicotinic acid into male Sprague-Dawley rats to decrease WAT lipolysis corrects the antagonistic effects of GCs on insulin actions [10]. Finally, GC treatment has been shown to increase hepatic ceramide levels [11] and Inhibition of ceramide synthesis by a small molecular inhibitor, myriocin, compromises GC-induced insulin resistance [11]. Also, the ability of GCs to cause insulin resistance is reduced in mice lacking Des2, an enzyme in ceramide biosynthesis pathway [11].

The biological responses of GCs are mainly mediated by the glucocorticoid receptor (GR) which directly regulates its primary target genes. Therefore, to understand the molecular mechanism of GC-induced insulin resistance, the first step is to identify GR primary target genes that participated in this GC-regulated process. We previously identified *angiopoietin-like 4* (*Angptl4*) as a GR primary target gene in hepatocytes and adipocytes [12, 13]. The *Angptl4* gene encodes a secreted protein that promotes adipocyte lipolysis [14] and inhibits extracellular lipoprotein lipase (LPL) [15, 16]. Mice lacking Angptl4 (*Angptl4*$^{-/-}$) display impaired GC-induced WAT lipolysis [14]. Thus, *Angptl4*$^{-/-}$ mice are perfect models to study the role of WAT lipolysis in GC-modulated metabolite changes in peripheral tissues that cause insulin resistance.

In this study, we analyzed the effects of GC on glucose homeostasis and insulin actions in *Angptl4*$^{-/-}$ mice. We also performed metabolomics in the liver and skeletal muscle of *Angptl4*$^{+/+}$ (will be called as wild type, WT, mice in the rest of the manuscript) and *Angptl4*$^{-/-}$ mice treated with or without GC. The goal of this report is to establish *Angptl4* as a GR primary target gene that potentially links GC-promoted WAT lipolysis to the changes of insulin resistance inducing metabolites in liver and/or skeletal muscle and to elucidate the mechanism governing this process.

Results

GC-induced insulin resistance is improved in Angptl4 null mice

WT and *Angptl4*$^{-/-}$ mice were treated with or without dexamethasone (Dex, a synthetic glucocorticoid) for 7 days. Intraperitoneal glucose tolerance tests (IPGTTs) were then performed on these mice. In WT mice, as expected, Dex treatment induced glucose intolerance (Fig. 1a and 1b). While there was no difference in glucose tolerance between control WT and *Angptl4*$^{-/-}$ mice with Dex treatment, (Fig. 1a and 1b), upon Dex treatment, *Angptl4*$^{-/-}$ mice did not show glucose intolerance observed in WT mice (Fig. 1a and 1b). After 7 days of Dex treatment, fasting plasma insulin levels were markedly higher in Dex-treated WT mice than those of WT and *Angptl4*$^{-/-}$ mice without Dex treatment as well as Dex-treated *Angptl4*$^{-/-}$ mice (Fig. 1c, 0 min). These results confirm that Dex treatment in mice causes insulin resistance resulting in hyperinsulinemia. More importantly, the observation that glucose tolerance was still impaired in Dex-treated WT mice despite the presence of hyperinsulinemia suggests that pancreatic islet beta cells were unable to compensate for insulin resistance. In control WT and *Angptl4*$^{-/-}$ mice, plasma insulin levels were increased 15 min after glucose administration but returned to basal levels within 30 min (Fig. 1c). For Dex-treated WT mice, plasma insulin levels were similar at all three time points we measured (Fig. 1c). Interestingly, in Dex-treated *Angptl4*$^{-/-}$ mice, plasma insulin levels remained elevated 30 mins after glucose administration (Fig. 1c). This sustained elevation of plasma insulin in *Angptl4*$^{-/-}$ mice presumably overcame insulin resistance, explaining the normal glucose tolerance observed in Dex-treated *Angptl4*$^{-/-}$ mice. This suggests that, in contrast to WT mice, pancreatic islet beta cells of *Angptl4*$^{-/-}$ mice were able to compensate better than WT mice for the presence of insulin resistance. The observation that insulin levels did not differ between Dex-treated *Angptl4*$^{-/-}$ and Dex-treated WT mice at the 30 min time point in the IPGTT, again demonstrates more severe insulin resistance in Dex-treated WT than in *Angptl4*$^{-/-}$ mice.

We assessed this hypothesis further by performing insulin tolerance test (ITTs) to monitor and compare the Dex effect on whole body insulin sensitivity of WT and *Angptl4*$^{-/-}$ mice. Dex treatment significantly worsened insulin sensitivity in WT mice (Fig. 1 d and 1e). *Angptl4*$^{-/-}$ mice were less insulin sensitive than WT mice in the absence of Dex treatment (Fig. 1d and 1e). However, Dex-treatment in *Angptl4*$^{-/-}$ mice did not impair insulin sensitivity to the same degree as in Dex-treated WT mice, having similar insulin sensitivity to control WT mice (Fig. 1d and 1e). These results demonstrate that a lack of Angptl4 prevented the whole body insulin insensitivity induced by GC exposure.

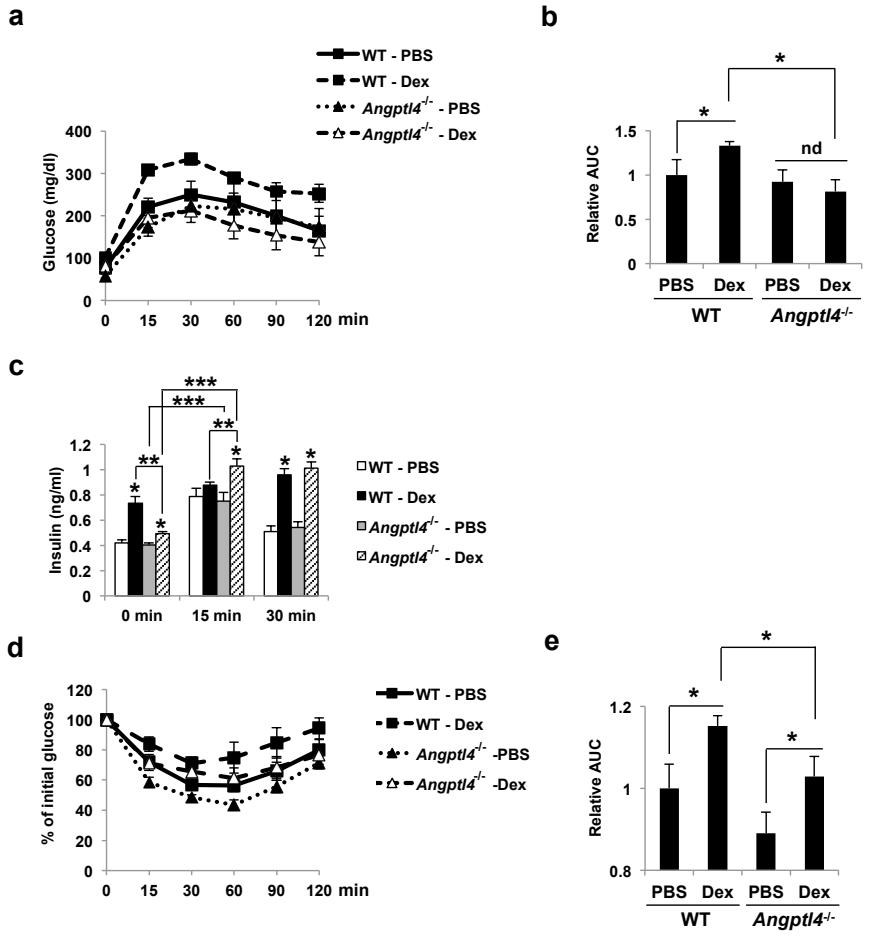

Fig1.Dex-induced glucose and insulin intolerance were improved in *Angptl4*$^{-/-}$ mice.

Male 8 weeks old WT and *Angptl4*$^{-/-}$ mice were treated with PBS or Dex via drinking water (≈0.42 mg/kg body weight) for 7 days. (a) On last day, mice were fasted for 16 hrs and GTT assay was performed. (b) Relative area under curve (AUC) for GTT results (relative to PBS-treated WT mice) was shown. Error bars represent S.E.M., n=5-7, *$p < 0.05$ (c) Plasma insulin level was measured before glucose injection (0 time point), and 15 min and 30 min after glucose injection. Error bars represent S.E.M., n=5-7, * indicates significant ($p < 0.05$) effect of Dex (compare to PBS) at the given time point, ** indicates significant difference ($p < 0.05$) between WT Dex and *Angptl4*$^{-/-}$ Dex at the given time point, whereas *** indicates significant ($p < 0.05$) difference between time points. (d) ITT was performed as described in Methods. ITT result was displayed as percentage of initial plasma glucose level at different time points. (e) Relative AUC for ITT results (relative to PBS-treated WT mice) was shown. Error bars represent S.E.M., n=5-7, *$p < 0.05$

To determine which organ contributes to the insulin sensitivity observed upon Angptl4 depletion, we monitored the activity of Akt in epididymal WAT (eWAT), liver, and gastrocnemius muscle after 10 min of insulin treatment in control- and Dex-treated WT and *Angptl4*$^{-/-}$ mice. Akt is known to be phosphorylated at serine 473 and threonine 308 residues upon insulin treatment [17]. We performed immunoblotting to detect threonine 308 phosphorylated Akt (p-Akt) as an indicator for Akt activation. In liver and gastrocnemius muscle of control WT mice, insulin treatment caused an increase in Akt phosphorylation. This effect, however, was not observed in Dex-treated WT mice (Fig. 2a and 2b). These results demonstrate that Dex treatment prevented insulin activation of Akt in these two tissues. In contrast, in liver and gastrocnemius muscle of control- and Dex-treated *Angptl4*$^{-/-}$ mice, insulin treatment markedly increased p-Akt levels (Fig. 2a and 2b). Thus, in the absence of Angptl4, insulin still had the ability to activate Akt in liver and gastrocnemius muscle even in the presence of Dex. For eWAT, insulin treatment increased p-Akt levels in both control- and Dex-treated WT mice, (Fig. 2c). Furthermore, insulin treatment also significantly elevated p-Akt levels in eWAT of control and Dex-treated *Angptl4*$^{-/-}$ mice (Fig. 2c). These results demonstrate that, in liver and skeletal muscle of WT mice, Dex treatment induced insulin resistance, which were substantially reversed in *Angptl4*$^{-/-}$ mice. In contrast, Dex treatment in eWAT had more complex effects on insulin signaling in which insulin-stimulated Akt activation was present both in the basal condition and upon Dex treatment. However, maximal Akt activation was somewhat reduced.

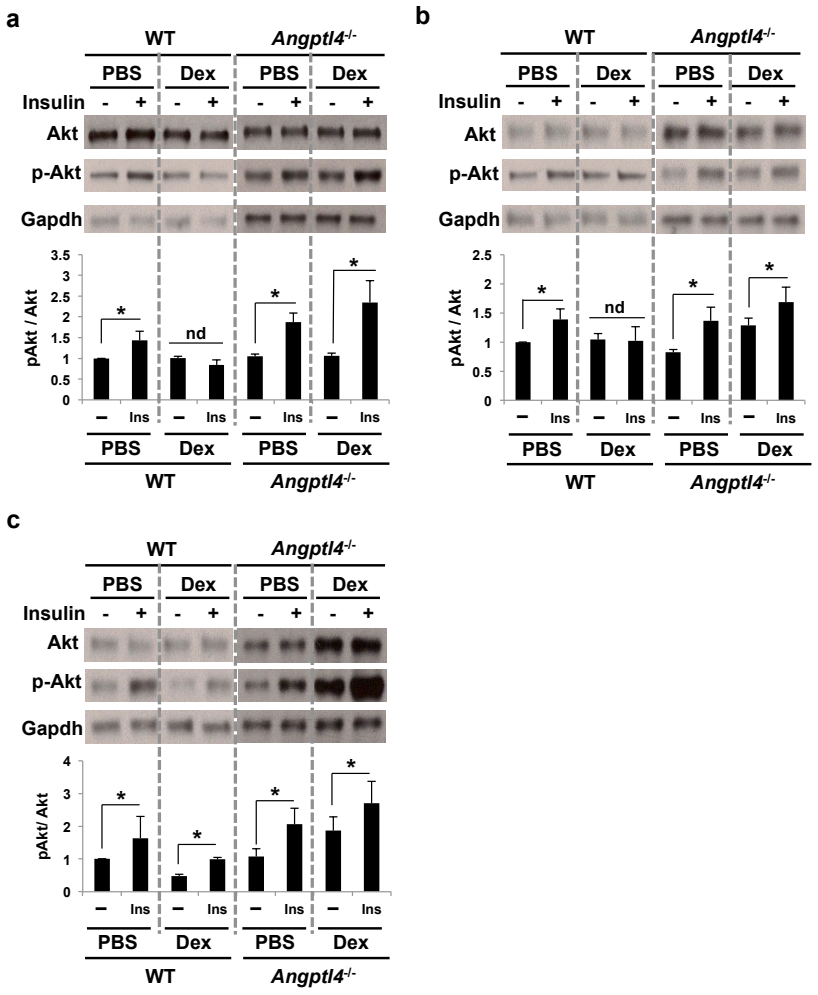

Fig. 2 Dex-induced insulin resistance in liver and gastrocnemius muscle was improved in *Angptl4*$^{-/-}$ mice.

Male 8 weeks old WT and *Angptl4*$^{-/-}$ mice were treated with PBS or Dex via drinking water (≈0.42 mg/kg body weight) for 7 days. These mice were injected with insulin (1 unit/body weight) for 10 min and various tissues were then isolated. Western blot was performed to monitor the levels of p-Akt and Akt in (a) liver, (b) gastrocnemius muscle and (c) eWAT. The levels of Gapdh were used as an internal control. The intensity of bands in western blots was measured by Image J. The intensity of bands are normalized with Gapdh levels. The relative ratio of p-Akt vs. Akt represents the Akt activity. Error bars represent S.E.M., n=3-4, and *p<0.05

Metabolomic analysis of gastrocnemius muscle and liver in control and Dex-treated WT and Angptl4$^{-/-}$ mice

With our observations of the differential effects of Dex in eWAT vs liver and muscle upon Angptl4 ablation, we hypothesized that Angptl4 is involved in GC-induced insulin resistance by mobilizing fatty acids from WAT that are then converted in liver and skeletal muscle to metabolites that can modulate insulin action. To test this model, we performed targeted metabolomics analyses in gastrocnemius muscle and liver of control and Dex–treated WT and *Angptl4*$^{-/-}$ mice. We focused on these two tissues because they become insulin resistant upon Dex treatment in our experimental system (Fig. 2). We used single reaction monitoring (SRM)-based targeted metabolomic analysis to quantify the levels of approximately 150 common lipid metabolites (Supplementary table 1). We found 11 metabolites whose levels were significantly increased under Dex treatment in liver of WT mice, whereas 48 metabolites had reduced levels (Fig. 3a and Supplementary table 1). Surprisingly, none of the lipid species identified in muscle tissues were significantly increased after Dex treatment in WT mice, although 9 metabolite species were reduced (Supplementary table 2). However, none of these 9 metabolites had previously been associated with the development of insulin resistance.

Among the 11 metabolites whose levels were increased by Dex treatment in WT mouse liver, the levels of 6 of these metabolites were significantly lower in Dex-treated *Angptl4*$^{-/-}$ mice. These were C18:0-ceramide, C16:0-sphingosine phosphate (S1P), C16:0/C18:1/C16:0-triacylglycerol (TAG), C18:0/C18:1/C18:0-TAG, C18:0/C18:1-DAG, and C16:0/C18:1-phosphatidylethanolamine (PE) (Fig. 3b). While the levels of ceramides, DAG [18, 19] and S1P [20, 21] have been all positively associated with the development of insulin resistance, only ceramides have been linked to the GC-induced modulation of insulin sensitivity [11]. We therefore focused on elucidating the role of Angptl4 in GC-induced hepatic ceramide production and insulin resistance.

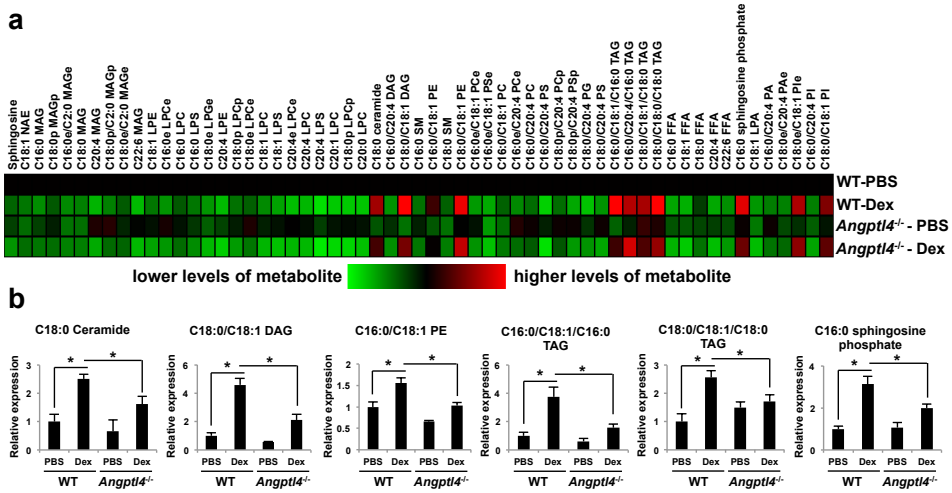

Fig. 3 Metabolomics analysis in liver and gastrocnemius muscle of control- and Dex-treated WT and *Angptl4*$^{-/-}$ mice.

Male 8 weeks old WT and *Angptl4*$^{-/-}$ mice were treated with PBS or Dex via drinking water (≈0.42 mg/kg body weight) for 7 days. (a) Liver was isolated from these mice and lipids were extracted for metabolomics analysis. The heat map shows metabolites that are significantly altered in content ($p < 0.05$) upon Dex treatment in liver of WT mice. The relative content was displayed in the heat map compared to WT-PBS group. Red shading on the heat map indicates higher relative levels, whereas green shading represents lower relative levels. (b) Six lipid metabolites that were found significantly elevated in Dex-treated WT mice liver but not Dex-treated *Angptl4*$^{-/-}$ mice were shown. Error bars represent S.E.M., n=4, and *$p < 0.05$

Activation of the hepatic ceramide synthetic program is attenuated in Angptl4$^{-/-}$ mice

Recent studies have shown that distinct ceramide species, defined by their fatty acyl chain length, can exert specific biological functions [22, 23]. Therefore, we expanded our initial SRM-based targeted metabolomic analysis by analyzing multiple ceramide species to determine whether their levels in liver were modulated by Dex treatment. For the 16 ceramide species we assayed, we found that their levels were similar between liver of control WT and *Angptl4*$^{-/-}$ mice (Fig. 4a). However, Dex treatment markedly elevated a series of ceramide species, including C16:0-, C18:0-, C20:0-, C20:2-, C20:1-, C22:1-, C22:0, C22:4-, C24:0-, C24:2- and C26:0-ceramides in liver of WT mice (Fig. 4a). In the liver of Dex-treated *Angptl4*$^{+/+}$ mice, the levels of these ceramide species were all significantly lower, compared to control WT mice (Fig. 4a). C24:1-ceramides were the only species that were reduced by Dex treatment in livers of WT mice (Fig. 4a) with a further decrease observed in livers of Dex-treated *Angptl4*$^{-/-}$ mice.

The simplest model to explain the overall reduction of ceramide species in livers of Dex-treated *Angptl4*$^{-/-}$ mice compared to Dex-treated WT mice is that the stimulation of lipolysis by Dex in WAT is diminished in *Angptl4*$^{-/-}$ mice, which then decreases the availability of palmitate for hepatic ceramide synthesis. We measured the levels of palmitate in plasma of control and Dex-treated WT and *Angptl4*$^{-/-}$ mice. We found that Dex treatment for 7 days elevated plasma palmitate for approximately 50% in WT mice (Fig. 4b). In Dex-treated *Angptl4*$^{-/-}$ mice, plasma palmitate levels, though not statistically significant, were trending toward to 27% lower than those of Dex-treated WT mice ($p=0.1$, Fig. 4b). Interestingly, plasma stearic acid (C18:0-FA) levels were also augmented by Dex treatment in WT mice and this induction was significantly reduced in Dex-treated *Angptl4*$^{-/-}$ mice (Fig. 4b). Dex treatment, however, did not affect the levels of C18:1-, C20:4-, and C22:6-FA in WT mice (Fig. 4b). Plasma C16:0-, C18:0-, and C20:4-FA levels were either significant or trending higher in control *Angptl4*$^{-/-}$ mice than those of control WT mice (Fig. 4b). These results likely reflect the higher activity of LPL in plasma of *Angptl4*$^{-/-}$ mice [24]. We also measured the levels of representative ceramide species in plasma of control and Dex-treated WT and *Angptl4*$^{-/-}$ mice. We found that the levels of C16:0-, C18:0- and C20:4-cermadies were increased by Dex in WT and this induction was attenuated in *Angptl4*$^{-/-}$ mice (Fig. 4c).

It is important to note that only 11 lipid species were increased by GC in livers of WT mice, despite the increase of fatty acid flux from WAT to liver by Dex treatment. This observation suggests that, in addition to increasing the availability of hepatic fatty acids, Dex may stimulate specific metabolic pathways that regulate ceramide synthesis. We therefore tested this idea by analyzing the expression of genes encoding enzymes involved in ceramide synthesis. We found that *Spt2, Cers3, Cers4, Cers5,* and *Cers6*, which are genes in the *de novo* ceramide synthetic pathway, were all induced by Dex treatment (Fig. 4d and Supplementary Figure S1). The expression of *Smpd1*, which encodes an enzyme that converts sphingomyelins to ceramides, was also augmented by Dex (Fig. 4d and Supplementary Figure S1). However, Dex also increased the expression of *Sgms1*, which encodes an enzyme that converts ceramides to sphingomyelins (Fig. 4e). Counterintuitively, the induction of *Sgms1* and *Smpd1* by Dex

promotes the bi-directional interconversion of ceramides and sphingomyelins. This resembles the unique effect of GC in both promoting hepatic glycogen synthesis and gluconeogenesis [3, 25]. Because we observed decreased levels of sphingomyelins upon Dex treatment (Fig. 3a), we postulated that induction of *Smpd1* likely dominates over the *Sgms1* induction by Dex. Finally, the stimulation of *Sphk1* expression, a gene that encodes an enzyme that converts sphingosine to S1P, likely explains the decreased sphingosine and increased S1P levels in the livers of Dex-treated WT mice (Fig. 3a).

Interestingly, in *Angptl4*$^{-/-}$ mice, the ability of Dex to augment the expression of *Cers3, Cers4, Cers5, Cers6,* and *Sphk1* was impaired, whereas the induction of *Spt1, Spt2* and *Smpd1* remained intact (Fig. 4b). The decreased expression of *Sphk1* likely explains the reduced S1P levels in liver of Dex-treated *Angptl4*$^{-/-}$ mice compared to Dex-treated WT mice (Fig. 3a and 3b). Overall, these results suggest that the reduction in ceramide production in livers of *Angptl4*$^{-/-}$ mice was due to both diminished substrate availability and impairment in the induction of ceramide synthetic enzymes by Dex. To confirm that the gene expression changes are reflected at the protein levels, we performed immunoblotting for Cers5 and Cers6, as the representative enzymes in ceramide synthesis. Indeed, we detected the levels of these two proteins to be increased by Dex in livers of WT mice, but not in *Angptl4*$^{-/-}$ mice (Fig. 4f). Overall, these gene expression analyses were in agreement with the metabolomic results, which demonstrated complex effects of Dex on ceramide metabolism.

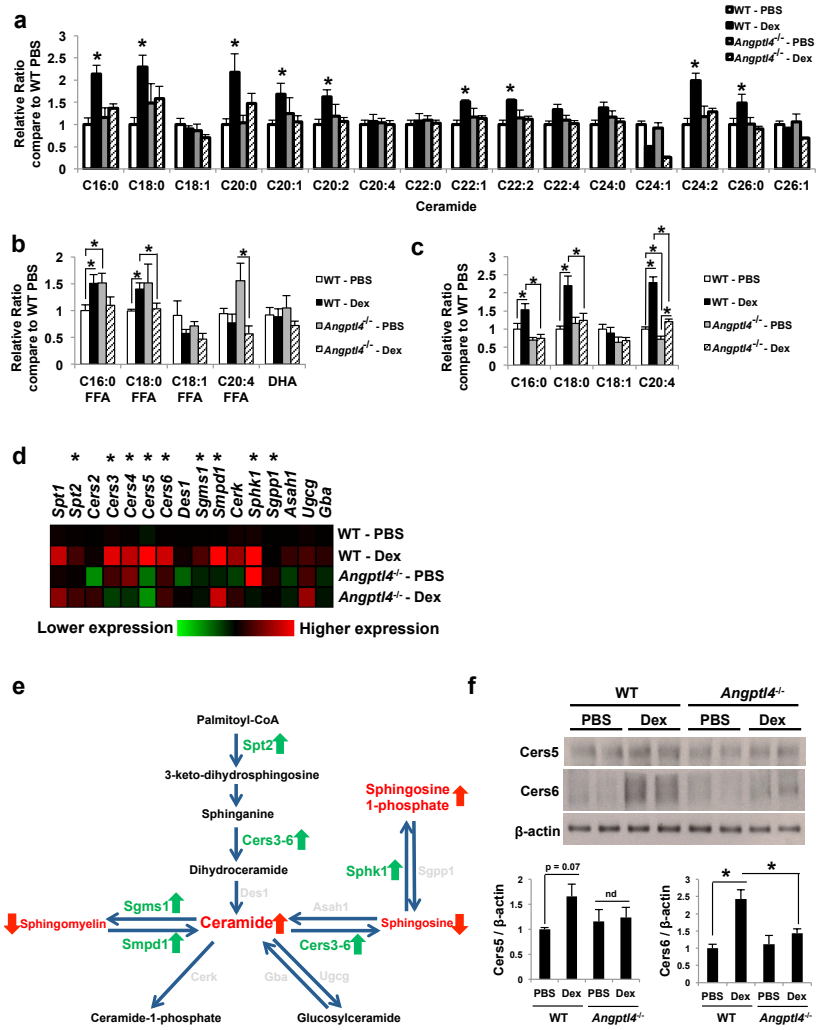

Fig. 4 Dex-activated hepatic ceramide synthetic program was attenuated in *Angptl4*$^{-/-}$ mice.

Male 8 weeks old WT and *Angptl4*$^{-/-}$ mice were treated with PBS or Dex via drinking water (≈0.42 mg/kg body weight) for 7 days and liver was isolated from these mice. (a) The levels of 16 different ceramide species in liver, (b) The levels of 5 different fatty acids in plasma, (c) The levels of 4 ceramide species in plasma of these mice were measured. (d) The expression of genes encoding enzymes involved in ceramide production was monitored using qPCR. The heat map showed the relative expression level compared to WT-PBS group. Red shading on the heat map indicates higher expression levels, whereas green shading represents lower expression levels. The exact numbers of fold induction were shown in Supplenmetary Fig. S1. These results were from 16 mice. (e) Schematic representation of ceramide synthesis pathways. The genes that were induced by Dex in WT mice liver are shown as green color. Those were not induced by Dex are shown as light gray color. (f) The expression of Cers5 and Cers6 proteins was monitored using western blot. The intensity of bands in western blots was measured by Image J. The bar graph represents average intensity of bands normalized with Gapdh levels. Error bars represent S.E.M., n=3-4, and *p<0.05.

The activation of downstream signaling effectors by ceramides is impaired in Dex-treated Angptl4$^{-/-}$ mice

Previous studies have shown that protein phosphatase 2A (PP2A) and protein kinase C ζ (PKCζ) act downstream of ceramide-initiated signaling [26, 27]. We therefore measured the activity of these two enzymes to further document that Dex treatment stimulates ceramide-initiated signaling. PP2A was immunoprecipitated from liver lysates using an antibody against PP2A catalytic subunit. To estimate the PP2A activity, we measured dephosphorylation of threonine-phosphopeptides using our immunoprecipitates. We found that Dex treatment increased PP2A activity in livers of WT mice (≈1.8 fold). In *Angptl4*$^{-/-}$ mice, however, the effect of Dex was markedly reduced (Fig. 5a). In addition, PKCζ activity was monitored based on autophosphorylation of threonine 560 residue of PKCζ (p-PKCζ), which is required for PKCζ activation [28]. We found that autophosphorylation of T560 of PKCζ was increased by Dex treatment in livers of WT mice (Fig. 5b). However, in *livers of Angptl4*$^{-/-}$ mice, this Dex effect was markedly reduced (Fig. 5a). These results validate the concept that Dex treatment stimulates ceramide-initiated signaling in liver, which is impaired in the absence of Angptl4.

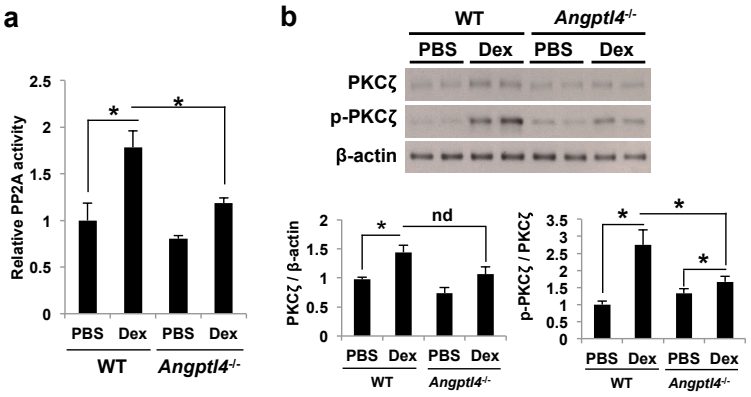

Fig. 5 Dex treatment activated PKCζ and PP2A in liver of WT mice but not *Angptl4*$^{-/-}$ mice.

Male 8 weeks old WT and *Angptl4*$^{-/-}$ mice were treated with PBS or Dex via drinking water (≈0.42 mg/kg body weight) for 7 days. (a) PP2A activity was measured in liver of these mice as described in Methods. The bar graph shows relative PP2A activity (to PBS-treated WT mice). Error bars represent S.E.M., n=3-4, and *p < 0.05. (b) The levels of p-PKCζ and PKCζ in liver of these mice were monitored by western blots. The intensity of bands in western blots was measured by Image J. The bar graph represents average intensity of bands normalized with β-actin levels. The ratio of p-PKCζ and PKCζ is an indicator of PKCζ activity. Error bars represent S.E.M., n=3-4, and *p<0.05.

The inhibition of ceramide synthesis by myriocin reduces Dex-induced insulin resistance in WT but not Angptl4$^{-/-}$ mice

Previous studies have shown that inhibiting ceramide synthesis by myriocin, an inhibitor of Spt1 and Spt2 [29], reduces Dex-induced insulin resistance. If the major role for Angptl4 in Dex-induced insulin resistance is to elevate hepatic ceramide production, we hypothesized that blocking ceramide synthesis would improve insulin sensitivity in Dex-treated WT but not in Dex-treated *Angptl4*$^{-/-}$ mice. Consistent with our model, we found that treatment with the ceramide synthase inhibitor myriocin attenuated Dex-induced glucose intolerance in WT mice. But we did not observe this effect in DEX-treated *Angptl4*$^{-/-}$ mice (Fig. 6a).

We also monitored the activity of PKCζ to validate our hypothesis that the effect of myriocin was mediated through ceramide generation. Indeed, in myriocin treatment, there was a marked decreased p-PKCζ levels in Dex-treated WT mice (Fig. 6b). These results confirm that myriocin treatment reduces the ceramide-initiated signaling that is induced by Dex. Contrastingly, in Dex-treated *Angptl4*$^{-/-}$ mice, myriocin treatment had no effect on p-PKCζ levels (Fig. 6b). These results are in agreement with the fact that myriocin did not affect glucose tolerance in Dex-treated *Angptl4*$^{-/-}$ mice (Fig. 6a).

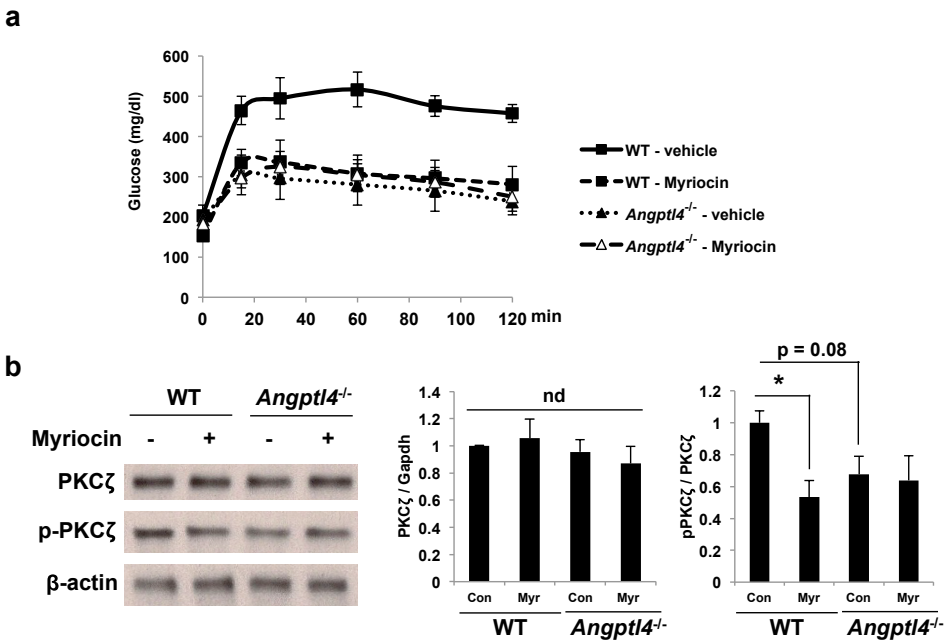

Fig. 6 Myriocin improved insulin sensitivity in Dex-treated WT but not *Angptl4*$^{-/-}$ mice.

Male 8 weeks old WT and *Angptl4*$^{-/-}$ mice were treated with Dex (≈0.42 mg/kg body weight) for 7 days. Myriocin (0.5 mg/kg body weight) was injected intraperitoneally into a half of mice at day 4 of the experiments. (a) Mice were fasted for 6 hrs and GTT was performed. (b) Western blots were performed in liver to monitor the levels of p-PKCζ and PKCζ. The intensity of bands in western blots was measured by Image J. The bar graph represents average intensity of bands normalized with β-actin levels. The ratio of p-PKCζ and PKCζ is an indicator of PKCζ activity. Error bars represent S.E.M., n=3-4, and *p<0.05.

Discussion

The GC's antagonistic effect on whole body insulin sensitivity is well established. However, the molecular mechanisms underlying such GC effect remain to be elucidated. Our present studies demonstrate that *Angptl4*, a primary target gene of GR in hepatocytes and adipocytes [12], plays a key role in GC-induced insulin resistance. We previously reported that Angptl4, a secreted protein, is required for GC-induced WAT lipolysis and purified Angptl4 proteins can directly enhance lipolysis in primary adipocytes [14]. Here we show that Angptl4 is required for GC-induced ceramide production and ceramide-initiated signaling in liver. Based on these results, we propose that Angptl4 participates in GC-induced insulin resistance by promoting lipolysis in WAT, which mobilizes fatty acids that are taken up by liver for ceramide production (Fig. 7). In addition to promoting adipocyte lipolysis, Angptl4 also inhibits extracellular LPL [15, 16]. Our present studies mainly focus on the lipolytic effect of Angptl4 in GC-induced insulin resistance. However, we do not exclude the involvement of Angptl4's LPL inhibitory effect in the regulation of insulin sensitivity. Reducing LPL activity may lead to hypertriglyceridemia, which could also contribute to insulin resistance.

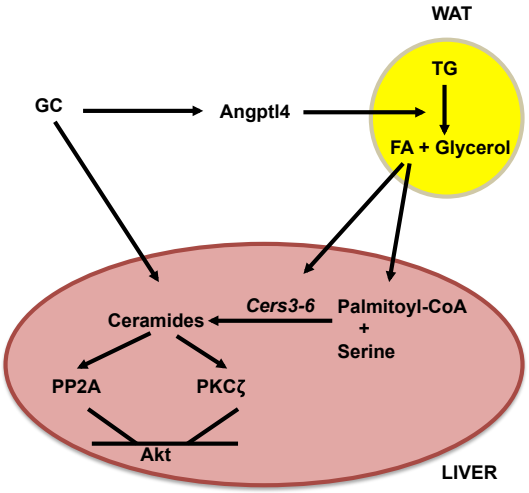

Fig. 7 The proposed model for the role of Angptl4 in GC-induced hepatic insulin resistance.

GC activates the expression of Angptl4, which promotes lipolysis in WAT. Fatty acids generated from lipolysis serve as both precursors (palmitate) for ceramide synthesis and also signals to act with GC to increase the expression of Cers3-6. Ceramides subsequently activate PKCζ and PP2A, which inhibit Akt and result in insulin resistance.

The simplest model for Angptl4 action in GC-induced insulin resistance is for the provision of precursors, such as palmitate, for hepatic ceramide production, through the promotion of WAT lipolysis. Based on our results, Angptl4 action also provides signals needed for GC to activate ceramide synthetic pathways in liver: as without Angptl4, the ability of Dex to activate ceramide synthetic genes was attenuated (Fig. 7). Previous studies have shown that GC treatment increases the expression of several genes involved in ceramide synthesis in liver [11]. However, the mechanism governing such GC effect has been unknown. Chromatin immunoprecipitation sequencing (ChIP-seq) analysis in mouse liver identifies GR binding sites in or nearby genomic regions of several ceramide synthetic genes, such as *Cers6, Cers3* and *Spt2 [30]*. However, whether these genes are indeed GR primary target genes would require further studies. In addition to the direct activation of ceramide synthetic genes by GR, another potential mechanism is that the fatty acids generated by Angptl4-induced lipolysis in WAT provide the signals to act with GC to regulate ceramide synthetic genes. Saturated fatty acids have been shown to activate nuclear factor κB (NFκB) to stimulate ceramide synthetic genes in liver [23, 31], although GR is known to antagonize NFκB responses [32, 33]. Alternatively, fatty acids can serve as ligands for peroxisome proliferator activated receptor α and γ (PPARα and PPARγ, respectively) [34, 35]. PPARα have been shown to increase ceramide production in heart [36], skin [37] and trophoblasts [38], whereas PPARγ have been shown to promote ceramide synthesis in keratinocytes [39].

It is intriguing that our results show increase in a wide variety of ceramide species by Dex in liver. Our results are supported by the fact that Dex treatment increased the expression of at least 4 ceramide synthases (Cers3-6). Each ceramide synthase is responsible for synthesizing different species of ceramides and recent studies indicate that different ceramide species exert distinct physiological functions [22, 23]. For example, the deletion of *Cers6* gene in liver, which results in decreased C16:0-ceramides levels, protected mice from high fat diet-induced insulin resistance [40]. In contrast, haploinsufficiency of *Cers2* gene in mice were susceptible for the development of insulin resistance [41]. In this case, the levels of C22:0-, C24:0-, and C24:1-ceramides were decreased, whereas the levels of C16:0-ceramides were increased in livers of these *Cers2* heterozygous mice. The increase in *Cers5* and *Cers6* expression in liver of these mice demonstrates its contribution to the elevated C16:0-ceramide levels. Another study showed that increasing acid ceramidase expression in liver decreased the levels of C16:0- and C18:0-ceramides that are correlated to the reduction protein kinase c ζ (PKCζ) activity and the development of insulin resistance [42]. Overall, these results suggest that C16:0-ceramides negatively regulate insulin sensitivity. Based on our results from Cers5 and Cers6 proteins, both are responsible for the synthesis of C16:0-ceramides and are found in low levels in liver. However, their expression is markedly induced by Dex. Moreover, in addition to ceramides, our metabolomics studies identified other lipid metabolites, including C18:0/18:1-DAG and C16:0-S1P, that are increased in insulin resistance and these metabolites are augmented by Dex in liver. DAG levels in liver have long been associated with the development of insulin resistance [18, 19] and levels of C18:0/18:1-DAG are positively correlated with homeostatic model assessment-insulin resistance (HOMA-IR) [43]. In contrast, S1P has been shown to negatively regulate insulin action through S1P

receptor 2 ($S1P_2$) in liver [20, 21]. The exact roles of these metabolites in GC-induced insulin resistance require further investigation in the future.

The induction of ceramide levels in liver explains the role of Angptl4 in GC-induced hepatic insulin resistance. However, insulin resistance in gastrocnemius muscle was also improved in *Angptl4* null mice. It is surprising that in gastrocnemius muscle only 9 metabolites were affected by Dex treatment and none of them have been previously linked to insulin sensitivity. It is possible that the metabolites modulated by Dex treatment to induce insulin resistance in gastrocnemius muscle were not in the list of target metabolomics experiments we conducted. Notably, ceramides are mainly associated with very low density lipoprotein (VLDL) in plasma [44] and plasma ceramide levels have been negatively associated with insulin sensitivity [45, 46]. Therefore, it is also possible that ceramides produced in liver are mobilized to gastrocnemius muscle to exert the inhibitory effect on insulin action [47]. This model is somewhat supported by our observation that plasma ceramide levels were augmented by Dex in WT but not in *Angptl4* null mice (Fig. 4d).

Recent studies have shown that high fat diet causes inflammation in WAT. Secretion of Interleukin-6 (IL-6) from macrophages in WAT has been shown to increase to promote WAT lipolysis, which in turn induces hepatic insulin resistance [48]. While the induction of WAT lipolysis is also involved in the development of insulin resistance by GC, GC exposure actually suppresses, rather than promotes, inflammation in WAT [49]. Thus, the GC increase in Angptl4 expression, rather than cytokines, to promote WAT lipolysis is the key step in GC-induced insulin resistance. However, Angptl4 alone is unlikely to confer the suppressive effect of GC on insulin action and a network of GC primary target genes likely are needed to exert GC response on whole body insulin sensitivity. Regardless, it is clear from our studies that Angptl4 plays a critical role in triggering inter-organ communication between WAT and liver, leading to the suppression of insulin action. Overall, these results fill an important gap in our understanding of the metabolic functions of GC. Furthermore, targeting Angptl4 may be a promising strategy to dissociate the beneficial anti-inflammatory effects of GCs from adverse effects such as insulin resistance.

Materials and Methods

Animals.

Angptl4$^{-/-}$ mice were provided by the laboratories of Andras Nagy (Samuel Lunenfeld Research Institute, Mount Sinai Hospital) and Jeff Gordon (Washington University) [50]. *Angptl4*$^{-/-}$ mice were generated on a mixed B6:129 Sv background. *Angptl4*$^{+/+}$ mice were the littermates of *Angptl4*$^{-/-}$ mice. Male 8-12 weeks old mice were used in this study. Genotyping method was as described previously [50]. The Office of Laboratory Animal Care at the University of California, Berkeley approved all the animal experiments (AUP-2014-08-6617).

Drug Administration.

Male 8-week-old *Angptl4*$^{+/+}$ and *Angptl4*$^{-/-}$ mice were treated with approximately 0.42 mg/kg of dexamethasone (Sigma D2915) for 7 days via drinking water (0.00025 g of Dex/L). In myriocin experiments, myriocin (0.5 mg/kg body weight) was given to mice on the last 4 days of Dex treatment.

IP Glucose Tolerance Test (IPGTT) and Insulin Tolerance Test (ITT)

Mice were injected with glucose (1 g/kg body weight) or insulin (1 unit/kg body weight, Sigma, I0516-5ML) intraperitoneally. Blood samples (one drop from tail vein) are obtained at 0, 30, 60, 90, 120 min time points to measure glucose levels using Blood Glucose meter (Contour, Bayer). Blood was also collected during different time points of GTT for measuring plasma insulin levels.

Lipidomic profiling

Liver tissues and gastrocnemius muscle tissues were used for lipidomic profiling. Lipid metabolites were extracted in 4 ml of a 2:1:1 mixture of chloroform:methanol:Tris buffer with inclusion of internal standards C12:0 dodecylglycerol (10 nmol) and pentadecanoic acid (10 nmol). Organic and aqueous layers were separated by centrifugation at 1000 × g for 5 min and the organic layer was collected, dried down under N_2 and dissolved in 120 µl chloroform, of which 10 µl was analyzed by both single-reaction monitoring (SRM)-based LC-MS/MS or untargeted LC-MS. LC separation was achieved with a Luna reverse-phase C5 column (50 mm × 4.6 mm with 5 µm diameter particles, Phenomenex). Mobile phase A was composed of a 95:5 ratio of water:methanol, and mobile phase B consisted of 2-propanol, methanol, and water in a 60:35:5 ratio. Solvent modifiers 0.1% formic acid with 5 mM ammonium formate and 0.1% ammonium hydroxide were used to assist ion formation as well as to improve the LC resolution in both positive and negative ionization modes, respectively. The flow rate for each run started at 0.1 ml/min for 5 min, to alleviate backpressure associated with injecting chloroform. The gradient started at 0% B and increased linearly to 100% B over the course of 45 min with a flow rate of 0.4 ml/min, followed by an isocratic gradient of 100% B for 17 min at 0.5 ml/min before equilibrating for 8 min at 0% B with a flow rate of 0.5 ml/min.

MS analysis was performed with an electrospray ionization (ESI) source on an Agilent 6430 QQQ LC-MS/MS. The capillary voltage was set to 3.0 kV, and the fragmentor voltage was set to 100 V. The drying gas temperature was 350°C, the drying gas flow rate was 10 l/min, and the nebulizer pressure was 35 psi. Representative metabolites were quantified by SRM of the transition from precursor to product ions at associated collision energies. Data was normalized to the internal standards and also external standard curves of metabolite classes against the internal standards and levels were expressed as relative metabolite levels compared to controls. These internal

standards were added alongside dodecylglycerol and pentadecanoic acid in the 2:1:1 chloroform:methanol:Tris buffer mixture.

Western Blot.

The protein concentration of samples were measured using BCA protein assay (Thermo Scientific, 23228). Proteins (~30 μg) were mixed with 1X NuPAGE LDS Sample Buffer (ThermoFisher, NP0007) and 1X NuPAGE Sample Reducing Agent (ThermoFisher, NP0009), boiled for 5 min before applying to SDS-PAGE. Following are the antibodies used in this study: anti-Gapdh (Santa Cruz, sc-25778), anti-Akt (Cell Signaling, 9272s), anti-phosphor-Akt (Cell Signaling, 9275s), anti-Cers5 (Life Technologies, PA-520570), anti-Cers6 (Santa Cruz, sc-100554), anti-β-actin (Santa Cruz, sc-47778), anti-PKCζ (Santa Cruz, sc-216), anti-phospho-PKCζ (T410, Cell Signaling, 2060S). The intensity of the bands was quantified using Image J software (National Institute of Health) and normalized to Gapdh or β-actin.

PP2A activity assay

The PP2A activity in liver lysate was detected using PP2A Immunoprecipitation Phosphatase Assay kit (Millipore, 17-313FR) following the manufacture's protocol.

Quantitative Real-Time PCR (qPCR).

Total RNA was isolated from liver tissues using TRIzol reagent (Invitrogen, 15596018). Reverse transcription was performed as following: 0.5 μg of total RNA, 4 μl of 2.5 mM dNTP and 2 μl of 15 μM random primers (New England Biolabs, S1254S) were mixed at a volume of 16 μl, and incubated at 70°C for 5 min. Then, a 4 μl cocktail containing 25 units of Moloney Murine Leukemia Virus (M-MuLV) Reverse Transcriptase (New England Biolabs, M0253S), 10 units of RNasin Plus (Promega, N261B) and 2 μl of 10x M-MuLV Reverse Transcriptase Reaction Buffer (New England Biolabs, B0253S) was added, and samples were incubated at 42°C for 1h and then at 95°C for 5 min. The cDNA was diluted and used for real-time quantitative PCR (qPCR) using the Power Eva qPCR SuperMix Kit (Biochain, K5057400), following manufacturer's protocol. The qPCR was performed on the StepOne PCR System (Applied Biosystems) and analyzed with the ΔΔ-Ct method, as supplied by the manufacturer (Applied Biosystems). Rpl19 gene expression was used for internal normalization. Primer sequences used in this study are listed in Supplementary table 3.

Statistics.

Data are expressed as standard error of the mean (S.E.M) for each group and comparisons were analyzed by Student's t test.

Reference

[1] R. C. Andrews and B. R. Walker, "Glucocorticoids and insulin resistance: old hormones, new targets," *Clin Sci (Lond),* vol. 96, pp. 513-23, May 1999.

[2] G. Di Dalmazi, U. Pagotto, R. Pasquali, and V. Vicennati, "Glucocorticoids and type 2 diabetes: from physiology to pathology," *J Nutr Metab,* vol. 2012, p. 525093, 2012.

[3] T. Kuo, A. McQueen, T. C. Chen, and J. C. Wang, "Regulation of Glucose Homeostasis by Glucocorticoids," *Adv Exp Med Biol,* vol. 872, pp. 99-126, 2015.

[4] K. Ohshima, N. S. Shargill, T. M. Chan, and G. A. Bray, "Effects of dexamethasone on glucose transport by skeletal muscles of obese (ob/ob) mice," *Int J Obes,* vol. 13, pp. 155-63, 1989.

[5] J. Buren, H. X. Liu, J. Jensen, and J. W. Eriksson, "Dexamethasone impairs insulin signalling and glucose transport by depletion of insulin receptor substrate-1, phosphatidylinositol 3-kinase and protein kinase B in primary cultured rat adipocytes," *Eur J Endocrinol,* vol. 146, pp. 419-29, Mar 2002.

[6] J. Ruzzin, A. S. Wagman, and J. Jensen, "Glucocorticoid-induced insulin resistance in skeletal muscles: defects in insulin signalling and the effects of a selective glycogen synthase kinase-3 inhibitor," *Diabetologia,* vol. 48, pp. 2119-30, Oct 2005.

[7] L. L. Gathercole, I. J. Bujalska, P. M. Stewart, and J. W. Tomlinson, "Glucocorticoid modulation of insulin signaling in human subcutaneous adipose tissue," *J Clin Endocrinol Metab,* vol. 92, pp. 4332-9, Nov 2007.

[8] T. C. Brennan-Speranza, H. Henneicke, S. J. Gasparini, K. I. Blankenstein, U. Heinevetter, V. C. Cogger*, et al.*, "Osteoblasts mediate the adverse effects of glucocorticoids on fuel metabolism," *J Clin Invest,* vol. 122, pp. 4172-89, Nov 2012.

[9] A. Ekstrand, C. Saloranta, J. Ahonen, C. Gronhagen-Riska, and L. C. Groop, "Reversal of steroid-induced insulin resistance by a nicotinic-acid derivative in man," *Metabolism,* vol. 41, pp. 692-7, Jul 1992.

[10] N. Venkatesan, M. B. Davidson, and A. Hutchinson, "Possible role for the glucose-fatty acid cycle in dexamethasone-induced insulin antagonism in rats," *Metabolism,* vol. 36, pp. 883-91, Sep 1987.

[11] W. L. Holland, J. T. Brozinick, L. P. Wang, E. D. Hawkins, K. M. Sargent, Y. Liu*, et al.*, "Inhibition of ceramide synthesis ameliorates glucocorticoid-, saturated-fat-, and obesity-induced insulin resistance," *Cell Metab,* vol. 5, pp. 167-79, Mar 2007.

[12] S. K. Koliwad, T. Kuo, L. E. Shipp, N. E. Gray, F. Backhed, A. Y. So*, et al.*, "Angiopoietin-like 4 (ANGPTL4, fasting-induced adipose factor) is a direct glucocorticoid receptor target and participates in glucocorticoid-regulated triglyceride metabolism," *J Biol Chem,* vol. 284, pp. 25593-601, Sep 18 2009.

[13] C. Y. Yu, O. Mayba, J. V. Lee, J. Tran, C. Harris, T. P. Speed*, et al.*, "Genome-wide analysis of glucocorticoid receptor binding regions in adipocytes reveal gene network involved in triglyceride homeostasis," *PLoS One,* vol. 5, p. e15188, 2010.

[14] N. E. Gray, L. N. Lam, K. Yang, A. Y. Zhou, S. Koliwad, and J. C. Wang, "Angiopoietin-like 4 (Angptl4) protein is a physiological mediator of intracellular lipolysis in murine adipocytes," *J Biol Chem,* vol. 287, pp. 8444-56, Mar 9 2012.

[15] K. Yoshida, T. Shimizugawa, M. Ono, and H. Furukawa, "Angiopoietin-like protein 4 is a potent hyperlipidemia-inducing factor in mice and inhibitor of lipoprotein lipase," *J Lipid Res,* vol. 43, pp. 1770-2, Nov 2002.

[16] W. Dijk and S. Kersten, "Regulation of lipoprotein lipase by Angptl4," *Trends Endocrinol Metab,* vol. 25, pp. 146-55, Mar 2014.

[17] D. R. Alessi, M. Andjelkovic, B. Caudwell, P. Cron, N. Morrice, P. Cohen*, et al.*, "Mechanism of activation of protein kinase B by insulin and IGF-1," *EMBO J,* vol. 15, pp. 6541-51, Dec 2 1996.

[18] V. T. Samuel, K. F. Petersen, and G. I. Shulman, "Lipid-induced insulin resistance: unravelling the mechanism," *Lancet,* vol. 375, pp. 2267-77, Jun 26 2010.

[19] F. R. Jornayvaz and G. I. Shulman, "Diacylglycerol activation of protein kinase Cepsilon and hepatic insulin resistance," *Cell Metab,* vol. 15, pp. 574-84, May 2 2012.

[20] S. Fayyaz, J. Henkel, L. Japtok, S. Kramer, G. Damm, D. Seehofer*, et al.*, "Involvement of sphingosine 1-phosphate in palmitate-induced insulin resistance of hepatocytes via the S1P2 receptor subtype," *Diabetologia,* vol. 57, pp. 373-82, Feb 2014.

[21] S. Fayyaz, L. Japtok, and B. Kleuser, "Divergent role of sphingosine 1-phosphate on insulin resistance," *Cell Physiol Biochem,* vol. 34, pp. 134-47, 2014.

[22] J. W. Park, W. J. Park, and A. H. Futerman, "Ceramide synthases as potential targets for therapeutic intervention in human diseases," *Biochim Biophys Acta,* vol. 1841, pp. 671-81, May 2014.

[23] B. Chaurasia and S. A. Summers, "Ceramides - Lipotoxic Inducers of Metabolic Disorders," *Trends Endocrinol Metab,* vol. 26, pp. 538-50, Oct 2015.

[24] A. Koster, Y. B. Chao, M. Mosior, A. Ford, P. A. Gonzalez-DeWhitt, J. E. Hale*, et al.*, "Transgenic angiopoietin-like (angptl)4 overexpression and targeted disruption of angptl4

and angptl3: regulation of triglyceride metabolism," *Endocrinology,* vol. 146, pp. 4943-50, Nov 2005.

[25] R. N. Margolis and R. T. Curnow, "The role of insulin and glucocorticoids in the regulation of hepatic glycogen metabolism: effect of fasting, refeeding, and adrenalectomy," *Endocrinology,* vol. 113, pp. 2113-9, Dec 1983.

[26] R. T. Dobrowsky, C. Kamibayashi, M. C. Mumby, and Y. A. Hannun, "Ceramide activates heterotrimeric protein phosphatase 2A," *J Biol Chem,* vol. 268, pp. 15523-30, Jul 25 1993.

[27] G. Muller, M. Ayoub, P. Storz, J. Rennecke, D. Fabbro, and K. Pfizenmaier, "PKC zeta is a molecular switch in signal transduction of TNF-alpha, bifunctionally regulated by ceramide and arachidonic acid," *EMBO J,* vol. 14, pp. 1961-9, May 1 1995.

[28] Y. Kanoh, G. Bandyopadhyay, M. P. Sajan, M. L. Standaert, and R. V. Farese, "Thiazolidinedione treatment enhances insulin effects on protein kinase C-zeta /lambda activation and glucose transport in adipocytes of nondiabetic and Goto-Kakizaki type II diabetic rats," *J Biol Chem,* vol. 275, pp. 16690-6, Jun 2 2000.

[29] Y. Miyake, Y. Kozutsumi, S. Nakamura, T. Fujita, and T. Kawasaki, "Serine palmitoyltransferase is the primary target of a sphingosine-like immunosuppressant, ISP-1/myriocin," *Biochem Biophys Res Commun,* vol. 211, pp. 396-403, Jun 15 1995.

[30] L. Grontved, S. John, S. Baek, Y. Liu, J. R. Buckley, C. Vinson*, et al.*, "C/EBP maintains chromatin accessibility in liver and facilitates glucocorticoid receptor recruitment to steroid response elements," *EMBO J,* vol. 32, pp. 1568-83, May 29 2013.

[31] W. L. Holland, B. T. Bikman, L. P. Wang, G. Yuguang, K. M. Sargent, S. Bulchand*, et al.*, "Lipid-induced insulin resistance mediated by the proinflammatory receptor TLR4 requires saturated fatty acid-induced ceramide biosynthesis in mice," *J Clin Invest,* vol. 121, pp. 1858-70, May 2011.

[32] K. De Bosscher, W. Vanden Berghe, and G. Haegeman, "The interplay between the glucocorticoid receptor and nuclear factor-kappaB or activator protein-1: molecular mechanisms for gene repression," *Endocr Rev,* vol. 24, pp. 488-522, Aug 2003.

[33] N. A. Rao, M. T. McCalman, P. Moulos, K. J. Francoijs, A. Chatziioannou, F. N. Kolisis*, et al.*, "Coactivation of GR and NFKB alters the repertoire of their binding sites and target genes," *Genome Res,* vol. 21, pp. 1404-16, Sep 2011.

[34] A. Georgiadi and S. Kersten, "Mechanisms of gene regulation by fatty acids," *Adv Nutr,* vol. 3, pp. 127-34, Mar 2012.

[35] L. Poulsen, M. Siersbaek, and S. Mandrup, "PPARs: fatty acid sensors controlling metabolism," *Semin Cell Dev Biol,* vol. 23, pp. 631-9, Aug 2012.

[36] M. Baranowski, A. Blachnio, P. Zabielski, and J. Gorski, "PPARalpha agonist induces the accumulation of ceramide in the heart of rats fed high-fat diet," *J Physiol Pharmacol,* vol. 58, pp. 57-72, Mar 2007.

[37] M. Rivier, I. Castiel, I. Safonova, G. Ailhaud, and S. Michel, "Peroxisome proliferator-activated receptor-alpha enhances lipid metabolism in a skin equivalent model," *J Invest Dermatol,* vol. 114, pp. 681-7, Apr 2000.

[38] I. L. Aye, X. Gao, S. T. Weintraub, T. Jansson, and T. L. Powell, "Adiponectin inhibits insulin function in primary trophoblasts by PPARalpha-mediated ceramide synthesis," *Mol Endocrinol,* vol. 28, pp. 512-24, Apr 2014.

[39] M. Baranowski, A. Blachnio, P. Zabielski, and J. Gorski, "Pioglitazone induces de novo ceramide synthesis in the rat heart," *Prostaglandins Other Lipid Mediat,* vol. 83, pp. 99-111, Feb 2007.

[40] S. M. Turpin, H. T. Nicholls, D. M. Willmes, A. Mourier, S. Brodesser, C. M. Wunderlich*, et al.*, "Obesity-induced CerS6-dependent C16:0 ceramide production promotes weight gain and glucose intolerance," *Cell Metab,* vol. 20, pp. 678-86, Oct 7 2014.

[41] S. Raichur, S. T. Wang, P. W. Chan, Y. Li, J. Ching, B. Chaurasia*, et al.*, "CerS2 haploinsufficiency inhibits beta-oxidation and confers susceptibility to diet-induced steatohepatitis and insulin resistance," *Cell Metab,* vol. 20, pp. 687-95, Oct 7 2014.

[42] J. Y. Xia, W. L. Holland, C. M. Kusminski, K. Sun, A. X. Sharma, M. J. Pearson*, et al.*, "Targeted Induction of Ceramide Degradation Leads to Improved Systemic Metabolism and Reduced Hepatic Steatosis," *Cell Metab,* vol. 22, pp. 266-78, Aug 4 2015.

[43] T. Galbo, R. J. Perry, M. J. Jurczak, J. P. Camporez, T. C. Alves, M. Kahn*, et al.*, "Saturated and unsaturated fat induce hepatic insulin resistance independently of TLR-4 signaling and ceramide synthesis in vivo," *Proc Natl Acad Sci U S A,* vol. 110, pp. 12780-5, Jul 30 2013.

[44] A. H. Merrill, Jr., S. Lingrell, E. Wang, M. Nikolova-Karakashian, T. R. Vales, and D. E. Vance, "Sphingolipid biosynthesis de novo by rat hepatocytes in culture. Ceramide and sphingomyelin are associated with, but not required for, very low density lipoprotein secretion," *J Biol Chem,* vol. 270, pp. 13834-41, Jun 9 1995.

[45] J. M. Haus, S. R. Kashyap, T. Kasumov, R. Zhang, K. R. Kelly, R. A. Defronzo*, et al.*, "Plasma ceramides are elevated in obese subjects with type 2 diabetes and correlate with the severity of insulin resistance," *Diabetes,* vol. 58, pp. 337-43, Feb 2009.

[46] X. Lopez, A. B. Goldfine, W. L. Holland, R. Gordillo, and P. E. Scherer, "Plasma ceramides are elevated in female children and adolescents with type 2 diabetes," *J Pediatr Endocrinol Metab,* vol. 26, pp. 995-8, 2013.

[47] J. P. Kirwan, "Plasma ceramides target skeletal muscle in type 2 diabetes," *Diabetes,* vol. 62, pp. 352-4, Feb 2013.

[48] R. J. Perry, J. P. Camporez, R. Kursawe, P. M. Titchenell, D. Zhang, C. J. Perry*, et al.*, "Hepatic acetyl CoA links adipose tissue inflammation to hepatic insulin resistance and type 2 diabetes," *Cell,* vol. 160, pp. 745-58, Feb 12 2015.

[49] D. Patsouris, J. G. Neels, W. Fan, P. P. Li, M. T. Nguyen, and J. M. Olefsky, "Glucocorticoids and thiazolidinediones interfere with adipocyte-mediated macrophage chemotaxis and recruitment," *J Biol Chem,* vol. 284, pp. 31223-35, Nov 6 2009.

[50] F. Backhed, H. Ding, T. Wang, L. V. Hooper, G. Y. Koh, A. Nagy*, et al.*, "The gut microbiota as an environmental factor that regulates fat storage," *Proc Natl Acad Sci U S A,* vol. 101, pp. 15718-23, Nov 2 2004.

Supplemental Materials

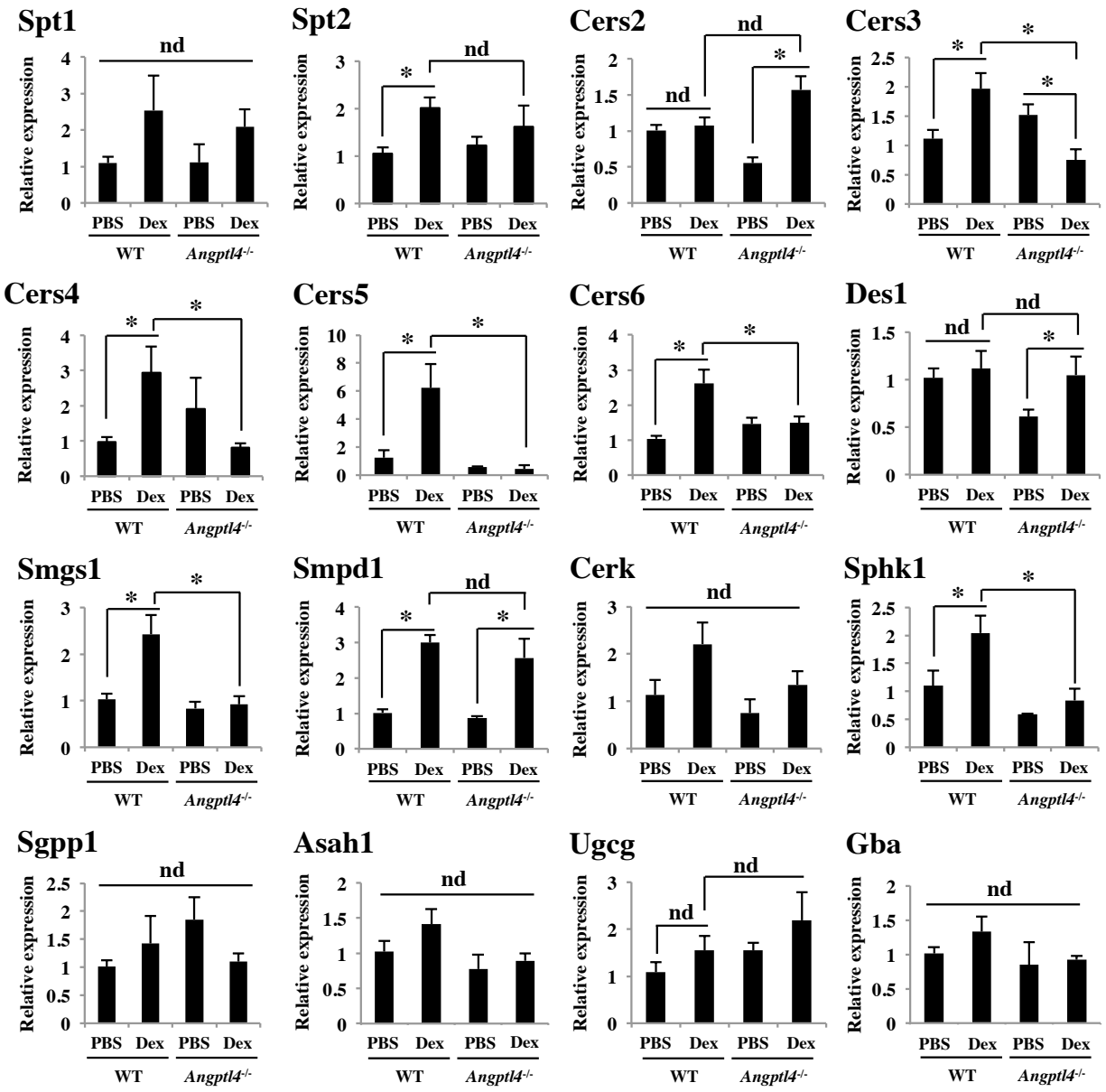

Fig.S1 Gene expression study on genes involved in ceramide metabolism.

Male 8-week-old WT and Angptl4$^{-/-}$ mice were treated with PBS or Dexamethasone (≈0.417 mg/kg of body weight) for 7 days prior to the collection of liver. Gene expression patterns were studied by RT-qPCR. Error bars represent S.E.M., n=3-4, and *p < 0.05

Table 1. Lipidomics data - Liver

Metabolite	C16:0 NAE	sphingosine	sphinganine	C16 MAGE	C18:1 NAE	C18:0 NAE	C16:0 MAG
WT PBS -1	0.693363725	0.658369365	0.622032041	0.826476251	0.856249222	0.865548774	0.764530273
WT PBS -2	1.586516428	0.97124944	0.87987114	0.971979768	1.408998563	1.45381677	1.155047416
WT PBS -3	1.02297112	1.387639121	1.366561264	1.340236387	0.915689823	0.965445461	1.299632513
WT PBS -4	0.697148726	0.982742074	1.131535555	0.861307595	0.819062392	0.715188995	0.780789799
WT Dex -1	0.677757023	0.585740546	0.590446505	1.036492082	0.55689241	1.35721912	0.505870463
WT Dex -2	0.547077076	0.526943234	0.621854544	0.763203135	0.527678704	0.777199128	0.354737271
WT Dex -3	0.516597432	0.570682557	0.655105	2.561474522	0.471837007	0.795390466	0.401655478
WT Dex -4	0.683090653	0.730251504	0.86569921	3.222802979	0.576180429	1.132237313	0.507066705
Angptl4$^{-/-}$ PBS-1	0.358342186	0.830239305	1.475829111	1.177186412	0.364628649	0.536003755	0.674691354
Angptl4$^{-/-}$ PBS-2	0.447466006	0.602855184	1.016450903	0.664223574	0.453362279	0.544653185	0.807750998
Angptl4$^{-/-}$ PBS-3	0.546602774	0.728387773	0.884443866	0.86513772	0.459459011	0.626252191	0.579637635
Angptl4$^{-/-}$ PBS-4	1.060295953	0.829716438	1.134095573	1.11573628	1.019634181	1.199885511	0.927432885
Angptl4$^{-/-}$ Dex-1	0.38608318	0.308051573	0.576685765	1.052361648	0.308354109	0.568976341	0.399055988
Angptl4$^{-/-}$ Dex-2	0.60714698	0.427899934	0.50256039	1.114346412	1.002737674	1.34129603	0.395931955
Angptl4$^{-/-}$ Dex-3	0.375727928	0.426419457	0.503332292	1.074270424	0.423459254	0.676258882	0.705183495
Angptl4$^{-/-}$ Dex-4	0.486785512	0.501759046	0.540118272	0.897356285	0.53083448	0.788211592	0.621043141
Metabolite	C16:0 NAE	sphingosine	sphinganine	C16 MAGE	C18:1 NAE	C18:0 NAE	C16:0 MAG
WT Con							
av	1	1	1	1	1	1	1
sem	0.210212966	0.149471293	0.160457545	0.117576928	0.137777216	0.159775394	0.13457292
WT Dex							
av	0.606130546	0.60340446	0.683276315	1.895993179	0.533147138	1.015511507	0.442332479
sem	0.043355797	0.044082525	0.062223885	0.593383314	0.02273862	0.140129425	0.03824824
FOLD (compare to WT PBS)	0.606130546	0.60340446	0.683276315	1.895993179	0.533147138	1.015511507	0.442332479
P value against WT PBS	0.116173024	0.043787632	0.115322843	0.18906448	0.015549177	0.94418746	0.007232646
Angptl4$^{-/-}$ PBS							
av	0.60317673	0.747799675	1.127704863	0.955570997	0.57427103	0.726698661	0.747378218
sem	0.157148651	0.053923075	0.126749323	0.118260943	0.150027495	0.159033642	0.076094699
FOLD (compare to WT PBS)	0.60317673	0.747799675	1.127704863	0.955570997	0.57427103	0.726698661	0.747378218
P value against WT PBS	0.181305465	0.16357393	0.555265208	0.79883532	0.081592326	0.270948528	0.153363484
Angptl4$^{-/-}$ Dex							
av	0.4639359	0.416032502	0.53067418	1.034583692	0.566346379	0.843685711	0.530303645
sem	0.053908264	0.040060003	0.017664043	0.047508372	0.152390726	0.171801821	0.078580276
FOLD (compare to Angptl4$^{-/-}$ PBS)	0.769154175	0.556342182	0.470578958	1.082686369	0.986200504	1.160984266	0.709551914
P valu against Angptl4$^{-/-}$ PBS	0.434082877	0.002606972	0.003448477	0.558075246	0.971641477	0.635072829	0.094435071
FOLD (compare to WT Dex)	0.765405906	0.689475352	0.776661166	0.545668467	1.062270318	0.830798771	1.198880185
P value aginst WT Dex	0.085595011	0.019924804	0.056341934	0.198029839	0.836538254	0.467758131	0.352982298

C-2 ceramide	C18:0p MAGp	C12:0 acyl carnitine	C18:0 MAGE	C20:4 NAE	MAG18:2	MAG18:1	C16:0e/C2:0 MAGe	C18:0 MAG
0.307138158	0.881548674	1.104313324	0.926020538	0.410508433	0.42664137	0.6211942	0.754453139	0.78623126
2.208861923	1.079616611	0.649959946	0.940932839	1.199671674	1.30371295	0.8570312	1.011520667	0.953019839
0.795578325	1.225343721	1.213575095	1.261412827	1.142629221	1.47721256	1.9327328	1.279315013	1.338357526
0.688421594	0.813490994	1.032151634	0.871633797	1.247190672	0.79243312	0.5890417	0.954711181	0.922391376
0.907471525	0.641039139	0.713817222	0.60311278	1.95599602	0.42886981	0.2254757	0.54828404	0.617345537
0.258718626	0.534593376	1.219019724	0.473888229	2.141884409	0.4396316	0.242928	0.413333948	0.384833249
1.271806647	0.645179332	0.852743534	1.394566643	0.820514922	0.50819537	0.2014191	0.289324733	0.283499377
0.205005516	0.767484137	1.0952646	1.92664972	0.230909023	0.47689354	0.2468946	0.589189652	0.694961582
0.568423956	0.982002102	2.530236087	0.996623772	0.274437407	1.60730138	0.6911899	0.398298153	0.411523103
1.070348156	0.702021519	2.54096518	0.330128121	0.420016202	2.62103144	1.3144461	0.503265428	0.519059469
0.810177368	0.841146643	3.692082692	0.622625463	0.325286028	1.42657015	0.6100758	0.589049453	0.568788207
0.838915315	1.001143272	4.300244286	0.732173321	0.496095257	2.19559914	0.9231682	0.695288999	0.755613175
1.224923573	0.517050884	3.066020052	0.552961013	0.429944091	0.37728198	0.1553162	0.37540173	0.426392583
0.392657626	0.590314328	2.579232873	0.798983775	0.558315483	0.24856199	0.1222049	0.40629239	0.428322646
0.857934364	0.566159193	2.358783128	0.590026078	0.268122582	0.53029408	0.188254	0.612434479	0.622688493
0.680189075	0.595331532	2.895956333	0.516502194	0.066646262	0.39022826	0.1529171	0.580380402	0.526913516
C-2 ceramide	C18:0p MAGp	C12:0 acyl carnitine	C18:0 MAGE	C20:4 NAE	MAG18:2	MAG18:1	C16:0e/C2:0 MAGe	C18:0 MAG
1	1	1	1	1	1	1	1	1
0.416360621	0.09395696	0.122493999	0.08840081	0.197656142	0.24010371	0.316598	0.108202719	0.118466987
0.660750578	0.647073996	0.97021127	1.099554343	1.287326094	0.46339758	0.2291794	0.460033093	0.495159936
0.258778219	0.047601209	0.114411742	0.342664964	0.457467584	0.0181337	0.010357	0.068185898	0.09653246
0.660750578	0.647073996	0.97021127	1.099554343	1.287326094	0.46339758	0.2291794	0.460033093	0.495159936
0.514795063	0.015404794	0.864790265	0.787915709	0.585198348	0.067402	0.0509267	0.005549265	0.016335116
0.821966199	0.881578384	3.265882061	0.670387669	0.378958723	1.96262553	0.88472	0.546475508	0.563745988
0.102633456	0.069675485	0.439529263	0.137932728	0.049339089	0.27407202	0.157857	0.063101529	0.071883664
0.821966199	0.881578384	3.265882061	0.670387669	0.378958723	1.96262553	0.88472	0.546475508	0.563745988
0.69245633	0.350423373	0.002536979	0.09091216	0.022555673	0.03844302	0.7555942	0.01108767	0.019858682
0.788926159	0.567213984	2.724998097	0.614618265	0.330757104	0.38659158	0.1546731	0.49362725	0.501079309
0.174094893	0.017892437	0.15834656	0.063261229	0.106183212	0.0575923	0.0134949	0.060031879	0.04684001
0.959803652	0.643407319	0.834383498	0.916810218	0.872805094	0.19697674	0.1748271	0.90329254	0.888838802
0.875502737	0.004718796	0.290963611	0.72585119	0.694879111	0.00134638	0.0036614	0.566230249	0.492667386
1.193984818	0.876582876	2.808664649	0.55897034	0.256933427	0.83425463	0.6748996	1.073025522	1.011954467
0.695373085	0.167373482	0.00010643	0.213423651	0.087825363	0.25043059	0.004669	0.724240703	0.957795419

C20:4 MAG	C18:0p/C2:0 MAGp	C18:0e/C2:0 MAGe	C16:0 acyl carnitine	C22:6 MAG	C18:0 acyl carnitine	C16:0 alkyl LPE
0.553522596	0.927039956	0.970047951	0.996373663	0.602743481	0.847674533	0.763847804
1.203377763	1.064808354	1.094015108	0.661418414	1.214805167	1.083313443	1.073083235
1.324920595	0.972501195	1.089839902	1.263388727	1.303467806	1.263231856	1.089353268
0.918179046	1.035650495	0.84609704	1.078819196	0.878983546	0.805780168	1.073715693
0.23689391	0.588131158	0.677229846	0.911620122	0.247527282	1.307907968	0.889367515
0.309235671	0.470492851	0.668193929	1.020833224	0.23765274	0.950810338	0.766637321
0.289055602	0.492394808	0.691665855	1.167448473	0.254933062	2.129764698	0.961154212
0.336180341	0.439555566	0.523207519	1.235300972	0.351485105	1.558285409	1.537889939
1.831326961	1.480632278	0.819234002	2.510964587	1.17085658	1.490676424	1.38625755
1.234868778	1.177878427	0.764914465	1.542119017	0.91288831	1.137631993	0.97226437
0.890140728	1.354929656	0.954413136	1.459206488	0.778197296	1.088478798	1.06575611
1.167682023	1.40999732	0.890341228	1.782488547	1.058961644	1.31710451	1.229232776
0.2391371	0.554686489	0.595429869	2.121986913	0.21380183	4.901116557	0.725493139
0.234310358	0.619476941	0.607663494	2.082762613	0.240988327	1.982016297	1.432051343
0.508832863	0.609988399	0.604233861	1.818821187	0.370486319	2.109959622	1.39637428
0.32530194	0.551273834	0.604934845	2.278279676	0.27757392	2.369199256	1.314320235
C20:4 MAG	C18:0p/C2:0 MAGp	C18:0e/C2:0 MAGe	C16:0 acyl carnitine	C22:6 MAG	C18:0 acyl carnitine	C16:0 alkyl LPE
1	1	1	1	1	1	1
0.171506231	0.031024765	0.058802845	0.125908938	0.160906726	0.106909826	0.078807269
0.292841381	0.497643596	0.640074287	1.083800698	0.272899547	1.486692103	1.038762247
0.020998988	0.032050651	0.039254279	0.072778395	0.026433208	0.247958497	0.171153494
0.292841381	0.497643596	0.640074287	1.083800698	0.272899547	1.486692103	1.038762247
0.006410047	2.93037E-05	0.002241597	0.585411024	0.004287586	0.121547569	0.843814464
1.281004623	1.35585942	0.857225708	1.82369466	0.980225957	1.258472931	1.163377701
0.198031939	0.064664053	0.041338813	0.239125903	0.085580995	0.09167727	0.091317486
1.281004623	1.35585942	0.857225708	1.82369466	0.980225957	1.258472931	1.163377701
0.324668756	0.002547956	0.094197991	0.022572235	0.917136966	0.11613338	0.2243681
0.326895565	0.583856416	0.603065517	2.075462597	0.275712599	2.840572933	1.217059749
0.064146505	0.01794485	0.002650533	0.095401512	0.034186061	0.691553112	0.165698627
0.255186874	0.430617221	0.703508436	1.138053778	0.281274533	2.257158547	1.046143267
0.00375668	2.5921E-05	0.000857519	0.365883556	0.000261558	0.063850889	0.786147352
1.116288838	1.173242097	0.942180509	1.914985478	1.010308011	1.910666591	1.171644188
0.631874531	0.057288414	0.383192835	0.000169804	0.950211751	0.114921635	0.482484202

C16:0 LPE	C18:1 alkyl LPE	C18:0 alkyl LPE	C16:0 alkyl LPG	C18:1 LPE	C16:0 alkyl LPC	C18:0 LPE	C16:0e LPCe
0.864928722	0.647344106	0.668008727	ND	0.915888797	0.909491015	0.78093511	0.782651506
0.825754101	1.301439196	1.094516889	ND	0.943670455	1.19601404	0.870009583	1.156366573
1.289299003	0.944392645	1.16991153	ND	1.392615574	1.072823078	1.309659253	0.901685202
1.020018174	1.106824053	1.067562855	ND	0.747825174	0.821671867	1.039396054	1.159296719
0.620331716	0.622988911	0.645282302	ND	0.376596486	1.059685031	0.861143135	0.450955794
0.769630425	0.548381424	0.465392867	ND	0.565767266	0.954146893	0.993036989	0.364591153
0.613135197	0.565661959	0.687367339	ND	0.458255947	0.801362454	0.806904855	0.349382064
0.901278609	0.84916586	0.977276832	ND	0.747072223	1.152489895	1.026722519	0.516337305
0.64574725	1.578108059	1.395669832	ND	0.954866685	1.121950779	0.803909063	1.701435336
0.620240969	1.096660091	1.15461116	ND	0.974534152	1.14214125	0.835785639	1.107204934
0.724918243	0.854078376	1.10983395	ND	0.908358703	1.176472687	0.889340181	1.046298324
0.65004942	1.24474133	1.194395631	ND	0.905283108	1.202329645	0.808945663	0.961598782
0.536600932	0.382864547	0.801079955	ND	0.470937631	1.061093658	0.661604572	0.341730041
0.422789359	0.593643831	1.740590293	ND	0.305087962	1.033948386	0.500092331	0.418940119
0.45870843	0.544754164	1.19644689	ND	0.364059288	1.197130611	0.598475526	0.428300193
0.470845728	0.474426048	1.379462445	ND	0.301158807	1.101089426	0.534895986	0.434503947
C16:0 LPE	C18:1 alkyl LPE	C18:0 alkyl LPE	C16:0 alkyl LPG	C18:1 LPE	C16:0 alkyl LPC	C18:0 LPE	C16:0e LPCe
1	1	1	ND	1	1	1	1
0.105158818	0.13836405	0.112763142	ND	0.13783651	0.083525198	0.116307006	0.094309825
0.726093987	0.646549538	0.693829835	ND	0.53692298	0.991921068	0.921951875	0.420316579
0.068635765	0.069395159	0.106036266	ND	0.080045708	0.075340215	0.052411434	0.039046735
0.726093987	0.646549538	0.693829835	ND	0.53692298	0.991921068	0.921951875	0.420316579
0.07194189	0.062507233	0.095287539	ND	0.027148043	0.945077	0.563117106	0.001284425
0.66023897	1.193396964	1.213627643	ND	0.935760662	1.16072359	0.834495137	1.204134344
0.022540862	0.151419395	0.063090745	ND	0.017195378	0.017859946	0.01957449	0.168433789
0.66023897	1.193396964	1.213627643	ND	0.935760662	1.16072359	0.834495137	1.204134344
0.019585584	0.382146869	0.149355374	ND	0.660040659	0.1088957	0.210113999	0.331000638
0.472236112	0.498922148	1.279394896	ND	0.360310922	1.09831552	0.573767104	0.405868575
0.023757004	0.04577317	0.195443995	ND	0.039582053	0.035707973	0.035666117	0.021617468
0.715250285	0.418068893	1.054190635	ND	0.385046024	0.946233478	0.68756195	0.337062535
0.001214532	0.004616866	0.759652082	ND	1.10063E-05	0.169054906	0.00068082	0.003323451
0.650378767	0.771668864	1.843960624	ND	0.671066308	1.107261006	0.622339538	0.9656259
0.012901883	0.126103007	0.038879072	ND	0.095315098	0.249085905	0.001525878	0.757137587

C16:0 alkyl LPS	C16:0 LPG	C20:4 alkyl LPE	C16:0 LPC	C18:1 alkyl LPG	C16:0 LPS	C18:0e LPGe	C20:4 LPE	C18:0p LPCp
0.621354152	ND	0.873339545	0.977825428	ND	0.893217218	0.983934213	0.825011873	0.926492039
1.992333513	ND	1.284464508	1.002241087	ND	1.031517824	0.775329548	1.211392789	1.100268309
0.708340812	ND	0.56638541	1.195593889	ND	1.336299713	1.217839956	1.008622776	1.133091966
0.677971522	ND	1.275810536	0.824339596	ND	0.738965246	1.022896283	0.954972561	0.840147686
0.722357564	ND	0.173783444	0.640087395	ND	0.487876176	0.278444902	0.24110062	0.445182185
0.596012473	ND	0.354372759	0.651602812	ND	0.482861592	0.368480283	0.256839406	0.515594371
0.197542577	ND	3.066281104	0.598710803	ND	0.545795799	0.455550782	0.217570425	0.446354659
1.735171647	ND	0.82045506	0.707111861	ND	0.615285386	0.541533725	0.350643179	0.814605369
1.940389435	ND	1.320321417	0.960916111	ND	0.812582919	0.698380384	0.782429826	0.979423729
1.136615765	ND	0.551950774	0.971019904	ND	0.69110509	0.646984181	0.718578661	0.95742728
0.9041934	ND	1.280485528	0.906721604	ND	0.881357345	0.638872655	0.64673172	0.775364559
0.675371367	ND	1.200266849	0.866658879	ND	0.752367132	0.526468872	0.79496637	0.83496964
0.803951835	ND	1.185219893	0.626027869	ND	0.490781035	0.21060822	0.172363531	0.476435841
73.4079081	ND	0.784770877	0.491272151	ND	0.389600377	0.268850367	0.189609007	0.31965671
0.804033706	ND	0.834398595	0.568621025	ND	0.431632787	0.349191039	0.217359988	0.408467328
0.496840283	ND	0.946440268	0.617455191	ND	0.46258799	0.297547015	0.187815936	0.345054882
C16:0 alkyl LPS	C16:0 LPG	C20:4 alkyl LPE	C16:0 LPC	C18:1 alkyl LPG	C16:0 LPS	C18:0e LPGe	C20:4 LPE	C18:0p LPCp
1	ND	1	1	ND	1	1	1	1
0.331268509	ND	0.173458927	0.076163356	ND	0.127027745	0.090697945	0.080316861	0.069954383
0.812771065	ND	1.103723092	0.649378218	ND	0.532954738	0.411002423	0.266538408	0.555434146
0.327170676	ND	0.668218303	0.022345075	ND	0.030936263	0.056570462	0.029172801	0.087944471
0.812771065	ND	1.103723092	0.649378218	ND	0.532954738	0.411002423	0.266538408	0.555434146
0.701523655	ND	0.885495737	0.00448365	ND	0.011751494	0.001500672	0.000137403	0.007484791
1.164142492	ND	1.088256142	0.926329124	ND	0.784353122	0.627676523	0.735676644	0.886796302
0.275346415	ND	0.180503064	0.024390091	ND	0.040748251	0.036217127	0.034040016	0.048880476
1.164142492	ND	1.088256142	0.926329124	ND	0.784353122	0.627676523	0.735676644	0.886796302
0.716291591	ND	0.736481553	0.39248287	ND	0.157113145	0.008838958	0.023094963	0.232926497
18.87818348	ND	0.937707408	0.575844059	ND	0.443650547	0.28154916	0.191787116	0.38740369
18.17671905	ND	0.089163233	0.030895632	ND	0.021690545	0.028903909	0.009361988	0.035063603
16.21638555	ND	0.861660571	0.621640888	ND	0.565626037	0.448557736	0.260694854	0.436857584
0.36747369	ND	0.482853758	0.000111827	ND	0.000317294	0.000297078	4.72835E-06	0.000165601
23.22693842	ND	0.849585748	0.886762203	ND	0.832435694	0.685030415	0.719547765	0.697479068
0.358731196	ND	0.813687386	0.102049445	ND	0.056005958	0.087714316	0.050484924	0.126285691

C18:0e LPCe	C18:0 alkyl LPC	C18:1 alkyl LPS	C18:1 LPG	C18:0 alkyl LPS	C18:0 LPG	C20:4 alkyl LPG	C18:1 LPC	C16:0 PAF/LPC
0.741555151	0.709832105	0.900156492	0.688916859	1.14913282	0.688687768	ND	0.945842657	0.841261762
1.140980579	1.239825111	1.143220543	1.188177518	0.462028131	0.427428435	ND	0.855460489	1.057139793
0.965476388	1.074843792	0.285617404	1.191631163	0.281261476	1.782351275	ND	1.290493515	1.162824591
1.151987882	0.975498992	1.671005562	0.93127446	2.107577572	1.101532522	ND	0.908203339	0.938773854
0.590538224	0.767068692	0.146919502	0.518004975	0.148670978	1.482759202	ND	0.342826429	0.798355877
0.657966008	0.723947836	0.083414429	1.550380762	0.3676042	0.297814552	ND	0.472464396	0.835155479
0.448857458	0.594867435	0.163884634	0.746315417	0.662469018	1.203167519	ND	0.338763299	0.716924611
0.804722788	0.959990077	0.777187635	0.581451664	0.627996045	0.730999346	ND	0.67388018	0.888061708
1.564337873	1.468985864	0.364615152	1.132476175	0.348216759	0.324167979	ND	0.991234862	1.158160154
1.364622329	1.216383773	0.432727504	1.108824493	4.080247289	0.324748019	ND	0.886421163	1.092586638
1.053748449	1.029656658	0.36700285	1.767299937	0.171066269	0.793515843	ND	0.835872004	1.105062339
1.033946998	1.250149019	0.826433453	0.815791911	2.609700275	2.703211686	ND	0.786686188	1.010539562
0.489871908	0.637586941	0.060704698	3.395258475	0.097084191	2.343367567	ND	0.341628376	0.716044479
0.45476308	0.516324101	0.66287184	0.761616376	0.244774911	0.710796338	ND	0.245687954	0.628728764
0.67639794	0.722799622	0.153851791	0.808051298	0.174432151	0.524845971	ND	0.300390141	0.621254274
0.509827945	0.579697423	0.132507994	0.694512751	0.601559612	0.330806919	ND	0.269577685	0.669435547
C18:0e LPCe	C18:0 alkyl LPC	C18:1 alkyl LPS	C18:1 LPG	C18:0 alkyl LPS	C18:0 LPG	C20:4 alkyl LPG	C18:1 LPC	C16:0 PAF/LPC
1	1	1	1	1	1	ND	1	1
0.096160222	0.11102379	0.287383572	0.120287573	0.413820359	0.295400276	ND	0.098589129	0.069954314
0.625521119	0.76146851	0.29285155	0.849038204	0.45168506	0.928685155	ND	0.456983576	0.809624419
0.073936775	0.075611889	0.162371482	0.23868021	0.120555162	0.261313352	ND	0.078682739	0.035968131
0.625521119	0.76146851	0.29285155	0.849038204	0.45168506	0.928685155	ND	0.456983576	0.809624419
0.021463433	0.126113352	0.075904223	0.592674476	0.250406166	0.862460776	ND	0.005065354	0.051845485
1.254163912	1.241293829	0.49769474	1.206098129	1.802307648	1.036410882	ND	0.875053554	1.091587173
0.128150561	0.090061498	0.110709993	0.200451317	0.940576978	0.566493373	ND	0.043752432	0.03052766
1.254163912	1.241293829	0.49769474	1.206098129	1.802307648	1.036410882	ND	0.875053554	1.091587173
0.163749494	0.142407787	0.154008293	0.41190591	0.464618166	0.956402769	ND	0.290721574	0.275381943
0.532715218	0.614102022	0.252484081	1.414859725	0.279462716	0.977454199	ND	0.289321039	0.658865766
0.049227903	0.04388518	0.138238934	0.660544114	0.111520925	0.461865119	ND	0.02072082	0.021802119
0.424757253	0.494727362	0.507307111	1.1730884	0.155058276	0.943114566	ND	0.33063238	0.603585112
0.001910049	0.000770948	0.215484202	0.772537046	0.159005029	0.938334267	ND	1.93623E-05	2.55197E-05
0.851634265	0.806470673	0.862157229	1.666426455	0.618711445	1.052514077	ND	0.633110366	0.813791866
0.336366854	0.142842639	0.856099951	0.451200831	0.33471634	0.929767525	ND	0.084984362	0.011581951

C16:0 PAF	C18:0 LPC	C18:1 LPS	C18:0 LPS	C20:4e LPCe	C20:4 alkyl LPS	C20:4 LPG	C16:0 Ceramide	C20:4 LPC	C20:4 LPS
0.856767463	0.856767463	0.747472698	0.688445144	1.010998075	0.713250384	0.44357217	0.813008162	0.834055973	0.603299611
1.041132465	1.041132465	1.056045019	1.00609246	1.05291121	1.965792706	1.21709108	1.079218808	1.229814616	1.471125197
1.223220254	1.223220254	1.290186844	1.490826351	0.866860671	1.052095581	1.57895263	1.313810953	1.07364876	1.069444864
0.878879819	0.878879819	0.906295438	0.814636045	1.069230044	0.268861329	0.76038412	0.793962077	0.86248065	0.856130328
0.794594905	0.794594905	0.264006293	0.460992655	0.229651859	0.407763234	0.67573403	0.780494581	0.284613459	0.121564495
0.786785199	0.786785199	0.320387638	0.543923213	0.271959159	0.522315544	0.38713911	0.683262354	0.278747924	0.099830201
0.71084146	0.71084146	0.335412837	0.625690426	0.138221691	0.346362851	0.22343396	0.869610382	0.258900246	0.114443741
0.872654834	0.872654834	0.525318897	0.733880808	0.370365245	0.672549366	0.72993483	0.620417847	0.294584861	0.154849237
1.16477717	1.16477717	0.964843147	0.858522639	1.096981843	0.524830266	0.27932589	1.671870221	1.11509917	0.847046124
1.047702573	1.047702573	0.824451394	0.811071396	1.01420667	0.393764495	0.62540863	1.026890121	0.925597059	0.712950581
1.04977675	1.04977675	0.939273252	1.040953485	0.963632493	1.064681195	0.68606806	0.783927319	0.901616907	0.693593325
1.017741754	1.017741754	0.989819934	0.940916162	0.911430513	0.8846291	1.06158541	0.825704676	0.841688245	0.761284154
0.689165726	0.689165726	0.298401844	0.503355775	0.31789182	1.055372483	0.41583348	0.612663881	0.313223695	0.090904836
0.596853168	0.596853168	0.191569498	0.373617265	0.262861311	1.265082989	0.61599198	0.544658895	0.275984699	0.085757267
0.58692185	0.58692185	0.25299953	0.370595282	0.267691432	1.187982351	0.49632894	0.466253471	0.251405454	0.073982983
0.621572555	0.621572555	0.23854556	0.37510908	0.265931933	1.320865191	1.84297283	0.636249962	0.265927382	0.07484167
C16:0 PAF	C18:0 LPC	C18:1 LPS	C18:0 LPS	C20:4e LPCe	C20:4 alkyl LPS	C20:4 LPG	C16:0 Ceramide	C20:4 LPC	C20:4 LPS
1	1	1	1	1	1	1	1	1	1
0.085002362	0.085002362	0.115433975	0.176156618	0.046042945	0.359659399	0.24989037	0.123210696	0.093402306	0.183677984
0.791219099	0.791219099	0.361281416	0.591121775	0.252549488	0.487247749	0.50406048	0.738446291	0.279211623	0.122671919
0.033069875	0.033069875	0.056798055	0.058264072	0.048177134	0.071724462	0.12003919	0.054732728	0.007518219	0.011640637
0.791219099	0.791219099	0.361281416	0.591121775	0.252549488	0.487247749	0.50406048	0.738446291	0.279211623	0.122671919
0.06202506	0.06202506	0.002540156	0.069746228	2.99986E-05	0.211574217	0.12383591	0.100439749	0.000252798	0.003104349
1.069999562	1.069999562	0.929596932	0.91286592	0.99656288	0.716976264	0.66309699	1.077098084	0.946000345	0.753718546
0.032429143	0.032429143	0.036535737	0.050422017	0.039504432	0.155561382	0.16021375	0.205228019	0.05906325	0.034210554
1.069999562	1.069999562	0.929596932	0.91286592	0.99656288	0.716976264	0.66309699	1.077098084	0.946000345	0.753718546
0.470844881	0.470844881	0.582094515	0.651218644	0.956659602	0.49730839	0.29968588	0.758315759	0.642441494	0.235534144
0.623628325	0.623628325	0.245379108	0.405669351	0.278594124	1.207325754	0.8427818	0.564956552	0.276635307	0.081371689
0.023028337	0.023028337	0.022006917	0.032575674	0.013137193	0.057511641	0.33592288	0.038202348	0.013198291	0.004156805
0.582830449	0.582830449	0.263962906	0.444390947	0.279554988	1.683913142	1.27097817	0.524517275	0.292426222	0.107960311
2.98966E-05	2.98966E-05	3.72796E-06	0.000150087	2.43462E-06	0.025396406	0.64634809	0.049565928	3.25159E-05	1.1748E-06
0.788186642	0.788186642	0.679191059	0.686270355	1.10312686	2.477847782	1.67198547	0.765061127	0.990772893	0.66332776
0.005952382	0.005952382	0.105762913	0.032072488	0.620661992	0.000228771	0.37901377	0.040704059	0.870889077	0.015586739

C20:1 LPC	C18:0p LPCp	C20:0 LPC	C18:1 Ceramide	C18:0 Ceramide	C20:4 Ceramide	C16:0/C18:1 DAG	C16:0/C20:4 DAG
0.870195209	0.91412307	0.874148826	1.179649148	0.996493832	0.643321075	1.213000445	1.08407649
0.709941672	0.692498378	0.938457003	0.65354339	1.123003655	1.428229758	0.624331977	1.124597517
1.317325438	1.378159311	1.166341826	1.842816636	1.589388625	1.316644162	1.83607327	1.268150169
1.102537682	1.015219242	1.021052345	0.323990826	0.291113887	0.611805005	0.326594308	0.523175824
0.126067008	0.122052069	0.242969936	1.066982017	2.328450867	0.927699898	1.424466598	0.414021414
0.217358114	0.224028049	0.188939204	2.803578946	2.797039787	0.978521249	1.131575525	0.334596398
0.131920928	0.138570235	0.156010624	0.835141319	2.765926077	1.019489192	1.53812953	0.520034398
0.36550106	0.349681004	0.309610253	0.857814611	2.147108743	0.93072218	1.183663004	0.390492858
1.139266387	1.302773867	1.086880771	1.187674089	0.031085551	0.772266645	0.24669588	1.170014233
1.070643749	1.025319158	0.878620156	0.075741224	0.050686619	0.671268754	0.181891693	0.622700184
0.733407796	0.75391244	0.87108363	0.431602899	0.820646155	0.894561004	0.281383634	0.811315309
0.748021689	0.768137637	0.889889395	0.773212964	1.751265161	1.352129166	0.186320833	0.647888244
0.164555025	0.16412959	0.225960825	1.99432	2.424129952	0.985358402	0.746217263	0.525030463
0.146214188	0.157474162	0.229671649	1.74477973	1.407642416	1.203906977	0.738528367	0.444562735
0.156471423	0.177422611	0.264051161	0.382020895	1.170416041	0.808820075	0.446540385	0.4158458
0.139849911	0.134114776	0.26036431	2.202668315	1.485682333	1.260589815	0.378092823	0.340222188
C20:1 LPC	C18:0p LPCp	C20:0 LPC	C18:1 Ceramide	C18:0 Ceramide	C20:4 Ceramide	C16:0/C18:1 DAG	C16:0/C20:4 DAG
1	1	1	1	1	1	1	1
0.132976353	0.142935937	0.063073279	0.331616531	0.268489706	0.216325268	0.334039592	0.163773015
0.210211778	0.208582839	0.224382504	1.390879223	2.509631368	0.96410813	1.319458664	0.414786267
0.055808923	0.052070934	0.033590925	0.473781983	0.161384532	0.021823117	0.096860789	0.038835485
0.210211778	0.208582839	0.224382504	1.390879223	2.509631368	0.96410813	1.319458664	0.414786267
0.001548406	0.002010138	3.62362E-05	0.524284518	0.002942763	0.874303698	0.393775227	0.013192197
0.922834905	0.962535776	0.931618488	0.617057794	0.663420871	0.922556392	0.22407301	0.812979492
0.106117989	0.1294276	0.051898126	0.237592884	0.406552191	0.150291105	0.024153661	0.126140765
0.922834905	0.962535776	0.931618488	0.617057794	0.663420871	0.922556392	0.22407301	0.812979492
0.66608157	0.852360515	0.434560045	0.384113949	0.515493102	0.778659126	0.059709188	0.400488123
0.151772637	0.158285285	0.245011986	1.580947235	1.621967685	1.064668817	0.577344709	0.431415296
0.005465923	0.009061202	0.009985225	0.410454991	0.27566166	0.103891379	0.09631078	0.038182944
0.164463477	0.164446131	0.262996054	2.562073197	2.444854776	1.154041992	2.576591932	0.530659506
0.00034815	0.000812401	1.28081E-05	0.088369315	0.098859659	0.466225043	0.011958015	0.027507097
0.721998733	0.758860533	1.091938907	1.136653139	0.646297184	1.104304366	0.437561801	1.040090597
0.337504667	0.378023241	0.577548938	0.77196767	0.032042864	0.380074672	0.001612921	0.770428922

C18:0/C18:1 DAG	C18:0/C20:4 DAG	C16:0/18:1 alkyl PE	C16:0 SM	C16:0/C18:1 PE	Plasmalogen PE 16:0/20:4	C16:0/20:4 alkyl PE
0.97209154	0.843382633	0.068543198	0.75856114	0.923250183	0.766023648	0.810313523
0.961706483	1.549707043	1.030973557	0.94183671	1.145070372	1.170730868	1.450862285
1.514533241	0.983283506	2.432986801	1.3236304	1.226243993	1.163855768	1.002783355
0.551668737	0.623626819	0.467496444	0.97597176	0.705435452	0.899389716	0.736040838
5.495438249	0.790973062	0.09552735	0.56715651	1.3522448	0.736683595	0.755160703
3.778498115	0.77812335	0.126844899	0.50932063	1.508757699	0.906136968	0.906282002
5.25787496	1.061132467	0.114891951	0.48924494	1.908985917	0.832252315	0.845613124
3.827919093	0.834929787	0.069319382	0.65211455	1.468449889	0.842621263	0.892510506
0.710403653	1.04268905	1.017598732	0.71987058	0.583121374	1.164161212	1.056231264
0.520340857	0.701097701	0.357660999	0.86572765	0.676749738	0.783202992	0.885060092
0.540695003	0.820350055	0.438871585	0.97121627	0.719423274	0.783523071	0.831744102
0.440010659	1.018286711	0.086361722	0.94974608	0.660967943	0.972890196	1.294813475
3.188716347	1.009868684	0.181898366	0.52557175	1.123833059	0.643961926	0.819313293
2.344969243	1.129139955	0.096952786	0.55493534	1.025076732	0.663922894	0.7995922
1.566339616	0.816673469	0.067584001	0.46884589	0.841091675	0.585226306	0.690118269
1.30706058	0.758013649	0.198594225	0.58546597	1.14963037	0.640934779	0.798292921
C18:0/C18:1 DAG	C18:0/C20:4 DAG	C16:0/18:1 alkyl PE	C16:0 SM	C16:0/C18:1 PE	Plasmalogen PE 16:0/20:4	C16:0/20:4 alkyl PE
1	1	1	1	1	1	1
0.197482204	0.197619805	0.516848007	0.11796528	0.117221501	0.100359813	0.160452471
4.589932604	0.866289666	0.101645895	0.55445916	1.559609576	0.829423535	0.849891584
0.456907903	0.066076376	0.012559485	0.03650135	0.121092244	0.03496168	0.034142467
4.589932604	0.866289666	0.101645895	0.55445916	1.559609576	0.829423535	0.849891584
0.000359978	0.544796846	0.132945862	0.01125653	0.015995893	0.159606189	0.395453398
0.552862543	0.895605879	0.47512326	0.87664015	0.660065582	0.925944368	1.016962233
0.056833425	0.081741929	0.195901067	0.05699774	0.028464777	0.091108956	0.10426221
0.552862543	0.895605879	0.47512326	0.87664015	0.660065582	0.925944368	1.016962233
0.072472172	0.642771421	0.37897507	0.38275458	0.030432578	0.604532853	0.932249472
2.101771446	0.928423939	0.136257344	0.53370474	1.034907959	0.633511476	0.776829171
0.424150818	0.085852587	0.031924215	0.02483744	0.069958506	0.016883496	0.029300923
3.801616646	1.036643417	0.286783149	0.60880709	1.567886565	0.684178767	0.763872192
0.011104609	0.791188883	0.138642849	0.00149286	0.002544657	0.019665133	0.068454651
0.457908999	1.071724592	1.340510051	0.96256818	0.66356861	0.763797323	0.914033255
0.007191855	0.587122483	0.35196075	0.65489371	0.009488114	0.002342784	0.155521197

C18:1 SM	C18:0 SM	C18:0/C18:1 alkyl PE	C16:0/18:1 alkyl PG	C16:0/C20:4 PE	C18:0/C18:1PE	C16:0e/C18:1 PCe	C16:0e/C18:1 PSe
1.0260668	1.06703052	1.10176361	1.092086918	0.890895395	0.771389709	0.994816025	0.599110055
0.77456946	0.68820584	0.732922694	0.736703216	1.281055173	1.130536391	1.238863512	1.519587097
1.30807071	1.35822573	1.559140174	1.290895471	1.143965295	1.25556662	1.073482232	1.255766052
0.89129303	0.88653791	0.606173523	0.880314395	0.684084136	0.84250728	0.692838231	0.625536797
0.63556757	0.56579077	1.428664498	1.090004305	0.733745421	2.244114007	0.366762775	0.290917134
0.77187899	0.72266498	1.706543445	1.077153024	0.732674191	3.354506318	0.39708784	0.411283719
0.54041908	0.53603323	0.340083898	0.896956236	0.939578391	4.41342027	0.413010368	0.344499935
0.80635109	0.66650335	1.273721621	1.390974228	0.781382775	2.90824613	0.380491899	0.270966584
0.61327833	0.48891467	0.876523017	0.886727056	0.97024795	0.826647241	1.399389017	0.487407751
0.52582374	0.48677402	0.589303884	0.788726142	0.903277676	0.980038781	0.888371527	0.272013399
0.60510141	0.66987693	1.343249224	0.746922183	0.858840811	1.017145162	0.639308898	0.427383163
0.66356218	0.56882219	1.112677417	0.704440219	0.988770532	1.150187823	0.786535517	0.335765516
0.60435743	0.51826385	1.61687804	0.981641685	0.869654055	3.588400456	0.414018746	0.128315998
0.52732054	0.46636236	2.921954241	0.836484887	0.797735171	2.365079778	0.457225243	0.141947694
0.48763506	0.43442789	1.491921529	0.769534957	0.610588358	2.11108446	0.366698301	0.53596642
0.60178393	0.59598387	2.008250504	0.824390013	0.851568832	3.17322602	0.442921679	0.124175334
C18:1 SM	C18:0 SM	C18:0/C18:1 alkyl PE	C16:0/18:1 alkyl PG	C16:0/C20:4 PE	C18:0/C18:1PE	C16:0e/C18:1 PCe	C16:0e/C18:1 PSe
1	1	1	1	1	1	1	1
0.11482711	0.14227556	0.21397491	0.121363784	0.132735534	0.115260816	0.11432069	0.230275643
0.68855418	0.62274808	1.187253365	1.113771948	0.796845195	3.230071681	0.38933822	0.329416843
0.06162435	0.04345641	0.296242354	0.102370245	0.048914339	0.455657225	0.01003467	0.031395787
0.68855418	0.62274808	1.187253365	1.113771948	0.796845195	3.230071681	0.38933822	0.329416843
0.0540345	0.04432509	0.626675209	0.500567093	0.200988752	0.003175874	0.001793133	0.027860636
0.60194141	0.55359696	0.980438385	0.7817039	0.930284242	0.993504752	0.92840124	0.380642457
0.02847445	0.04320681	0.161478447	0.039007071	0.030071114	0.066540223	0.165109088	0.047782261
0.60194141	0.55359696	0.980438385	0.7817039	0.930284242	0.993504752	0.92840124	0.380642457
0.01514166	0.02393984	0.944199807	0.137658825	0.626784648	0.962659642	0.733649748	0.038875099
0.55527424	0.50375949	2.009751078	0.853012885	0.782386604	2.809447678	0.420215992	0.232601361
0.02876453	0.03526227	0.323343667	0.045282793	0.059267757	0.344513682	0.01997453	0.101192921
0.92247224	0.90997519	2.049849443	1.091222502	0.841018872	2.827815039	0.452623256	0.611075714
0.29276655	0.4059346	0.029260305	0.277857942	0.067696596	0.002063579	0.022350852	0.2340513
0.80643507	0.80892982	1.692773537	0.765877509	0.981855208	0.86977874	1.07930835	0.70610039
0.09772279	0.07761668	0.109827638	0.05868185	0.856960698	0.489302317	0.21641282	0.39607049

C16:0/C18:1 PG	Plasmalogen PE 18:0/20:4	C18:0/C20:4 alkyl PE	C20:4 SM	C16:0/20:4 alkyl PG	C16:0/C18:1 PC	C16:0/C18:1 PS
0.856224319	0.706432619	1.668309719	0.88667809	0.684731327	0.969931915	1.223235855
1.627498513	1.633797397	0.847197882	1.00563377	0.023227929	0.992450227	0.755127521
0.810989173	0.936099067	0.899891963	1.19392322	2.451062426	1.304621046	1.336696123
0.705287995	0.723670918	0.584600435	0.91376492	0.840978317	0.732996812	0.684940501
0.665659769	0.570792157	1.545088698	0.71946411	1.368547428	0.528565862	0.43741692
0.557757653	0.632132459	2.875168615	0.95587923	1.370692277	0.626529471	1.374640524
0.566834642	0.72053269	0.557811681	0.77920124	0.585410585	0.629171798	1.44061782
0.776509272	0.472375979	0.624279498	0.94761128	2.22321167	0.665655761	1.550904342
1.143302988	1.566989884	0.555475974	0.90005988	3.354206147	0.525932433	0.996341075
1.003727013	1.190278186	1.328501291	0.72275773	0.342829183	0.53439374	2.082732643
0.811834828	1.00738476	0.377159067	0.83372339	0.205122851	0.635818721	2.636782972
1.311559814	1.24310631	0.761170692	0.85788543	0.468414977	0.590181212	1.560104348
1.179258977	1.002893804	1.285015114	0.56039452	1.943415183	0.570451705	1.541884863
1.047940109	0.942176015	0.521687435	0.518374	1.296627298	0.507697237	3.208117826
0.774678081	0.838493414	0.883635373	0.46483584	1.260600255	0.447015194	0.665610582
0.732896004	1.050437501	0.921686807	0.55071999	0.896373481	0.574541032	0.801266697
C16:0/C18:1 PG	Plasmalogen PE 18:0/20:4	C18:0/C20:4 alkyl PE	C20:4 SM	C16:0/20:4 alkyl PG	C16:0/C18:1 PC	C16:0/C18:1 PS
1	1	1	1	1	1	1
0.211543157	0.217623918	0.233196052	0.069472	0.515133322	0.117276657	0.16391653
0.641690334	0.598958321	1.400587123	0.85053897	1.38696549	0.612480723	1.200894901
0.051152346	0.052199356	0.540693633	0.05971411	0.334464993	0.029361607	0.257076489
0.641690334	0.598958321	1.400587123	0.85053897	1.38696549	0.612480723	1.200894901
0.150793331	0.123312402	0.521684417	0.15390197	0.551890115	0.018474163	0.534406384
1.067606161	1.251939785	0.755576756	0.82860661	1.09264329	0.571581527	1.81899026
0.105964976	0.116527503	0.206461071	0.03785167	0.755768994	0.025721484	0.351439725
1.067606161	1.251939785	0.755576756	0.82860661	1.09264329	0.571581527	1.81899026
0.784684514	0.346824744	0.462439775	0.07342605	0.922620017	0.011809133	0.079157993
0.933693293	0.958500183	0.903006182	0.52358109	1.349254054	0.524926292	1.554219992
0.107610497	0.045726877	0.156007213	0.02154427	0.217707245	0.03014018	0.58395887
0.874567165	0.765612049	1.195121707	0.63188138	1.234853192	0.918375188	0.854441074
0.409374874	0.057514779	0.589545254	0.00042235	0.755300823	0.283596631	0.711071743
1.455052762	1.6002786	0.644734032	0.61558742	0.972810112	0.857049491	1.294218162
0.049741464	0.002052219	0.410618723	0.00211438	0.927791606	0.082645687	0.599752707

C18:0/C18:1 alkyl PG	Plasmalogen PC 16:0/20:4	C18:0/C20:4 PE	C16:0e/C20:4 PCe	C16:0/20:4 alkyl PS	C16:0/C20:4 PG
0.986094315	0.793615211	0.950096771	0.844949572	0.218350948	1.023483027
1.227406322	1.524147836	1.277623291	1.438146653	3.439369371	1.181048418
1.18212536	1.039609004	1.10355035	1.004867156	0.250871503	1.18149375
0.604374004	0.642627949	0.668729588	0.71203662	0.091408178	0.613974804
0.90753986	1.499696391	0.87139217	0.540136941	0.068359259	0.640785087
0.73068175	1.434692481	0.878017947	0.380685796	0.103442206	0.43531967
0.821702441	1.70417699	0.941879862	0.488007947	0.198215989	0.918148113
0.816885761	1.180672958	0.694615385	0.447977238	0.088314293	0.691218744
0.769937978	1.236177909	1.112066906	2.167914932	0.494935176	0.898405624
0.745238417	1.172872018	0.818883644	1.12461117	0.320486404	0.698531753
0.740889969	1.068343536	0.927697986	0.936997591	0.753937909	0.783307645
0.900063675	1.197527774	0.988933495	1.006924582	1.001135214	1.100410905
1.268343921	1.601818111	0.785857631	0.498123405	0.427944323	1.056223397
1.044621784	1.652152513	0.898433395	0.724876113	0.274795218	0.958481489
0.65536289	1.451095924	0.579050119	0.522875442	0.392643494	0.705747031
0.897935112	1.710169277	0.683403759	0.538068313	0.050725833	0.935377877
C18:0/C18:1 alkyl PG	Plasmalogen PC 16:0/20:4	C18:0/C20:4 PE	C16:0e/C20:4 PCe	C16:0/20:4 alkyl PS	C16:0/C20:4 PG
1	1	1	1	1	1
0.141890973	0.192918223	0.129108412	0.157839508	0.813850456	0.13394197
0.819202453	1.454809705	0.846476341	0.464201981	0.114582937	0.671367904
0.036114435	0.107917606	0.053055987	0.033629151	0.028788414	0.099141568
0.819202453	1.454809705	0.846476341	0.464201981	0.114582937	0.671367904
0.263054463	0.085353004	0.313552759	0.016003258	0.318659657	0.096071975
0.78903251	1.168730309	0.961895508	1.309112069	0.642623676	0.870163982
0.037559007	0.0359086	0.061172138	0.288872723	0.149026199	0.086992759
0.78903251	1.168730309	0.961895508	1.309112069	0.642623676	0.870163982
0.200659433	0.422890541	0.798619936	0.383960997	0.680878399	0.447304357
0.966565927	1.603808957	0.736686226	0.570985818	0.286527217	0.913957449
0.128685726	0.055508896	0.068476357	0.051952963	0.085146636	0.074180188
1.225001397	1.372266077	0.765869286	0.436162672	0.445870932	1.050327832
0.233601913	0.000590727	0.049608092	0.045603452	0.083340845	0.714880816
1.179886514	1.102418379	0.87029748	1.230037445	2.500609819	1.361336227
0.312472454	0.265507809	0.251973893	0.135200896	0.104272375	0.097805129

C18:0/C18:1 alkyl PC	C18:0/C18:1 alkyl PS	C18:0/C18:1 PG	C16:0/C20:4 PC	C16:0/C20:4 PS	C18:0/C20:4 alkyl PG	C18:0/C18:1PC
0.970690218	0.752350331	0.38728063	0.787288274	0.886799327	0.852935858	0.971357044
1.264010309	1.682572477	1.133654109	1.40010837	1.14069278	1.497259521	1.048731315
1.055971086	1.525355038	1.636895196	1.061281774	1.194775624	0.720861121	1.275382477
0.709328388	0.039722154	0.842170065	0.751321582	0.777732269	0.9289435	0.704529164
0.742378614	0.090881602	1.840857222	0.507236709	0.172857874	0.868609661	0.902263671
0.70819853	1.175902596	1.71694776	0.532937125	0.136910065	0.691089325	1.042867115
0.743872624	0.095865046	1.694646946	0.660426638	0.197667247	0.805308522	0.984377059
0.771507316	0.079697682	0.827627603	0.575721205	0.214213697	1.465554224	1.071658953
0.716102793	0.040407729	0.253362743	1.185889567	1.064033352	1.699953968	0.679927856
0.715396235	0.862850218	0.332994367	1.079018744	0.845630165	1.92641739	0.677261244
0.779626993	0.091269752	0.447731838	0.981571723	0.842652828	1.468485199	0.780045864
0.861747347	0.047389506	0.793064873	1.13186056	0.75344861	2.86401353	0.72158987
0.857776215	0.087389139	2.3913735	0.686684302	0.128207204	1.965303801	0.903122483
0.805049808	1.17324532	2.892799775	0.667512272	0.111502097	1.726121172	0.716985771
0.804475489	0.804249227	3.260577751	0.532254302	0.089023167	1.284445313	0.634413237
0.896189634	1.457614077	1.719729636	0.671693782	0.111531637	1.373272882	0.744829962
C18:0/C18:1 alkyl PC	C18:0/C18:1 alkyl PS	C18:0/C18:1 PG	C16:0/C20:4 PC	C16:0/C20:4 PS	C18:0/C20:4 alkyl PG	C18:0/C18:1PC
1	1	1	1	1	1	1
0.114812621	0.379184102	0.262016893	0.150257944	0.099978889	0.171236297	0.117733344
0.741489271	0.360586731	1.520019883	0.569080419	0.180412221	0.957640433	1.0002917
0.012960928	0.271792973	0.233026978	0.03356488	0.016807194	0.173242942	0.037381726
0.741489271	0.360586731	1.520019883	0.569080419	0.180412221	0.957640433	1.0002917
0.066586812	0.219571542	0.188590178	0.031209802	0.000191975	0.867664047	0.998192389
0.768218342	0.260479301	0.456788455	1.094585149	0.876441239	1.989717522	0.714706209
0.034621811	0.201105559	0.118978586	0.043531885	0.066086412	0.306056431	0.024028307
0.768218342	0.260479301	0.456788455	1.094585149	0.876441239	1.989717522	0.714706209
0.101447386	0.135666936	0.107997318	0.567575367	0.342307526	0.030270523	0.055197549
0.840872787	0.880624441	2.566120165	0.639536164	0.110066026	1.587285792	0.749837863
0.022274291	0.296310569	0.333654541	0.035996666	0.008042152	0.158031315	0.056216366
1.094575254	3.380784717	5.617743039	0.584272649	0.125582893	0.79774429	1.049155379
0.128037937	0.134037229	0.001003679	0.000195761	2.58208E-05	0.286987804	0.586415345
1.134032304	2.442198684	1.688214868	1.123806307	0.610080768	1.657496632	0.749619199
0.008396812	0.243447138	0.042309824	0.202243193	0.009228708	0.03628708	0.009971395

C18:0/C18:1 PS	C18:0p/C20:4 PCp	C18:0p/C20:4 PSp	C18:0/C20:4 alkyl PC	C18:0/C20:4 alkyl PS	C18:0/C20:4 PG	C18:0/C20:4 PC
0.804991311	0.946707442	0.827785619	0.707113469	0.733035462	1.119699303	0.810894465
1.445072827	1.391223805	1.372345899	1.813411757	1.777307539	1.220947734	1.433541676
1.115376054	0.980468157	1.141670115	0.85686166	0.861619388	1.168661107	1.094972128
0.634559808	0.681600596	0.658198366	0.622613114	0.628037611	0.490691857	0.660591731
0.733553684	0.60025097	0.322316141	0.616332078	0.332922481	0.189250672	0.709029432
0.926170533	0.551403776	0.350209823	0.612275076	0.408061742	0.238428004	0.686812956
1.052446179	0.629950563	0.413395869	0.697807221	0.415451295	0.275508351	0.784564556
0.736535258	0.487493552	0.271037759	0.540120683	0.364943894	0.236357274	0.596949529
1.068894366	1.541958451	1.245912786	1.673631347	1.386122059	0.889699766	1.168692278
0.92683739	0.991841863	1.044269655	1.20770175	1.129584291	0.62346997	1.003457643
0.827979299	0.848865359	1.052921211	0.901251733	1.067961312	0.794546655	0.973205326
1.115547218	1.026731109	0.997120956	1.281902276	1.232717358	0.892070812	1.129016115
1.005312682	0.624006347	0.386539992	0.850523283	0.470371569	0.334470511	0.913284433
0.912497291	0.72865708	0.379558434	0.929927128	0.374234337	0.480107065	0.898901144
0.641514354	0.597784477	0.409036039	0.754356288	0.253460088	0.400766131	0.583854525
1.002140792	0.676376177	0.411427364	0.781807647	0.339895177	0.47241502	0.752808636
C18:0/C18:1 PS	C18:0p/C20:4 PCp	C18:0p/C20:4 PSp	C18:0/C20:4 alkyl PC	C18:0/C20:4 alkyl PS	C18:0/C20:4 PG	C18:0/C20:4 PC
1	1	1	1	1	1	1
0.178646853	0.146530951	0.159477804	0.275428553	0.263467627	0.17102319	0.17027844
0.862176414	0.567274715	0.339239898	0.616633765	0.380344853	0.234886075	0.694339118
0.077796389	0.031134943	0.029661131	0.032226375	0.019336406	0.017671703	0.038619738
0.862176414	0.567274715	0.339239898	0.616633765	0.380344853	0.234886075	0.694339118
0.505893763	0.027742638	0.006550514	0.216087993	0.057401685	0.004328913	0.130581396
0.984814568	1.102349196	1.085056152	1.266121776	1.204096255	0.799946801	1.06859284
0.065903397	0.151503663	0.055002764	0.158864754	0.06954454	0.063057951	0.047444917
0.984814568	1.102349196	1.085056152	1.266121776	1.204096255	0.799946801	1.06859284
0.939030238	0.64447822	0.632098605	0.43467505	0.482177221	0.314496481	0.711375924
0.89036628	0.65670602	0.396640457	0.829153586	0.359490293	0.421939682	0.787212184
0.085694846	0.02901851	0.007990192	0.039209102	0.044850137	0.034193542	0.076869249
0.904095358	0.595733206	0.365548323	0.654876649	0.298556109	0.527459678	0.736681133
0.415893977	0.027731454	1.69028E-05	0.037005062	5.15442E-05	0.001883755	0.020717608
1.032696169	1.157650787	1.169203444	1.344645126	0.945169338	1.796358855	1.133757502
0.815684815	0.080339992	0.110893924	0.005766429	0.684283929	0.002823464	0.321794934

C18:0/C20:4 PS	C16:0/C16:0/C16:0 TAG	C16:0/C18:1/C16:0 TAG	C16:0/C20:4/C16:0 TAG	C18:0/C18:1/C18:0 TAG	C18:0/C18:0/C18:0 TAG
0.767532782	1.320067734	0.774441985	1.332781092	0.578008708	0.836380066
1.459414407	0.785677385	0.779517471	0.59688209	1.798142796	1.550163457
1.132683984	0.520495211	1.75081943	1.600097607	0.868641235	0.921152732
0.640368827	1.37375967	0.695221115	0.470239211	0.75520726	0.692303745
0.388201176	0.535200954	3.326860758	2.490157104	3.232901249	4.95977425
0.411465226	3.035735344	2.554312146	2.425009688	2.18915309	3.183711224
0.470458901	5.757475845	5.754517936		2.496530018	3.303483419
0.391097263	0.785927394	3.382764454	3.152382948	2.36104948	2.792773573
1.169997024	1.040062647	0.651859456	0.814831399	1.953430977	1.82477457
1.017359263	2.58069052	0.189642872	0.752280079	1.150030188	0.975604795
1.12017584	6.938679157	1.103682487	0.887042584	1.188970696	0.947089438
1.121207037	5.506772807	0.502163019	1.015463178	1.710791859	1.368204972
0.437674378	0.939809462	2.301031802	2.691211281	2.36517109	3.323071011
0.325608168		1.435330431	3.399624063	1.217832718	1.573592294
0.261238975	0.22263355	1.011603224	2.728424854	1.536294892	1.734522087
0.354089391	1.275676762	1.497165272	3.194210617	1.745928945	2.949517135
C18:0/C20:4 PS	C16:0/C16:0/C16:0 TAG	C16:0/C18:1/C16:0 TAG	C16:0/C20:4/C16:0 TAG	C18:0/C18:1/C18:0 TAG	C18:0/C18:0/C18:0 TAG
1	1	1	1	1	1
0.185302056	0.207765627	0.251016093	0.275984742	0.272685286	0.18937291
0.415305641	2.528584884	3.754613824	2.689183247	2.569908459	3.559935617
0.019099146	1.214268403	0.692915652	0.201231533	0.229771727	0.479183187
0.415305641	2.528584884	3.754613824	2.689183247	2.569908459	3.559935617
0.020100305	0.260986211	0.009648616	0.006734948	0.004555424	0.00253096
1.107184791	4.016551283	0.611836959	0.86740431	1.50080593	1.278918444
0.032118781	1.344146949	0.190129352	0.05651297	0.197747389	0.205758891
1.107184791	4.016551283	0.611836959	0.86740431	1.50080593	1.278918444
0.589409176	0.06839779	0.263801282	0.654493541	0.18762945	0.357071549
0.344652728	0.812706591	1.561282682	3.003367704	1.716306911	2.395175632
0.036586231	0.268952299	0.269157835	0.174755859	0.242002589	0.435865674
0.311287448	0.202339404	2.551795311	3.462477266	1.143590172	1.872813426
4.29079E-06	0.103499423	0.028015805	2.43448E-05	0.516240496	0.059781399
0.829877309	0.321407676	0.41583043	1.116832669	0.667847489	0.672814312
0.137755524	0.292818236	0.025593694	0.318682806	0.043028006	0.122268655

C16:0 FFA	C18:1 FFA	C18:0 FFA	C20:4 FFA	C22:6 FFA	C16:0 sphingosine phosphate	C16:0 alkyl glycerone phosphate	C16:0 alkyl LPA
0.86046742	0.87090373	0.9683983	0.846783425	0.64488407	0.948288388	1.407067144	1.145324262
1.16775614	0.96156429	1.18686072	1.156260654	1.2035266	0.704513564	0.653732427	0.691976443
1.10238353	1.25857043	0.92175908	0.957370077	0.92330198	1.005583034	1.189447766	1.113742335
0.86939291	0.90896154	0.92298191	1.039585844	1.22828735	1.341615014	0.749752663	1.04895696
0.42143731	0.34005541	0.76793515	0.373875917	0.39112265	2.454405536	1.591750243	0.899321394
0.34015824	0.29429878	0.74917943	0.269723848	0.36958137	2.528054777	0.616838987	1.013556105
0.32558383	0.27602418	0.81489859	0.328161594	0.46344971	3.763170214	1.057575199	1.973300816
0.30516159	0.30174766	0.72476693	0.388930492	0.5214992	3.794402574	1.015834237	1.549217511
0.68915449	0.61086435	0.74841192	0.926535825	0.67005488	0.877823084	0.512087414	1.359421563
0.67937566	0.72749952	0.64201778	0.674809288	0.61245477	0.627000871	0.951138108	0.915622043
0.56146558	0.48033627	0.51002386	0.491640823	0.53809674	1.025580432	1.175857884	1.132143233
0.76744704	0.80030607	0.99987472	0.916171844	0.98568027	1.743260807	1.280844265	1.274342452
0.271482	0.18672282	0.58946752	0.225467028	0.29985771	1.4763408	0.974582021	0.936548729
0.25798706	0.18805355	0.4732451	0.239625863	0.35795863	2.354658643	1.498544476	1.084055944
0.31590071	0.23003082	0.50333936	0.254074353	0.36648161	1.995397233	1.224901713	1.126468305
0.33897467	0.21321464	0.61458275	0.297534573	0.59061655	2.170555771	0.978966582	0.933451476
C16:0 FFA	C18:1 FFA	C18:0 FFA	C20:4 FFA	C22:6 FFA	C16:0 sphingosine phosphate	C16:0 alkyl glycerone phosphate	C16:0 alkyl LPA
1	1	1	1	1	1	1	1
0.07913705	0.08817115	0.06322514	0.065368864	0.13709124	0.131249861	0.178913172	0.104615071
0.34808524	0.30303151	0.76419503	0.340172963	0.43641323	3.135008275	1.070499667	1.358848957
0.02548221	0.01347242	0.01907197	0.026802575	0.0347471	0.372044005	0.200138603	0.249028782
0.34808524	0.30303151	0.76419503	0.340172963	0.43641323	3.135008275	1.070499667	1.358848957
0.00022735	0.00023178	0.0117744	8.54088E-05	0.00724159	0.001645603	0.801629946	0.232297204
0.67436069	0.65475155	0.72508207	0.752289445	0.70157166	1.068416299	0.979981918	1.170382323
0.04247978	0.07001497	0.10376455	0.104546688	0.0984788	0.239517462	0.170451063	0.097000245
0.67436069	0.65475155	0.72508207	0.752289445	0.70157166	1.068416299	0.979981918	1.170382323
0.01102353	0.02204196	0.06432452	0.091281759	0.12747941	0.810559368	0.93806964	0.27743579
0.29608611	0.20450546	0.54515868	0.254175454	0.40372863	1.999238112	1.169248698	1.020131113
0.01890535	0.01046535	0.03379274	0.015588157	0.06403026	0.189100909	0.124376902	0.049911052
0.43906194	0.31234055	0.7518579	0.337869229	0.57546313	1.871216411	1.193132931	0.871622113
0.00018534	0.0007089	0.15029855	0.003283658	0.04434351	0.022506423	0.404282825	0.217580983
0.8506138	0.67486533	0.71337638	0.747194758	0.92510629	0.637713823	1.092245738	0.750731793
0.15236089	0.00117717	0.00132526	0.032269413	0.66943117	0.034577275	0.689752576	0.230716764

C16:0 LPA	C18:0 alkyl LPA	C18:1 LPA	C18:0 LPA	C20:4 LPA	C16:0 alkyl LPI	C18:1 alkyl LPI	C18:0 alkyl LPI	C18:1 LPI	C18:0 LPI
0.862733288	0.84214642	1.18502266	0.92767266	1.175748726	1.394589644	1.335605082	1.148424972	0.93100581	0.98764502
0.410356299	1.12924859	0.79314393	0.90767465	0.897943943	0.997949421	0.891445426	1.03772098	0.99654242	0.68483731
0.993469812	1.157603981	1.31674877	1.16246155	1.140989441	0.933921833	0.81700955	1.019565958	1.27686761	1.69004753
1.733440602	0.87100101	0.70508464	1.00219115	0.78531789	0.673539102	0.955939942	0.79428809	0.79558417	0.63747014
0.666728804	1.313165264	0.63804341	1.33562521	1.215707513	1.109051897	1.194109838	0.563354341	0.40527386	1.22297843
0.419163719	0.890799511	0.43219771	1.00475623	1.011373051	0.887018931	0.770319546	1.147325956	0.53728672	1.01179954
0.991452364	2.425754918	0.347839	1.71299025	1.446094582	0.72929337	1.080052309	1.726156949	0.75388968	1.54887692
0.834475297	1.618308663	0.20532485	1.43219156	1.026788998	0.98771853	0.876371674	0.452715949	1.08759838	1.21712867
1.060651566	0.96744372	0.60468388	1.08117504	0.744086949	0.982833892	0.714501195	0.576147016	0.89934751	0.68487806
1.270840616	1.093557084	0.35431945	0.63955149	0.670858392	0.438672251	0.549402837	0.792999398	0.75379619	0.7537758
1.40588728	1.077688338	0.39385154	0.71899946	0.768159527	0.880591472	2.155605448	1.154556491	1.02548739	0.96594141
1.493318025	1.022665439	0.75221065	0.9567234	0.767249105	0.700278789	1.065071994	0.5279552	0.77026215	0.63421729
0.693877292	1.173415619	0.50247084	1.99814658	1.248188678	1.002990021	0.411001375	1.02647198	0.60429513	1.26397979
0.921355572	1.500009251	0.19581001	0.75293285	1.005929132	1.174762828	0.571448074	0.168656627	0.34381566	0.66837982
0.935258405	1.435334523	0.08635113	0.79223781	1.110755655	0.616839826	0.957268864	0.896786325	0.34599146	0.59462396
0.912862892	0.343411281	0.25315511	0.64825909	0.646298491	0.519210849	0.531697259	1.465409872	0.21233102	0.3871006
C16:0 LPA	C18:0 alkyl LPA	C18:1 LPA	C18:0 LPA	C20:4 LPA	C16:0 alkyl LPI	C18:1 alkyl LPI	C18:0 alkyl LPI	C18:1 LPI	C18:0 LPI
1	1	1	1	1	1	1	1	1	1
0.274545018	0.083217939	0.14841599	0.05784589	0.094546939	0.149066046	0.115412904	0.07424793	0.10133018	0.2427402
0.727955046	1.562007089	0.40585124	1.37139081	1.174991036	0.928270682	0.980213342	0.972388299	0.69601216	1.25019589
0.122433021	0.324251966	0.09045422	0.14608417	0.101607764	0.080368719	0.095985254	0.293844984	0.14900003	0.11100954
0.727955046	1.562007089	0.40585124	1.37139081	1.174991036	0.928270682	0.980213342	0.972388299	0.69601216	1.25019589
0.400351612	0.144190193	0.01417126	0.05599744	0.254184651	0.686654515	0.899440838	0.930375667	0.14256887	0.38475959
1.307674372	1.040338645	0.52626638	0.84911235	0.737588493	0.750594101	1.121145369	0.762914526	0.86222331	0.75970314
0.094201174	0.028654863	0.09322891	0.10258263	0.022930105	0.119255156	0.361190264	0.142704974	0.06340785	0.07298108
1.307674372	1.040338645	0.52626638	0.84911235	0.737588493	0.750594101	1.121145369	0.762914526	0.86222331	0.75970314
0.329935292	0.662850411	0.0354387	0.24740179	0.035705423	0.239232063	0.760184962	0.1909656	0.29291227	0.379724
0.86583854	1.113042668	0.25944677	1.04789408	1.002792989	0.828450881	0.617853893	0.889331201	0.37660832	0.72852104
0.057505956	0.266081526	0.08808709	0.31820463	0.128767602	0.1556718	0.118169001	0.26927397	0.08207774	0.18815538
0.662120906	1.069884959	0.49299515	1.23410534	1.359556173	1.103726875	0.551091687	1.165702278	0.43678745	0.95895489
0.007091905	0.794982378	0.08270261	0.57385497	0.088951445	0.705086923	0.233597401	0.692697767	0.00338854	0.8822744
1.189412101	0.712572098	0.63926568	0.76411047	0.853447352	0.892466925	0.630325937	0.914584433	0.54109445	0.58272551
0.347363798	0.325612185	0.29028363	0.39117122	0.334239927	0.589515146	0.054754516	0.841817943	0.10951581	0.05417782

C20:4 LPI	C16:0/18:1 alkyl PA	C16:0/20:4 alkyl PA	C18:0/C18:1 alkyl PA	C16:0/C20:4 PA	C18:0/C18:1 PA	C18:0e/C20:4 PAe
0.91218822	0.848288601	0.71834577	0.765175459	0.858438877	0.927725415	0.769754756
0.84685862	1.126419976	1.236059334	1.388010686	1.271472271	0.982117389	1.281980815
1.38945004	1.155298185	1.003439716	0.876324543	0.953921829	1.316146403	0.798663879
0.85150313	0.869993239	1.04215518	0.970489311	0.916167024	0.774010792	1.149600551
0.55506937	0.506321575	0.539395428	0.987665803	0.439864515	1.454548258	0.439316659
0.78687901	0.935602105	0.786228871	0.766942481	0.542592611	1.208178003	0.386888919
1.01705909	0.99621035	0.957063341	1.146789328	0.501357173	1.46450302	0.548772576
0.84735211	0.88622698	1.634715332	0.967275581	0.536764924	1.074709001	0.577099966
0.65614557	1.043143867	1.957146498	0.985659439	1.193008991	0.551186525	0.63435672
0.52964089	0.747528883	0.904589899	0.828083943	1.078653617	0.655873314	0.468437749
0.65595979	0.943580026	1.271820551	1.062331319	1.042347034	1.363791261	0.842411458
0.68052554	0.909934741	1.08105118	0.986748506	1.082712119	0.747590533	0.911096217
0.58090332	0.916022903	1.443676736	1.103094882	0.704710883	1.54972842	0.462643316
0.50160218	0.677109872	0.750194228	1.175227967	0.520324145	1.516736915	0.5956654
0.43129705	0.660028624	1.365022958	0.98896992	0.47257703	1.183909837	0.561583385
0.26919932	0.336503785	0.902840326	0.965692111	0.462621731	1.29027694	0.735963199
C20:4 LPI	C16:0/18:1 alkyl PA	C16:0/20:4 alkyl PA	C18:0/C18:1 alkyl PA	C16:0/C20:4 PA	C18:0/C18:1 PA	C18:0e/C20:4 PAe
1	1	1	1	1	1	1
0.13066683	0.081658661	0.106787173	0.135972227	0.092595856	0.114223127	0.127620078
0.8015899	0.831090253	0.979350743	0.967168298	0.505144806	1.30048457	0.48801953
0.0955292	0.110567523	0.234672859	0.077875034	0.02359031	0.095800479	0.044931083
0.8015899	0.831090253	0.979350743	0.967168298	0.505144806	1.30048457	0.48801953
0.26620358	0.265132312	0.938770577	0.840969519	0.002056694	0.090449871	0.009136535
0.63056795	0.911046879	1.303652032	0.965705802	1.09918044	0.829610408	0.714075536
0.03413331	0.061405342	0.230374692	0.049258848	0.032565817	0.182524172	0.100821736
0.63056795	0.911046879	1.303652032	0.965705802	1.09918044	0.829610408	0.714075536
0.03393798	0.417420715	0.276866457	0.820442373	0.351282412	0.458877705	0.129249485
0.44575047	0.647416296	1.115433562	1.05824622	0.540058447	1.385163028	0.588963825
0.06631046	0.118973694	0.170448942	0.049211787	0.056310193	0.088458876	0.056539283
0.70690315	0.71062896	0.855622156	1.095826719	0.491328291	1.669654834	0.82479205
0.04792765	0.09647406	0.535682456	0.232136415	0.000136334	0.033780224	0.320666863
0.55608294	0.778996377	1.138952076	1.094169672	1.069116105	1.065113004	1.206844785
0.02222547	0.301279001	0.655502339	0.361000679	0.588179525	0.540126508	0.211678452

C18:0/C20:4 PA	C16:0/C16:0 PI	C16:0/18:1 alkyl PI	C16:0/C18:1 PI	C18:0e/C18:1 Pie	C16:0/C20:4 PI	C18:0/C18:1 PI
0.72363497	1.293492259	0.891844608	0.900130652	0.657647497	0.935882307	0.780941613
1.192516712	0.344360679	1.175320833	1.00190619	1.596363964	0.901721715	1.262727534
1.094662573	1.771218042	1.123193912	1.274010512	0.936355209	1.307761298	1.150912883
0.989185744	0.590929019	0.809640647	0.823952646	0.80963333	0.85463468	0.80541797
0.479155996	0.425538659	0.809086012	0.89566362	2.241481163	0.455375957	1.756981925
0.862758498	0.576484079	0.928931388	1.05805276	2.558743043	0.425142252	2.181314307
0.91682418	0.504001833	1.139654222	1.393775666	3.36000825	0.57243818	2.790536805
0.871479367	0.668824173	1.122783817	1.144480608	2.373783081	0.548065671	2.041263835
1.019388546	0.093186196	0.622890906	0.529417287	0.698498817	0.607243523	0.841725759
0.814508246	0.087534036	0.587279581	0.462054405	0.659772095	0.542277821	0.813722119
0.912742541	0.344111415	0.911096651	0.864775284	0.900175405	0.796550832	1.032635748
0.887708558	0.121569225	0.589652082	0.599980407	0.996570473	0.566743163	0.982205415
0.90888233	0.289158811	1.000049008	0.967623175	2.821212437	0.387858255	2.467740794
0.938049068	0.19641475	0.78007016	0.827708754	2.281484396	0.358450699	1.942020164
0.89878983	0.191847907	0.846272179	0.729117848	2.241942947	0.292632429	1.60187879
0.705151205	0.219995383	0.820103189	0.754207531	1.999536344	0.36125791	1.487498375
C18:0/C20:4 PA	C16:0/C16:0 PI	C16:0/18:1 alkyl PI	C16:0/C18:1 PI	C18:0e/C18:1 Pie	C16:0/C20:4 PI	C18:0/C18:1 PI
1	1	1	1	1	1	1
0.101043829	0.32635831	0.088434725	0.098341222	0.206790019	0.103930182	0.1216721
0.78255451	0.543712186	1.00011386	1.122993164	2.633503884	0.500255515	2.192524218
0.101824732	0.051856293	0.079623078	0.10395546	0.250754609	0.035534403	0.218006404
0.78255451	0.543712186	1.00011386	1.122993164	2.633503884	0.500255515	2.192524218
0.180348114	0.216571799	0.999267587	0.423076179	0.002390232	0.003892364	0.003073653
0.908586973	0.161600218	0.677729805	0.614056846	0.813754197	0.628203835	0.91757226
0.042407716	0.061291038	0.078212487	0.088188472	0.08056297	0.057692244	0.05319351
0.908586973	0.161600218	0.677729805	0.614056846	0.813754197	0.628203835	0.91757226
0.436117054	0.044993508	0.03419773	0.026569566	0.433506811	0.02038218	0.557605129
0.862718109	0.224354213	0.861623634	0.819664327	2.336044031	0.350049823	1.874784531
0.053177679	0.022464618	0.048107664	0.053572218	0.173315121	0.020253458	0.219959441
0.949516265	1.388328651	1.271337969	1.334834605	2.870699824	0.557223315	2.043200968
0.525189047	0.373509974	0.092082467	0.093378197	0.000208486	0.003895307	0.005501129
1.102438357	0.412634144	0.861525541	0.729892535	0.887047878	0.699742057	0.855080421
0.51140259	0.001317715	0.187139709	0.041006656	0.366825856	0.010424242	0.344470349

C18:0/C20:4 alkyl PI	C18:0/C20:4 PI
0.776888402	0.778633762
1.411132856	1.032466711
1.033904627	1.217143753
0.778074115	0.971755774
0.767366874	0.888945828
0.718021322	1.020840468
1.084948299	1.301885693
0.802129754	1.036879859
0.922436564	0.827021396
0.806333717	0.822154037
0.900029518	1.060210409
0.851522414	0.909058353
0.786768159	0.915974818
0.771065466	0.895339928
0.641144655	0.642395365
0.689409921	0.689651758
C18:0/C20:4 alkyl PI	C18:0/C20:4 PI
1	1
0.149780292	0.09037249
0.843116562	1.062137962
0.082436512	0.086514905
0.843116562	1.062137962
0.394206736	0.63708869
0.870080553	0.904611049
0.025894266	0.055565466
0.870080553	0.904611049
0.42551187	0.403214307
0.72209705	0.785840467
0.034402031	0.069972522
0.829919767	0.86870536
0.013854809	0.232072053
0.856461707	0.739866661
0.224270157	0.047603082

Table 2. Lipidomics data - Muscle

Metabolite	C12 MAGE	C16:0 NAE	C16: 0 MAGE	C18:1 NAE	C18:0 NAE	C18:1 MAGE	C12:0 acyl carnitine	C18:0 MAGE
WT PBS -1	1.03946029	0.99127059	0.948215657	0.863477	0.8771568	0.913159816	0.967941639	0.912591292
WT PBS -2	0.93327632	1.01288008	1.00026112	1.1286038	1.1103172	0.753140425	0.73572808	0.793518893
WT PBS -3	0.72074876	0.92305402	0.849574267	0.9663671	0.8224482	0.968971765	0.86189013	0.899295808
WT PBS -4	1.30651463	1.07279531	1.201948956	1.041552	1.1900778	1.364727994	1.434440151	1.394594007
WT Dex -1	0.89887317	0.8218863	0.808219818	1.0715167	0.9747847	0.185750153	0.886808014	0.856052208
WT Dex -2	0.77146473	0.43078846	0.584219606	0.6456985	0.6120945	0.056945281	1.060342527	1.012367066
WT Dex -3	0.96728064	1.96024352	0.792296928	1.0778835	1.1446626	4.161405492	1.001915343	1.038554078
WT Dex -4	1.07530405	1.24405811	0.449307612	1.039931	1.2130639	1.451198858	1.243652013	1.200245694
Angptl4$^{-/-}$ PBS-1	0.77393914	0.5319215	0.744419392	0.7467774	0.8439289	0.061106785	0.894561978	0.902051979
Angptl4$^{-/-}$ PBS-2	1.43935979	0.82837141	1.073663303	1.2806665	1.1961087	0.399561237	1.008823444	1.052285327
Angptl4$^{-/-}$ PBS-3	0.92464807	0.58654494	0.782775222	1.14373	0.8468509	0.062216113	1.039493686	1.032265664
Angptl4$^{-/-}$ PBS-4	1.1141231	0.70495425	0.963940128	1.4277786	0.9729419	0.130293356	1.852606226	1.707896783
Angptl4$^{-/-}$ Dex-1	1.85424749	1.31066577	1.405726699	1.7303571	1.7999203	0.769629517	1.575753027	1.645472206
Angptl4$^{-/-}$ Dex-2	0.97400177	0.70721677	0.803497537	1.163067	1.0658444	0.098052888	1.668278432	1.593334857
Angptl4$^{-/-}$ Dex-3	1.4467655	1.01765961	0.993632428	1.772665	1.4934405	0.072325753	1.953707441	1.855309511
Angptl4$^{-/-}$ Dex-4	0.69989458	1.13447616	0.596475852	0.6737583	1.4826263	0.110865293	0.702509373	0.715088602
Metabolite	C12 MAGE	C16:0 NAE	C16: 0 MAGE	C18:1 NAE	C18:0 NAE	C18:1 MAGE	C12:0 acyl carnitine	C18:0 MAGE
WT Con								
av	1	1	1	1	1	1	1	1
sem	0.1217722	0.03090569	0.074214199	0.0562992	0.0889356	0.129894229	0.152392029	0.134201495
WT Dex								
av	0.92823065	1.1142441	0.658510991	0.9587574	0.9861514	1.463824946	1.048179474	1.026804762
sem	0.06363496	0.32725517	0.086408272	0.1046823	0.1343698	0.952622949	0.074463957	0.070465526
FOLD (compare to WT PBS)	0.92823065	1.1142441	0.658510991	0.9587574	0.9861514	1.463824946	1.048179474	1.026804762
P value against WT PBS	0.62014263	0.7400444	0.024068993	0.7404519	0.9343076	0.64659663	0.785914669	0.865452562
Angptl4$^{-/-}$ PBS								
av	1.06301753	0.66294803	0.891199511	1.1497381	0.9649576	0.163294373	1.198871334	1.173624938
sem	0.14345664	0.06591333	0.077397493	0.1463051	0.0827102	0.080400153	0.220131197	0.181177634
FOLD (compare to WT PBS)	1.06301753	0.66294803	0.891199511	1.1497381	0.9649576	0.163294373	1.198871334	1.173624938
P value against WT PBS	0.74910201	0.00357813	0.349426224	0.3763678	0.7826501	0.00154756	0.48565888	0.470482316
Angptl4$^{-/-}$ Dex								
av	1.24372733	1.04250458	0.949833129	1.3349619	1.4604579	0.262718363	1.475062068	1.452301294
sem	0.25535356	0.12695287	0.172248076	0.2605538	0.1507022	0.169160264	0.269785454	0.252174484
FOLD (compare to Angptl4$^{-/-}$ PBS)	1.16999702	1.57252837	1.065791797	1.1611008	1.5134943	1.608863541	1.230375627	1.237449245
P valu against Angptl4$^{-/-}$ PBS	0.55991249	0.03785502	0.766686058	0.5581465	0.027971	0.614593768	0.457871554	0.404037209
FOLD (compare to WT Dex)	1.3398904	0.93561598	1.442395255	1.3923875	1.4809672	0.179473894	1.407260974	1.414388936
P value aginst WT Dex	0.27577721	0.84481587	0.181354583	0.2288286	0.057126	0.260779506	0.178036169	0.155275555

C20:4 NAE	C18:1 MAG	C16:0 AcMAGE	C18:2 MAGE	C20:4 MAG	C18:0 AcMAGE	C16:0 acyl carnitine	C16:0 alkyl LPE	C16:0 LPE
0.84688643	0.134995641	0.922906071	0.965497783	0.34938716	1.092346777	0.738839645	0.790237073	0.97543887
1.24329532	1.29193222	1.216565534	1.237467483	2.31763942	0.99626087	0.993940524	1.235697905	0.964002291
0.99589365	1.99155744	0.821988371	0.804261937	1.00310358	0.732079464	0.774550589	0.89340374	0.885575098
0.9139246	0.581514699	1.038540024	0.992772797	0.32986984	1.179312888	1.492669242	1.080661282	1.174983741
0.97995335	0.522823463	0.763767268	0.722700744	0.45142046	0.65193896	0.625483981	0.664968888	0.718394719
0.57034276	0.136993633	0.856176724	0.776637175	0.19583473	0.725365644	1.027922068	0.714023106	0.782793308
1.33624501	1.173249363	1.264136438	1.174593979	1.51907356	1.07529556	0.898523382	1.048938847	0.972488167
0.73209599	0.375004139	1.239231634	1.150525089	0.57946971	0.828347946	0.840834947	0.84746065	0.958459356
1.02227918	0.581645459	1.016856462	0.95128696	0.88132033	0.77018272	0.952569547	1.091009552	0.944460819
1.37975501	1.412923008	1.168090083	1.069114528	0.51916621	0.985958984	0.437562947	1.210537159	1.018052494
0.75996164	0.337813986	0.919252121	0.864578852	0.32024571	0.715117052	0.970336548	0.631789693	0.694730638
0.83068562	0.686294541	0.904057058	0.852159675	0.25212161	0.867549005	1.374346457	1.157156232	0.986019551
0.9976519	0.860607858	2.416027473	2.150421069	0.85311803	1.99646574	0.62727401	1.371882255	1.473531542
0.91804103	0.682914708	0.818460455	0.71605423	0.75301653	0.705061802	1.173253848	0.79229013	0.761854307
1.13342065	0.56369696	1.207112527	1.14767042	0.32921804	0.995698881	1.467436106	0.797553865	0.838893069
0.98304285	0.407680454	0.582470209	0.531409169	0.35956016	0.576987096	0.822817819	0.912587518	0.679389524
C20:4 NAE	C18:1 MAG	C16:0 AcMAGE	C18:2 MAGE	C20:4 MAG	C18:0 AcMAGE	C16:0 acyl carnitine	C16:0 alkyl LPE	C16:0 LPE
1	1	1	1	1	1	1	1	1
0.08663247	0.407407767	0.084664819	0.089417947	0.46623982	0.096814442	0.173635602	0.09892042	0.06165188
0.90465928	0.552017649	1.030828016	0.956114247	0.68644962	0.820237027	0.848191095	0.818847873	0.858033887
0.1667036	0.22180319	0.128999162	0.119799434	0.28876879	0.092396546	0.083909243	0.085842647	0.063472631
0.90465928	0.552017649	1.030828016	0.956114247	0.68644962	0.820237027	0.848191095	0.818847873	0.858033887
0.62992611	0.37146805	0.848243352	0.778977544	0.58826603	0.22777279	0.461120716	0.215897536	0.159748824
0.99817036	0.754669249	1.002063931	0.934285004	0.49321347	0.83470194	0.933703875	1.022623159	0.910815875
0.13873915	0.231242775	0.060722487	0.050059618	0.14122783	0.059456495	0.191924371	0.132551347	0.073586739
0.99817036	0.754669249	1.002063931	0.934285004	0.49321347	0.83470194	0.933703875	1.022623159	0.910815875
0.99143775	0.619261299	0.984837678	0.545051048	0.33829863	0.195932714	0.806387934	0.895676182	0.388733931
1.00803911	0.628724995	1.256017666	1.136388722	0.57372819	1.06855338	1.022695446	0.968578442	0.93841711
0.04523355	0.095653682	0.407547232	0.361832169	0.13411939	0.321467036	0.186362386	0.137269784	0.181319746
1.00988683	0.833113309	1.253430672	1.216319129	1.16324519	1.28016161	1.095310273	0.947150897	1.030303858
0.94827904	0.632703803	0.560321483	0.60006076	0.69368598	0.501286088	0.75070893	0.786525304	0.892446359
1.11427488	1.13895814	1.218455113	1.188549094	0.83579068	1.302737311	1.205737071	1.182855173	1.09368304
0.57139296	0.761577017	0.617238753	0.652945511	0.73542543	0.485887202	0.425974624	0.39073482	0.690199079

C18:1 alkyl LPE	C18:0 alkyl LPE	C16:0 alkyl LPG	C18:1 LPE	C16:0 alkyl LPC	C18:0 LPE	lyso PAF C16:0	C16:0 alkyl LPS	C16:0 LPG
0.830542384	0.89550801	ND	1.15677493	1.201536779	0.92055511	0.907035204	ND	ND
1.511832104	0.863302611	ND	1.39642963	1.086465882	0.84544217	1.255433965	ND	ND
0.734024809	1.008725688	ND	0.78172709	0.658581014	0.94927149	0.632219276	ND	ND
0.923600704	1.232463691	ND	0.66506834	1.053416325	1.28473123	1.205311556	ND	ND
0.629526147	0.720463039	ND	0.41986552	0.87454901	0.71378118	0.700562077	ND	ND
0.938634642	0.808768612	ND	1.03565863	0.60980704	0.8170788	0.812382837	ND	ND
0.746198613	0.94161092	ND	0.59122583	1.112882884	0.99370528	0.926466207	ND	ND
1.30171318	0.851394496	ND	2.39126243	0.913244155	0.79339045	1.148190001	ND	ND
0.865187483	0.952292212	ND	0.81383251	0.948433665	1.33979631	0.910999724	ND	ND
1.484153245	1.29422452	ND	1.75133783	1.211366253	1.5084003	1.189841724	ND	ND
0.732530255	0.706799578	ND	0.65259778	0.565803445	0.94937913	0.663234344	ND	ND
1.110634778	0.959111817	ND	1.15679246	0.568475477	1.16384583	0.969205804	ND	ND
1.28749185	2.024074384	ND	2.20227216	1.607854272	1.92241448	1.313257678	ND	ND
1.164693809	0.874191765	ND	1.39664493	0.878966987	1.00505845	0.963991027	ND	ND
0.937473645	0.820473769	ND	1.05686528	0.817552321	0.85306429	1.083844762	ND	ND
0.874065615	0.904083718	ND	0.82648224	0.739460442	1.3249857	0.883756496	ND	ND
C18:1 alkyl LPE	C18:0 alkyl LPE	C16:0 alkyl LPG	C18:1 LPE	C16:0 alkyl LPC	C18:0 LPE	lyso PAF C16:0	C16:0 alkyl LPS	C16:0 LPG
1	1	ND	1	1	1	1	ND	ND
0.174944668	0.083526571	ND	0.16871009	0.118150204	0.0974016	0.144713642	ND	ND
0.904018146	0.830559267	ND	1.1095031	0.877620772	0.82948893	0.896900281	ND	ND
0.147086285	0.045973351	ND	0.44652093	0.103421032	0.05902853	0.095617535	ND	ND
0.904018146	0.830559267	ND	1.1095031	0.877620772	0.82948893	0.896900281	ND	ND
0.689151667	0.125867855	ND	0.82617242	0.465374158	0.18500363	0.573953807	ND	ND
1.048126441	0.978107032	ND	1.09364015	0.82351971	1.24035539	0.933320399	ND	ND
0.165099536	0.120611368	ND	0.24313322	0.157452022	0.11981147	0.108218776	ND	ND
1.048126441	0.978107032	ND	1.09364015	0.82351971	1.24035539	0.933320399	ND	ND
0.848034832	0.886264571	ND	0.76240095	0.404511178	0.17056474	0.724797293	ND	ND
1.06593123	1.155705909	ND	1.37056615	1.010958505	1.27638073	1.061212491	ND	ND
0.096676833	0.289972461	ND	0.30094996	0.201002377	0.23673731	0.093533256	ND	ND
1.016987253	1.181574073	ND	1.25321492	1.227606933	1.02904437	1.13702914	ND	ND
0.928884201	0.592235168	ND	0.50102528	0.490565227	0.89643899	0.405695131	ND	ND
1.179103799	1.391479158	ND	1.23529727	1.151930922	1.5387556	1.183200088	ND	ND
0.393111214	0.310502265	ND	0.64499379	0.57680491	0.11672376	0.265280732	Nd	ND

C16:0 LPC	C18:1 alkyl LPG	C16:0 LPS	C18:0 alkyl LPG	C20:4 LPE	C18:0p LPCp	lyso PAF C18:0	C18:0 alkyl LPC	18:1 alkyl LP
0.936423149	ND	0.998965072	ND	0.83854211	0.94115124	0.962295439	0.948549702	ND
1.11769653	ND	1.040541695	ND	1.5002912	1.070602027	1.434800689	1.131575622	ND
0.79860003	ND	0.758547528	ND	0.87281756	0.847198787	0.665936974	0.74505857	ND
1.147280291	ND	1.201945705	ND	0.78834912	1.141047947	0.936966898	1.174816105	ND
0.084591619	ND	0.889165141	ND	0.64499924	0.664139213	0.513925908	0.889473049	ND
0.694163648	ND	0.690293443	ND	0.48014798	0.59336459	0.590914467	0.736832789	ND
1.036576232	ND	1.004312282	ND	0.79850884	0.990612344	0.914654545	1.125462815	ND
0.954648426	ND	0.860700864	ND	1.11341438	0.659074177	0.804099474	1.147699639	ND
0.920156913	ND	0.898724179	ND	1.00641412	0.899845103	1.122887506	0.885204778	ND
1.102505817	ND	1.103854372	ND	1.21063523	1.312186746	1.011175455	1.317868068	ND
0.712966965	ND	0.700906461	ND	0.64594085	0.605207558	0.521750769	0.786066473	ND
0.90581283	ND	0.864958017	ND	1.00443654	0.709757138	0.803179874	0.820868248	ND
1.450707553	ND	1.50370991	ND	1.73893601	1.599878027	0.90238185	1.505008695	ND
0.8567628	ND	0.734299628	ND	0.78013622	1.066735843	0.619114881	1.022422585	ND
1.108607625	ND	0.993152301	ND	1.18030515	0.713251235	0.715073826	1.268830758	ND
0.712309123	ND	0.708591569	ND	0.7095848	0.605594054	0.554888946	0.844987346	ND
C16:0 LPC	C18:1 alkyl LPG	C16:0 LPS	C18:0 alkyl LPG	C20:4 LPE	C18:0p LPCp	lyso PAF C18:0	C18:0 alkyl LPC	18:1 alkyl LP
1	ND	1	ND	1	1	1	1	ND
0.081725109	ND	0.091617895	ND	0.1676632	0.065631901	0.159698818	0.098113489	ND
0.692494981	ND	0.861117932	ND	0.75926761	0.726797581	0.705898598	0.974867073	ND
0.215380597	ND	0.064853969	ND	0.13476054	0.089403171	0.092779901	0.098531988	ND
0.692494981	ND	0.861117932	ND	0.75926761	0.726797581	0.705898598	0.974867073	ND
0.230337724	ND	0.262211881	ND	0.30587837	0.048897665	0.16240784	0.862516242	ND
0.910360631	ND	0.892110757	ND	0.96685668	0.881749136	0.864748401	0.952501892	ND
0.079582599	ND	0.082752366	ND	0.1173996	0.155900741	0.132134634	0.123507594	ND
0.910360631	ND	0.892110757	ND	0.96685668	0.881749136	0.864748401	0.952501892	ND
0.461871293	ND	0.415777489	ND	0.87667792	0.510679657	0.538247261	0.773481465	ND
1.032096775	ND	0.984938352	ND	1.10224054	0.99636479	0.697864876	1.160312346	ND
0.161785619	ND	0.184476447	ND	0.23618583	0.223985745	0.075700627	0.144058802	ND
1.133722988	ND	1.10405389	ND	1.14002474	1.129986692	0.807014937	1.218173272	ND
0.524707941	ND	0.662312342	ND	0.62609106	0.689116764	0.315159086	0.315453027	ND
1.490403256	ND	1.143790316	ND	1.45171548	1.370897229	0.988619155	1.190226215	ND
0.254223401	ND	0.549955109	ND	0.25403135	0.306419965	0.94868932	0.32887933	ND

C18:1 LPG	C18:0 alkyl LPS	C18:0 LPG	C20:4 alkyl LPG	C18:1 LPC	C18:0 LPC	C18:1 LPS	C18:0 LPS	C20:4 alkyl LPC	C20:4 alkyl LPS
ND	1.495994542	ND	ND	0.69345912	0.95750399	1.228320279	1.1249659	ND	1.467329113
ND	0.663882517	ND	ND	1.63461319	1.14126541	1.607123303	0.8073825	ND	0.840389244
ND	0.69929847	ND	ND	0.99134787	0.82295537	0.63581539	0.8594288	ND	0.360827381
ND	1.140824472	ND	ND	0.68057982	1.07827523	0.528741028	1.2082228	ND	1.331454262
ND	0.556609376	ND	ND	0.63538522	0.72698882	0.349914357	0.5954694	ND	0.890396765
ND	0.308820297	ND	ND	0.40636456	0.68710789	1.190848822	0.9435642	ND	0.774649529
ND	1.211943791	ND	ND	0.82034119	0.87778439	0.400986157	0.8672855	ND	0.277632964
ND	1.036499096	ND	ND	0.62320232	0.84834482	2.106425193	0.7900121	ND	0.132712882
ND	0.355285095	ND	ND	0.70335209	0.86128587	0.573686815	1.3091175	ND	0.048449116
ND	0.789788299	ND	ND	0.76104148	1.10958675	1.718987117	1.9001943	ND	0.45378661
ND	0.443373909	ND	ND	0.58097735	0.74278292	0.507141968	1.0378832	ND	0.37803888
ND	0.570272109	ND	ND	0.79622966	0.82982275	1.077110977	1.3706865	ND	0.710703193
ND	1.749793407	ND	ND	0.82320843	1.12949592	1.190681152	1.5134178	ND	2.73021686
ND	0.615785915	ND	ND	0.58082433	0.85440284	1.768802814	1.1767918	ND	1.302413711
ND	0.705442287	ND	ND	0.70269011	1.23699875	1.020333807	0.9149926	ND	0.510877992
ND	0.34802981	ND	ND	0.52359119	0.70837104	0.877142982	1.0462097	ND	0.053344473
C18:1 LPG	C18:0 alkyl LPS	C18:0 LPG	C20:4 alkyl LPG	C18:1 LPC	C18:0 LPC	C18:1 LPS	C18:0 LPS	C20:4 alkyl LPC	C20:4 alkyl LPS
ND	1	ND	ND	1	1	1	1	ND	1
ND	0.19774531	ND	ND	0.22338407	0.07025764	0.254205347	0.0982493	ND	0.252037639
ND	0.77846814	ND	ND	0.62132332	0.78505648	1.012043632	0.7990828	ND	0.518848035
ND	0.20901984	ND	ND	0.08466436	0.04616064	0.412456938	0.0747592	ND	0.185015299
ND	0.77846814	ND	ND	0.62132332	0.78505648	1.012043632	0.7990828	ND	0.518848035
ND	0.470568573	ND	ND	0.1640254	0.04308995	0.980974486	0.1547731	ND	0.174746694
ND	0.539679853	ND	ND	0.71040014	0.88586957	0.969231719	1.4044704	ND	0.39774445
ND	0.094324963	ND	ND	0.04719744	0.0786706	0.280439209	0.1803612	ND	0.136467163
ND	0.539679853	ND	ND	0.71040014	0.88586957	0.969231719	1.4044704	ND	0.39774445
ND	0.080360328	ND	ND	0.25163864	0.32078886	0.937856029	0.0964403	ND	0.080333783
ND	0.854762855	ND	ND	0.65757851	0.98231714	1.214240189	1.162853	ND	1.149213259
ND	0.307850705	ND	ND	0.06665341	0.1217692	0.19564614	0.1284946	ND	0.586759681
ND	1.583833174	ND	ND	0.92564524	1.10887332	1.252786268	0.8279655	ND	2.889325698
ND	0.365575934	ND	ND	0.54172566	0.53059532	0.500594314	0.3171112	ND	0.25872492
ND	1.098006213	ND	ND	1.05835157	1.25126939	1.199790355	1.4552347	ND	2.214932276
ND	0.844322919	ND	ND	0.74797587	0.18060692	0.673344467	0.0499944	ND	0.345079065

C20:4 LPG	C16:0 Ceramide	C20:4 LPC	C20:4 LPS	C18:1 Ceramide	C18:0 Ceramide	C20:4 Ceramide	C16:0/C18:1 DAG	C18:0/C18:1 DAG
ND	0.911497286	0.3280279	1.0467147	0.644232208	0.876799378	0.891197971	0.770268135	0.591164536
ND	1.133992939	2.3169322	0.9236576	0.9347265	1.040280142	0.721728151	0.956177357	1.251148501
ND	0.87686561	1.0408266	0.5988502	0.939496979	0.839196877	0.862004769	1.132944826	1.217321041
ND	1.077644165	0.3142134	1.4307775	1.481544313	1.243723603	1.525069109	1.140609681	0.940365922
ND	0.964148554	0.6130121	11.139856	1.150933623	1.174448875	1.26043932	1.308585324	0.961003272
ND	0.632458158	0.1950623	0.6509753	0.575187995	0.786697524	0.552270133	0.490839757	0.382962389
ND	1.322952573	0.8485818	0.9962691	1.878883471	1.652938291	1.916263315	1.465940894	1.182143191
ND	0.836704196	0.37339	1.3035886	0.921122986	1.049324072	0.68734749	0.505214579	0.615932329
ND	1.008643485	0.5493285	0.7016748	0.747049779	1.003079464	0.805819087	0.828522065	0.748041246
ND	1.30381938	0.4828005	1.3297788	1.2377617	1.368005129	0.874885172	0.830387485	1.102972003
ND	1.032891243	0.4872856	1.2283801	0.810226386	0.892988993	1.008468286	0.701494687	0.570474302
ND	1.093003286	0.3567436	1.2175845	0.758021873	1.002844325	0.684494936	0.876809367	0.789368387
ND	2.058690036	0.6906533	1.6698639	1.546183337	2.26942143	1.597969694	1.280388674	1.758015853
ND	1.310813507	0.5903442	0.6243867	1.147900554	1.429240688	0.817903179	0.645586019	0.771903424
ND	1.576663739	0.6716386	1.7226757	1.440117452	1.665788667	1.219703862	1.078729525	1.11551346
ND	0.766302089	0.5355324	0.7541224	0.526663578	0.677615563	0.64545204	0.436187368	0.474396656
C20:4 LPG	C16:0 Ceramide	C20:4 LPC	C20:4 LPS	C18:1 Ceramide	C18:0 Ceramide	C20:4 Ceramide	C16:0/C18:1 DAG	C18:0/C18:1 DAG
ND	1	1	1	1	1	1	1	1
ND	0.062568318	0.4706226	0.1718771	0.174732389	0.092222431	0.178888549	0.087627318	0.153026867
ND	0.93906587	0.5075116	3.5226722	1.131532019	1.16585219	1.104080064	0.942645139	0.785510295
ND	0.145052962	0.1423237	2.5425573	0.275786942	0.18135229	0.311214033	0.25871868	0.177697529
ND	0.93906587	0.5075116	3.5226722	1.131532019	1.16585219	1.104080064	0.942645139	0.785510295
ND	0.713004084	0.3551775	0.360439	0.701000383	0.446111996	0.781617319	0.840638362	0.3956497
ND	1.109589349	0.4690395	1.1193545	0.888264934	1.066729478	0.84341687	0.809303401	0.802713985
ND	0.06712741	0.0403928	0.141501	0.117311188	0.103716525	0.067639977	0.037631624	0.110776562
ND	1.109589349	0.4690395	1.1193545	0.888264934	1.066729478	0.84341687	0.809303401	0.802713985
ND	0.27745271	0.3039315	0.6111645	0.614549846	0.647686997	0.444229857	0.092474036	0.336577214
ND	1.428117343	0.6220421	1.1927622	1.16521623	1.510516587	1.070257194	0.860222896	1.029957348
ND	0.269482154	0.0361201	0.292103	0.228902443	0.329187873	0.213103409	0.193683493	0.275775958
ND	1.28706836	1.3262041	1.0655803	1.311789068	1.416025917	1.26895398	1.062917684	1.283093815
ND	0.295071857	0.030211	0.8285786	0.322972567	0.245898509	0.349458136	0.804973425	0.473481027
ND	1.520785057	1.2256708	0.3385959	1.029768677	1.295633014	0.969365564	0.91256281	1.311195225
ND	0.16115928	0.4650427	0.3977206	0.928182239	0.394478631	0.93146612	0.807215799	0.484358388

C18:0/C20:4 DAG	C16:0/18:1 alkyl PE	C16:0 Sphingomyelin PC	C16:0/C18:1 PE	Plasmalogen PE 16:0/20:4	C16:0/20:4 alkyl PE
0.938116282	0.876792801	0.351720024	1.091694483	0.85294077	0.941966383
1.433461476	1.268913775	2.976276073	1.302789605	1.188688514	1.37502902
0.810865585	0.855013352	0.287509462	0.741154815	0.755110978	0.733163054
0.817556657	0.999280072	0.384494441	0.864361096	1.203259738	0.949841543
0.819015215	0.915730936	0.212440363	0.606431437	0.691262669	0.58166944
2.527457107	0.817072005	0.188962081	0.700263811	0.483128588	0.665150887
1.347188926	1.032400609	0.293394431	0.847431799	0.95509147	0.766591277
0.43734089	1.122488174	0.297304283	0.925633277	0.684302051	1.044331314
1.151202145	0.909343159	0.306898794	0.75859894	0.780501235	0.608971536
0.906185855	1.557456585	0.495934661	1.369984325	1.359993323	1.646470654
0.728819929	1.177959509	0.34471832	0.894852399	0.892453014	0.746752293
0.620151379	1.193349773	0.389743959	1.029392155	1.166337047	1.054854718
1.39320485	1.826549104	0.591310933	1.74858143	1.692156375	1.76094795
0.596669264	1.314222852	0.44669731	1.163541503	0.833328847	1.311875431
1.00659911	1.555759862	0.519851201	1.282481064	1.367084823	1.332761574
0.4389754	0.73455409	0.291569729	0.690325642	0.549319532	0.569607129
C18:0/C20:4 DAG	C16:0/18:1 alkyl PE	C16:0 Sphingomyelin PC	C16:0/C18:1 PE	Plasmalogen PE 16:0/20:4	C16:0/20:4 alkyl PE
1	1	1	1	1	1
0.147415469	0.095094812	0.659066505	0.12432758	0.114932925	0.134701056
1.282750535	0.971922931	0.248025289	0.769940081	0.703446194	0.764435729
0.4549006	0.066748153	0.027751168	0.071783933	0.096772986	0.100667432
1.282750535	0.971922931	0.248025289	0.769940081	0.703446194	0.764435729
0.575907147	0.817088095	0.297756594	0.160164385	0.095849819	0.210807784
0.851589827	1.209527257	0.384323934	1.013206955	1.049821155	1.0142623
0.115968556	0.13304872	0.040875408	0.131144035	0.131364848	0.230426661
0.851589827	1.209527257	0.384323934	1.013206955	1.049821155	1.0142623
0.458923436	0.247407999	0.387125247	0.94411498	0.78490991	0.959120109
0.858862156	1.357771477	0.462357294	1.22123241	1.110472394	1.243798021
0.214553475	0.232602712	0.064127619	0.217378055	0.257537582	0.247407635
1.008539708	1.12256377	1.203040594	1.205313884	1.057772925	1.226308048
0.977179159	0.600103835	0.344412671	0.443878041	0.840774628	0.522504358
0.669547299	1.396995001	1.864153832	1.586139545	1.578617388	1.627079914
0.431653599	0.161938909	0.022015955	0.096168225	0.189508082	0.122856509

C18:1 Sphingomyelin PC	Sphingomye	C18:0/C18:1 alkyl PE	C16:0/18:1 alkyl PG	C16:0/C20:4 PE	C18:0/C18:1PE	C16:0e/C18:1 PCe
0.977353629	0.9548402	1.087208022	1.204985681	0.861688176	1.082496896	0.956138233
1.131920545	0.8952652	1.458691937	0.782365054	1.052365547	1.3274775	1.225797336
0.750539674	0.863135	0.72378389	0.854255976	0.835329784	0.783220474	0.725507482
1.140186152	1.2867595	0.730316151	1.158393289	1.250616494	0.80680513	1.092556949
1.052954367	0.8560241	0.440437089	0.78495295	0.735827442	0.454345063	0.676976395
0.645299072	0.6379222	0.951558419	0.650782696	0.574553272	0.858970892	0.614693666
1.109637498	1.0678273	0.59730237	0.970843223	0.956267255	0.812427918	0.82267293
0.857724394	1.0296388	1.242432787	0.940674832	0.845984873	1.10812421	0.703731318
1.040879702	1.0085442	0.483314356	0.851344361	0.87911957	0.779875937	0.670809222
1.657504538	0.1899173	1.636081635	1.151999175	1.103440031	1.731744905	1.233298143
0.924081541	1.0370198	0.631358031	0.849593065	0.86921254	0.89819644	0.646009211
1.141226662	1.1627081	0.971383092	1.563857788	1.148265696	1.257091017	0.963079815
2.04704689	1.7632429	1.602100018	1.46335942	1.225585942	1.996924062	1.697154741
1.099429204	1.6335264	1.379265929	1.105207128	0.69363728	1.50087069	0.985719814
1.467381329	1.8304349	1.271392549	1.316870159	1.090514923	1.368246212	1.100048273
0.76119295	0.8861557	0.752812205	0.750218994	0.597997771	8.986269468	0.575328374
C18:1 Sphingomyelin PC	Sphingomye	C18:0/C18:1 alkyl PE	C16:0/18:1 alkyl PG	C16:0/C20:4 PE	C18:0/C18:1PE	C16:0e/C18:1 PCe
1	1	1	1	1	1	1
0.091195075	0.0974559	0.174887642	0.106346076	0.096521681	0.128570626	0.106779064
0.916403833	0.8978531	0.807932666	0.836813425	0.778158211	0.808467021	0.704518577
0.105248264	0.0981378	0.180008526	0.074189015	0.081430007	0.13471053	0.043577667
0.916403833	0.8978531	0.807932666	0.836813425	0.778158211	0.808467021	0.704518577
0.570280014	0.4880496	0.473121117	0.254961561	0.129483237	0.34336244	0.042789055
1.190923111	0.8495473	0.930534278	1.104198597	1.000009459	1.166727075	0.878299098
0.161731623	0.2224124	0.256414018	0.168901033	0.073257533	0.213926252	0.138510749
1.190923111	0.8495473	0.930534278	1.104198597	1.000009459	1.166727075	0.878299098
0.343471201	0.5583081	0.830330555	0.620334962	0.999940245	0.528973829	0.512551541
1.343762593	1.52834	1.251392675	1.158913925	0.901933979	3.463077608	1.089562801
0.275223634	0.2179269	0.179891099	0.154799117	0.151678964	1.846027923	0.231750283
1.128336986	1.7990051	1.344810938	1.049552072	0.901925447	2.968198547	1.24053731
0.649042388	0.0720685	0.345171641	0.81919373	0.581603796	0.262763152	0.463678357
1.46634327	1.702216	1.548882386	1.38491316	1.159062472	4.283511285	1.546535231
0.197151527	0.0386452	0.132041949	0.109701389	0.499185429	0.20151081	0.153621089

C16:0/18:1 alkyl PS	C16:0/C18:1 PG	Plasmalogen PE 18:0/20:4	C18:0/C20:4 alkyl PE	C20:4 Sphingomyelin PC	C16:0/20:4 alkyl PG
ND	1.052000571	0.912920529	0.934431704	0.930371153	ND
ND	1.173710585	1.039886719	1.027398061	1.126959533	ND
ND	0.722528392	0.789496611	0.795706683	0.813215177	ND
ND	1.051760452	1.257696142	1.242463551	1.129454137	ND
ND	0.714299099	0.7706803	0.694858796	0.956514563	ND
ND	0.405023621	0.542438172	0.602954488	0.779375905	ND
ND	0.832927998	0.985735129	0.964584546	1.337068583	ND
ND	0.628429219	0.820861261	0.845086707	0.926222981	ND
ND	0.726419483	0.94886724	0.886487417	1.084583212	ND
ND	1.123932559	1.411548642	1.514278867	1.390513217	ND
ND	0.725568752	0.961685515	0.985170988	0.913135285	ND
ND	0.752682743	1.226692972	1.213492122	1.150107375	ND
ND	1.259562178	1.754194518	1.776456088	1.54513063	ND
ND	0.646561419	0.971166624	0.996062658	0.858092546	ND
ND	1.078963474	1.477253939	1.318652787	1.400683221	ND
ND	0.609019667	0.670220752	0.65162641	0.777577462	ND
C16:0/18:1 alkyl PS	C16:0/C18:1 PG	Plasmalogen PE 18:0/20:4	C18:0/C20:4 alkyl PE	C20:4 Sphingomyelin PC	C16:0/20:4 alkyl PG
ND	1	1	1	1	ND
ND	0.096845695	0.099955308	0.09379685	0.077789161	ND
ND	0.645169984	0.779928716	0.776871134	0.999795508	ND
ND	0.090361513	0.091523697	0.080032656	0.118892138	ND
ND	0.645169984	0.779928716	0.776871134	0.999795508	ND
ND	0.036590987	0.155541296	0.120336478	0.99889828	ND
ND	0.832150884	1.137198592	1.149857349	1.134584772	ND
ND	0.09746393	0.111635841	0.139444656	0.098860319	ND
ND	0.832150884	1.137198592	1.149857349	1.134584772	ND
ND	0.267665666	0.395183942	0.406882985	0.325817398	ND
ND	0.898526684	1.218208958	1.185699486	1.145370965	ND
ND	0.160780614	0.244217426	0.239420502	0.192092228	ND
ND	1.079764141	1.07123678	1.031170942	1.009506731	ND
ND	0.736134307	0.773072709	0.901298867	0.961801043	ND
ND	1.392697593	1.561949103	1.526249894	1.145605232	ND
ND	0.21864764	0.143859849	0.156469399	0.543151202	ND

C16:0/C18:1 PC	C16:0/C18:1 PS	C18:0/C18:1 alkyl PG	Plasmalogen PS 16:0/20:4	C18:0/C20:4 PE	C16:0/20:4 alkyl PC
0.958127097	1.07317241	1.177628533	ND	0.925465259	0.865760883
1.041217424	1.630616136	1.012993801	ND	1.007028393	1.05318585
0.784167097	0.727747286	0.817434765	ND	0.830309437	0.692495997
1.216488382	0.568464169	0.991942901	ND	1.237196911	1.38855727
0.817351987	0.448156291	0.648786921	ND	0.827171136	0.803784487
0.632144096	0.6546916	0.468289142	ND	0.639707881	0.570342379
1.058736199	0.655675743	0.08294493	ND	1.0567512	1.034652689
0.757753229	1.272577498	0.577471642	ND	0.773332744	1.067289576
0.761645658	0.679804942	0.66515372	ND	1.066097101	0.077709175
1.262810077	1.945706922	1.036487112	ND	1.335228596	1.579738707
0.819287782	0.788290451	0.768997328	ND	1.075986321	0.785722596
1.001192916	1.012603233	0.7470596	ND	1.369340009	1.021918675
1.777706124	0.806874803	1.173066423	ND	1.608520713	1.84462278
0.961581552	1.287526243	0.704635546	ND	0.862051481	0.99822868
1.233120272	1.458009942	1.056786627	ND	1.415628516	1.198794776
0.606290946	0.837484875	0.587685948	ND	0.72683524	0.609771007
C16:0/C18:1 PC	C16:0/C18:1 PS	C18:0/C18:1 alkyl PG	Plasmalogen PS 16:0/20:4	C18:0/C20:4 PE	C16:0/20:4 alkyl PC
1	1	1	ND	1	1
0.089862524	0.235119761	0.07366349	ND	0.086920504	0.148992265
0.816496378	0.757775283	0.444373159	ND	0.82424074	0.869017283
0.089497386	0.17840399	0.126062991	ND	0.086945242	0.115545448
0.816496378	0.757775283	0.444373159	ND	0.82424074	0.869017283
0.198077653	0.443192533	0.008910644	ND	0.20276477	0.513231577
0.961234108	1.106601387	0.80442444	ND	1.211663007	0.866272288
0.112741992	0.288156614	0.080516676	ND	0.081510781	0.311124327
0.961234108	1.106601387	0.80442444	ND	1.211663007	0.866272288
0.797026111	0.784033187	0.123286654	ND	0.126022546	0.711645386
1.144674724	1.097473966	0.880543636	ND	1.153258987	1.16285431
0.246970236	0.162826149	0.139445465	ND	0.212669547	0.258054048
1.190838646	0.991751843	1.094625663	ND	0.951798463	1.34236582
0.52441106	0.978893797	0.653113978	ND	0.806182201	0.490782487
1.401934846	1.448284195	1.981541005	ND	1.399177365	1.338125643
0.258076556	0.209226541	0.059425511	ND	0.202102292	0.338746247

C16:0/20:4 alkyl PS	C16:0/C20:4 PG	C18:0/C18:1 alkyl PC	C18:0/C18:1 alkyl PS	C18:0/C18:1 PG	C16:0/C20:4 PC	C16:0/C20:4 PS
ND	1.157750675	1.220876725	1.004672256	1.040420389	0.935866244	ND
ND	0.846927352	0.784503411	1.660266475	0.858216408	0.994389518	ND
ND	0.8354898	0.786180516	0.70559804	0.785299406	0.832905387	ND
ND	1.159832173	1.208439348	0.629463229	1.316063798	1.236838851	ND
ND	0.67458874	0.699835933	0.330571346	0.741231208	0.795879881	ND
ND	0.484366919	0.740335739	0.754562293	0.470926888	0.643072833	ND
ND	0.899006272	0.924295913	0.541138099	0.828081134	1.056041965	ND
ND	0.55214199	0.576509964	1.049762016	0.714801068	0.875133359	ND
ND	0.730630322	0.843175369	0.541794088	0.72826134	0.87172262	ND
ND	1.09616343	1.107971459	1.79654905	1.178573014	1.382894415	ND
ND	0.905866768	0.601882667	0.558814459	0.824592698	0.918976541	ND
ND	0.857342232	0.937055856	0.825162859	0.73740885	1.100081239	ND
ND	1.042067828	1.715500365	0.79882712	1.50984808	1.772339486	ND
ND	0.390825462	0.865150161	1.327858506	0.869585509	0.943718957	ND
ND	0.5549765	0.680734243	1.155300931	1.019153568	1.304407162	ND
ND	0.512788092	0.509829935	0.60726528	0.706046385	0.674419854	ND
C16:0/20:4 alkyl PS	C16:0/C20:4 PG	C18:0/C18:1 alkyl PC	C18:0/C18:1 alkyl PS	C18:0/C18:1 PG	C16:0/C20:4 PC	C16:0/C20:4 PS
ND	1	1	1	1	1	ND
ND	0.091708978	0.123959349	0.234510778	0.118226148	0.085711662	ND
ND	0.65252598	0.735244387	0.669008439	0.688760075	0.842532009	ND
ND	0.091101461	0.072005079	0.153618369	0.076535944	0.085931045	ND
ND	0.65252598	0.735244387	0.669008439	0.688760075	0.842532009	ND
ND	0.03614742	0.114287493	0.28241875	0.069150542	0.242134067	ND
ND	0.897500688	0.872521338	0.930580114	0.867208976	1.068418704	ND
ND	0.07582617	0.105557228	0.295857408	0.10603389	0.115801482	ND
ND	0.897500688	0.872521338	0.930580114	0.867208976	1.068418704	ND
ND	0.422120341	0.463416976	0.86016429	0.435092212	0.651653947	ND
ND	0.62516447	0.942803676	0.972312959	1.026158386	1.173721365	ND
ND	0.143259084	0.267587507	0.164127587	0.173443446	0.237631637	ND
ND	0.69656155	1.080550854	1.044846053	1.183288475	1.098559358	ND
ND	0.14392525	0.815117029	0.905859507	0.464004694	0.70415934	ND
ND	0.958068321	1.282299726	1.453364267	1.489863341	1.393088158	ND
ND	0.877252508	0.482163688	0.225958549	0.125425324	0.237907157	ND

C18:0/C20:4 alkyl PG	C18:0/C18:1PC	C18:0/C18:1 PS	Plasmalogen PC 18:0/20:4	Plasmalogen PS 18:0/20:4	C18:0/C20:4 alkyl PC
1.090171437	1.027091383	1.052310965	0.994839466	ND	1.084391561
1.069471092	1.084110608	1.703348088	0.945267125	ND	0.760948362
0.768861027	0.793995518	0.671128533	0.777536962	ND	0.873377726
1.071496444	1.094802492	0.573212414	1.282356448	ND	1.28128235
0.704255732	0.713914527	0.322284636	0.847170637	ND	0.794435576
0.505770223	0.745476884	0.765799211	0.705174053	ND	0.85392171
0.912160916	0.928272589	0.489505049	1.129133233	ND	1.035414518
0.724085248	0.928126816	1.149180941	0.790418617	ND	0.399983378
0.848148493	0.805283614	0.491659568	0.825554121	ND	1.278822349
1.305966435	0.146659651	0.183165146	1.295683291	ND	1.612074361
0.994972427	0.089903992	0.590091964	0.689268287	ND	0.754181608
1.016479339	1.160436484	0.8977408	0.788795409	ND	1.16975489
1.695889879	1.765714914	0.799240278	1.986206117	ND	2.151028437
0.891941734	1.390680385	1.322024016	1.073111173	ND	1.324475787
1.329638291	1.287572214	1.199278556	1.07517202	ND	0.766829813
0.79430203	0.707725649	0.655349121	0.635951288	ND	0.724459917
C18:0/C20:4 alkyl PG	C18:0/C18:1PC	C18:0/C18:1 PS	Plasmalogen PC 18:0/20:4	Plasmalogen PS 18:0/20:4	C18:0/C20:4 alkyl PC
1	1	1	1	ND	1
0.077187049	0.070257797	0.256212649	0.10497511	ND	0.115260785
0.71156803	0.828947704	0.681692459	0.867974135	ND	0.770938795
0.083066436	0.057664214	0.180676832	0.091813028	ND	0.133851159
0.71156803	0.828947704	0.681692459	0.867974135	ND	0.770938795
0.043863966	0.10886286	0.34914169	0.380348199	ND	0.242341532
1.041391673	0.550570935	0.54066437	0.899825277	ND	1.203708302
0.095794094	0.260155866	0.147239552	0.135056053	ND	0.176925606
1.041391673	0.550570935	0.54066437	0.899825277	ND	1.203708302
0.747981037	0.146402736	0.17108527	0.579470484	ND	0.371941408
1.177942984	1.287923291	0.993972993	1.19261015	ND	1.241698488
0.208218145	0.218988828	0.158733216	0.283979954	ND	0.332511784
1.131123874	2.339250419	1.838428883	1.325379693	ND	1.031560958
0.573093513	0.073229963	0.081178808	0.387744794	ND	0.922945364
1.655418645	1.55368461	1.458095919	1.37401577	ND	1.610631734
0.082689309	0.08905802	0.241799359	0.318466775	ND	0.237050896

C18:0/C20:4 alkyl PS	C18:0/C20:4 PG	C18:0/C20:4 PC	C18:0/C20:4 PS	C16:0/C16:0/C16:0 TAG	C16:0/C18:1/C16:0 TAG
ND	ND	1.008749894	1.072247365	0.765020924	0.803017349
ND	ND	0.908275307	1.19456632	1.167096402	1.154726747
ND	ND	0.825093927	0.704597713	0.803227629	0.8570579
ND	ND	1.257880872	1.028588602	1.264655045	1.185198005
ND	ND	0.776794635	0.550754852	0.948967921	1.028478481
ND	ND	0.647338605	0.467059054	0.898566397	0.91405457
ND	ND	1.008244369	0.805908966	1.135530802	1.209916869
ND	ND	0.82219154	0.672321661	0.866427329	0.79665394
ND	ND	0.934970219	0.693740593	0.855642457	0.827863772
ND	ND	1.445155443	1.257814226	1.162970289	1.00344699
ND	ND	1.011578108	0.663624822	1.083969269	0.963483353
ND	ND	1.103692435	0.831645846	1.135273684	0.108137936
ND	ND	1.897074544	0.640636687	1.568252551	1.629421347
ND	ND	1.024931358	0.706960469	0.846985141	0.972666585
ND	ND	1.336445996	1.132812054	1.137099791	1.286453233
ND	ND	0.745178438	0.509572337	0.694739278	0.740777542
C18:0/C20:4 alkyl PS	C18:0/C20:4 PG	C18:0/C20:4 PC	C18:0/C20:4 PS	C16:0/C16:0/C16:0 TAG	C16:0/C18:1/C16:0 TAG
ND	ND	1	1	1	1
ND	ND	0.093801501	0.104544868	0.126457513	0.098941597
ND	ND	0.813642287	0.624011133	0.962373112	0.987275965
ND	ND	0.074698128	0.073836061	0.060166557	0.088017398
ND	ND	0.813642287	0.624011133	0.962373112	0.987275965
ND	ND	0.171145803	0.026027098	0.797172082	0.926582377
ND	ND	1.123849051	0.861706372	1.059463925	0.725733013
ND	ND	0.11251817	0.137007868	0.069883468	0.209265511
ND	ND	1.123849051	0.861706372	1.059463925	0.725733013
ND	ND	0.430278972	0.452896179	0.694956126	0.2808734
ND	ND	1.250907584	0.747495387	1.061769191	1.157329677
ND	ND	0.246927078	0.134826485	0.19214648	0.193037038
ND	ND	1.113056582	0.86745951	1.002175879	1.594704466
ND	ND	0.656140584	0.574107903	0.991369675	0.180313933
ND	ND	1.537417122	1.197887902	1.103282269	1.172245368
ND	ND	0.141015494	0.452438733	0.639095946	0.453379504

C16:0/C20:4/C16:0 TAG	C18:0/C18:1/C18:0 TAG	C18:0/C18:0/C18:0 TAG	C18:0/C20:4/C18:0 TAG	C16:0 FFA	C18:1 FFA	C18:0 FFA
0.927913679	0.911831566	1.007991243	1.00267419	0.672467158	0.232086789	0.961621451
1.075356061	1.1044991	0.962176483	1.037490215	1.407006297	1.391854242	1.392066585
0.87012929	0.841731223	0.719650112	0.873610211	1.374950436	1.930189101	1.104391544
1.126600969	1.141938111	1.310182162	1.086225384	0.545576109	0.445869868	0.54192042
1.111273464	1.083250772	0.855941353	1.024007528	0.682538757	0.619180557	0.602443056
0.8047739	0.936262229	0.854519763	0.936727994	0.401430028	0.235892368	0.5258323
1.114132548	1.270507915	1.14723228	1.096024116	1.016589797	1.023443494	1.222825867
0.98801591	1.2321877	1.444408323	1.02601271	5.212759831	1.460706822	5.066512956
0.955878973	1.196337498	1.095295728	0.833404347	0.957977739	0.67523028	1.257540707
1.241469387	1.191837573	1.38533418	1.047213934	0.89779271	0.902270108	1.061636591
0.813103675	0.865590462	0.831274267	0.812032868	0.440607718	0.333368261	0.475220007
1.408457254	1.437596081	1.014130481	1.072586602	0.731940058	0.621485837	0.939789483
2.33403459	2.711072451	2.856929849	1.827224653	0.998879318	0.519831453	1.843593041
1.432622607	1.671896272	1.33066128	1.078712439	0.861213729	0.797990082	1.138761292
1.639455914	1.704151093	1.288602163	1.157787906	0.705840821	0.477488918	1.087610212
0.931545529	0.95111934	0.729826158	0.650408573	0.827747483	0.679402455	1.014601056
C16:0/C20:4/C16:0 TAG	C18:0/C18:1/C18:0 TAG	C18:0/C18:0/C18:0 TAG	C18:0/C20:4/C18:0 TAG	C16:0 FFA	C18:1 FFA	C18:0 FFA
1	1	1	1	1	1	1
0.060393971	0.072966412	0.121210393	0.04548064	0.227306839	0.399536441	0.17699426
1.004548955	1.130552154	1.07552543	1.020693087	1.828329603	0.83480581	1.854403544
0.072790853	0.076323541	0.140912837	0.032614139	1.135127326	0.263395744	1.082013703
1.004548955	1.130552154	1.07552543	1.020693087	1.828329603	0.83480581	1.854403544
0.96320159	0.262511546	0.698595312	0.724271706	0.501171017	0.741723926	0.465428663
1.104727322	1.172840404	1.081508664	0.941309438	0.757079557	0.633088622	0.933546697
0.134830278	0.117406381	0.115346254	0.068802493	0.115811158	0.116976319	0.166203055
1.104727322	1.172840404	1.081508664	0.941309438	0.757079557	0.633088622	0.933546697
0.505002188	0.257722661	0.643446516	0.503421766	0.377751777	0.412041663	0.793493978
1.58441466	1.759559789	1.551504863	1.178533393	0.848420338	0.618678227	1.2711414
0.290723022	0.361675191	0.456177963	0.243260967	0.060248002	0.073906066	0.192510177
1.434213337	1.500255094	1.434574603	1.252014848	1.120648855	0.97723795	1.361625942
0.185076194	0.173782271	0.356428914	0.384273092	0.510325384	0.920447697	0.232650431
1.577239866	1.556372064	1.442555257	1.15464032	0.464041241	0.741104362	0.685471835
0.101163214	0.139716532	0.357290716	0.543939899	0.421773721	0.459584046	0.614674591

C20:4 FFA	PGD2/PGE2	C16:0 alkyl LPA	C16:0 LPA	C18:1 alkyl LPA	C18:0 alkyl LPA	C18:1 LPA	C18:0 LPA
0.37967339	ND	0.892449212	0.900055024	1.074411982	0.97986939	0.681638177	0.963485552
1.649373621	ND	0.964516952	1.012164037	0.951014484	0.935381771	1.39961434	1.086136541
1.705727286	ND	1.00222543	1.173897241	1.043353976	1.065963702	1.331683072	1.080360667
0.265225703	ND	1.140808406	0.913883698	0.931219558	1.018785137	0.587064411	0.87001724
0.577909198	ND	0.778615217	0.898092379	0.682534584	1.073986927	0.69027637	0.811496641
0.263667937	ND	0.988547044	0.844660246	1.287708756	0.740826228	0.536776813	0.744813282
1.242933195	ND	1.112127666	1.086826268	0.747087914	1.249345691	0.85064301	0.828172765
1.258338888	ND	2.652064959	2.519471268	14.26400172	5.797174104	3.398701304	3.404047083
1.082695116	ND	1.227408756	1.228634781	1.043478936	1.106091962	0.955576524	1.086870438
0.533968231	ND	0.907964626	0.732256886	0.9205673	0.907088819	0.538330844	0.849866385
0.386607283	ND	0.775944117	0.891635164	0.880461631	0.865204164	0.689675886	0.70811625
0.34142393	ND	0.99212186	1.39671976	1.227399912	0.831253127	1.05263447	1.25850552
0.348457637	ND	0.827386828	0.834051828	1.359771597	0.909817033	0.474102903	0.625597601
0.502402761	ND	0.7258254	0.882936509	1.114964403	1.007059479	0.572334511	0.78827886
0.442931608	ND	0.836122282	0.827658226	0.620739392	0.880945666	0.51009547	0.824477022
0.609519836	ND	1.542301572	1.616306927	1.440399273	1.569764941	1.130396283	1.455912365
C20:4 FFA	PGD2/PGE2	C16:0 alkyl LPA	C16:0 LPA	C18:1 alkyl LPA	C18:0 alkyl LPA	C18:1 LPA	C18:0 LPA
1	ND	1	1	1	1	1	1
0.392049686	ND	0.05216814	0.063109184	0.034817429	0.027816135	0.212441233	0.051725367
0.835712304	ND	1.382838722	1.33726254	4.245333244	2.215333237	1.369099374	1.447132443
0.248015336	ND	0.428638512	0.397477804	3.342311019	1.19859495	0.679561287	0.652553386
0.835712304	ND	1.382838722	1.33726254	4.245333244	2.215333237	1.369099374	1.447132443
0.735350495	ND	0.409416796	0.434131938	0.369079263	0.349848939	0.622732266	0.520056833
0.58617364	ND	0.97585984	1.062311648	1.017976945	0.927409518	0.809054431	0.975839648
0.170535464	ND	0.094919864	0.152085168	0.077946259	0.061546665	0.11844213	0.122397206
0.58617364	ND	0.97585984	1.062311648	1.017976945	0.927409518	0.809054431	0.975839648
0.370456531	ND	0.831024235	0.718140711	0.840184984	0.32378719	0.4622882	0.861708508
0.47582796	ND	0.982909021	1.040238372	1.133968666	1.09189678	0.671732292	0.923566462
0.054684784	ND	0.188136811	0.192419261	0.184538192	0.161557202	0.154228297	0.182642423
0.811752573	ND	1.007223559	0.979221469	1.113943368	1.177362059	0.830268356	0.946432607
0.56042814	ND	0.974399249	0.931218279	0.583643931	0.378120563	0.506563691	0.819982384
0.56936814	ND	0.710790785	0.777886422	0.267109459	0.492881505	0.490638083	0.638204517
0.206247496	ND	0.425701506	0.526240283	0.388502846	0.388785965	0.35558205	0.469067474

C20:4 LPA	C16:0 alkyl LPI	C16:0 LPI	C18:1 alkyl LPI	C18:0 alkyl LPI	C18:1 LPI	C18:0 LPI	C20:4 alkyl LPI
0.334948993	ND	1.524341867	ND	ND	1.265767673	1.405827535	ND
2.048207212	ND	0.521396943	ND	ND	0.809279846	0.627595001	ND
1.346233277	ND	1.050415996	ND	ND	0.907687205	0.882571764	ND
0.270610517	ND	0.903845194	ND	ND	1.017265276	1.0840057	ND
0.653256539	ND	0.722622204	ND	ND	0.797919404	0.870067734	ND
0.241072016	ND	0.833983568	ND	ND	0.980346149	1.186702268	ND
0.833715932	ND	0.596070121	ND	ND	0.769577722	0.902376391	ND
1.260168444	ND	2.75863148	ND	ND	7.049480251	6.778120804	ND
0.723321255	ND	0.926978508	ND	ND	1.068665168	1.204810339	ND
0.345080042	ND	0.736247339	ND	ND	0.781165418	0.927718929	ND
0.587256343	ND	0.737907774	ND	ND	1.050045549	1.100453417	ND
0.534413016	ND	0.949011607	ND	ND	0.755825544	1.145774386	ND
0.345665068	ND	0.622774205	ND	ND	0.563975639	0.847492152	ND
0.453582323	ND	0.549571824	ND	ND	0.487378911	0.939899634	ND
0.432894237	ND	0.362568972	ND	ND	0.361241738	0.57849185	ND
1.131398281	ND	0.824514721	ND	ND	1.045722003	1.215656134	ND
C20:4 LPA	C16:0 alkyl LPI	C16:0 LPI	C18:1 alkyl LPI	C18:0 alkyl LPI	C18:1 LPI	C18:0 LPI	C20:4 alkyl LPI
1	ND	1	ND	ND	1	1	ND
0.427484668	ND	0.207320766	ND	ND	0.0982456	0.164374527	ND
0.747053233	ND	1.227826843	ND	ND	2.399330881	2.434316799	ND
0.211268481	ND	0.51257712	ND	ND	1.550753067	1.449680764	ND
0.747053233	ND	1.227826843	ND	ND	2.399330881	2.434316799	ND
0.6148406	ND	0.694622516	ND	ND	0.4025249	0.363522653	ND
0.547517664	ND	0.837536307	ND	ND	0.91392542	1.094689268	ND
0.078336235	ND	0.058174987	ND	ND	0.084209	0.059615895	ND
0.547517664	ND	0.837536307	ND	ND	0.91392542	1.094689268	ND
0.337933786	ND	0.479108795	ND	ND	0.530644918	0.607641432	ND
0.590884977	ND	0.58985743	ND	ND	0.614579573	0.895384942	ND
0.181682078	ND	0.09549456	ND	ND	0.149667582	0.13142493	ND
1.079207149	ND	0.704276848	ND	ND	0.672461406	0.817935252	ND
0.83376677	ND	0.068669537	ND	ND	0.131941999	0.216499551	ND
0.790954314	ND	0.480407668	ND	ND	0.256146235	0.367817756	ND
0.595459467	ND	0.266979091	ND	ND	0.295600643	0.331103196	ND

C20:4 LPI	C16:0/18:1 alkyl PA	C16:0/C18:1 PA	C16:0/20:4 alkyl PA	C18:0/C18:1 alkyl PA	C16:0/C20:4 PA	C18:0/C18:1 PA
1.17178536	1.000093292	0.982950293	0.834370503	1.134789197	0.854869291	1.019438452
0.88237034	1.077699511	1.080521321	1.099786576	0.744749535	1.128415674	0.85904928
1.0198342	0.924091889	1.116095323	1.507590869	1.172662193	1.297594914	1.169238095
0.9260101	0.998115307	0.820433063	0.558252052	0.947799075	0.719120122	0.952274174
1.02168556	0.748674495	0.838498115	1.357505082	0.835373284	1.058587628	0.878067814
0.99386724	0.854226447	1.03026597	0.93026877	0.74125916	0.720663657	0.962131195
0.80882126	0.809805315	0.901136175	1.015784839	0.986539255	1.077530156	1.080752921
7.27795115	3.120818039	6.440799029	4.103447085	2.217278947	3.91645586	2.716659329
1.25181927	1.023064073	0.930482343	0.930786489	0.94680216	0.882124837	1.273082455
1.0641222	1.048846578	0.955192143	0.631055456	0.751940682	0.577031509	0.886148937
1.14451181	0.607923444	0.725450459	1.049569386	0.633407516	0.571510061	0.767079728
1.14091847	1.265841406	1.570452501	0.829125534	1.240356671	0.666713044	1.630250165
0.51738083	0.820509013	0.771640032	0.79884693	0.801621121	0.721398473	0.822073186
0.82663719	1.129650318	1.055095129	0.926993125	0.809679391	0.629787573	0.996589062
0.73707035	1.065533	0.896842296	1.134226981	0.982601525	0.740955216	1.006026722
1.6102151	1.623610172	1.743343514	1.885227134	2.199948345	1.219074581	2.249881826
C20:4 LPI	C16:0/18:1 alkyl PA	C16:0/C18:1 PA	C16:0/20:4 alkyl PA	C18:0/C18:1 alkyl PA	C16:0/C20:4 PA	C18:0/C18:1 PA
1	1	1	1	1	1	1
0.0640409	0.031361888	0.066141757	0.202109754	0.098259053	0.130706333	0.065296916
2.5255813	1.383381074	2.302674822	1.851751444	1.195112662	1.693309325	1.409402815
1.5848274	0.57954964	1.379952301	0.756217738	0.344446682	0.745568895	0.437730809
2.5255813	1.383381074	2.302674822	1.851751444	1.195112662	1.693309325	1.409402815
0.37327778	0.533426188	0.382123432	0.318299832	0.605583099	0.395021023	0.390628562
1.15034294	0.986418875	1.045394362	0.860134216	0.893126757	0.674344863	1.139140321
0.03857275	0.137409313	0.182435231	0.088654782	0.132551013	0.072615223	0.19612137
1.15034294	0.986418875	1.045394362	0.860134216	0.893126757	0.674344863	1.139140321
0.09102817	0.926373328	0.822820369	0.549630866	0.541141731	0.072264229	0.525926552
0.92282587	1.159825626	1.116730243	1.186323542	1.198462596	0.827803961	1.268642699
0.23816084	0.168333379	0.21677197	0.242997029	0.336427957	0.132654947	0.329802325
0.80221805	1.175794234	1.068238249	1.37923073	1.341872904	1.227567683	1.113684306
0.38207492	0.455273281	0.809612101	0.254104273	0.430817827	0.349385933	0.747233587
0.36539147	0.838399229	0.484970883	0.640649449	1.002803028	0.488867538	0.900127831
0.35588063	0.723786845	0.428449327	0.434264928	0.994674314	0.296618891	0.805890123

C18:0/C20:4 alkyl PA	C18:0/C20:4 PA	C16:0/C16:0 PI	C16:0/18:1 alkyl PI	C16:0/C18:1 PI	C16:0/20:4 alkyl PI	C18:0/C18:1 alkyl PI
1.070126193	1.041539847	1.081948228	0.909087064	0.993051369	0.89002432	1.249598923
0.92739884	1.174591313	0.897686666	1.068744791	0.958474339	1.231720122	0.959664008
1.185398778	0.944595806	1.458710155	1.29961102	1.313957076	0.926025738	1.065646514
0.817076189	0.839273034	0.561654952	0.722557126	0.734517216	0.95222982	0.725090555
0.956521171	0.869080866	0.783042705	0.850296749	0.886955351	0.851034475	0.639683648
0.921763406	0.815517855	0.897093204	0.941098326	0.877694679	1.168403878	0.766934088
1.011096275	1.062428445	0.888417293	0.969165881	0.913578413	1.103586181	1.025810441
10.32923651	5.676718157	2.845570112	5.615850415	2.855252944	11.61963692	16.11938937
1.055960794	1.152568391	1.524658936	1.432101279	1.337080442	1.477966355	0.989881928
0.975398591	0.642070402	1.137346849	1.385740712	1.125827831	1.283658287	1.142033808
0.968529615	0.709776932	1.119297292	1.321562649	1.122516475	1.101947513	0.763851382
2.017861732	0.901591912	1.618477376	1.55916042	1.810371305	1.234315178	1.997826459
0.96106519	0.890970856	0.56813008	0.802680061	0.563399949	1.099866833	0.789608826
0.977645902	0.787273033	0.764526633	1.042809106	0.755607182	0.981725012	0.967588934
0.879947802	0.655491608	0.995102683	0.972935619	1.055970658	1.237744623	0.805198397
2.079155645	1.238657573	3.103164885	2.192763589	2.971377908	1.177199084	2.39887915
C18:0/C20:4 alkyl PA	C18:0/C20:4 PA	C16:0/C16:0 PI	C16:0/18:1 alkyl PI	C16:0/C18:1 PI	C16:0/20:4 alkyl PI	C18:0/C18:1 alkyl PI
1	1	1	1	1	1	1
0.080634173	0.071362028	0.187026049	0.122383387	0.119311504	0.078285294	0.109472707
3.304654341	2.105936331	1.353530828	2.094102843	1.383370347	3.685665363	4.637954386
2.341599558	1.191441104	0.498021404	1.174189868	0.490686472	2.645543032	3.827987942
3.304654341	2.105936331	1.353530828	2.094102843	1.383370347	3.685665363	4.637954386
0.363279076	0.389897188	0.531031187	0.389801424	0.476504937	0.349395848	0.378807009
1.254437683	0.851501909	1.349945113	1.424641265	1.348949013	1.274471833	1.223398394
0.255247526	0.114417933	0.12943175	0.050240678	0.161788481	0.077927108	0.269578749
1.254437683	0.851501909	1.349945113	1.424641265	1.348949013	1.274471833	1.223398394
0.378545989	0.313003435	0.174825148	0.018371208	0.133271854	0.047493772	0.471731191
1.224453635	0.893098267	1.35773107	1.252797094	1.336588924	1.124133888	1.240318827
0.285699044	0.12485714	0.588316792	0.317353609	0.554274496	0.05522114	0.38827749
0.976097618	1.048850575	1.00576761	0.879377233	0.990837245	0.882039021	1.013830681
0.940162608	0.814163924	0.990106534	0.611996793	0.983615676	0.166537215	0.972605957
0.370523967	0.424086073	1.003103174	0.598250033	0.966183009	0.305001615	0.267427992
0.411800157	0.350411458	0.995828884	0.514996558	0.951663598	0.37041263	0.411191638

C16:0/C20:4 PI	C18:0/C18:1 PI	C18:0/C20:4 alkyl PI	C18:0/C20:4 PI
1.04098327	0.993994229	1.061633358	1.05091908
0.971240496	1.021539231	1.091661596	1.068028672
1.194871192	1.295361771	1.142944157	1.111350511
0.792905042	0.689104769	0.703760889	0.769701737
0.919271784	0.882933923	0.979412009	1.056795864
0.826969429	0.930891027	0.90907441	1.03948756
1.084486693	1.056043848	1.079197868	1.300150324
2.831683562	5.719409473	6.18666626	13.23686396
1.163158443	1.179075602	1.13290745	1.389948729
1.048937886	1.157441965	1.413565901	1.245424134
0.926799905	1.107939913	0.904500892	1.108806681
1.945019043	1.809962187	1.814257992	2.181319917
0.567174542	0.619837112	0.761980483	0.77036975
0.764343755	0.939650166	1.249673257	1.196037181
0.970580782	1.008419166	1.145935326	1.095461996
2.006244194	2.840177719	2.672911708	2.802005127
C16:0/C20:4 PI	C18:0/C18:1 PI	C18:0/C20:4 alkyl PI	C18:0/C20:4 PI
1	1	1	1
0.083351585	0.123960487	0.100162851	0.077812209
1.415602867	2.147319568	2.288587637	4.158324428
0.475022484	1.191255586	1.299828134	3.026764804
1.415602867	2.147319568	2.288587637	4.158324428
0.421926183	0.375082104	0.361114698	0.337086635
1.270978819	1.313604917	1.316308059	1.481374865
0.229803677	0.166120849	0.195923911	0.24027096
1.270978819	1.313604917	1.316308059	1.481374865
0.31008652	0.181043202	0.20061605	0.105289189
1.077085818	1.352021041	1.457625194	1.465968513
0.320480852	0.503224237	0.418453249	0.454513428
0.847445923	1.029244808	1.10735871	0.989599964
0.640421365	0.944566363	0.770053809	0.977065425
0.76086722	0.629631966	0.636910368	0.352538273
0.576243484	0.561143722	0.565146487	0.412887761

Table 3. Primer List

Primer	Forward	Reverse
mSpt1	TACTCAGAGACCTCCAGCTG	CACCAGGGATATGCTGTCATC
mSpt2	GGAGATGCTGAAGCGGAAC	GTATGAGCTGCTGACAGGCA
mCers2	GGCGCTAGAAGTGGGAAAC	TCGAATGACGAGAAAGAGCA
mCers3	GCTACACCTCTAGCAAATGCAC	ATCTTTCAACCTGGCGCTCT
mCers4	TGTCGTTGACGTTGAGTGAG	AGCAGGCTTCACAGAATTTC
mCers5	ACACTAGCCAATCAGGGCG	GCTGCACTCTCAGGCTCC
mCers6	ACAAAGCAAGATGGCAGGGA	TCCGTGTTCTTCAGGTCTGC
mDes1	CACCGGTACCTCGGAGCGGA	GTTTGGGATTGATGAACAGGGGT
mSgms1	CTCATGAGGCCCAACAAGAT	CACCTTCTTGGGTGACCAGT
mSmpd1	GGCGAGTACAGCAAGTGTGA	AAGCCATTGACAGGAGTGCT
mCerk	CGGTACTGGTGTCGGAGATCA	GTGAATGCGAACGGATTTTCC
mSphk1	TCCTGGAGGAGGCAGAGATA	CATTAGCCCATTCACCACCT
mSgpp1	TACCCATTGGTGGACCTGAT	CAGGGTATAAGCAGCGTGT
mAsah1	ATCAAAAGCTGCCTGGTATGAT	TCCACCCAAGAAATATTCCAA
mUgcg	GGAATGGCCTTGTTCGGCT	CGGCTGTTTGTCTGTTGCC
mGba	ATCTGCTTGGCTCACGAGTT	TGTCGATGAAAGGGGTCTTC

Chapter II:

Pik3r1 is Required for Glucocorticoid-induced Perilipin 1 Phosphorylation in Lipid Droplet for Adipocyte Lipolysis

Abstract

Glucocorticoids promote lipolysis in white adipose tissue (WAT) to adapt to energy demands under stress, while superfluous lipolysis causes metabolic disorders, including dyslipidemia and hepatic steatosis. Glucocorticoid-induced lipolysis requires the phosphorylation of cytosolic hormone sensitive lipase (HSL) and perilipin 1 (Plin1) in the lipid droplet by protein kinase A (PKA). We previously identified *Pik3r1* (a.k.a. *p85α*) as a glucocorticoid receptor target gene. Here, we found that glucocorticoids increased HSL phosphorylation, but not Plin1 phosphorylation in adipose tissue-specific *Pik3r1*-null (AKO) mice. Furthermore, in lipid droplets, glucocorticoid-increased phospho-HSL, and catalytic and regulatory subunits of PKA were attenuated in AKO mice. In agreement with reduced WAT lipolysis, glucocorticoid-initiated hepatic steatosis and hypertriglyceridemia were improved in AKO mice. Our data demonstrated a novel role of Pik3r1, independent of its regulatory function of phosphoinositide 3-kinase, in mediating the metabolic action of glucocorticoids. The inhibition of Pik3r1 may alleviate lipid disorders caused by excess glucocorticoid exposure.

Introduction

Endogenous glucocorticoids (GC) are steroid hormones released from the adrenal gland in response to stress signals. During fasting, GC promote lipolysis in white adipose tissue (WAT), where triglycerides (TG) are hydrolyzed to glycerol and fatty acids as energy fuels. Glycerol serves as a precursor for hepatic gluconeogenesis, whereas mobilized fatty acids are oxidized in energy-requiring tissues to produce ATP. However, prolonged GC exposure results in dyslipidemia, hepatic steatosis, and insulin resistance [1-3]. While exogenous GC are frequently prescribed as effective anti-inflammatory agents, their actions in metabolic tissues pose a therapeutic conundrum [4].

GC relay their message through the intracellular GC receptor (GR), which is a transcription factor. GC-induced adipocyte lipolysis requires *de novo* protein synthesis [5-7], which is consistent with the concept that GR exerts its main function through modulating gene expression. Several mechanisms are documented: first, GC increase the transcription of genes encoding lipolytic enzymes, including adipose triglyceride lipase (ATGL, a.k.a. desnutrin) and hormone sensitive lipase (HSL) [7-9]. ATGL catalyzes the hydrolysis of TG to diacylglycerol (DAG), whereas HSL hydrolyzes DAG to monoacylglycerol (MAG) [10, 11]. Second, GC elevate the levels of cyclic AMP (cAMP) [12-15], which activates protein kinase A (PKA). PKA phosphorylates HSL in the cytosol and perilipin 1 (Plin1) on lipid droplets [10, 11]. Phosphorylated HSL (pHSL) are mobilized to lipid droplets and associate with phosphorylated Plin1 (pPlin1) [16-18]. This anchoring of pHSL to lipid droplet is critical, since TG are stored within lipid droplets. Upon phosphorylation of Plin1, the interaction between Plin1 and CGI-58 is disrupted, which allows the activation of ATGL by CGI-58 [11, 19, 20]. Third, GC decrease the expression of Akt [21] and cAMP phosphodiesterase 3B (PDE3B) to augment cAMP levels [13]. Fourth, GC induce the transcription of Angiopoietin-like 4 (*Angptl4*) [22], which encodes a secreted protein that activates cAMP-PKA signaling in adipocytes to stimulate lipolysis [14]. Overall, we propose that GC promote WAT lipolysis through a network of GR primary target genes, including *ATGL*, *HSL* and *Angptl4*, most of which remain to be discovered.

We identified *Pik3r1* (a.k.a. *p85α*) as a GR primary target gene in both adipocytes and myotubes with RNA profiling and chromatin immunoprecipitation sequencing (ChIPseq) analysis [9, 23]. *Pik3r1* encodes a regulatory subunit of phosphoinositide 3-kinase (PI3K). Overexpression of Pik3r1 reduces insulin signaling in myotubes and hepatocytes [23-26]. Monomeric Pik3r1 competes with heterodimeric PI3K, which composes of Pik3r1 and p110 (the catalytic subunit of PI3K), for the binding to insulin receptor substrate-1 (IRS-1) [27, 28]. Since Pik3r1 lacks the catalytic capacity, insulin signaling is attenuated. Alternatively, Pik3r1 can potentiate phosphatase and tensin homolog (PTEN) to inhibit PI3K [29, 30]. These data illustrated that increased Pik3r1 is negatively associates with insulin sensitivity.

In adipocytes, insulin suppresses lipolysis partly through PI3K-Atk-PDE3B pathway to decrease the levels of cAMP [31-33]. Therefore, GC-induced, excess Pik3r1 could attenuate insulin signaling and in turn promote lipolysis. To investigate the role of Pik3r1 in lipolysis, we generated adipose tissue-specific Pik3r1 knockout (AKO) mice. Surprisingly, lack of Pik3r1 did not attenuate PI3K-Atk-PDE3B pathway. Instead, we found that the levels of pPlin1 were significantly decreased in inguinal and epididymal WAT of AKO mice in response to GC. Furthermore, in lipid droplets of WT mice, subunits of PKA were increased by GC treatment. However, this action was abolished in AKO mice. Moreover, pHSL levels in lipid droplets were augmented by Dex in WT mice, and this effect was not seen in AKO mice. Finally, Dex-induced hepatic steatosis and hypertriglyceridemia were dramatically improved in AKO mice. In summary, we have shown that Pik3r1 mediates the metabolic actions of GC in WAT. Our data underscore the possibility that antagonists of WAT Pik3r1 may improve the adverse effects of GC therapeutics.

Results

Dex treatment increased Pik3r1 protein in WAT depots

We have previously identified *Pik3r1* as a GC primary target genes in 3T3-L1 adipocytes, and here we examined whether GC induces Pik3r1 protein levels *in vivo*. Dexamethasone (Dex), a synthetic glucocorticoid, was administered intraperitoneally for 1, 4, or 7 days in floxed Pik3r1 mice [34] (*Pik3r1* $^{flox/flox}$, referred to as WT) mice. Compared to PBS injection, Dex treatment increased the levels of Pik3r1 protein as soon as in 1 day by 2-fold, in both inguinal (iWAT, Fig. 1a) and epididymal white adipose tissues (eWAT, Fig. 2b). By the end of 7 days, Dex elevated Pik3r1 protein levels by approximately 3-fold in both adipose depots (Fig. 1a and 1b). These results demonstrated that GC increases Pik3r1 protein expression in iWAT and eWAT *in vivo*.

To study the role of Pik3r1 in GC-promoted lipolysis, we generated adipose tissue-specific *Pik3r1*-null mice with AdipoQ-Cre [35] and floxed Pik3r1 mice [34] and termed AKO mice for simplicity. To confirm the knockout efficiency and tissue specificity, we isolated iWAT, eWAT, liver, and gastrocnemius muscle (GA) from 8-week old AKO mice and control littermates. Immunoblotting showed total ablation of Pik3r1 protein in iWAT and eWAT from AKO mice, while their expressions are present in both depots from WT mice (Fig. 1c). Furthermore, Pik3r1 expressions are intact in the liver and gastrocnemius muscle of AKO mice (Fig. 1d). These data demonstrated extremely high efficiency and specificity for the knockout line. Importantly, AKO mice showed no gross phenotype and maintained a similar body weight to their control littermates (Fig. 1e).

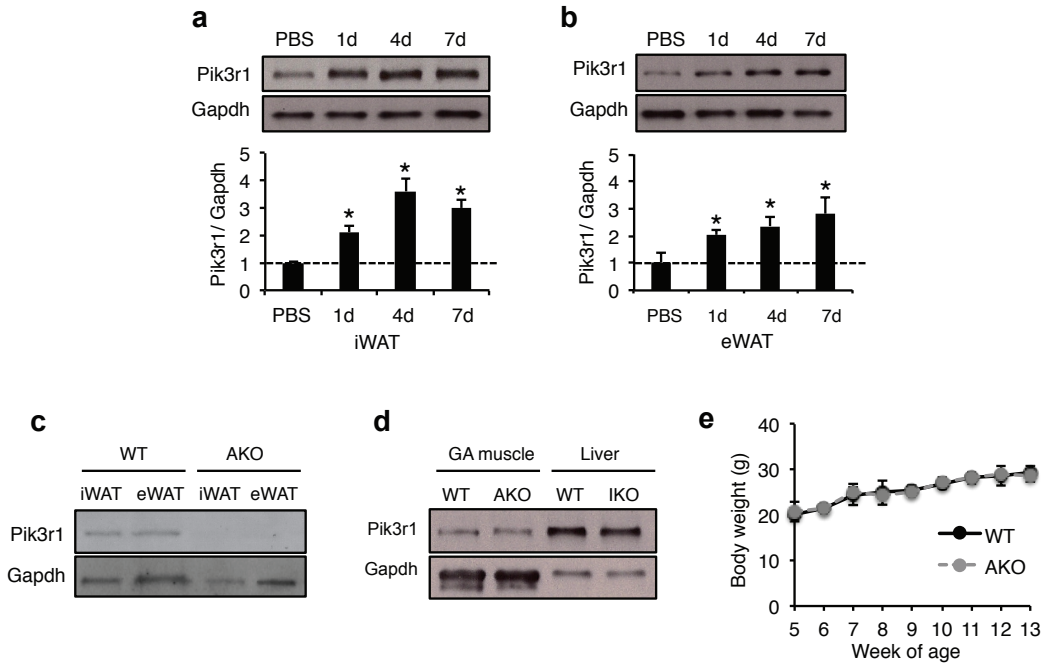

Fig. 1. Dex induced Pik3r1 protein expression in iWAT and eWAT.

(a-b) Eight-week old male WT mice were injected intraperitoneally with control PBS or Dex (5mg/kg body weight) for 1-, 4- or 7- day. Pik3r1 protein expression was measured with immunobloting in (a) iWAT and (b) eWAT, and normalized to internal control Gapdh. Representative immunoblots are shown (n=3). Error bars represent the S.E.M. of relative Pik3r1 expression level (Dex *vs.* PBS), and *p < 0.05. (c-d) In 8-week old male WT and AKO mice, Pik3r1 expressions were examined in (c) iWAT and eWAT, and (d) gastrocnemius (GA) muscle and liver. (e) Body weight of WT and AKO mice were monitored from age of 5 to 13 week, and n=6. Error bars represent the S.E.M., and *p < 0.05.

Dex-induced WAT lipolysis was absent in AKO mice

We hypothesize that Pik3r1 mediates Dex-induced lipolysis in iWAT and eWAT. We injected a single dose of Dex or control PBS in AKO and WT mice. After 24 h, glycerol release from isolated iWAT and eWAT was measured. The amount of released glycerol indicates the degree of lipolysis. In WT mice, Dex induces glycerol release in both iWAT and eWAT explants (Fig. 2a and 2b). In contrast, in AKO mice, the Dex-stimulated glycerol release was absent (Fig. 2a and 2b). Furthermore, we also measured the levels of plasma free fatty acid (FFA), the other product of lipolysis. Plasma FFA levels were increased in Dex-treated WT mice (Fig. 2c). However, Dex failed to elevate plasma FFA in AKO mice (Fig. 2c). These results illustrated that Pik3r1 is required for Dex-initiated WAT lipolysis.

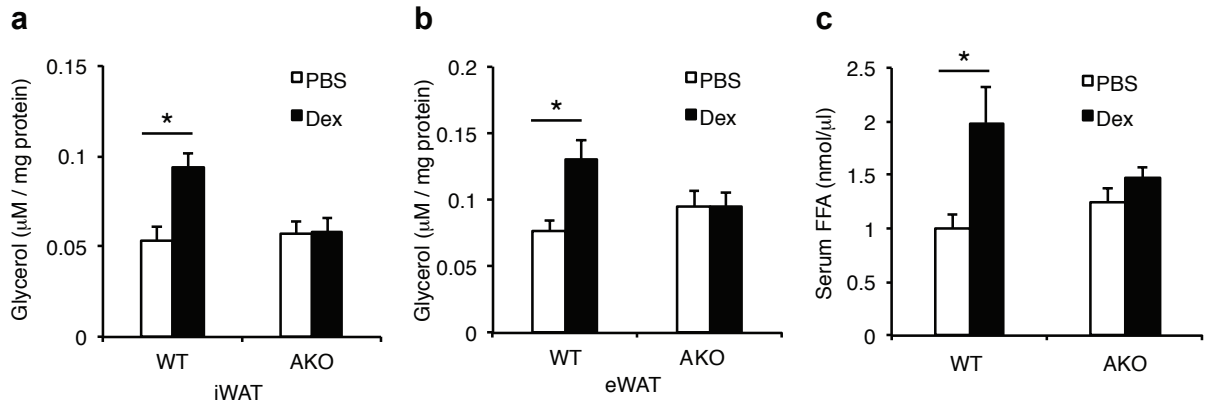

Fig. 2. Dex stimulated WAT lipolysis was abolished in AKO mice.

Eight-week old male WT and AKO mice were administered PBS or Dex (10mg/kg body weight) for 24 h. (a-b) glycerol release was measured from (a) iWAT and (b) eWAT explants. (c) The levels of serum free fatty acids were measured. Error bars represent S.E.M., n=7, and *p < 0.05.

Dex-stimulated ATGL expression was unaffected in AKO mice

To understand the mechanism of impaired Dex-induced WAT lipolysis in the absence of Pik3r1, we first examined ATGL, the rate-controlling enzyme in lipolysis. Previous studies have shown that the expression of ATGL was highly induced by GC [8, 9]. To examine if Dex-increased ATGL expression was affected in the absence of Pik3r1, we treated AKO and WT mice with Dex or PBS for 24 h and performed protein expression analysis. Consistent with previous reports, Dex-elevated ATGL protein levels in iWAT and eWAT of WT mice (Fig. 3). Notably, the absence of Pik3r1 did not affect the ability of Dex to elevate the expression of ATGL (Fig. 3).

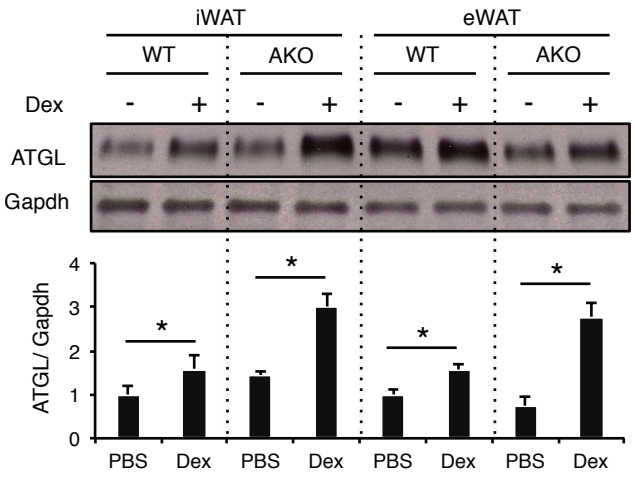

Fig. 3. Dex increased ATGL protein expression in WT and AKO mice.

Eight-week old male WT and AKO mice were administered PBS or Dex (10mg/kg body weight) for 24 h. In both iWAT and eWAT, the expression of ATGL was monitored in by immunoblots. Representative result from three independent experiments is shown. Bar graphs show the average intensity of bands. Gapdh was used as an internal control. Error bars represent S.E.M., and *p < 0.05.

Dex induced the phosphorylation of HSL but not Plin1 in AKO mice

A second mechanism in which GC induces lipolysis is through phosphorylation of HSL and Plin1 indirectly, and we tested whether Pik3r1 was required in this process. HSL and Plin1 are phosphorylated by PKA, at serine 660 for HSL [36] and serine 492 for Plin1 [37]. In iWAT and eWAT, the levels of total HSL showed an upward trend in WT and AKO mice treated with Dex, but did not reach statistical significance (Fig. 4a and 4b). In contrast, phosphorylated HSL levels were increased by Dex in iWAT and eWAT from WT and AKO mice (Fig. 4c). These data showed that lack of Pik3r1 did not affect Dex-increased pHSL levels.

In both adipose depots, the levels of total Plin1 displayed similar levels in WT and AKO mice treated with Dex (Fig. 4d and 4e). Dex increased pPlin1 in WT mice, but failed to do so in AKO mice (Fig. 4f). Thus, Pik3r1 is essential for Dex to induce phosphorylation of Plin1. Since Plin1 localized to lipid droplets while HSL resides in the cytosol, it suggests that the impaired PKA phosphorylation is cellular compartment-specific.

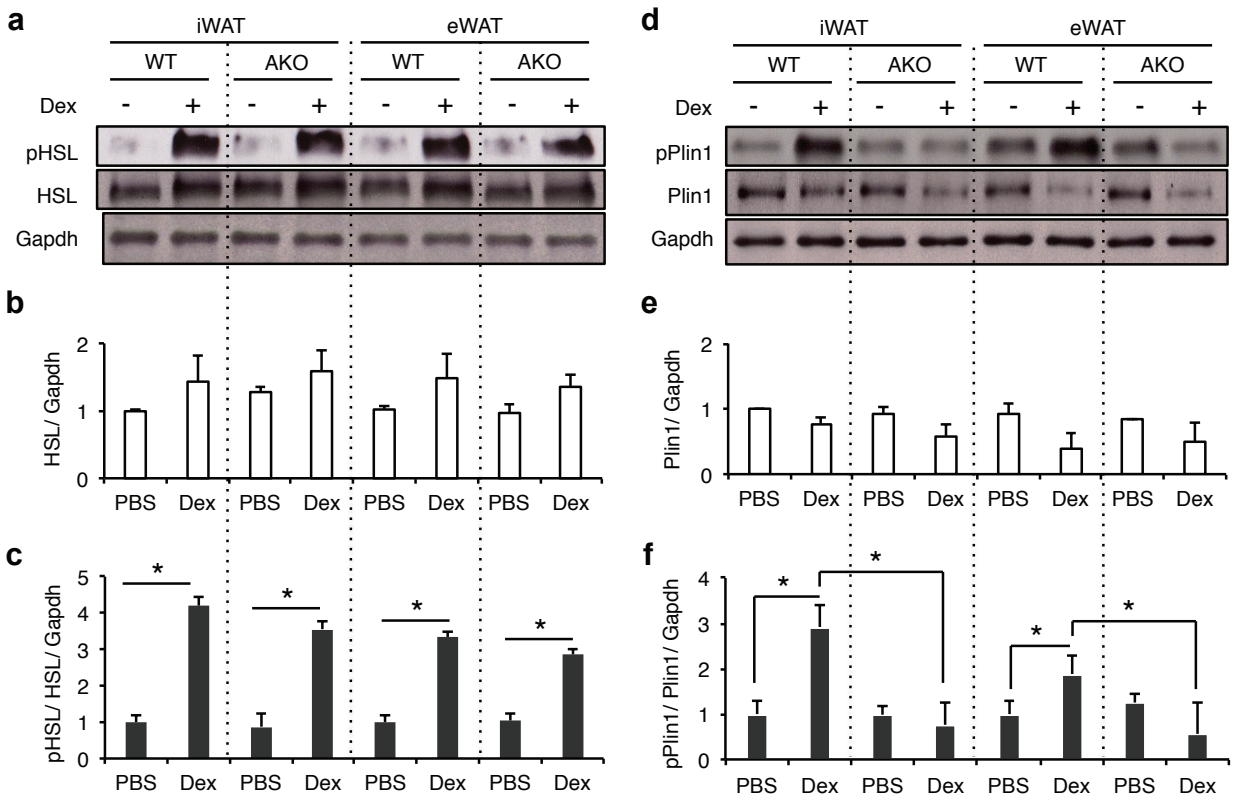

Fig. 4. Dex effects on HSL and Plin1 phosphorylation in WT and AKO mice.

Eight-week old male WT and AKO mice were administered PBS or Dex (10mg/kg body weight) for 24 h. (a) In iWAT and eWAT, HSL and pHSL levels are displayed in immunoblots, and Gapdh was used as an internal control. (b) Bar graphs show normalized total HSL protein levels. (c) Bar graphs illustrate normalized pHSL protein levels. (d) In iWAT and eWAT, Plin1 and pPlin1 levels are displayed in immunoblots, and Gapdh was used as an internal control. (e) Bar graphs show normalized total Plin1 protein levels. (f) Bar graphs illustrate normalized pPlin1 protein levels. Error bars represent S.E.M., n=3, and *p < 0.05.

Pik3r1 is dispensable in Dex-modulated Akt and PDE activities

Insulin suppresses WAT lipolysis in part through PI3K-Akt-PDE3B pathway, through inducing the degradation of the secondary messenger cAMP which is critical for the PKA activation. In iWAT depot, total Akt protein levels were decreased by Dex in WT mice, but upregulated by Dex in AKO mice (Fig. 5a and 5b). In contrast, no difference was observed in eWAT depot (Fig. 5a and 5b). It suggested that GC exert a depot-specific effect on total Akt protein expression.

Because Pik3r1 serves as the regulatory unit of PI3K, the absence of Pik3r1 could lead to inhibition of Akt signaling. The phosphorylation status of Akt at serine 308 [38] was assessed. In both iWAT and eWAT, Dex-induced phosphorylation of Akt displayed the same trend in WT and AKO mice (Fig. 5c). The results proved that PI3K-Akt signaling is intact in Pik3r1-null mice, likely due to the redundant function of Pik3r2.

We further examined PDE activities. Compared to control-treated WT mice, control-treated AKO and Dex-treated WT and AKO mice all showed increased PDE activities in iWAT depot. In eWAT depot, only Dex-treated WT mice showed significant PDE activity induction. Although the elevation of control- and Dex-treated eWAT in AKO mice did not reach statistical significance, the upward trend demonstrated that their PDE signaling was unchanged.

It was to our surprise that Dex treatment increased PDE activities, since GC has been shown to antagonize insulin signaling in adipocytes [22, 39-42]. Moreover, GC-induced excess Pik3r1 did not inhibit Akt and PDE activities. Notably, treatment of GC *in vivo* causes hyperinsulinemia, which could explain the elevated PDE activities. To examine, we measured the plasma insulin in Dex-treated WT and AKO mice. Indeed, we found that Dex increased insulin levels in WT mice, and a similar upward trend was observed in AKO mice (Fig. 5e). These data demonstrated that PI3K-Akt-PDE3B pathway was intact even in the absence of Pik3r1. Thus, Dex-induced PKA signaling was independent of PI3K-Akt-PDE3B pathway.

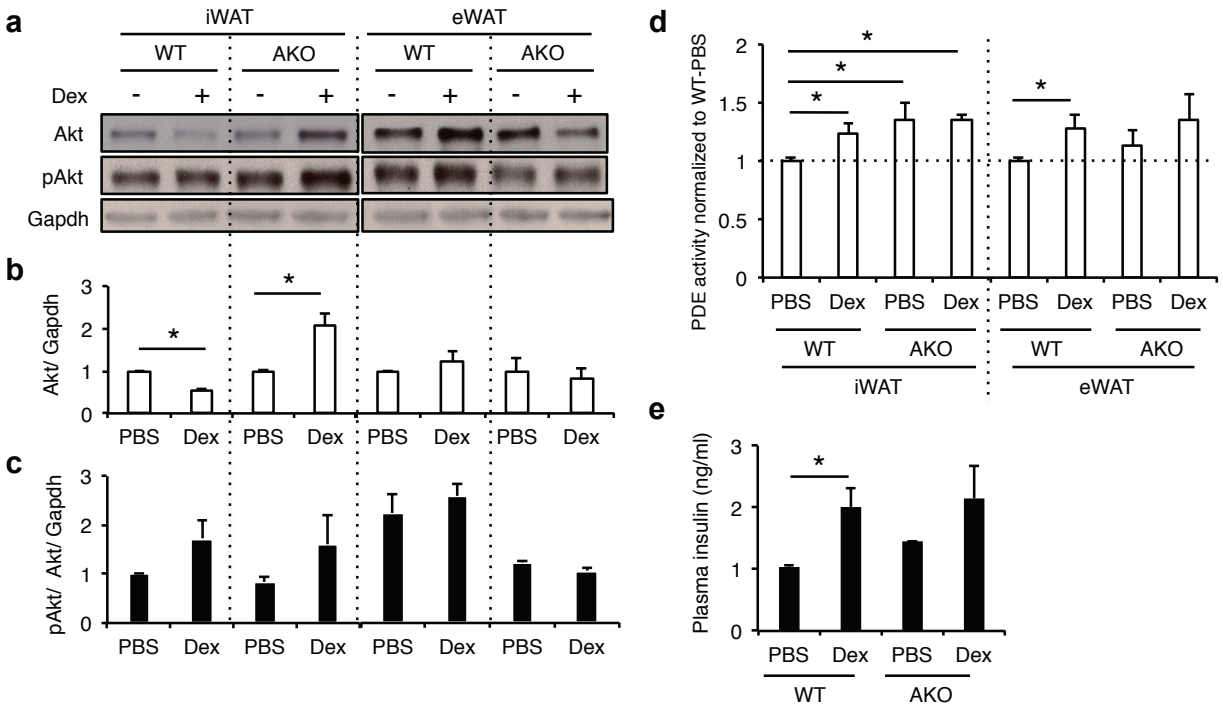

Fig. 5. Dex actions on Akt and PDE activities are intact in the absence of Pik3r1

Eight-week old male WT and AKO mice were administered PBS or Dex (10mg/kg body weight) for 24 h. (a) In iWAT and eWAT, Akt and pAkt levels are displayed in immunoblots, and Gapdh was used as an internal control. (b) Bar graphs show normalized total Akt protein levels. (c) Bar graphs illustrate normalized pAkt protein levels. (d) In iWAT and eWAT, PDE activities are normalized to PBS-treated WT mice. (e) Plasma insulin levels were measured. Error bars represent S.E.M., n=6, and *p < 0.05.

In the lipid droplets, Dex-increased pHSL and subunits of PKA was attenuate in AKO mice

We further explored the mechanism of compromised Dex-induced Plin1 phosphorylation in the absence of Pik3r1 in the lipid droplet, and proposed three scenarios. First, the amount of PKA in lipid droplet could be reduced. Second, the levels of lipid droplet A kinase anchoring protein (AKAP), optic atrophy 1 (OPA1) [43], could be decreased resulting in less anchored PKA in lipid droplets. Third, phosphorylated Plin1 could be de-phosphorylated more rapidly. We isolated lipid droplets from eWAT from control- or Dex-treated WT and AKO mice and tested these possibilities.

Pik3r1 is present in lipid droplets in WT but not AKO mice. Interestingly, Dex did not modulate Pik3r1 protein levels in these lipid droplets (Fig. 6a). In contrast, Dex induced HSL phosphorylation in WT, and this effect was abolished in AKO mice (Fig. 6b). Furthermore, Dex increased the levels of PKA catalytic and regulatory RIIβ subunit in lipid droplets of WT but not AKO mice (Fig. 6c and 6d). OPA1, however, showed no difference between WT and AKO mice. Protein Phosphatase 1 (PP1) de-phosphorylates lipid droplet-anchored Plin1 [44], and similar levels of PP1 were detected in WT and AKO mice. It eliminates the possibility of rapid de-phosphorylation of Plin1. To test if Dex generally increases PKA levels, we monitored different subunits of PKA in whole cell lysates of eWAT from WT and AKO mice treated with Dex, and no difference was found (Fig. 6e, 6f and 6g). Overall, these results indicated that Pik3r1 is indispensable for Dex-induced pHSL and PKA levels in lipid droplets.

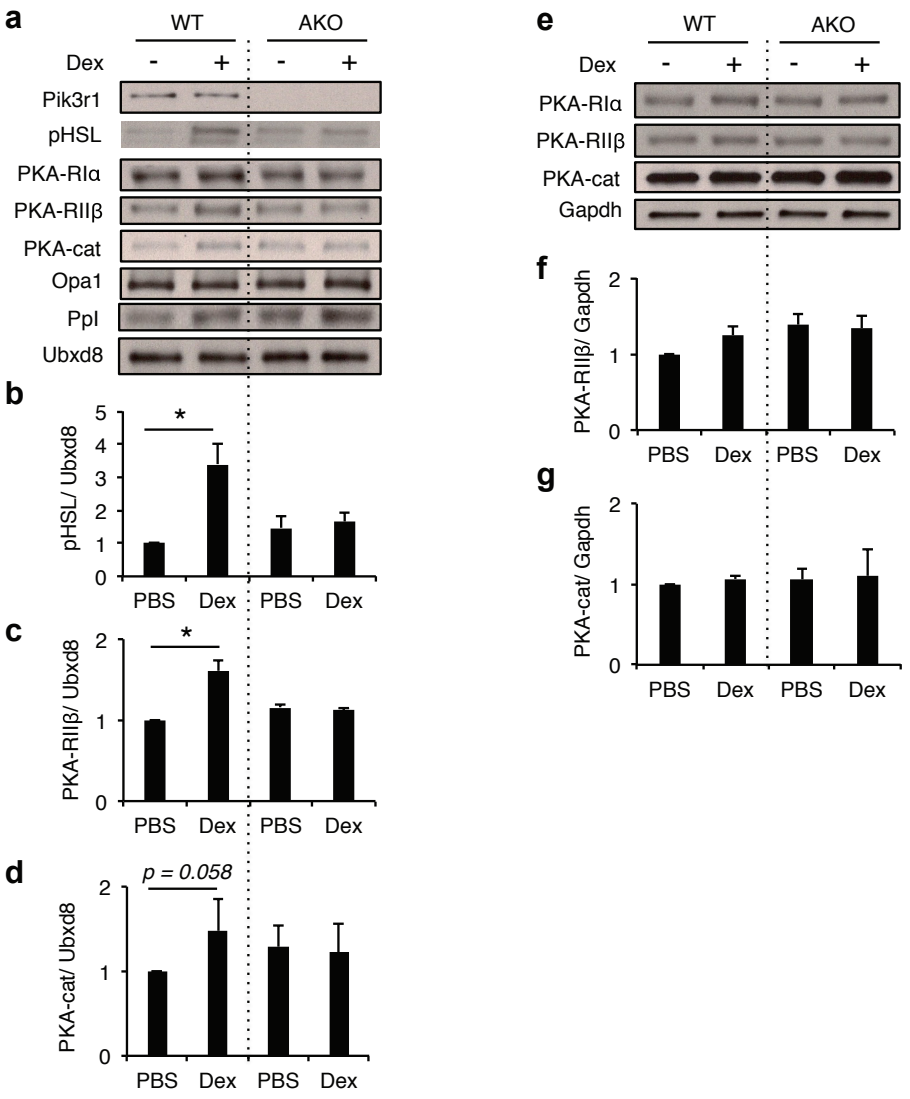

Fig. 6. In lipid droplets, Dex induced the levels of pHSL and subunits of PKA in WT but not AKO mice.

Eight-week old male WT and AKO mice were administered PBS or Dex (10mg/kg body weight) for 24 h. (a-d) Lipid droplets were isolated from eWAT. (a) Immunoblots display the levels of Pik3r1, pHSL, regulatory subunits of PKA (PKA-RIa and PKA-RIIb), catalytic subunit of PKA (PKA-cat), Optic Atrophy 1 (OPA1), protein phosphatase 1 (PP1), and lipid droplet internal control Ubxd8. (b) Bar graphs show normalized pHSL protein levels. (c) Bar graphs illustrate normalized PKA-RIIb protein levels. (d) Bar graphs demonstrate normalized PKA-RIa protein levels. (e-g) Whole cell lysate collected from eWAT. (e) Immunoblots display the levels of PKA-RIa, PKA-RIIb, PKA-cat and internal control Gapdh. (f) Bar graphs illustrate normalized PKA-RIIb protein levels. (g) Bar graphs demonstrate normalized PKA-RIa protein levels. Error bars represent S.E.M., n=3, and *p < 0.05.

AKO mice were protected by Dex-induced hepatic steatosis and hypertriglyceridemia

Superfluous adipose tissue lipolysis caused by GC can result in excess lipid mobilization from WAT to liver, leading to hepatic steatosis and hypertriglyceridemia. We explored the possibility that Pik3r1 ablation can relieve GC-induced symptoms. Dex was administered to WT and AKO mice for 4 days, and their plasma and hepatic TG levels were measured. Similar levels of hepatic TG were found in control-treated WT and AKO mice (Fig. 7a). Dex stimulated hepatic TG levels by 10-fold in WT mice (Fig. 7a). Markedly, this adverse Dex effect was reduced to only 2-fold in AKO mice (Fig. 7a). For plasma TG, their levels were similar between control-treated WT and AKO mice (Fig. 7b). In WT mice, Dex increased their plasma TG levels by 2-fold (Fig. 7b). However, this effect was abolished in AKO mice (Fig. 7b). In summation, these results demonstrated that Pik3r1 ablation improves GC-induced hepatic steatosis and hypertriglyceridemia, and Pik3r1 mediates adverse metabolic actions of GC.

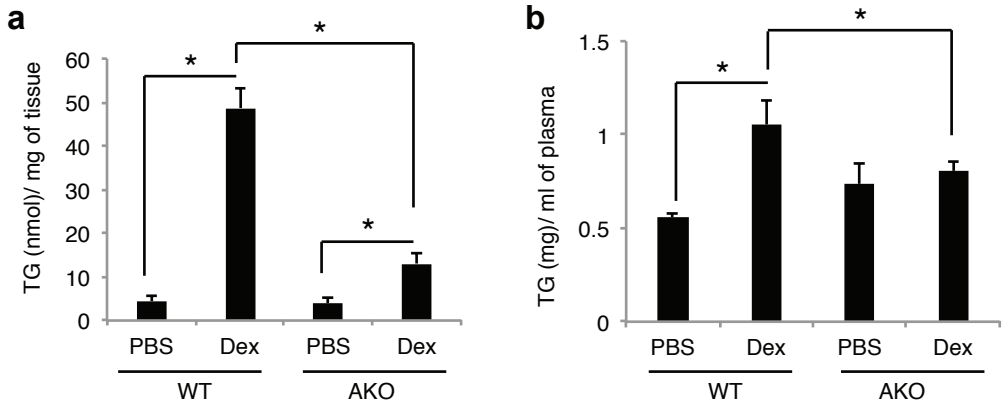

Fig. 7. AKO mice are protected from Dex-induced hepatic steatosis and hypertriglyceridemia

Eight-week old male WT and AKO mice were administered PBS or Dex (10mg/kg body weight) for 4-day. (a) Hepatic TG and (b) plasma TG levels were assessed. For plasma TG, mice were fasted for 6 h prior to sample collection. Error bars represent S.E.M., n=6, and *p < 0.05.

Discussion

Endogenous GC are essential for metabolic adaptation in stressful conditions, such as fasting. During fasting, GC promote lipolysis in adipose tissues to release glycerol for hepatic gluconeogenesis and fatty acids as energy fuels for peripheral tissues. However, during prolonged GC exposure, such as exogenous GC treatment for anti-inflammation, excess lipolysis can cause metabolic disorders, including dyslipidemia and insulin resistance. Therefore, identification of GC targets in adipose tissue is critical to eliminate the adverse metabolic actions in GC therapeutics. Here, we report that Pik3r1, a regulatory subunit of PI3K and a GC primary target gene, mediates GC-stimulated adipocyte lipolysis. With the deletion of Pik3r1 specifically in white adipose tissues, the ability of GC to induce lipolysis was abolished, and GC-initiated hepatic steatosis and hypertriglyceridemia were alleviated. We then explored the potential mechanisms of the reduced GC-stimulated lipolysis in the absence of Pik3r1.

Because Pik3r1 participates in PI3K-Akt-PDE3B axis, Pik3r1 deletion could impair this axis therefore antagonizing cAMP-PKA induced lipolysis. Unexpectedly, this axis was very much intact in Pik3r1-null adipocytes, as evident by similar levels of phosphorylated HSL in whole cell lysates in WAT of WT and AKO mice in response to GC treatment. Instead, we found PKA signaling was impaired in lipid droplets. First, subunits of PKA in lipid droplets were increased by GC treatment in WT but not AKO mice, while their levels in whole cell lysates were similar in both mouse models (Fig. 8). Second, in the lipid droplet, GC-induced phosphorylation of Plin1 by PKA was stopped when Pik3r1 was removed (Fig. 8). Because Plin1 was not phosphorylated, it cannot be dissociated from CGI-58 to anchor phosphorylated HSL in lipid droplets. As a result, we observed the levels of GC-induced pHSL levels were eradicated in the lipid droplets in the absence of Pik3r1. These data pointed to a compartment-specific role for Pik3r1 in conveying GC-induced adipocyte lipolysis.

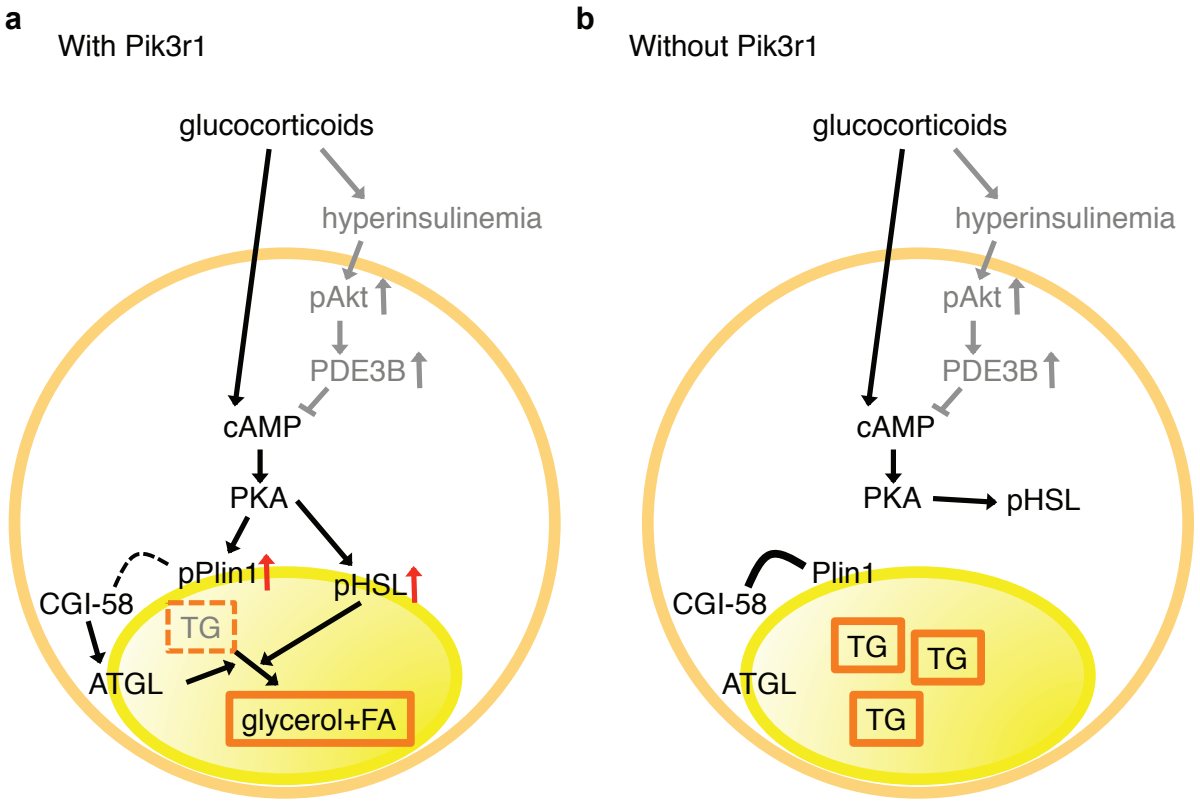

Fig. 8. A Model for the role of Pik3r1 in GC-stimulated WAT lipolysis.

In WAT, PI3K-Akt-PDE3B signaling was intact in the absence of Pik3r1 (in gray). (a) In the presence of Pik3r1, glucocorticoid treatment augments cAMP-PKA signaling, leading to the phosphorylation of HSL in the cytosol. In the lipid droplets, PKA levels are increased, which in turn phosphorylate Plin1. pPlin1 can then anchor pHSL from the cytosol to lipid droplets for TG hydrolysis. (b) In the absence of Pik3r1, GC-induced cAMP-PKA signaling is still able to phosphorylate cytosolic HSL. However, GC did not increase PKA levels in the lipid droplet. Plin1 cannot be phosphorylated and pHSL is unable to anchor to lipid droplet, therefore minimal lipolysis was observed.

The next question we asked was how Pik3r1 is involved in GC-increased PKA levels in lipid droplets. Our studies showed that Pik3r1 was localized in lipid droplet but its levels were not affected by GC treatment. Similarly, GC treatment did not affect the levels of OPA1, an A kinase anchoring protein, in lipid droplets. However, we cannot exclude the possibility that GC induce post-translational modifications of Pik3r1 and/or OPA1 to increase the retention of PKA in lipid droplet. Alternatively, GC could increase the trafficking of PKA to lipid droplets. Pik3r1 has been shown to participate in the trafficking of receptor tyrosine kinases, as it interacts and activates small GTPase Rab4 and Rab5 [45-47]. This GTPase activating (GAP) activity of Pik3r1 is required for intracellular trafficking of PDGF receptor [46]. In addition, Pik3r1 is involved in the trafficking of erythropoietin receptor. Erythropoietin induces Cbl-dependent ubiquitination of Pik3r1, which binds to phosphotyrosines of erythropoietin receptor and an endocytic protein, epsin-1, to drive endocytosis of erythropoietin receptor [48]. Moreover, Pik3r1 interacts with X-box binding protein 1 (XBP1), a transcription factor that confers endoplasmic reticulum (ER) stress responses, and is required for the nuclear localization of XBP1 [49, 50], although the exact mechanism of how Pik3r1 promotes XBP1 nuclear translocation is unclear. Another possible mechanism is that Pik3r1 is involved in PKA stability specifically in lipid droplet. Pik3r1 has been shown to interact with PTEN and blocks ubiquitination of PTEN and its eventual proteasomal degradation [51]. Future experiments will be necessary to determine which of these mechanisms are exerted by Pik3r1 to increase PKA levels in lipid droplet upon GC treatment.

We have previously showed that Angiopoietin-like 4 (Angptl4), another GR primary target gene in hepatocytes and adipocytes [22], is involved in GC-induced adipocyte lipolysis. *Angptl4* encodes a secreted protein that directly increases cAMP levels in adipocytes to promote lipolysis. In *Angptl4* null mice, PKA-initiated phosphorylation of HSL and Plin1 induced by Dex are significantly reduced [14]. Thus, Angptl4 acts upstream of Pik3r1 in GC-induced adipose lipolysis. In this view, it would be interesting to examine whether Angptl4-induced adipose lipolysis requires Pik3r1. It is also unclear whether Pik3r1 is required for lipolysis induced by catecholamine in adipocytes. In contrast to GC, catecholamine does not increase Pik3r1 expression in adipocytes. Thus, the intracellular levels of Pik3r1 in GC-treated adipocytes should be more abundant than those of catecholamine-treated adipocytes. Pik3r1 usually forms heterodimers with p110 catalytic subunit of PI3K. Pik3r1 also form homodimers to interact with PTEN [30]. As Pik3r1 has been shown to associate with many other signaling molecules [47], its intracellular levels may determine its availability to participate in different biological functions. In any case, the role of Pik3r1 in Angptl4 null mice and catecholamine-induced lipolysis shall be determined by future experiments.

In summary, our studies have identified a novel role of Pik3r1 in GC-augmented PKA levels in lipid droplet to promote lipolysis. Removal of Pik3r1 in WAT dampens the ability of GC to promote lipolysis, which leads to hypertriglyceridemia and fatty liver. Thus, WAT Pik3r1 is a potential target to lessen lipid disorders caused by GC. The mechanisms underlying the regulation of PKA levels in lipid droplet that leads to the modulation of lipolysis is mostly unknown, and future studies are warranted.

Material and methods

Mice and treatment

Mice with conditional allele of Pik3r1 gene flanked with LoxP sites at exon7 (*Pik3r1*$^{flox/flox}$) were provided by the laboratory of Lewis Cantley (Weill Cornell Medical College, New York) [34]. Mice expressing Cre recombinase driven by adiponectin promoter (AdipoQ-*Cre*) [35] were purchased from Jackson Laboratory. Adipocyte specific *Pik3r1* knockout mice (AKO) were generated by crossing *Pik3r1* $^{flox/flox}$ with AdipoQ-*Cre* mice. The Office of Laboratory Animal Care at the University of California, Berkeley (Approval number AUP-2014-08-6617) approved all animal experiments conducted. The following primers were used for genotyping: Pik3r1_loxP_F (CACCGAGCACTGGAGCACTG), Pik3r1_loxP_R (CCAGTTACTTTCAAATCAGCACAG), AdipoQ_Cre_F (GCGGTCTGGCAGTAAAAACTATC), AdipoQ_Cre_R (GTGAAACAGCATTGCTGTCACTT). In AKO mice, ~310 bps amplified by Pik3r1_loxP_F and Pik3r1_loxP_R primers and ~100 bps amplified by AdipoQ_Cre_F and AdipoQ_Cre_R primers were observed. In *Pik3r1* $^{flox/flox}$ (WT) mice only ~310 bps were observed.

Eight-week old male AKO and WT mice were injected 10 mg/kg body weight of dexamethasone (Dex, water soluble dexamethasone, Sigma D2915) or PBS (control) for 1, 4 or 7 days. At the end of the treatment period, blood, inguinal and epididymal adipose tissues, liver and gastrocnemius muscle were isolated from mice for protein expression and TG analyses.

Free fatty acid measurement

Plasma was isolated from whole blood immediately after collection, and a free fatty acid quantitation kit (Sigma-Aldrich, MAK044) was used to measure plasma FFA levels.

Ex vivo lipolysis assay

Lipolysis was assessed as previously described [14]. Briefly, explants from freshly removed epididymal and inguinal WAT depots (~100mg) were incubated at 37°C in 500 µL of Krebs-Ringer Buffer (12 mM HEPES, 121 mM NaCl, 4.9 mM KCl, 1.2 mM $MgSO_4$ and 0.33mM $CaCl_2$) with 3% BSA and 3 mM glucose. Glycerol release was determined over time with free glycerol reagent (Sigma-Aldrich, F6428). Measurements were normalized to total protein content of the explants with Bio-Rad protein dye reagent (Bio-Rad, 500-0006).

Isolation of lipid droplets

The isolation of lipid droplets was based on a previous report [52]. Briefly, freshly removed epididymal and inguinal WAT depots were incubated at 37°C in Krebs Ringer Buffer (12 mM HEPES, 121 mM NaCl, 4.9 mM KCl, 1.2 mM $MgSO_4$ and 0.33 mM $CaCl_2$) with 3% BSA, 3 mM glucose and collagenase (0.033 g/100 ml). The adipocyte solution was washed twice with PBS to remove extra collagenase, followed by re-suspension in 3 ml of disruption buffer (25 mM Tris-HCl, 100 mM KCl, 1 mM EDTA, 5 mM EGTA, and protease inhibitor). Cells were disrupted, and the lysate was collected and mixed with an equal volume of disruption buffer containing 1.08 M sucrose. It was then sequentially overlaid with 2 ml of 270 mM sucrose buffer, 135 mM sucrose buffer, and Tris/EDTA/EGTA buffer (25 mM Tris-HCl, 1 mM EDTA, 1 mM EGTA, pH 7.4). Following centrifugation at 150,000 g for 1 h, lipid droplet enriched fractions were collected from the top of the gradient, and subjected for immunoblotting.

Plasma insulin measurement

Plasma samples were collected 24 h after 10 mg/kg of Dex administered with intraperitoneal injection, and plasma insulin levels were assessed with ultra sensitive mouse insulin ELISA kit (Crystal Chem Inc., 90080).

Western blot and antibodies

The following antibodies were used in this study: anti-Gapdh (Santa Cruz, sc-25778), anti-Pik3r1 (Cell Signaling, 4292s), anti-ATGL (Cell Signaling, 2138s), anti-Akt (Cell Signaling, 9272s), anti-phosphor-Akt (T308) (Cell Signaling, 9275s), anti-perilipin A (Abcam, ab3526), anti-phospho-perilipin (VALA Sciences, 4856), anti-HSL (Cell Signaling, 4107s), anti-phospho-HSL (S660) (Cell Signaling, 4126s), anti-PKA-RIα (BD Biosciences, 610609), anti-PKA-RIIβ (BD Biosciences, 610625), and anti-PKAα catalytic subunit (C-20) (Santa Cruz, sc-903). Anti-Ubxd8 antibody was provided by the laboratory of Dr. James Olzmann (UC Berkeley, Berkeley, CA). The intensity of the bands was quantified using Image J software (National Institute of Health) and normalized to Gapdh or Ubxd8 as indicated.

PDE Activity Assay

Total protein lysates were prepared from fresh tissues, and PDE activity was measured with PDELight HTS cAMP phosphodiesterase kit (Lonza, LT07-600).

Statistics

We utilized Student's t test, and data were expressed as standard error of the mean (S.E.M) for each group. *P* values below 0.05 were considered significant.

References

[1] D. P. Macfarlane, S. Forbes, and B. R. Walker, "Glucocorticoids and fatty acid metabolism in humans: fuelling fat redistribution in the metabolic syndrome," *J Endocrinol,* vol. 197, pp. 189-204, May 2008.

[2] T. Kuo, A. McQueen, T. C. Chen, and J. C. Wang, "Regulation of Glucose Homeostasis by Glucocorticoids," *Adv Exp Med Biol,* vol. 872, pp. 99-126, 2015.

[3] R. M. de Guia and S. Herzig, "How Do Glucocorticoids Regulate Lipid Metabolism?," *Adv Exp Med Biol,* vol. 872, pp. 127-44, 2015.

[4] T. Rhen and J. A. Cidlowski, "Antiinflammatory action of glucocorticoids--new mechanisms for old drugs," *N Engl J Med,* vol. 353, pp. 1711-23, Oct 20 2005.

[5] J. N. Fain, A. Dodd, and L. Novak, "Enzyme regulation in gluconeogenesis and lipogenesis. Relationship of protein synthesis and cyclic AMP to lipolytic action of growth hormone and glucocorticoids," *Metabolism,* vol. 20, pp. 109-18, Feb 1971.

[6] J. E. Campbell, A. J. Peckett, M. D'Souza A, T. J. Hawke, and M. C. Riddell, "Adipogenic and lipolytic effects of chronic glucocorticoid exposure," *Am J Physiol Cell Physiol,* vol. 300, pp. C198-209, Jan 2011.

[7] A. J. Peckett, D. C. Wright, and M. C. Riddell, "The effects of glucocorticoids on adipose tissue lipid metabolism," *Metabolism,* vol. 60, pp. 1500-10, Nov 2011.

[8] J. A. Villena, S. Roy, E. Sarkadi-Nagy, K. H. Kim, and H. S. Sul, "Desnutrin, an adipocyte gene encoding a novel patatin domain-containing protein, is induced by fasting and glucocorticoids: ectopic expression of desnutrin increases triglyceride hydrolysis," *J Biol Chem,* vol. 279, pp. 47066-75, Nov 5 2004.

[9] C. Y. Yu, O. Mayba, J. V. Lee, J. Tran, C. Harris, T. P. Speed*, et al.*, "Genome-wide analysis of glucocorticoid receptor binding regions in adipocytes reveal gene network involved in triglyceride homeostasis," *PLoS One,* vol. 5, p. e15188, 2010.

[10] R. E. Duncan, M. Ahmadian, K. Jaworski, E. Sarkadi-Nagy, and H. S. Sul, "Regulation of lipolysis in adipocytes," *Annu Rev Nutr,* vol. 27, pp. 79-101, 2007.

[11] S. G. Young and R. Zechner, "Biochemistry and pathophysiology of intravascular and intracellular lipolysis," *Genes Dev,* vol. 27, pp. 459-84, Mar 1 2013.

[12] R. G. Yip and H. M. Goodman, "Growth hormone and dexamethasone stimulate lipolysis and activate adenylyl cyclase in rat adipocytes by selectively shifting Gi alpha2 to lower density membrane fractions," *Endocrinology,* vol. 140, pp. 1219-27, Mar 1999.

[13] C. Xu, J. He, H. Jiang, L. Zu, W. Zhai, S. Pu*, et al.*, "Direct effect of glucocorticoids on lipolysis in adipocytes," *Mol Endocrinol,* vol. 23, pp. 1161-70, Aug 2009.

[14] N. E. Gray, L. N. Lam, K. Yang, A. Y. Zhou, S. Koliwad, and J. C. Wang, "Angiopoietin-like 4 (Angptl4) protein is a physiological mediator of intracellular lipolysis in murine adipocytes," *J Biol Chem,* vol. 287, pp. 8444-56, Mar 9 2012.

[15] S. K. Koliwad, N. E. Gray, and J. C. Wang, "Angiopoietin-like 4 (Angptl4): A glucocorticoid-dependent gatekeeper of fatty acid flux during fasting," *Adipocyte,* vol. 1, pp. 182-187, Jul 1 2012.

[16] H. P. Moore, R. B. Silver, E. P. Mottillo, D. A. Bernlohr, and J. G. Granneman, "Perilipin targets a novel pool of lipid droplets for lipolytic attack by hormone-sensitive lipase," *J Biol Chem,* vol. 280, pp. 43109-20, Dec 30 2005.

[17] D. L. Brasaemle, V. Subramanian, A. Garcia, A. Marcinkiewicz, and A. Rothenberg, "Perilipin A and the control of triacylglycerol metabolism," *Mol Cell Biochem,* vol. 326, pp. 15-21, Jun 2009.

[18] C. Sztalryd and A. R. Kimmel, "Perilipins: lipid droplet coat proteins adapted for tissue-specific energy storage and utilization, and lipid cytoprotection," *Biochimie,* vol. 96, pp. 96-101, Jan 2014.

[19] V. Subramanian, A. Rothenberg, C. Gomez, A. W. Cohen, A. Garcia, S. Bhattacharyya*, et al.*, "Perilipin A mediates the reversible binding of CGI-58 to lipid droplets in 3T3-L1 adipocytes," *J Biol Chem,* vol. 279, pp. 42062-71, Oct 1 2004.

[20] J. G. Granneman, H. P. Moore, R. Krishnamoorthy, and M. Rathod, "Perilipin controls lipolysis by regulating the interactions of AB-hydrolase containing 5 (Abhd5) and adipose triglyceride lipase (Atgl)," *J Biol Chem,* vol. 284, pp. 34538-44, Dec 11 2009.

[21] J. Buren, Y. C. Lai, M. Lundgren, J. W. Eriksson, and J. Jensen, "Insulin action and signalling in fat and muscle from dexamethasone-treated rats," *Arch Biochem Biophys,* vol. 474, pp. 91-101, Jun 1 2008.

[22] S. K. Koliwad, T. Kuo, L. E. Shipp, N. E. Gray, F. Backhed, A. Y. So*, et al.*, "Angiopoietin-like 4 (ANGPTL4, fasting-induced adipose factor) is a direct glucocorticoid receptor target and participates in glucocorticoid-regulated triglyceride metabolism," *J Biol Chem,* vol. 284, pp. 25593-601, Sep 18 2009.

[23] T. Kuo, M. J. Lew, O. Mayba, C. A. Harris, T. P. Speed, and J. C. Wang, "Genome-wide analysis of glucocorticoid receptor-binding sites in myotubes identifies gene networks modulating insulin signaling," *Proc Natl Acad Sci U S A,* vol. 109, pp. 11160-5, Jul 10 2012.

[24] L. A. Barbour, S. Mizanoor Rahman, I. Gurevich, J. W. Leitner, S. J. Fischer, M. D. Roper*, et al.*, "Increased P85alpha is a potent negative regulator of skeletal muscle insulin signaling and induces in vivo insulin resistance associated with growth hormone excess," *J Biol Chem,* vol. 280, pp. 37489-94, Nov 11 2005.

[25] B. Draznin, "Molecular mechanisms of insulin resistance: serine phosphorylation of insulin receptor substrate-1 and increased expression of p85alpha: the two sides of a coin," *Diabetes,* vol. 55, pp. 2392-7, Aug 2006.

[26] C. M. Taniguchi, J. O. Aleman, K. Ueki, J. Luo, T. Asano, H. Kaneto*, et al.*, "The p85alpha regulatory subunit of phosphoinositide 3-kinase potentiates c-Jun N-terminal kinase-mediated insulin resistance," *Mol Cell Biol,* vol. 27, pp. 2830-40, Apr 2007.

[27] K. Ueki, D. A. Fruman, S. M. Brachmann, Y. H. Tseng, L. C. Cantley, and C. R. Kahn, "Molecular balance between the regulatory and catalytic subunits of phosphoinositide 3-kinase regulates cell signaling and survival," *Mol Cell Biol,* vol. 22, pp. 965-77, Feb 2002.

[28] J. Luo, S. J. Field, J. Y. Lee, J. A. Engelman, and L. C. Cantley, "The p85 regulatory subunit of phosphoinositide 3-kinase down-regulates IRS-1 signaling via the formation of a sequestration complex," *J Cell Biol,* vol. 170, pp. 455-64, Aug 1 2005.

[29] R. B. Chagpar, P. H. Links, M. C. Pastor, L. A. Furber, A. D. Hawrysh, M. D. Chamberlain*, et al.*, "Direct positive regulation of PTEN by the p85 subunit of phosphatidylinositol 3-kinase," *Proc Natl Acad Sci U S A,* vol. 107, pp. 5471-6, Mar 23 2010.

[30] L. W. Cheung, K. W. Walkiewicz, T. M. Besong, H. Guo, D. H. Hawke, S. T. Arold*, et al.*, "Regulation of the PI3K pathway through a p85alpha monomer-homodimer equilibrium," *Elife,* vol. 4, p. e06866, 2015.

[31] E. Degerman, T. R. Landstrom, J. Wijkander, L. S. Holst, F. Ahmad, P. Belfrage*, et al.*, "Phosphorylation and activation of hormone-sensitive adipocyte phosphodiesterase type 3B," *Methods,* vol. 14, pp. 43-53, Jan 1998.

[32] T. Kitamura, Y. Kitamura, S. Kuroda, Y. Hino, M. Ando, K. Kotani*, et al.*, "Insulin-induced phosphorylation and activation of cyclic nucleotide phosphodiesterase 3B by the serine-threonine kinase Akt," *Mol Cell Biol,* vol. 19, pp. 6286-96, Sep 1999.

[33] E. Degerman, F. Ahmad, Y. W. Chung, E. Guirguis, B. Omar, L. Stenson*, et al.*, "From PDE3B to the regulation of energy homeostasis," *Curr Opin Pharmacol,* vol. 11, pp. 676-82, Dec 2011.

[34] J. Luo, J. R. McMullen, C. L. Sobkiw, L. Zhang, A. L. Dorfman, M. C. Sherwood*, et al.*, "Class IA phosphoinositide 3-kinase regulates heart size and physiological cardiac hypertrophy," *Mol Cell Biol,* vol. 25, pp. 9491-502, Nov 2005.

[35] J. Eguchi, X. Wang, S. Yu, E. E. Kershaw, P. C. Chiu, J. Dushay*, et al.*, "Transcriptional control of adipose lipid handling by IRF4," *Cell Metab,* vol. 13, pp. 249-59, Mar 2 2011.

[36] C. L. Su, C. Sztalryd, J. A. Contreras, C. Holm, A. R. Kimmel, and C. Londos, "Mutational analysis of the hormone-sensitive lipase translocation reaction in adipocytes," *J Biol Chem,* vol. 278, pp. 43615-9, Oct 31 2003.

[37] H. H. Zhang, S. C. Souza, K. V. Muliro, F. B. Kraemer, M. S. Obin, and A. S. Greenberg, "Lipase-selective functional domains of perilipin A differentially regulate constitutive and protein kinase A-stimulated lipolysis," *J Biol Chem,* vol. 278, pp. 51535-42, Dec 19 2003.

[38] D. R. Alessi, M. Andjelkovic, B. Caudwell, P. Cron, N. Morrice, P. Cohen*, et al.*, "Mechanism of activation of protein kinase B by insulin and IGF-1," *EMBO J,* vol. 15, pp. 6541-51, Dec 2 1996.

[39] H. Masuzaki, J. Paterson, H. Shinyama, N. M. Morton, J. J. Mullins, J. R. Seckl*, et al.*, "A transgenic model of visceral obesity and the metabolic syndrome," *Science,* vol. 294, pp. 2166-70, Dec 7 2001.

[40] J. Buren, H. X. Liu, J. Jensen, and J. W. Eriksson, "Dexamethasone impairs insulin signalling and glucose transport by depletion of insulin receptor substrate-1, phosphatidylinositol 3-kinase and protein kinase B in primary cultured rat adipocytes," *Eur J Endocrinol,* vol. 146, pp. 419-29, Mar 2002.

[41] E. E. Kershaw, N. M. Morton, H. Dhillon, L. Ramage, J. R. Seckl, and J. S. Flier, "Adipocyte-specific glucocorticoid inactivation protects against diet-induced obesity," *Diabetes,* vol. 54, pp. 1023-31, Apr 2005.

[42] N. Houstis, E. D. Rosen, and E. S. Lander, "Reactive oxygen species have a causal role in multiple forms of insulin resistance," *Nature,* vol. 440, pp. 944-8, Apr 13 2006.

[43] G. Pidoux, O. Witczak, E. Jarnaess, L. Myrvold, H. Urlaub, A. J. Stokka*, et al.*, "Optic atrophy 1 is an A-kinase anchoring protein on lipid droplets that mediates adrenergic control of lipolysis," *EMBO J,* vol. 30, pp. 4371-86, Nov 2 2011.

[44] G. M. Clifford, D. K. McCormick, C. Londos, R. G. Vernon, and S. J. Yeaman, "Dephosphorylation of perilipin by protein phosphatases present in rat adipocytes," *FEBS Lett,* vol. 435, pp. 125-9, Sep 11 1998.

[45] M. D. Chamberlain, T. R. Berry, M. C. Pastor, and D. H. Anderson, "The p85alpha subunit of phosphatidylinositol 3'-kinase binds to and stimulates the GTPase activity of Rab proteins," *J Biol Chem,* vol. 279, pp. 48607-14, Nov 19 2004.

[46] M. D. Chamberlain, J. C. Oberg, L. A. Furber, S. F. Poland, A. D. Hawrysh, S. M. Knafelc*, et al.*, "Deregulation of Rab5 and Rab4 proteins in p85R274A-expressing cells alters PDGFR trafficking," *Cell Signal,* vol. 22, pp. 1562-75, Oct 2010.

[47] P. Mellor, L. A. Furber, J. N. Nyarko, and D. H. Anderson, "Multiple roles for the p85alpha isoform in the regulation and function of PI3K signalling and receptor trafficking," *Biochem J,* vol. 441, pp. 23-37, Jan 1 2012.

[48] G. B. Bulut, R. Sulahian, H. Yao, and L. J. Huang, "Cbl ubiquitination of p85 is essential for Epo-induced EpoR endocytosis," *Blood,* vol. 122, pp. 3964-72, Dec 5 2013.

[49] S. W. Park, Y. Zhou, J. Lee, A. Lu, C. Sun, J. Chung*, et al.*, "The regulatory subunits of PI3K, p85alpha and p85beta, interact with XBP-1 and increase its nuclear translocation," *Nat Med,* vol. 16, pp. 429-37, Apr 2010.

[50] J. N. Winnay, J. Boucher, M. A. Mori, K. Ueki, and C. R. Kahn, "A regulatory subunit of phosphoinositide 3-kinase increases the nuclear accumulation of X-box-binding protein-1 to modulate the unfolded protein response," *Nat Med,* vol. 16, pp. 438-45, Apr 2010.

[51] L. W. Cheung, B. T. Hennessy, J. Li, S. Yu, A. P. Myers, B. Djordjevic*, et al.*, "High frequency of PIK3R1 and PIK3R2 mutations in endometrial cancer elucidates a novel mechanism for regulation of PTEN protein stability," *Cancer Discov,* vol. 1, pp. 170-85, Jul 2011.

[52] C. M. Blouin, S. Le Lay, A. Eberl, H. C. Kofeler, I. C. Guerrera, C. Klein*, et al.*, "Lipid droplet analysis in caveolin-deficient adipocytes: alterations in surface phospholipid composition and maturation defects," *J Lipid Res,* vol. 51, pp. 945-56, May 2010.

Chapter III:

Glucocorticoid-activated Skeletal Muscle Pik3r1 Transcription is Associated with Glucocorticoid-induced Insulin Resistance

Abstract

Phosphoinositide-3-Kinase Regulatory Subunit 1 (*Pik3r1*) encodes a regulatory subunit of phosphatidylinositol 3-kinase (PI3K) that is previously identified as a glucocorticoid receptor (GR) primary target gene in mouse C2C12 myotubes. Here, we showed that the glucocorticoid treatment increased GR occupancy, the acetylation of histone H3 and H4, and the monomethylation of histone H3 lysine 4 residue (H3K4) at the glucocorticoid response element (GRE) in gastrocnemius muscle. The recruitment of histone acetyltransferase p300 to the GRE was also elevated by glucocorticoid treatment. Reducing p300 expression using RNA interference (RNAi) in C2C12 myotubes markedly decrease the ability of glucocorticoids to induce Pik3r1 expression. These results supported the role of p300 in glucocorticoid-activated Pik3r1 gene transcription. Treating mice with glucocorticoids for one week resulted in glucose intolerance. This effect, however, was compromised in skeletal muscle specific Pik3r1 knockout (MKO) mice. Glucocorticoid treatment reduced insulin action, monitored by the activity of protein kinase Akt, in gastrocnemius muscle, liver, and epididymal white adipose tissue (eWAT). In glucocorticoid-treated MKO mice Akt activity was restored in gastrocnemius muscle but not in liver and eWAT. Overall, our results identified the mechanism of glucocorticoid-stimulated skeletal muscle Pik3r1 gene transcription *in vivo* and established the key role of Pik3r1 in glucocorticoid-induced skeletal muscle insulin resistance.

Introduction

Glucocorticoids are steroid hormones that are required for metabolic adaptation under stress conditions. In skeletal muscle, glucocorticoids suppress insulin-stimulated glucose utilization, inhibit protein synthesis and facilitate protein degradation [1-3]. Inhibition of insulin-stimulated glucose utilization preserves plasma glucose whereas amino acids generated from protein degradation are used as precursors for hepatic gluconeogenesis. These processes are necessary during stress, such as fasting, to maintain plasma glucose, which is the major energy source for the brain and red blood cells [4]. However, prolonged or excess glucocorticoids exposure could lead to pathological outcomes including hyperglycemia, glucose intolerance, hyperinsulinemia, insulin resistance and muscle atrophy [4-7].

Glucocorticoids convey their function through an intracellular glucocorticoid receptors (GR). Once binding to glucocorticoids, GR translocates into nucleus, occupies genomic glucocorticoid response element (GRE) and recruits transcription coregulators to modulate the transcription of its primary target genes [8, 9]. These primary target genes then directly or indirectly trigger the downstream physiological and/or pathophysiological processes. Phosphoinositide-3-Kinase Regulatory Subunit 1 (*Pik3r1*), also as known as *p85α*, was identified as a glucocorticoids primary target gene in mouse C2C12 myotubes by RNA profiling and chromatin immunoprecipitation sequencing (ChIPseq) analysis [10, 11]. Pik3r1 encodes a regulatory subunit of phosphoinositide 3-kinase (PI3K). In activated insulin signaling, PI3K is recruited to the tyrosine phosphorylated- insulin receptor substrate-1 (IRS-1) through SH2 domain of Pik3r1. The catalytic subunit of PI3K, p110 then convert phosphatidylinositol-4, 5 bisphosphate (PIP_2) to phosphatidylinositol-3, 4, 5 triphosphate (PIP_3). PIP_3 then recruit protein kinase Akt to membrane, where it can be fully activated. Although Pik3r1 is a key component for insulin pathway, overexpression of monomeric Pik3r1 is found to suppress insulin signaling in myotubes and hepatocytes [11-14] through at least two potential mechanisms. First, Pik3r1 monomer competes with heterodimeric PI3K for binding towards IRS-1. Preventing the binding of active PI3K to IRS-1 reduced insulin signaling [15, 16]. Alternatively, Pik3r1 associates and is required for the activation of phosphatase and tensin homolog (PTEN) that reduces the levels of PIP_3 and therefore inhibit PI3K pathway [17, 18]. Thus, excess Pik3r1 levels negatively regulate insulin action. Interestingly, previous studies have shown that Pik3r1 levels are elevated in skeletal muscle of insulin resistant individuals. This indicates the potential contribution of Pik3r1 in the development of insulin resistance in human.

We previously show that reducing the expression of Pik3r1 in C2C12 myotubes compromises the inhibitory effect of glucocorticoids on the activity of signaling molecules in insulin signaling pathway [11]. We also identified a GRE, which is located at -43kb (relative to transcription start site) of mouse *Pik3r1* gene in C2C12 myotbes. In this report we analyze the mechanism of glucocorticoid-regulated Pik3r1 gene transcription in vivo. We examine the recruitment of GR and various transcription

coregulators to the previously identified GRE from the study in C2C12 myotubes. We also analyze the patterns of histone acetylation and methylation in genomic regions surrounding the GRE. We focus on specific transcription coregulators and test their role in glucocorticoid-activated Pik3r1 gene transcription in C2C12 myotubes. Finally, skeletal muscle specific Pik3r1 knockout (MKO mice) were generated to study the function of Pik3r1 in glucocorticoid-modulated glucose homeostasis and insulin sensitivity.

Results

Dex induces Pik3r1 expression in skeletal muscle in vivo

Pik3r1 mRNA expression was previously shown to be increased in gastrocnemius muscle by dexamethasone (Dex, a synthetic glucocorticoid) treatment for 1 or 4 days. Here, 8-weeks old male *Pik3r1*$^{Flox/Flox}$ mice (will be referred as wild type WT mice in the rest of this report) were injected intraperitoneally with Dex or PBS for 1, 4 or 7 days to monitor the effect of glucocorticoids on Pik3r1 protein expression. We found that Pik3r1 protein levels were markedly elevated after 4 and 7 days Dex treatment (≅3.3 and 2.8 fold, respectively) (Fig. 1a). In contrast, in liver Pik3r1 protein levels were only augmented upon 4 days (≅1.4 fold) but not 7 days Dex treatment (Fig. 1b). These results demonstrated that despite the induction of Pik3r1 mRNA by 24 hr Dex treatment in gastrocnemius muscle, the change of protein levels occurred at later time points. However, the elevation of Pik3r1 protein levels remained for at least 1 week. Finally, Dex effect on Pik3r1 expression was more profound in skeletal muscle than in liver.

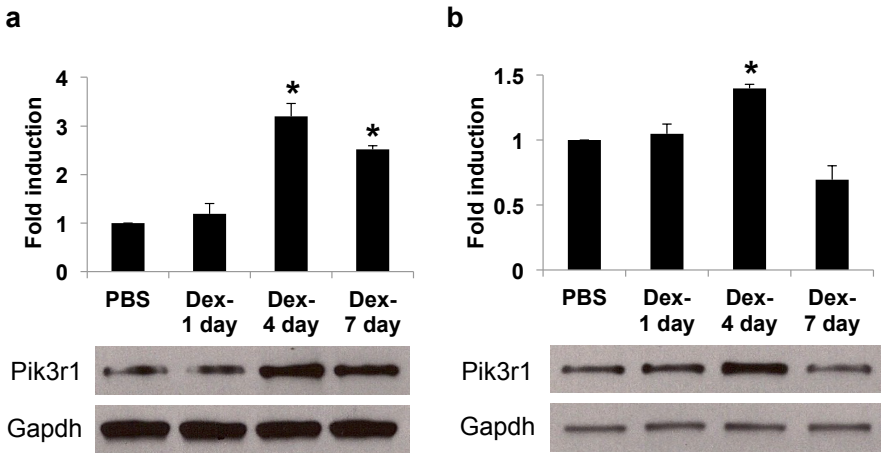

Fig. 1. Dex induced Pik3r1 expression in skeletal muscle *in vivo*.

Male 8-week-old WT mice were treated with PBS or 5 mg/kg of Dex for 1, 4, 7 days. The Pik3r1 expression was measured by immunoblot in both gastrocnemius (GA) muscle (a) and liver (b) and normalized to internal control Gapdh. Representative immunoblots are shown (n=3). Error bars represent the S.E.M. of relative Pik3r1 expression level (Dex vs. PBS), and *p < 0.05

Dex treatment induced the recruitment of GR and transcriptional coregulators to the Pik3r1 GRE

We previously identified a GRE located approximately -43kb of mouse Pik3r1 gene in C2C12 myotubes. We examined whether GR was recruited to the same GRE identified in cell culture study in gastrocnemius muscle. Eight-week old male WT mice were injected with PBS or Dex intraperitoneally for 4 days. Chromatin immunoprecipitation (ChIP) was then performed on gastrocnemius muscle isolated from these mice. We found a significant occupancy of GR on the Pik3r1 GRE in PBS-treated animals (Fig. 2a). This result is not surprising, as endogenous corticosterone levels could provide certain numbers of active GR to be recruited to the GRE. Dex treatment markedly increased GR occupancy on the GRE (approximately 3 fold from PBS-treated mice) (Fig. 2a). These results suggested that previously identified GRE in C2C12 myotubes also served as a GRE for Pik3r1 in gastrocnemius muscle.

We further analyze the status of histone acetylation and methylation in genomic regions surrounding the GRE. If this GRE participates in the Dex-activated Pik3r1 gene transcription, we expect that active epigenetic marks in this region, such as histone H3 and H4 acetylation and histone H3 lysine 4 (H3K4) methylation, will be increased upon Dex treatment [19-24]. Total H3 and H4 levels were also monitored by ChIP, because the levels of acetylated and methylated histones are associated with the overall density of histone in each genomic region. We found that the level of total histone H3 and H4 was not significantly affected by PBS or Dex treatment (Fig. 2b). However, compared to IgG control, the level of acetylated H3 (AcH3)/H3, acetylated H4 (AcH4)/H4 and monomethylated H3K4 (H3K4me1)/H3 were all significantly increased by 2.7, 4.8, and 4.6 fold respectively, in the PBS-treated group (Fig. 2b). These results were in agreement with the observation of GR occupancy on the GRE in PBS-treated animals.

Additionally, Dex treatment elevated both AcH3/H3 and AcH4/H4 levels in the Pik3r1 GRE (Fig. 2b). These results suggested that Dex treatment augmented Pik3r1 transcription through enhancing both histone H3 acetylation and histone H4 acetylation.

We next monitored the recruitment of previously identified transcriptional coregulators for GR, including p300 (a histone acyltransferase) [25], Tip60 [26], CCAR1 [27], MLL1 [28] and GCN5 [29], to the Pik3r1 GRE using ChIP. We found that none of them were significantly recruited to the GRE in PBS-treated animals (Fig. 2c). However, p300 occupancy was markedly increased upon Dex treatment (Fig. 2c). As p300 is a histone acetyltransferase, it is a potential transcriptional coregulator that contributed to elevated acetylated H3 and acetylated H4 levels in the Pik3r1 GRE after Dex treatment.

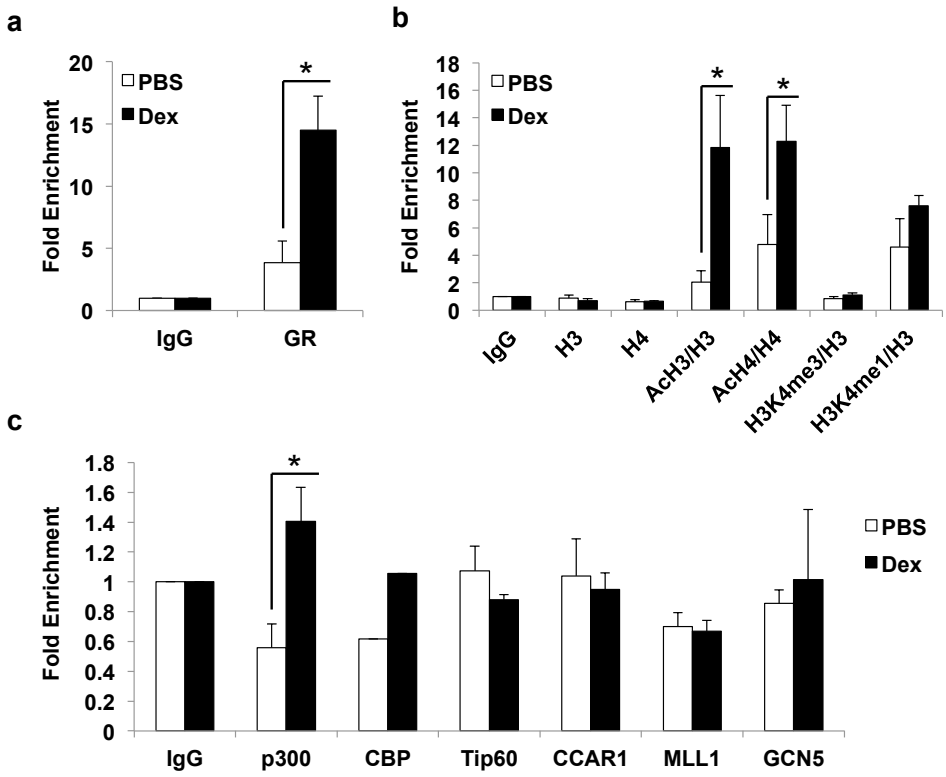

Fig. 2. Dex treatment induced the recruitment of GR and transcriptional coregulators to the Pik3r1 GRE.

Male, 8-week-old Pik3r1 Flox (WT) mice were treated with 5 mg/kg of Dex for 4 days. Then, their GA muscles were collected. ChIP experiments were performed on these GA muscles to study the recruitment of; glucocorticoid receptor (GR) (a), histone modifications (b) and recruitment of transcription cofactors p300, Tip60, CCAR1, MLL1, and GCN5 (c) on GRE of Pik3r1. Primer flanking the Pik3r1 GRE and Rpl19 (internal control) were used in qPCR. Error bars represent the S.E.M. of relative fold enrichment compared to IgG control from four independent experiments (*$p < 0.05$).

Reducing p300 expression in C2C12 myotubes impaired Dex-induced Pik3r1 expression

To study the role of p300 in glucocorticoid-induced Pik3r1 expression, we used C2C12 myotubes as a model. We first performed ChIP to monitor the recruitment of p300 to the Pik3r1 GRE. As shown in Fig. 3a, p300 was not seen on the GRE under EtOH (vehicle control) treatment. Dex treatment, however, significantly elevated GR recruitment to the GRE. CBP is another transcriptional coregulator that is highly related to p300 and shares overlapping functions with p300. However, CBP was not recruited to the GRE upon Dex treatment. To examine whether p300 is required for Dex-activated Pik3r1 expression, C2C12 myoblasts were infected with lentivirus expressing small hairpin RNA against p300 (sh-p300) or scramble shRNA (sh-scrRNA, control). After puromycin selection, cells were differentiated into myotubes, then treated with 1 μM Dex or equal amounts of EtOH (control) for 6 hr. RNA was isolated from these cells and real-time PCR was performed to monitor the expression of Pik3r1. In sh-scrRNA expressing C2C12 myotubes, Dex treatment increased the expression of Pik3r1 approximately 3 fold (Fig. 3b). However, in sh-p300 expressing C2C12 myotubes, such Dex effect was abolished (Fig. 3b). Overall, these results demonstrated that p300 is required for Dex to stimulate Pik3r1 gene transcription.

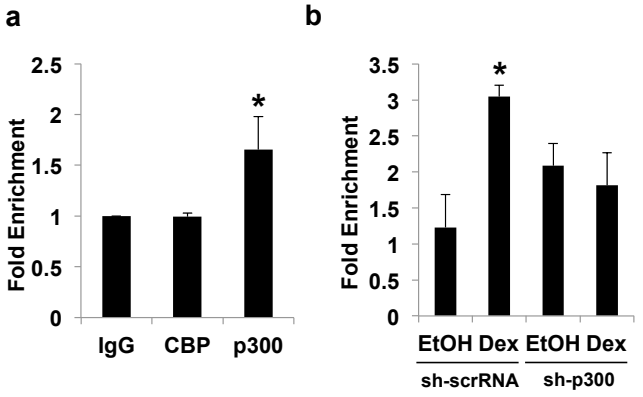

Fig. 3. Reducing p300 expression in C2C12 myotubes impaired Dex-induced Pik3r1 expression.

Fully differentiated C2C12 myotubes were treated with 1 μM Dex or EtOH (control) for 30 min. Cells were then collected for ChIP to study the recruitment of CBP and p300 to the GRE of Pik3r1. (a) To further examine the participation of p300 in *Pik3r1* transactivation, C2C12 myoblasts were infected with lentivirus particles expressing scramble sh-RNA (sh-scrRNA control) or sh-p300. After puromycin selection, cells were differentiated into myotubes and were then treated with 1 μM Dex or EtOH (control) for 6 hrs. At the end of the experiments, cells were collected for RT-qPCR to monitor the expression of *Pik3r1* (b).

GC-induced glucose intolerance was compromised in MKO mice

We generated skeletal muscle specific Pik3r1 knockout (MKO) mice to analyze the role of Pik3r1 in glucocorticoid-modulated glucose homeostasis and insulin sensitivity. MKO mice were generated by crossing *Pik3r1*$^{Flox/Flox}$ with transgenic mice carrying myosin light chain kinase promoter-driven Cre recombinase [30]. Immunoblotting confirmed that Pik3r1 expression was depleted in skeletal muscle, including gastrocnemius muscle (GA muscle), tibialis anterior muscle (TA muscle) and soleus muscle (Fig. 4a). To investigate the role of skeletal muscle Pik3r1 in glucocorticoid-regulated glucose homeostasis WT and MKO mice were treated with Dex or PBS via drinking water for 7 days. Mice were fasted for 16 hr and intraperitoneal glucose tolerance test (IPGTT) was performed. We found that Dex treatment induced glucose intolerance in WT mice (Fig. 4b and 4c). Glucose tolerance was similar between PBS-treated WT and MKO mice (Fig, 4b and 4c). Interestingly, Dex-treated MKO mice not only were more glucose tolerant than Dex-treated WT mice but also PBS-treated WT and MKO mice (Fig. 4b and 4c). Dex treatment caused hyperinsulinemia in WT mice (Fig. 4d). In MKO mice, Dex treatment still resulted in elevated plasma insulin levels (Fig. 4d). In fact, plasma insulin levels were trending higher in Dex-treated MKO mice than those of Dex-treated WT mice, though they were not statistically significant (Fig. 4d).

These results suggested that in MKO mice Dex treatment resulted in hyperinsulinemia, which subsequently improved glucose intolerance. In contrast, in WT mice Dex treatment also induced hyperinsulinemia, but such compensatory mechanism still cannot reduce plasma glucose levels. Thus, Dex-treated MKO mice should have better insulin sensitivity comparing to Dex-treated WT mice. We performed insulin tolerance test (ITT) to examine this hypothesis. Indeed we found that Dex-treated MKO mice were more insulin tolerant than Dex-treated WT mice (Fig. 4e and 4f). Notably, Dex-treated MKO mice were more insulin resistant than those PBS-treated WT and MKO mice (Fig. 4e and 4f). These results suggested that the better glucose tolerance observed in Dex-treated MKO mice was due to markedly higher plasma insulin levels in these mice. Overall, these results indicate skeletal muscle Pik3r1 is involved in glucocorticoid-regulated whole body glucose homeostasis and insulin sensitivity.

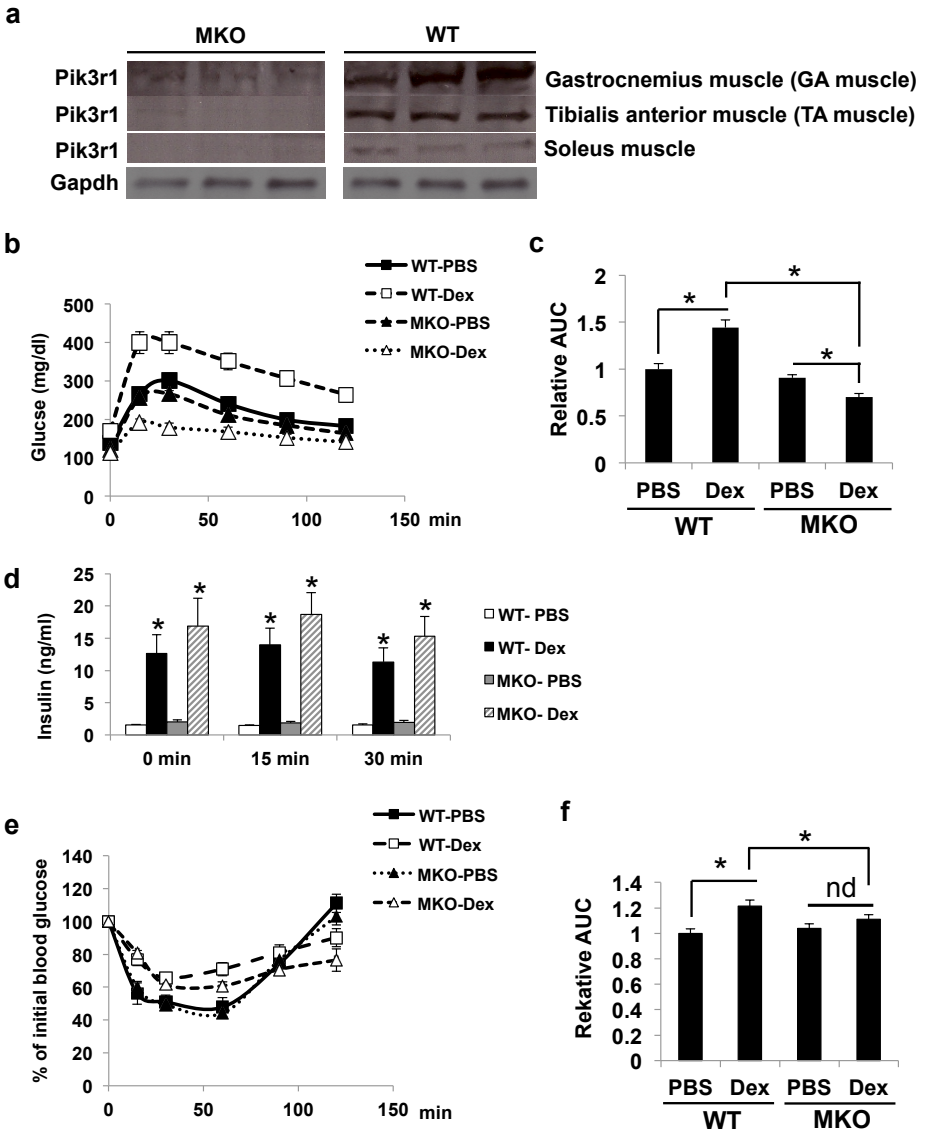

Fig. 4. GC-induced glucose intolerance was compromised in MKO mice.

Muscle specific Pik3r1 knockout (MKO) mice were generated. The expression of Pik3r1 in gastrocnemius (GA) muscle, tibialis anterior (TA) muscle and soleus muscle of WT and MKO was examined by immunoblots and normalized to internal control, Gapdh. Representative immunoblots are shown (n=3). (a) Male 8-week-old WT mice and MKO mice were treated with 10 mg/kg of Dex for 7days. On the last day, mice were fasted for 16 hrs and the GTT was performed. (b) Relative area under curve (AUC) for GTT results (relative to PBS-treated WT mice) was displayed. Error bars represent the S.E.M., n=3-7 and *$p < 0.05$. (c) Plasma insulin level was measured before glucose injection (0 min time point), 15 min and 30 min after glucose injection. Error bars represent the S.E.M., n=3-7 and *$p < 0.05$. (d) ITT was performed in mice as described in Methods. ITT results were depicted as percentage of initial plasma glucose level (the plasma glucose level before insulin injection). Error bars represent the S.E.M., n=3-7. (e) Relative area under curve (AUC) for ITT results (relative to PBS-treated WT mice) was shown. Error bars represent the S.E.M., n=3-7 and *$p < 0.05$.

Pik3r1 deletion in skeletal muscle restored insulin response inhibited by Dex

To further analyze insulin response in distinct tissues, PBS- or Dex-treated WT and MKO mice were injected with insulin for 10 min and gastrocnemius muscle, liver and epididymal white adipose tissue (eWAT) were then isolated. The activity of Akt, a downstream signaling molecule of insulin action, was then monitored. Akt is phosphorylated at serine 473 and threonine 308 residues upon insulin treatment (*17*). We performed ELISA to detect threonine 473 phosphorylated Akt (pAkt) and total Akt levels. Because insulin response mainly results in the increased phosphorylation of pAkt instead of total Akt levels, the ratio of pAkt/Akt represents the intensity of insulin action. In PBS-treated WT and MKO mice, insulin treatment increased pAkt/Akt ratio in gastrocnemius muscle, liver and eWAT (Fig. 5a, 5b and 5c). In contrast, Dex treatment suppressed the ability of insulin to elevate pAkt/Akt ratio (Fig. 5a, 5b and 5c). Interestingly, in Dex-treated MKO mice the ability of insulin to enhance the ratio of pAkt/Akt was restored in gastrocnemius muscle but not liver and eWAT (Fig. 5a, 5b and 5c). These results demonstrated that deletion of skeletal muscle Pik3r1 specifically reverse glucocorticoid-induced insulin resistance in skeletal muscle.

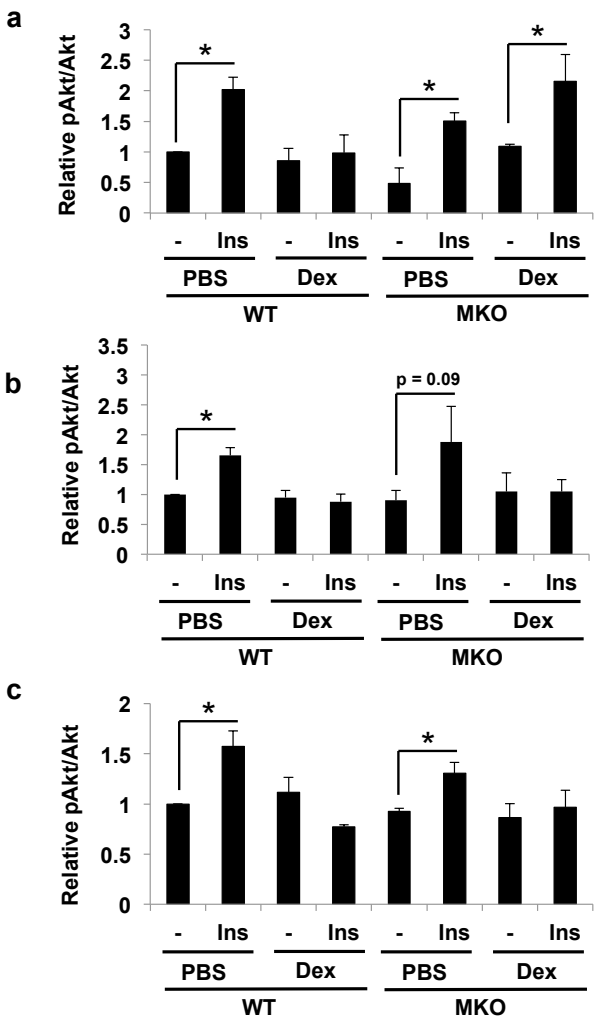

Fig. 5. Pik3r1 deletion in skeletal muscle restored insulin response inhibited by Dex.

Male 8-week-old WT and MKO mice were treated with 10 mg/kg of PBS or Dex for 7 days. On the last day, mice were injected with insulin (1 unit/body weight) for 10 min, and after various tissues were collected. ELISA kits were used to monitor the level of Akt and phosphor-Akt in GA muscle (a), liver (b) and eWAT (c). The results were presented as relative Akt/pAKt level. Error bars represent the S.E.M., n=3 and *$p < 0.05$.

Discussion

Our previous studies identified *Pik3r1* as a GR primary target gene in mouse C2C12 myotubes and reducing *Pik3r1* expression diminishes the ability of glucocorticoids to repress the activity of signaling molecules in insulin signaling pathway. However, the transcriptional activation of *Pik3r1* gene by glucocorticoids and the role of Pik3r1 in glucocorticoid-modulated insulin action *in vivo* have not been established. In this report we confirmed that GR was recruited to previously identified Pik3r1 GRE. In fact GR was found to occupy the GRE in PBS-treated mice. These results indicate that endogenous corticosterone levels in our experimental condition were enough to activate certain numbers of GR to enter nucleus and occupy the GRE. Similar results were observed in our previous studies on the transcriptional regulation of FoxO3 gene by glucocorticoids. However, it is unclear whether GR participates in the expression of Pik3r1 in this physiological state. Dex treatment, not surprisingly, augmented the recruitment of GR to the GRE. Interestingly, while AcH3, AcH4 and H4K4me1 levels in genomic regions surrounding the Pik3r1 GRE were already significant in PBS-treated animals, only AcH3 and AcH4 levels were further enhanced by Dex treatment. These results indicate that Dex treatment mainly increases the recruitment of histone acetyltransferase(s) to assist the transcriptional activation of Pik3r1 gene. Indeed, p300, which can acetylate histone H3 and H4 at multiple lysine residues, was specifically recruited to the GRE upon Dex treatment. Using C2C12 myotubes as a model we showed that reducing p300 expression decreased the ability of Dex to stimulate Pik3r1 gene expression. This confirms that importance of p300 in glucocorticoid response on Pik3r1 gene. Surprisingly, p300 and all other transcriptional coregulators we examined were not recruited to the GRE in PBS-treated animals. There are two potential explanations for these results. First, histone acetyltransferases and methyltransferases other than we tested are involved in establishing epigenetic marks in the genomic regions surrounding the Pik3r1 GRE. Second, these epigenetic marks are established by other transcription factors binding in these genomic regions and are independent of GR. Many pioneering transcription factors have been shown to establish epigenetic marks and chromatin environment in enhancers that are necessary for the further induction of transcription of specific genes [31-33]. To clarify these two models we could monitor the status of AcH3, AcH4 and H3K4me1 levels in adrenalectomized or skeletal muscle specific GR knockout mice in future study. If GR is required to establish these epigenetic marks, we should not observe AcH3, AcH4 and H3K4me1 levels in the Pik3r1 GRE in gastrocnemius muscle of adrenalectomized or skeletal muscle specific GR knockout mice.

Previous studies showed that heterozygous deletion of *Pik3r1* gene improved whole body insulin sensitivity in mice fed with high-fat diet [31, 32]. However, insulin sensitivity of MKO mice fed with high-fat diet was not improved [34]. In contrast, in this study, insulin sensitivity and glucose tolerance of Dex-treated MKO mice were markedly improved. These results highlighted the critical role of Pik3r1 in glucocorticoid response on glucose homeostasis and insulin

sensitivity. It is important to note that Dex-treated MKO mice still had hyperinsulinemia. Thus, comparing to control WT and MKO mice they were still insulin resistant. But compensation from pancreas β cells secreted more insulin to suppress plasma glucose levels. This is in agreement with the fact that other mechanisms have been identified to confer insulin resistance caused by glucocorticoids. Our previous studies showed that Dex-induced insulin resistance is improved in angiopoietin-like 4 (Angptl4) null mice (*Angptl4*$^{-/-}$). Angptl4 is a GR primary target gene encoding a secreted protein in liver and adipose tissue. Glucocorticoid-induced insulin resistance was improved in both liver and skeletal muscle of *Angptl4*$^{-/-}$ mice (see Chapter 1). Other reports showed that the reduction of osteoclacin expression by glucocorticoids in osteoblasts play a role in the development of insulin resistance [35]. Interestingly, while deletion of skeletal muscle Pik3r1 reversed Dex-inhibited insulin response only in skeletal muscle but not in liver and eWAT, insulin sensitivity of both liver and skeletal muscle is improved in Dex-treated *Angptl4*$^{-/-}$ mice. In contrast, osteoclacin appears to reverse glucocorticoid-induced hepatic insulin resistance. It is conceivable that more GR primary target genes are involved in the development of insulin resistance, which is a necessary physiological responding to stress.

Overall, in this report we showed that GR occupies the Pik3r1 GRE previously identified in C2C12 myotubes in gastrocnemius muscle and identify the mechanism of glucocorticoid-activated Pik3r1 gene transcription *in vivo*. The key role of Pik3r1 in glucocorticoid-induced skeletal muscle insulin resistance is also established. This work also highlights the potential of reducing skeletal muscle Pik3r1 as a potential approach to improve metabolic disorders caused by excess or chronic exposure to glucocorticoids.

Material and methods

Mice and treatment

Mice with conditional allele of Pik3r1 gene flanked with LoxP sites at exon7 ($Pik3r1^{Flox/Flox}$) were provided by the laboratory of Lewis Cantley (Weill Cornell Medical College, New York). Mice expressing Cre recombinase driven by muscle creatine kinase promoter (Ckmm-Cre) were purchased from Jackson Laboratory. Muscle specific Pik3r1 knockout mice (MKO) were generated by crossing $Pik3r1^{Flox/Flox}$ with Ckmm-Cre mice. The Office of Laboratory Animal Care at the University of California, Berkeley (Approval number AUP-2014-08-6617) approved all animal experiments conducted.

The following primers were used for genotyping: Pik3r1_loxP_F (CACCGAGCACTGGAGCACTG), Pik3r1_loxP_R (CCAGTTACTTTCAAATCAGCACAG), Ckmm_Cre_F (TAAGTCTGAACCCGGTCTGC), Ckmm_Cre_R (GTGAAACAGCATTGCTGTCACTT). In MKO mice, ~310 bps amplified by Pik3r1_loxP_F and Pik3r1_loxP_R primers and ~500 bps amplified by Ckmm_Cre_F and Ckmm_Cre_R primers were observed. In Pik3r1 flox/flox (WT) mice only ~310 bps amplified by Pik3r1_loxP_F and Pik3r1_loxP_R primers were observed.

Eight-weeks old male MKO and WT mice were injected intraperitoneally with 10 mg/kg body weight of dexamethasone (Dex, water soluble dexamethasone, Sigma D2915) or PBS (control) for 1, 4 or 7 days. At the end of the treatment period, blood, inguinal and epididymal adipose tissues, liver and gastrocnemius muscle were isolated from mice for protein expression analysis. The Office of Laboratory Animal Care at the University of California, Berkeley (Approval number R306-0111) approved all animal experiments conducted in this paper.

Western Blot.

The protein concentration for samples were measured with Bradford protein dye (BioRad). Proteins (~ 30 μg) were mixed with sample buffer and boiled for 5 min before apply to SDS PAGE. Following are the antibodies we used in this study: anti-Gapdh (Santa Cruz, sc-25778), anti-Pik3r1 (Cell Signaling, 4292s). The intensity of the bands was quantified using Image J software (National Institute of Health) and normalized to Gapdh.

Intraperitoneal Glucose Tolerance Test (GTT)

Eight-weeks old male MKO and WT mice were treated with 4 mg/kg body weight of Dex or PBS control via drinking water. After 15 hr fasting, mice for intraperitoneal glucose tolerance test (GTT) were injected with 1g/kg body weight glucose intraperitoneally. Tail vein blood was used to monitor blood glucose level at different time points: 0 (before glucose injection), 15, 30, 60 90, and 120 mins after glucose injection using a Blood Glucose meter (Contour, Bayer).

Insulin Tolerance Test (ITT)

Fed mice for experiment were injected with 1 unit/kg body weight insulin (Sigma, I0516-5ML) intraperitoneally. Tail vein blood was used to monitor blood glucose level at different time points: 0 (before glucose injection), 15, 30, 60 90, and 120 mins after glucose injection using a Blood Glucose meter (Contour, Bayer).

Muscle Chromatin Immunoprecipitation

Wild type mice were intraperitoneally injected with 10 mg/kg body weight of dexamethasone (Dex, water soluble dexamethasone, Sigma D2915) for 4 days. On the last day, gastrocnemius muscles were harvested and snap frozen with liquid nitrogen. Frozen muscles were ground to fine powder with pestle. Then, tissue powder was cross-linked with 1% formaldehyde in 20 ml PBS at 37°C for 10 min with gentle shaking. After quenching the cross-linking reaction with 125 mM glycine, samples were centrifuged at 1,000 rpm, 4°C for 5 min. Pellets were washed with ice-cold PBS, then resuspended in 3 ml buffer S (50 mM Tris pH 8.0, 1% SDS, 10 mM EDTA, 1mM DTT, 100 mM MG 132 and protease inhibitor cocktail). Samples were incubated on ince for 10 min, then sonicated with Branson Sonifier 250 sonicator for 50 seconds (60% output, 10s pulse with 40s reset). After spin for 10 min at 32,000 rpm, 4°C, supernatant, which contains sheared DNA fragments, was collected and mixed with one sample volume of buffer D (0.01% SDS, 1.1% Triton x-100, 1.2 mM EDTA, 16.7mM Tris [pH 8.0], 167 mM NaCl, 100 mM MG132 and protease inhibitor cocktail). Diluted sample was then incubated with 100 µl of 50% protein A/G agarose beads (sc-2003, Santa Cruz) for 1hr at 4°C with gentle shaking to pre-clean the sample. After spinning at 4,000 rmp for 3 min at 4°C to pellet the agarose beads, supernatant was used to set up the IP reactions. The following antibodies were used in this study: anti-IgG (sc-2027, Santa Cruz), anti-GR (a gift from Pufall lab, USC), anti-H3 histone (ab1791, abcam), anti-H4 (05-858, Millipore), anti-AcH3 (ab47915, abcam), anti-AcH4 (06-866, Millipore), anti-H3K4me3 (ab8580, abcam), anti-H3K4me1 (ab8895, abcam), and anti-p300 (sc-584, Santa Cruz). Samples were allowed to react with antibody for 18 hrs (overnight incubation) at 4C with gentle shaking. Then, 50 µl of 50% protein A/G agarose beads were added into each IP reaction and rotate for 2 hr at 4°C. Then, agarose beads were washed with the following conditions: 1x low-salt wash buffer (0.1% SDS, 1% Triton X-100, 2 mM EDTA, 20 mM Tris [pH 8.0] and 150 mM NaCl), 1x high-salt wash buffer (0.1% SDS, 1% Triton X-100, 2mM EDTA, 20 mM Tris [pH 8.0], and 500 m NaCl), 1x LiCl wash buffer (0.25M LiCl, 1% NP-40, 1% sodium deoxycholate, 1mM EDTA and 10 mM Tris [pH 8.0]) and 2x Tris-EDTA buffer. After last wash, all supernatant was removed, then 400 µl of elution buffer (10 mM DTT, 1% SDS and 0.1M NaHCO3) was added. Samples were rotated at room temperature for 1hr, then spin at 8,000 rmp for 1 min. Supernatant was transferred to new tube and mix with 16 µl of 5M NaCl, then incubated at 65°C for overnight. On the last day, 16 µl of Tirs [pH 6.5], 8 µl of 0.5 M EDTA, and 1.5 µl of protease K were added into the sample and incubate at 55°C for 3hr. The immune-precipitated DNA fragment were extracted with PCR clean up kit, then applied to qPCR to quantify the IP result.

Cell culture

The C2C12 cells were purchased from the Cell and Tissue Culture Facility at the University of California, Berkeley. They were maintained in Dulbecco's modified Eagle's medium (DMEM; Mediatech) containing 10% fetal bovine serum (FBS; Tissue Culture Biologicals) and incubated at 37°C with 5% CO2. The 95~100 % confluent C2C12 myoblasts were differentiated into myotubes with 2% horse serum (J.R. Scientific) in DMEM. The C2C12 cells were maintained in 2% horse serum-containing DMEM, changed every 2 days, until fully differentiated into myotubes, taking about 4-6 days.

Cell ChIP

Fully differentiated C2C12 myotubes were treated with 1 μM Dex or EtOH (control) for 30 min, cross-linked with 2% formaldehyde for 3 min at room temperature and reactions were quenched with 0.125 M glycine. The cells were washed with ice-cold 1x PBS, scraped and resuspended in cell lysis buffer (50 mM HEPES-KOH at pH 7.4, 1 mM EDTA, 150 mM NaCl, 10% glycerol, 0.5% Triton X-100, supplemented with protease inhibitor cocktails (Calbiochem)). The cell lysates were then incubated for 1h at 4°C, and the nuclei was collected by centrifugation at 500xg for 5 min at 4°C. The nuclei were resuspended in 1 mL of ice-cold RIPA buffer (10 mM Tris-HCL at pH 8.0, 1 mM EDTA, 150 mM NaCl, 5% glycerol, 1% Triton X-100, 0.1% sodium deoxycholate, 0.1% SDS, supplemented with protease inhibitor). The chromatin was fragmented with Branson Sonifier 250 sonicator (13 min sonication with 20 sec pulse at 35% power followed by 40 sec pause). Samples were the spun at 13,000 rpm for 15 min at 4°C to remove the cell debris. Supernatants were used for IP with the following antibody: anti-IgG (negative control, sc-2027, Santa Cruz Biotechnology) and anti-CCAR1 (A300-435A, Bethyl Laboratories) with overnight incubation. On next day, 50 μL of 50% protein A/G agarose beads (sc-2003, Santa Cruz Biotechnology) were added into each IP reaction then incubated at 4°C for 2h with rotation. The beads were then washed twice with RIPA buffer, twice with RIPA buffer containing 500 mM NaCl, twice with LiCl buffer (20 mM Tris at pH 8.0, 1 mM EDTA, 250 mM LiCl, 0.5% NP-40, 0.5% sodiumdeoxycholate) and one time with RIPA buffer, all supplemented with protease inhibitor. After removing the remaining wash buffer, 75 μL of proteinase K solution (TE buffer [pH 8.0] with 0.7% SDS and 200 μg/ml proteinase K) was added to each IP reaction, followed by incubation at 55°C for 3h, then 65°C for overnight to reverse formaldehyde cross-linking. ChIP DNA fragments were purified with QIAquick PCR purification kit (Qiagen) and used for qPCR reaction to quantify the IP results.

Lentiviral infection

Mouse C2C12 myoblasts were grown to 70-80% confluent, then infected with p300 shRNA lentiviral particle (sc-29432v, Santa Cruz Biotechnology) or control shRNA lentiviral particle (sc-108080, Santa Cruz Biotechnology) expressing scramble shRNA. Infected cells were then selected with 5 μg/ml puromycin for several days. Sh-p300 or scramble-shRNA control myoblasts were then differentiated into myotubes. Three days after differentiation, cells were treated with1 μM Dex or EtOH (control) for 6 h, followed by RNA extraction, RT-qPCR gene expression assay.

Plasma insulin analysis

Plasma insulin level were examined by using ultra sensitive mouse insulin ELISA kit (Crystal Chem Inc., Cat. No: 90080).

Akt pAkt ELISA

The Akt and pAkt levels were studied by using Akt (Total) ELISA kit (Invitrogen, KHO0101) and Akt (pS473) ELISA kit (Invitrogen, KHO0111) respectively.

Statistics

We utilized Student's t test, and data were expressed as standard error of the mean (S.E.M) for each group. *P* values below 0.05 were considered significant.

References

[1] B. R. Odedra, P. C. Bates, and D. J. Millward, "Time course of the effect of catabolic doses of corticosterone on protein turnover in rat skeletal muscle and liver," *Biochem J,* vol. 214, pp. 617-27, Aug 15 1983.

[2] A. G. Kayali, V. R. Young, and M. N. Goodman, "Sensitivity of myofibrillar proteins to glucocorticoid-induced muscle proteolysis," *Am J Physiol,* vol. 252, pp. E621-6, May 1987.

[3] D. Auclair, D. R. Garrel, A. Chaouki Zerouala, and L. H. Ferland, "Activation of the ubiquitin pathway in rat skeletal muscle by catabolic doses of glucocorticoids," *Am J Physiol,* vol. 272, pp. C1007-16, Mar 1997.

[4] M. McMahon, J. Gerich, and R. Rizza, "Effects of glucocorticoids on carbohydrate metabolism," *Diabetes Metab Rev,* vol. 4, pp. 17-30, Feb 1988.

[5] R. C. Andrews and B. R. Walker, "Glucocorticoids and insulin resistance: old hormones, new targets," *Clin Sci (Lond),* vol. 96, pp. 513-23, May 1999.

[6] J. N. Clore and L. Thurby-Hay, "Glucocorticoid-induced hyperglycemia," *Endocr Pract,* vol. 15, pp. 469-74, Jul-Aug 2009.

[7] T. Kuo, A. McQueen, T. C. Chen, and J. C. Wang, "Regulation of Glucose Homeostasis by Glucocorticoids," *Adv Exp Med Biol,* vol. 872, pp. 99-126, 2015.

[8] M. Arango-Lievano, W. M. Lambert, and F. Jeanneteau, "Molecular Biology of Glucocorticoid Signaling," *Adv Exp Med Biol,* vol. 872, pp. 33-57, 2015.

[9] S. H. Meijsing, "Mechanisms of Glucocorticoid-Regulated Gene Transcription," *Adv Exp Med Biol,* vol. 872, pp. 59-81, 2015.

[10] C. Y. Yu, O. Mayba, J. V. Lee, J. Tran, C. Harris, T. P. Speed*, et al.*, "Genome-wide analysis of glucocorticoid receptor binding regions in adipocytes reveal gene network involved in triglyceride homeostasis," *PLoS One,* vol. 5, p. e15188, 2010.

[11] T. Kuo, M. J. Lew, O. Mayba, C. A. Harris, T. P. Speed, and J. C. Wang, "Genome-wide analysis of glucocorticoid receptor-binding sites in myotubes identifies gene networks modulating insulin signaling," *Proc Natl Acad Sci U S A,* vol. 109, pp. 11160-5, Jul 10 2012.

[12] L. A. Barbour, S. Mizanoor Rahman, I. Gurevich, J. W. Leitner, S. J. Fischer, M. D. Roper*, et al.*, "Increased P85alpha is a potent negative regulator of skeletal muscle insulin signaling and induces in vivo insulin resistance associated with growth hormone excess," *J Biol Chem,* vol. 280, pp. 37489-94, Nov 11 2005.

[13] B. Draznin, "Molecular mechanisms of insulin resistance: serine phosphorylation of insulin receptor substrate-1 and increased expression of p85alpha: the two sides of a coin," *Diabetes,* vol. 55, pp. 2392-7, Aug 2006.

[14] C. M. Taniguchi, J. O. Aleman, K. Ueki, J. Luo, T. Asano, H. Kaneto*, et al.*, "The p85alpha regulatory subunit of phosphoinositide 3-kinase potentiates c-Jun N-terminal kinase-mediated insulin resistance," *Mol Cell Biol,* vol. 27, pp. 2830-40, Apr 2007.

[15] K. Ueki, D. A. Fruman, S. M. Brachmann, Y. H. Tseng, L. C. Cantley, and C. R. Kahn, "Molecular balance between the regulatory and catalytic subunits of phosphoinositide 3-kinase regulates cell signaling and survival," *Mol Cell Biol,* vol. 22, pp. 965-77, Feb 2002.

[16] J. Luo, S. J. Field, J. Y. Lee, J. A. Engelman, and L. C. Cantley, "The p85 regulatory subunit of phosphoinositide 3-kinase down-regulates IRS-1 signaling via the formation of a sequestration complex," *J Cell Biol,* vol. 170, pp. 455-64, Aug 1 2005.

[17] R. B. Chagpar, P. H. Links, M. C. Pastor, L. A. Furber, A. D. Hawrysh, M. D. Chamberlain*, et al.*, "Direct positive regulation of PTEN by the p85 subunit of phosphatidylinositol 3-kinase," *Proc Natl Acad Sci U S A,* vol. 107, pp. 5471-6, Mar 23 2010.

[18] L. W. Cheung, K. W. Walkiewicz, T. M. Besong, H. Guo, D. H. Hawke, S. T. Arold*, et al.*, "Regulation of the PI3K pathway through a p85alpha monomer-homodimer equilibrium," *Elife,* vol. 4, p. e06866, 2015.

[19] J. E. Brownell and C. D. Allis, "Special HATs for special occasions: linking histone acetylation to chromatin assembly and gene activation," *Curr Opin Genet Dev,* vol. 6, pp. 176-84, Apr 1996.

[20] M. Grunstein, "Histone acetylation in chromatin structure and transcription," *Nature,* vol. 389, pp. 349-52, Sep 25 1997.

[21] B. D. Strahl and C. D. Allis, "The language of covalent histone modifications," *Nature,* vol. 403, pp. 41-5, Jan 6 2000.

[22] T. Jenuwein and C. D. Allis, "Translating the histone code," *Science,* vol. 293, pp. 1074-80, Aug 10 2001.

[23] H. Santos-Rosa, R. Schneider, A. J. Bannister, J. Sherriff, B. E. Bernstein, N. C. Emre*, et al.*, "Active genes are tri-methylated at K4 of histone H3," *Nature,* vol. 419, pp. 407-11, Sep 26 2002.

[24] I. Garcia-Bassets, Y. S. Kwon, F. Telese, G. G. Prefontaine, K. R. Hutt, C. S. Cheng*, et al.*, "Histone methylation-dependent mechanisms impose ligand dependency for gene activation by nuclear receptors," *Cell,* vol. 128, pp. 505-18, Feb 9 2007.

[25] H. M. Chan and N. B. La Thangue, "p300/CBP proteins: HATs for transcriptional bridges and scaffolds," *J Cell Sci,* vol. 114, pp. 2363-73, Jul 2001.

[26] V. Sapountzi, I. R. Logan, and C. N. Robson, "Cellular functions of TIP60," *Int J Biochem Cell Biol,* vol. 38, pp. 1496-509, 2006.

[27] C. Y. Ou, T. C. Chen, J. V. Lee, J. C. Wang, and M. R. Stallcup, "Coregulator cell cycle and apoptosis regulator 1 (CCAR1) positively regulates adipocyte differentiation through the glucocorticoid signaling pathway," *J Biol Chem,* vol. 289, pp. 17078-86, Jun 13 2014.

[28] A. J. Ruthenburg, W. Wang, D. M. Graybosch, H. Li, C. D. Allis, D. J. Patel*, et al.*, "Histone H3 recognition and presentation by the WDR5 module of the MLL1 complex," *Nat Struct Mol Biol,* vol. 13, pp. 704-12, Aug 2006.

[29] E. Zelin, Y. Zhang, O. A. Toogun, S. Zhong, and B. C. Freeman, "The p23 molecular chaperone and GCN5 acetylase jointly modulate protein-DNA dynamics and open chromatin status," *Mol Cell,* vol. 48, pp. 459-70, Nov 9 2012.

[30] J. Luo, J. R. McMullen, C. L. Sobkiw, L. Zhang, A. L. Dorfman, M. C. Sherwood*, et al.*, "Class IA phosphoinositide 3-kinase regulates heart size and physiological cardiac hypertrophy," *Mol Cell Biol,* vol. 25, pp. 9491-502, Nov 2005.

[31] K. S. Zaret and J. S. Carroll, "Pioneer transcription factors: establishing competence for gene expression," *Genes Dev,* vol. 25, pp. 2227-41, Nov 1 2011.

[32] E. Calo and J. Wysocka, "Modification of enhancer chromatin: what, how, and why?," *Mol Cell,* vol. 49, pp. 825-37, Mar 7 2013.

[33] S. Heinz, C. E. Romanoski, C. Benner, and C. K. Glass, "The selection and function of cell type-specific enhancers," *Nat Rev Mol Cell Biol,* vol. 16, pp. 144-54, Mar 2015.

[34] J. Luo, C. L. Sobkiw, M. F. Hirshman, M. N. Logsdon, T. Q. Li, L. J. Goodyear*, et al.*, "Loss of class IA PI3K signaling in muscle leads to impaired muscle growth, insulin response, and hyperlipidemia," *Cell Metab,* vol. 3, pp. 355-66, May 2006.

[35] H. A. Ferris and C. R. Kahn, "New mechanisms of glucocorticoid-induced insulin resistance: make no bones about it," *J Clin Invest,* vol. 122, pp. 3854-7, Nov 2012.